MAXIMIZING CAPACITY OF UNDERGROUND MINE WATER CHILLING MACHINES REJECTING HEAT INTO A LIMITED SUPPLY OF WATER PUMPED TO SURFACE

Clifford Dale Wright

A project report submitted to the Faculty of Engineering and the Built Environment, University of the Witwatersrand, Johannesburg, in partial fulfilment of the requirements for the degree of Master of Science in Engineering.

Johannesburg, 2016

DECLARATION

I declare that this project report is my own, unaided work. It is being submitted in partial fulfilment of the requirements for the Degree of Master of Science in the University of the Witwatersrand, Johannesburg. It has not been submitted before for any degree or examination in any other University.

……..

Clifford Dale Wright

11th day of JANUARY year 2016

ABSTRACT

Underground chilling installations have an important role in deep mining operations because the total cost of cooling a mine is minimized when underground machines deliver as high a proportion of the required cooling as practicable. Thus the refrigerating load of an underground installation should be maximized to the extent permitted both by the environment in which the installation operates, and by the physical characteristics of the machines in the installation. This study analyses how, and to what extent, the refrigerating load of older, already installed water chilling machines rejecting heat into a limited supply of return water may be maximized through configuration of their water circuits and capacity control of their compressors. Multiple-machine installations are simulated in a range of scenarios, using the thermodynamically efficient series-counterflow arrangement, to predict both the potential maximum refrigerating load and the expected refrigerating load of such installations. The simulation results indicate significant potential for installations to chill water more efficiently and thus deliver larger, maximized, refrigerating loads. For scenarios where a larger-than-design flowrate of return water is available, so permitting machines to be operated with little or no capacity control, the simulated chilling efficiency and thus the expected refrigerating loads tend toward, and in some cases almost match, the potential maximum values. For simulations in which compressor capacity control is used to prevent the return water temperature from exceeding its maximum permitted value, expected refrigerating loads fall short of their potential values, by varying amounts, due to the low machine cycle efficiency caused largely by reduced compressor isentropic efficiency at part load. For a limited supply of return water for heat rejection, the simulations indicate that load maximization efforts should focus on the machines in an installation being connected in a series-counterflow arrangement and operated, as far as practicable, at or near full capacity to create the best prospect for approaching potential maximum refrigerating load.

This work is dedicated to

dearest Indrė, my darling wife
and to dearest Sofia, our precious daughter

my parents, Alan Dale Wright and Felicity Mae Wright

my parents-in-law, Mečislovas Andriuškevičius and Dainora Andriuškė

my grandmother Olive Henrietta Adams
and to the memory of my late grandfather Alexander Davidson Adams

the memory of my late grandparents
Walter Stockdale Wright and Lillian Maude Wright

ACKNOWLEDGEMENTS

I extend sincere thanks to my supervisor for his expertise, insight, enthusiasm, guidance, dedication, patience and encouragement.

My grateful thanks go to the CSIR, Division of Mining Technology, for financial assistance received as a bursary through the FutureMine Co-operative Research Programme.

Heartfelt thanks go to my parents for their support and encouragement.

To my precious wife, for her patience, selflessness, keen interest and perceptiveness, thank you.

TABLE OF CONTENTS

LIST OF FIGURES

LIST OF TABLES

Table

TABLE OF SYMBOLS

Symbol	Quantity	Unit
$\dot{m}_{RW}$	Mass flowrate of return water	kg/s
t_{WARM}	Return water available temperature	°C
t_{COOL}	Cool water available temperature	°C
η	Cycle efficiency	%
UA_E	Evaporator overall thermal conductance	kW/°C
UA_C	Condenser overall thermal conductance	kW/°C
$t_{(w)Ei}$	Evaporator inlet water temperature	°C
$t_{(r)E}$	Evaporator refrigerant temperature	°C
$LMTD_E$	Evaporator log mean temperature difference	°C
$t_{(w)Ci}$	Condenser inlet water temperature	°C
$t_{(r)C}$	Condenser refrigerant temperature	°C
$LMTD_C$	Condenser log mean temperature difference	°C
$\dot{W}_{IN}$	Compressor absorbed power	kW(M)
COP_{Carnot}	Carnot coefficient of performance	-
COP	Coefficient of performance	-
COP_{Lorenz}	Lorenz coefficient of performance	-
$t_{(w)Eo}$	Evaporator outlet water temperature	°C
$\dot{m}_{(w)E}$	Evaporator water flowrate	kg/s
$\dot{Q}_{(w)E}$	Evaporator water heat load	kW(R)
$\dot{Q}_{(w)C}$	Condenser water heat load	kW(R)
$t_{(w)Co}$	Condenser outlet water temperature	°C
$\dot{m}_r$	Refrigerant mass flowrate	kg/s
h	Refrigerant enthalpy	kJ/kg
$\dot{V}_r$	Refrigerant volume flowrate	m^3/s
v_r	Refrigerant specific volume	m^3/kg
$T_{(r)E}$	Evaporator refrigerant absolute temperature	K
$T_{(r)C}$	Condenser refrigerant absolute temperature	K
$\dot{m}_{(w)C}$	Condenser water flowrate	kg/s

Symbol	Quantity	Unit
c_p	Specific heat capacity of water at constant pressure	kJ/kg.K
$t_{(w)Co[max]}$	Specific maximum allowed return water temperature	°C
$\overline{T}_{(w)E}$	Evaporator water log mean temperature	K
$\overline{T}_{(w)C}$	Condenser water log mean temperature	K

GLOSSARY

chiller
A packaged water chilling machine with one evaporator, one condenser, a single- or multi-stage refrigerant compressor and one or more expansion valves as main components.

centrifugal chiller
A chiller using a single- or multi-stage centrifugal compressor.

centrifugal compression
An increase in temperature and pressure of refrigerant vapour by an addition of kinetic energy in a radial flow impeller, the resulting dynamic pressure is converted to static pressure in a diffuser.

condenser internal refrigerant stream
A flow of refrigerant condensing at constant, uniform temperature and pressure in the condenser of a chiller.

condenser water
Synonymous with '*heat removing water*' and '*return water*' in this glossary.

cycle efficiency
The ratio of COP to Carnot COP for a single chiller.

evaporator external water stream
A flow of water having its temperature lowered in one or more evaporators by heat transfer to boiling refrigerant.

evaporator internal refrigerant stream
A flow of refrigerant boiling at uniform temperature and pressure in the evaporator of a chiller.

expected performance

The values of key operating parameters and the accompanying refrigerating load that might be expected from a multiple-chiller installation, in any given operating regime, if all the chillers in the installation were to operate with realistic, degraded values of cycle efficiency when presented with less than ideal conditions in their water circuits and for varying amounts of compressor capacity control. Expected performance, simulated by models of real machines by the CHILLER computer program, usually delivers a lower refrigerating load than the '*potential performance'* in this glossary.

external regime

For a chiller, the mass flows and incoming properties of the two external water streams of evaporator water and heat removing water.

full capacity

The maximum water chilling load that a chiller can achieve for a given external regime. For a model of a real chiller at full capacity in the CHILLER program, the inlet guide vanes are fully open.

heat removing water

The flow of water increasing in temperature through one or more chiller condensers in removing the heat rejected by condensing refrigerant. In this study, return water is used as heat removing water. Refer also to the entry '*return water*' in this glossary.

lead lag

The configuration of a pair or group of chillers in series-counterflow in their water circuits. Refer also to the entry '*series-counterflow*' in this glossary.

return water utilization

For a water chilling installation, the quantitative measure of obtainable chilling (see the entry in this glossary), defined as the ratio of the sum of the total chilling load to the mass flowrate of return water. This ratio allows the obtainable chilling of installations with different return water flow rates, or of varying return water flow rates for one installation, to be compared.

Lorenz coefficient of performance

This is the maximum theoretical coefficient of performance of a water chilling machine. In calculating this COP, all heat transfer processes are assumed to occur reversibly.

obtainable chilling

A qualitative description of the degree of success of chillers in using return water available to them, individually and as a group, to provide a maximum amount of chilling. The obtainable chilling is quantified by the measure '*return water utilization*' in this glossary.

operating COP

In a water chilling machine, the ratio of evaporator chilling load to mechanical power input.

operating regime

An operating regime consists of the prevailing inputs to, and the control philosophy of, a chiller or group of chillers. The inputs consist of the starting temperature of the water to be chilled, the temperature of the return water before use and the mass flowrates provided to the chiller installation by each of these water sources. The control philosophy includes the desired final temperature of the chilled water and the final temperature of the return water, which may not exceed some specified maximum value.

potential performance

The values of key operating parameters and the accompanying maximum refrigerating load that could potentially be delivered by a multiple-chiller installation, in any given operating regime, if all the chillers in the installation were to operate with close-to-design values of cycle efficiency despite less than ideal conditions in their water circuits and for varying amounts of compressor capacity control. Potential performance is simulated in this report by a spreadsheet model developed for the task. Refer also to the term '*expected performance*' in this glossary.

refrigerating lift

The difference between the mean temperature of heat rejection, and the mean temperature of heat extraction, inside the machine's refrigerant circuit (Bailey-McEwan and Burrows, 2014:6)

return water

Water originating from several sources in a mine and being returned to surface, continuously or in batches, by the mine dewatering system. In this study, return water serves as heat removing water and is assumed to be available continuously at the flow rates considered. Refer also to the entry '*heat removing water*' in this glossary.

series-counterflow

Where the evaporators in a pair or group of chillers are connected in series in their water circuits, the chiller that receives the evaporator water stream first is termed the lead chiller. The chiller receiving the evaporator water stream last is correspondingly the lag chiller. If the condenser water circuits of these chillers are likewise connected in series, and the lag chiller condenser is the first in the group to receive the condenser water stream, then this series arrangement of chillers is described additionally as having a counterflow configuration.

1 INTRODUCTION

This chapter begins with a brief description of South Africa's position in the global gold mining industry, highlighting several of the economic features of the local industry. It goes on to explain the role that refrigeration is to play in the future of South African gold mining, with a focus on the current and future use of existing cooling infrastructure, particularly existing underground refrigeration installations and the heat rejection facilities[1] serving such installations.

1.1 Background

South Africa's contribution to global gold supply decreased from 79% in 1970 to 13.9% in 2004. From being ranked as the world's number one gold producer ahead of the United States and Australia in 2004 (Facts and Figures, 2004), South Africa slipped to the position of sixth largest global gold producer in 2012, with China remaining in first position since 2008 (Thomson Reuters GFMS, 2013). In addition to the slip in ranking, South Africa's annual gold output has markedly declined in recent years from 398.3 tonnes in 2003 to 177.8 tonnes in 2012 (Thomson Reuters GFMS, 2013). Gold's sliding price and surging costs are hitting a South African industry that has been slowly declining for decades as ore grades decline and shafts reach depths of up to 4km, the world's deepest (Stoddard and Lakmidas, 2013).

While South African deposits may account in 2011 for almost 12% of the world's proven remaining reserves (Facts and Figures, 2012), much of these resources are found at depths of 4000m and below.

[1] A stream of heat removing water accepts the heat rejected from the condensers and either transfers this heat (in underground cooling towers) to used ventilation air exiting the mine, or is itself pumped out of the mine. In the latter case, which applies to the present work, the heat removing water is return water (see Glossary).

Ramokgopa (2001) described mine management as recognizing that the capital cost of new shaft sinking with high costs for new infrastructure is far in excess of the capital cost of expanding production at an existing mine with good reserves. Dixon (1998) has described the long-term international competitiveness of the South African gold mining industry as relying on its ability to maintain or increase the grade recovered from existing underground operations, and control production costs as mining moves below current depths.

In the broad context of keeping South African gold mining viable in extended ultra-deep operations, Marx et al (2000) have reported that deeper mines may be most efficiently cooled, from a thermodynamic perspective, if 100% of the required chilling is generated underground. Practically, Hattingh et al (2000) suggest that, at best, approximately 80% of a mine's required total cooling might be generated underground, when taking into account the limited sources of heat rejection available to underground chillers. These findings led to the recommendation that, in conjunction with the use of ice plants on surface, the proportion of underground cooling should be maximized within the limits of heat rejection (Bluhm et al, 2000).

Thus, an ultra-deep mine will be cooled for the lowest total cost when underground heat sinks are made as large as possible and underground chilling installations are optimized to produce as much chilling as possible, using these heat sinks. Of these underground heat sinks, the largest single source is used ventilation air. Conventionally, heat is rejected into this air in underground cooling towers, as it passes out of the mine. The cooling towers almost always suffer from a shortage of air (van der Walt and de Kock, 1984) and as mines implement controlled recirculation of ventilation air to contain ventilation costs (Ramsden et al, 2001), the amount of air leaving a mine will decrease, making heat rejection to return water an essential feature for ultra-deep operations (Thom et al, 2002).

In summary, the need to make best use of existing infrastructure, the cost minimization achieved by generating more cooling underground, and the foreseen reduction in magnitude of presently available heat sinks for an ultra-deep mine, in particular used ventilation air, make it desirable to maximize the chilling load of underground machines for the available heat sinks, including return water.

1.2 Return water as a heat sink

The present work began as part of the FutureMine Co-Operative Research Programme Task 7.1.3[2], created to study the use of return water for heat rejection in underground refrigeration plants (Thom et al, 2002 and Thom et al, 2003).

Gold mines use water in mining operations including drilling, dust suppression and backfilling, environmental cooling and in the condenser circuits of underground chiller installations. Potable water is sent underground for drinking purposes. The actual volumes of water circulated, consumed and discharged vary greatly from mine to mine (Pulles, 1992). In addition, many mines must deal with extensive water seepage. This fissure water, together with used mine service water, wasted drinking water and water from backfilling operations, drains to the lowest levels in a mine before being treated prior to pumping to surface or re-use underground (Tedder, 1982).

[2] Research Task 7.1.3 *Improved Underground Heat Rejection* (subsequently updated in name to *Improved Heat Rejection for Underground Refrigeration Machines*) formed part of the FutureMine Co-Operative Research Programme, conducted by the CSIR, Division of Mining Technology.

The quality and contamination levels of such water vary considerably within a mine and from one mine to another. In many cases the water contains significant concentrations of dissolved solids leached from the geological formations and suspended material entrained from the mining operations (Tedder, 1982). Water from all these sources is collectively termed return water and ranges in available temperature from 18.9°C to 33.5°C (Pulles, 1992).

Even at its warmest, the available temperature of return water is relatively low compared to the refrigerant condensing temperature in underground chillers[3]. Thus, there is considerable potential to use it as heat removing water.

1.3 Aim of the study

The study aimed to assess how the refrigerating load of older, already installed chillers rejecting heat into a limited supply of return water[4] could be maximized, by configuration of their water circuits and control of their compressors.

[3] The maximum practicable refrigerant condensing temperature in underground chillers must be considerably below the refrigerants critical temperature (above which temperature the refrigerant does not condense to liquid), otherwise the required mass flow of refrigerant for a given refrigerating load becomes impractically high. For example R-134a, the preferred refrigerant for underground chillers (and the replacement for R-12) has a critical temperature of 101.6°C. As the condensing temperature increases (for a fixed cooling load), the mass flow of refrigerant increases dramatically. The reason is that a higher and higher percentage of flash gas is generated as the condensing temperature approaches the critical temp. of 101,6°C – so, to maintain the same cooling load, a higher and higher mass flow-rate of refrigerant is required to yield the mass flow of refrigerant liquid necessary, in the evaporator, to give this cooling load.

[4] The return water supply was assumed to be continuous in each case, but limited to the design water flow rate for the particular chiller condenser.

The first objective was to identify practicable, thermodynamically efficient arrangements of chiller water circuits that would permit a limited supply of return water to be used for heat rejection.

The second objective was to orientate the investigation in an appropriate theoretical framework, and so identify and quantify the thermodynamic limits that would govern or restrict efforts, at a fundamental level, to maximize an installation's refrigerating load.

The third objective was to assess the practicability of maximizing total refrigerating load in multiple-chiller installations, by simulating a range of scenarios, using the chiller arrangements identified earlier and variations of compressor control, to calculate both the potential maximum refrigerating load and expected refrigerating load of different installations.

The fourth objective, as an extension of the third, was to compare these simulations and identify the main reasons for the similarities and differences between potential maximum- and expected refrigerating loads, by analysis of key simulation outputs and parameter trends.

The fifth objective, supported by the results of the simulation work, was to address

- the viability of including additional chillers in an installation to increase refrigerating load
- the benefits presented by increasing the maximum allowed temperature of return water.
- the impact, on efforts to maximize refrigerating load, of restrictions on the maximum temperature of return water.

1.4 Outline of the simulations

1.4.1 Simulation group

The simulations were divided into two groups, belonging either to the Kloof mine or the Tau Tona mine[5]. Each simulation had four items specified by its containing group.

- A particular, fixed, continuously available mass flowrate of return water at a particular, constant temperature
- A particular, constant temperature of the evaporator water stream before chilling
- A specified, fixed, final temperature of chilled water to be delivered and
- the relevant chiller parameters and constants

1.4.2 Type of simulation

The groups above held two types of simulation: The first type used a spreadsheet based chiller model, and the second type used the CHILLER computer program[6] for modelling chillers at a more fundamental level, in much greater detail.

1.4.3 Quantity of chillers in a simulation

All simulations used a series-counterflow arrangement of chillers, so that configuration of a given simulation was defined simply by the quantity of

[5] Sections 3.2 and 3.3 introduce and outline the water chilling machines for the respective mines.

[6] The CHILLER computer program, developed by the Chamber of Mines of South Africa for the South African mining industry, is introduced in Section 4.1.1.

identical chillers in the simulation. The configurations in the Kloof and Tau Tona groups were similar, except that the Kloof group did not include five- or six-machine configurations and the Tau Tona group did not include a single-machine configuration.

1.4.4 Methodology of the simulations

The investigation took the following general form, proceeding in two parallel streams defined by the Kloof and Tau Tona simulation groups.

Within *each* of the Kloof and Tau Tona groups, first using the spreadsheet model,

- All configurations were simulated to quantify potential performance
- The relative performances of the individual chillers *within* each simulation were compared.
- An individual chiller's performance was compared with its equivalent chiller (that is, one holding the same position) in both the previous and subsequent configurations.

Secondly, and also within each of the groups, using the CHILLER program,

- all configurations were simulated again, now to model expected performance
- the relative performances of the individual chillers *within* each simulation were compared, based on the more detailed modelling of CHILLER.
- an individual chiller's performance was compared with its equivalent chiller (that is, one holding the same position) in both the previous and subsequent configurations.

Thirdly, CHILLER and spreadsheet model results were compared, for

simulations having the same quantity of chillers, to explain and quantify the differences between *potential* performance and expected performance, with a view to maximizing any given installation's chilling capacity.

1.5 Summary of the Project Report

Chapter 2 describes the main components of the water chilling machines in this study. The concept of using return water as heat-removing water is introduced. Performance parameters and definitions are listed to allow analysis of chiller performance.
Chiller capacity controls are described, along with the effects of capacity control on compressor efficiency and cycle efficiency.

The Carnot coefficient of performance is the theoretical maximum performance for any chiller operating between uniform evaporating and condensing refrigerant temperatures. The Carnot COP is introduced in the context of the semi-ideal refrigerating machine in section 2.2.5.
Although individual machine performance has an upper limit defined by the Carnot COP, an installation's theoretical maximum performance for any operating regime depends only on the four characteristic temperatures of that regime. These are the four external water circuit temperatures: the evaporator water inlet and outlet temperatures, and the condenser water inlet and outlet temperatures. The Lorenz coefficient of performance (refer to the glossary definition and section 2.3.6) is calculated with these four temperatures, and defines the upper performance limit for a chiller or group of chillers working within that regime.

Series and parallel heat exchanger configurations are discussed, along with the operating regime for which each is most appropriate. Lastly, the series-counterflow arrangement of chillers is introduced as a more thermodynamically efficient method of chilling water where heat is to be rejected into a limited supply of return water.

Chapter 3 uses a spreadsheet model to analyse the theoretical increase in chilling capacity afforded by arranging multiple chillers in a series configuration. The effects of using a limited supply of return water and changes in temperature of this water supply are modelled. Several important assumptions in the model are presented. In theory, a marked increase in refrigerating load is possible, even with the imposition of a limited amount of return water for condenser cooling.

In Chapter 4, simulations are performed with the CHILLER program (Bailey-McEwan and Penman, 1987), more realistically modelling real chillers for the same operating regimes as the spreadsheet model simulations. These simulations evaluate the effects on centrifugal compressor performance of placing machines in series. These effects directly affect the ability of a series arrangement of chillers to deliver the theoretical chilling increases predicted by the spreadsheet simulations.

Chapter 5 reviews and compares the results of the spreadsheet and CHILLER simulations. The best approach for maximizing the chilling capacity while limiting the condenser water outlet temperature is identified. The lead machine receives the warmest condenser water, and an important factor in the success of the multiple machine arrangement is the ability of this machine to lift its refrigerant to a relatively high condensing temperature while maintaining stable operation.

Chapter 6 summarizes the ability of existing machines to increase chilling capacity for several arrangements and operating regimes. Finally, several opportunities for further research are suggested, including development of algorithms based on the models, enhanced where necessary, used in this report, to control multiple-machine arrangements to maximize chilling. Another suggestion is for the development of a software toolbox to systematically evaluate the technical feasibility and cost-effectiveness of upgrading a mine’s infrastructure to accommodate hotter return water.

2 BACKGROUND

2.1 Underground water chilling installations

Prior to 1970, refrigeration plants were generally installed underground. Since then, there has been a trend to locate installations on surface (Ramsden et al, 2001). Surface plants operate with lower condenser water inlet temperatures, which reduces electricity consumption. Service water, which has a high return temperature, would be pumped to surface for re-cooling (Stroh, 1982, p. 656). Pre-cooling towers are one of the features which make surface plants economically justifiable (Stroh, p. 669) because a certain amount of 'free' cooling is available from such towers, especially in the winter months (van der Walt and de Kock, 1984). These qualities made surface plants attractive for more shallow mines. For ultra-deep mines, surface plant savings are exceeded by the cost of reticulation infrastructure to provide water from surface to the workings underground and increased water pumping costs (Hattingh et al, 2000).

Presently, refrigeration equipment is a combination of surface and underground installations. Surface plants may include screw compressor equipment with ammonia as refrigerant and single stage centrifugal compressor equipment using refrigerant R134a. In several cases, the surface plants produce ice which is sent to underground melting dams (Wilson et al, 2012).

2.2 Conventional water chilling machines used in mine cooling installations

Chilled water reticulation forms a vital link in the refrigeration system of most modern mines (Stroh, p. 685), with hot mines usually incorporating chilled service water in their refrigeration strategy. It is most common to distribute chilled water from water chilling machines to mine workings and open spray air coolers via an insulated pipe network (Stroh, p. 690).

2.2.1 Main components of a conventional water chiller

Figure 2.1 represents the main components of a packaged water chiller of the type used in this study. Water to be chilled passes into the evaporator, a heat exchanger in which liquid refrigerant boils at low temperature and pressure. The water is chilled to the desired temperature in one or more passes through tubes immersed in the boiling liquid refrigerant.

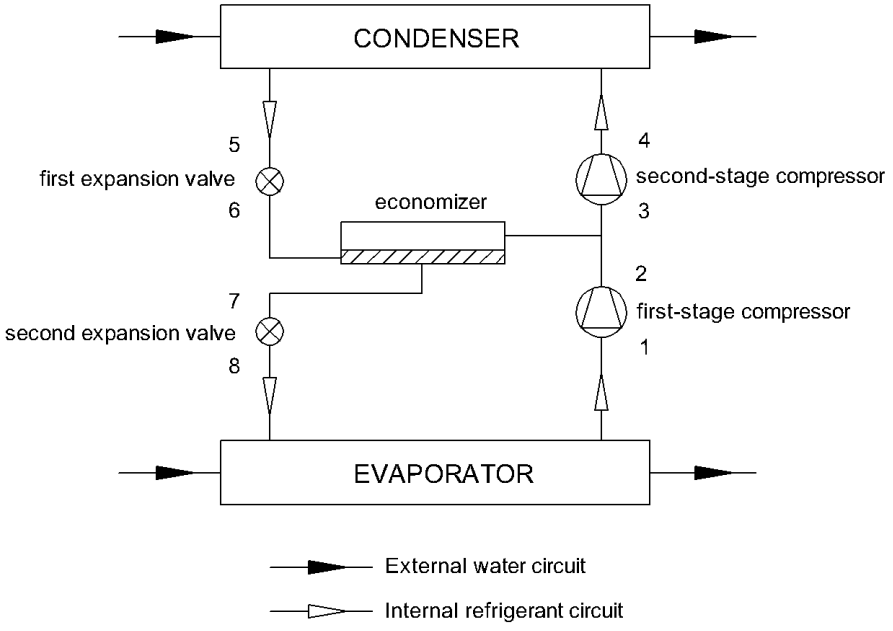

Figure 2.1 Packaged water chiller with flash gas economizer and two-stage centrifugal compression

The first stage of the two-stage centrifugal compressor draws refrigerant vapour (1) from the evaporator and increases the vapour temperature and pressure to the intermediate level of compression (2). At this point, a secondary flow of refrigerant flash vapour, from the economizer[7], is introduced to the second compressor stage (3) along with the main flow delivered from the first stage. The second stage of compression lifts the refrigerant temperature and pressure further (4), so that it may be condensed at the higher temperature in the condenser.

The refrigerant vapour condenses in the shell of the condenser at constant temperature[8] while rejecting energy (as latent heat of condensation) to the return water flowing through the condenser tubes. The return water is warmed as it receives this energy in passing through the condenser tubes. The entire liquid flow is expanded to a lower intermediate pressure and temperature through the first of two expansion valves (5)-(6) into the economizer, which holds liquid and flash vapour at saturated intermediate pressure. The flash vapour so generated is the secondary flow entering the compressor at the second stage (3), as stated above. (ASHRAE Handbook—HVAC Systems and Equipment, 2012, p. 43.1)

The liquid refrigerant in the economizer flows through the second expansion valve (7)-(8), with a proportion of the liquid again flashing to vapour, cooling the liquid further to the low temperature required in the evaporator shell.

---

[7] Because this gas has performed its function in taking enthalpy of evaporation from the cooled liquid refrigerant, it serves essentially no purpose in expanding through the second valve to evaporator pressure. Compressing this gas from the intermediate pressure achieves a reduction in the work of compression (Gosney, p. 362), hence the use of the term ‘economizer’. Also, the specific refrigerating effect of liquid refrigerant supplied to the evaporator is increased, with a consequent increase of the refrigerating capacity available from a given volume flow rate in the first-stage compressor (Gosney, p. 363).

[8] The compressed refrigerant vapour is actually delivered to the condenser with a degree of superheat. But, due to the relatively high latent heat of each of the preferred refrigerants, this superheat plays a negligible role in influencing the refrigerant condensing temperature.

2.2.2 Refrigerants suitable for underground installations

Several refrigerants have been used in underground installations: Refrigerant R11 was the most widely used until it was replaced by R12 and R22. R12 has in turn been almost entirely replaced by the new, more environmentally acceptable R134a which has similar properties. Although R22 provides greater capacity than R134a for a given compressor capacity[9], as an HCFC it is scheduled for phase out (ASHRAE Handbook 2012, HVAC systems and equipment, p. 43.6).

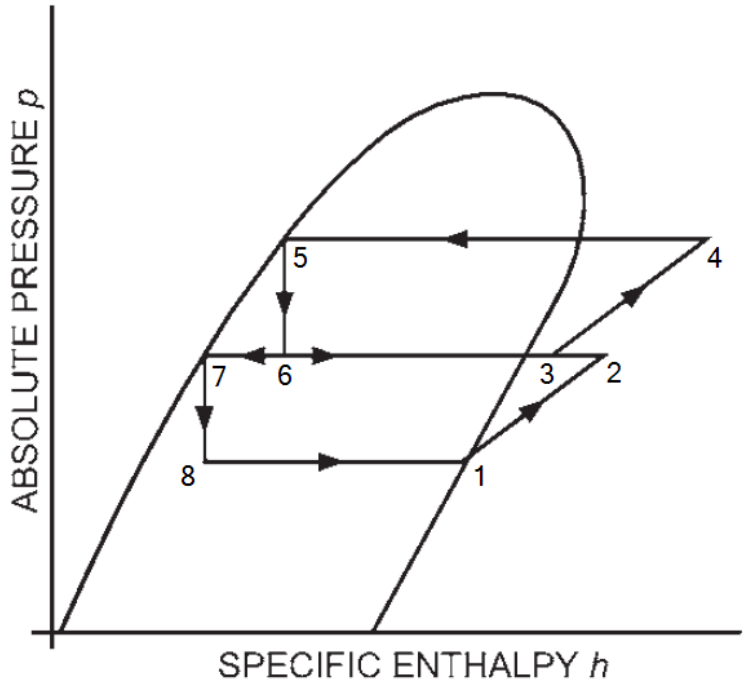

Figure 2.2 Two-stage compression cycle with flash cooling (Adapted from 2012 ASHRAE handbook - HVAC systems and equipment, p. 38.29)

Table 2.1 lists the theoretical calculated performance of a number of refrigerants for a standard cycle of 258 K evaporation and 303 K condensation.

[9] A given capacity refers, in the case of a centrifugal compressor, to a given physical size and rotational speed. The term *displacement* is reserved for positive displacement compressors.

Table 2.1 Comparative refrigerant performance per ton of refrigeration (extracted from ASHRAE Handbook 2009, Fundamentals, Table 9, p. 29.9)

Refrigerant	Evaporator pressure (MPa)	Condenser pressure (MPa)	Compression ratio	Net refrigerating effect (kJ/kg)	Specific volume of suction gas (m^3/kg)	Compressor displacement (ℓ/s)
R11	0.02	0.125	6.25	155.95	0.7689	4.891
R12	0.181	0.741	4.09	117.02	0.0923	0.784
R22	0.295	1.187	4.02	162.67	0.0779	0.478
R134a	0.163	0.767	4.71	148.03	0.1213	0.814

Ammonia is not suitable for use in centrifugal compressors due to its low molecular mass. In contrast, R-11 with its relatively high molecular mass and low volumetric refrigeration capacity represented a good candidate for application in centrifugal compressors (Gosney, 1982, p. 208). Centrifugal compressors are well suited to halocarbon refrigerants because of their ability to produce a high pressure ratio (ASHRAE Handbook 2012, HVAC systems and equipment, p. 38.28). Although refrigerant R11 was the first widely used refrigerant in centrifugal chillers, it has a relatively low vapour density at evaporator pressures typical in underground installations, thus requiring a relatively high volume flowrate for a given refrigerating capacity. However, R12, R134a and R22 have higher vapour densities than R11, meaning that for a given compressor size and speed, these latter refrigerants deliver a larger refrigerating effect than R11. Alternatively, for a fixed refrigerating load, compressor capacity may be reduced as the refrigerant volumetric refrigeration capacity increases, resulting in a smaller compressor. For safety reasons, ammonia cannot be used as a refrigerant underground.

Each chiller (following the layout of Figure 2.1) in an underground installation typically has a design capacity of the order of 3,500 kW(R) or more, requiring a large volume flowrate of halocarbon refrigerant.

2.2.3 Compressor operating characteristics

Refrigerant vapour enters the impeller in the axial direction and is discharged radially at a higher velocity. The kinetic energy imparted by the impeller increases the velocity of the gas flow. The corresponding dynamic pressure is then converted to static pressure, through a diffusion process, which generally begins within the impeller and ends in a radial diffuser and scroll outboard of the impeller (ASHRAE Systems and Equipment Handbook Chapter 34, 2000).

Because centrifugal compressors are not constant displacement, they offer a wide range of capacities continuously modulated over a limited range of pressure ratios (ASHRAE Handbook, HVAC systems and equipment, 2012, p. 43.7)

Compressor characteristic curves

Centrifugal compressor stage performance is generally specified by means of a characteristic curve, which is a plot of the isentropic head developed by the compressor against the volume flow rate at the compressor inlet. Isentropic head is easily obtained from the pressure-enthalpy diagram; the corresponding work is also called the ideal adiabatic work of compression.

Figure 2.3 shows a centrifugal compressor performance map at constant rotational speed, using prerotation vanes to modulate capacity. Typical curves for five different vane positions are shown in the figure. In addition to the head and flow characteristics, it shows the prerotation vane position and fraction of peak efficiency at which the compressor operates at any point on the map.

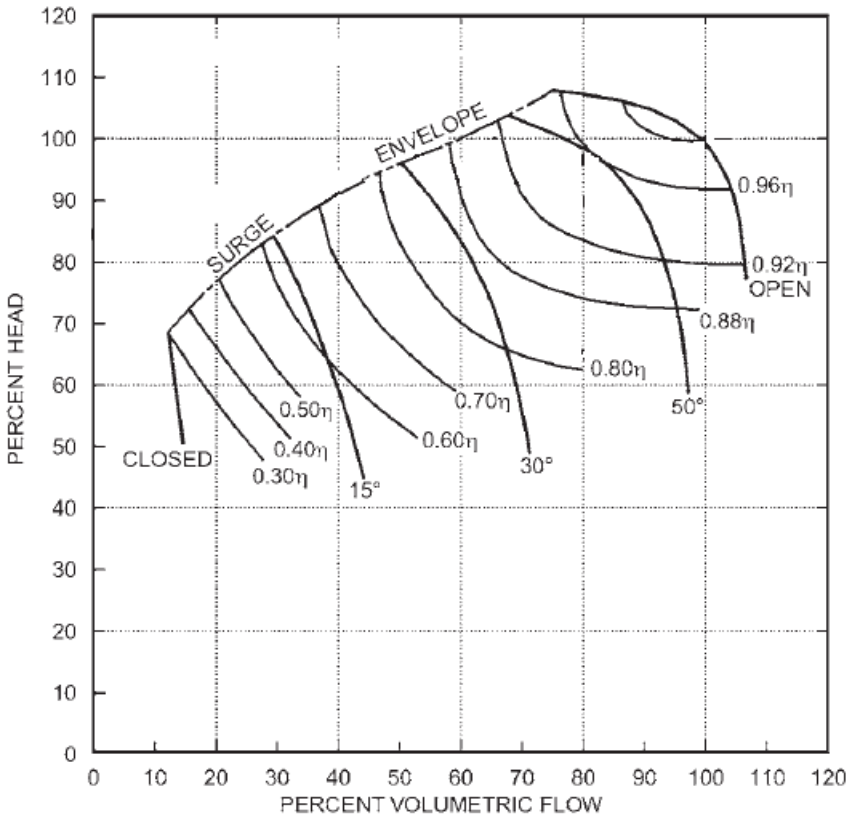

Figure 2.3 Typical compressor performance with various pre-rotation vane settings (Adapted from 2012 ASHRAE handbook - HVAC systems and equipment, p. 38.33)

Efficiency

The efficiency curves in Figure 2.3 refer to isentropic efficiency, defined as the ratio of the work required for isentropic (that is, reversible adiabatic) compression of the refrigerant gas to work input to the compressor shaft (ASHRAE Systems and Equipment Handbook Chapter 34, 2000). If a compressor's maximum efficiency is at design duty, any significant departure from this duty will reduce the isentropic efficiency of the compressor.

Operating limits

The range of compressor part-load performance is limited by surging. Surging describes an instability of operation caused by mismatch between the impeller and diffuser at low refrigerant flow rates (Gosney, p.350). Refrigerant alternatively flows backward and forward through the compressor, accompanied by increased noise, vibration and heat (ASHRAE Handbook – HVAC Systems and Equipment, Chapter 34, p. 38.33, 2012). Surging occurs when the system specific work, characterized by high condensing temperature, is greater than the compressor developed specific work (ASHRAE Handbook – HVAC systems and equipment, Chapter 43, 2012, pp. 43.10); the compressor does not develop adequate steady-state lift to match condenser pressure. Surging does not occur explicitly as a result of capacity control. All that is required is that a given condenser temperature is high enough that the compressor operates on its particular curve at a point at the surge envelope.

When the refrigerant velocity has approached a sonic value at the impeller eye, increasing speed does not produce a corresponding increase in capacity. The flow becomes choked; it represents the maximum capacity of an impeller (ASHRAE Handbook Chapter 34, 2000).

Stages of centrifugal compression required for high refrigerating lift in chillers installed underground

Heat-removing water presented to the condenser inlets of underground chillers may be relatively warm, of the order of 30°C (Biffi and Steenkamp, 1996). A chiller's evaporating and condensing refrigerant temperatures must be lower and higher, respectively, than the outlet water temperatures of these heat exchangers.

So, if a chiller must chill water to between 6°C and 10°C, but must reject its heat into water entering its condenser at 30°C, the ‘temperature lift’ which the centrifugal compressor must provide between its evaporating and condensing temperatures must be accordingly higher.

The change of specific enthalpy which can be produced (by a single compression stage) is related to the size of the compressor if peak efficiency is to be maintained (Gosney, p. 354). So, two- or multi-stage compression allows the compressor to develop the higher lift *and* maintain efficiency.

Capacity control

For a constant impeller speed, capacity control may be achieved with inlet guide vanes. Setting these vanes to pre-whirl the flow in the direction of rotation as it enters the impeller eye produces a new compressor performance curve at the same speed (ASHRAE Handbook Chapter 34, 2000). Inlet guide vanes operate most efficiently up to about 50% closure, after which efficiency begins to drop off rapidly.

In two- or multi-stage compressors, gas discharged from the first stage is directed to the inlet of the second stage through a return channel. The return channel can contain a set of fixed-flow straightening vanes or an additional set of adjustable inlet guide vanes.

Capacity control by inlet guide vanes in chillers installed underground

Underground water chillers operate at relatively constant condensing pressure. (This would also be the case for such chillers receiving a steady supply of return water at a given temperature for heat rejection.)

As their evaporating pressure is also relatively constant, so is their refrigerating lift, so constant-speed drive is appropriate for their centrifugal compressors. Capacity regulation is achieved with inlet vane openings from 100% down to approximately 50%. The disadvantage of such control is that the refrigerant velocity remains high at the compressor inlet. Down to about 50% capacity reduction, Figure 2.3 shows that the compressor isentropic efficiency is acceptable. But for larger values of capacity reduction, the inlet vanes tend to throttle the refrigerant flow rather than efficiently impart a prerotation velocity.

2.2.4 Chiller duty

The refrigerating load of a chiller is given by the product of the refrigerant mass flow rate in the evaporator and the change in the enthalpy of the refrigerant in the evaporator (Burrows, 1982). With reference to the state points in Figure 2.2:

$$\dot{Q}_E = \dot{m}_{(r)E} (h_1 - h_8) \qquad \text{(Equation 2.1)}$$

Due to the fixed speed, centrifugal compressors of the type in this study operate over a fairly small range in inlet volume flow rate, when the compressor is at full capacity. At full capacity, the volume flowrate is mainly a function of compressor physical dimensions and speed, as well as inlet refrigerant properties and evaporator pressure. At part capacity, the inlet prerotation guide vanes reduce the inlet volume flowrate.

A refrigerant's volume and mass flowrates are related by:

$$\dot{V}_r = \dot{m}_r \nu_r \qquad \text{(Equation 2.2)}$$

where ν_r is the refrigerant specific volume at the compressor inlet.

Substituting for the mass flowrate gives:

$$\dot{Q}_E = \frac{\dot{V}_{r,1}\,(h_1 - h_8)}{v_{r,1}} \qquad \text{(Equation 2.3)}$$

The ratio $\frac{(h_1 - h_8)}{v_{r,1}}$ in Equation 2.3 is dependent on the refrigerant properties at the evaporator's inlet and outlet . At part load, in addition to variation of this term, the volumetric flowrate $\dot{V}_{r,1}$ decreases with closure of the prerotation guide vanes.

Changes in operating conditions, for example inlet water temperatures, generally result in changes in the evaporating and condensing pressures. Changes to evaporator shell pressure affect the load of the chiller and the lift, and therefore input power, developed by the compressor. Changes in the condensing pressure change the compressor lift, as well as affecting the load of the chiller: a higher condenser pressure may reduce the refrigerating effect $(h_1 - h_8)$ in Equation 2.3, reducing the chiller load if the compressor is at full capacity.

2.2.5 The semi-ideal refrigerating machine

This is termed semi-ideal because although the internal refrigeration cycle is assumed free of irreversibility in all processes, the heat transfer in the evaporator from the water stream undergoing chilling to the refrigerant, and the heat transfer from the refrigerant to the heat removing condenser water stream, must occur across the finite heat transfer areas in the evaporator and condenser.

Thus the refrigerant temperatures must be maintained at the 'approach' temperatures, which are above the return water exit temperature in the condenser and below the chilled water delivery temperature in the evaporator. Although the machine may lift energy reversibly, it neither extracts nor rejects energy as heat reversibly, and so the machine is termed semi-ideal.

Apart from the flash gas therein, the refrigerant stream in the evaporator undergoes a phase change from liquid to vapour at uniform temperature. Similarly, refrigerant vapour in the condenser (after de-superheating) undergoes a phase transition to liquid, again at uniform temperature. These constant temperature processes mean that the highest level of performance a conventional vapour-compression centrifugal water chiller may achieve is quantified by the Carnot COP for a semi-ideal water-chilling machine:

$$COP_{Carnot} = \frac{T_{(r)E}}{T_{(r)C} - T_{(r)E}} \qquad \text{(Equation 2.4)}$$

where $T_{(r)E}$ and $T_{(r)C}$ are the uniform boiling and condensing refrigerant temperatures in the evaporator and condenser respectively. The Carnot COP defines the minimum, theoretical input power (when all the processes within a chiller are thermodynamically reversible) to achieve a given chilling load for a chiller operating with these uniform refrigerant temperatures.

The external irreversibilities of heat transfer through a machine's evaporator and condenser, whilst not explicitly appearing in the Carnot COP, nevertheless affect it. For example, condenser and evaporator fouling factors increase the resistances to heat transfer. Fouling influences the extents to which the heat exchanger refrigerant temperatures and the machine load differ from design duty (van der Walt, 1979).

The increased resistance to heat transfer is described mathematically by reduced overall heat transfer coefficients. In an evaporator, for example, Equation F.5 shows that a fouling factor reduces the UA product, requiring (for the same heat transfer rate) a compensating increase in the LMTD term. By Equation F.4, this increase in LMTD is achieved by reducing the evaporator refrigerant temperature. A fouled evaporator alone will therefore lower the Carnot COP.

If the condenser is also fouled, the condenser refrigerant temperature will be raised, contributing to a further reduction in Carnot COP for the semi-ideal machine. This means that a machine will consume more power than before.

2.2.6 The real refrigerating machine *(having internal, not only external, irreversibilities)*

The actual power consumption of a machine is higher than that predicted by the Carnot COP. This is due to internal irreversibilities in the refrigerant circuit, namely:

- Less-than-100% isentropic efficiency of the compressor components including impeller(s), diffuser(s) and regulating guide vanes.
- Fluid friction in the refrigerant piping
- Sliding friction in compressor bearings, and in any internal speed-increasing gearbox
- Irreversible constant-enthalpy expansion in the expansion valves

These internal irreversibilities vary with variations in chiller duty due to changes in operating regime. In particular, compressor isentropic efficiency declines markedly under severe part-duty. This is one aspect that the CHILLER program models, but the spreadsheet models do not.

2.3 Maximizing chilling load of machines by making best use of return water

In a multiple-chiller installation with condensers in series[10], each machine rejects all the heat energy it removes from the chilled water stream, along with its compressor work, into the single common return water stream. In doing so, the return water stream progressively increases in temperature as it passes through each successive condenser.

Thus, the heat rejection facility provided by return water is limited both by the continuously available flowrate of such water and its permitted final temperature[11], these being key variables of any operating regime. This in turn limits an installation's maximum refrigerating load, being maximum chilled water output at a specified temperature, because once sufficient chillers are installed to raise the return water temperature to its permitted final value, there is no scope for adding additional chillers to the installation.

Also, if operation of the chillers at full load would result in the return water exceeding its permitted final temperature, then the chiller loads must be reduced using capacity control[12], to cap the final temperature of return water at this limit, and in doing, reducing the chilled water output.

2.3.1 Operating regimes

An operating regime consists of the prevailing inputs to, and the control philosophy of, a chiller. For a single chiller, the operating regime comprises the evaporator and condenser water flows, and evaporator and

[10] Section 2.3.5 discusses water circuit arrangements for heat exchangers

[11] Section 2.3.3 and section 2.3.4 present these factors in more detail

[12] Section 2.2.3 deals with compressor capacity control in the context of compressor operating characteristics

condenser inlet water temperatures; plus the control philosophy of desired evaporator outlet water temperature and the maximum allowed temperature of return water at outlet.

For an installation with multiple chillers, the operating regime is defined similarly, but with evaporator water inlet temperature and maximum allowed return water outlet temperature referred to the first chiller, and condenser water inlet temperature and desired evaporator water outlet temperature referred to the last chiller in the arrangement[13]. The quantities in this operating regime are denoted by:

- $\dot{m}_{(w)E:}$ The flowrate of the evaporator water stream
- $\dot{m}_{RW}$: The flowrate of the available heat removing water
- t_{COOL}: The temperature of the cool water stream, at inlet to the lead evaporator.
- t_{WARM}: The temperature of the warm return water stream, at inlet to the lag condenser
- $t_{(w)Eo}$: The final chilled water temperature, measured at outlet to the lag evaporator
- $t_{(w)Co[max]}$: The specified maximum allowed temperature of the return water stream, measured at outlet of the lead condenser

[13] Refer to Section 2.3.5 for chiller arrangements.

2.3.2 A limited supply of return water

The constraint of having return water as the heat-removing water is relevant for two reasons.

a) Because the supply of return water is limited, as identified in Section 1.2, it may undergo a large temperature increase as it accepts heat energy from chiller condensers. This hot water is subsequently handled by the mine's dewatering system. So, whatever the chilling load, the final return water temperature leaving the installation must be controlled to remain at or below a predefined, maximum allowed value. The temperature value is decided by the ability of the mine's dams, dewatering pumps and piping system to handle hot return water.

b) The low available flowrate of return water precludes the arrangement of condenser in parallel in their water circuits, which adversely affects the efficiency of chilling.

2.3.3 Making best use of return water

There are two complementary aspects to making best use of return water.

a) Increase the chilling load as much as possible without exceeding the specified temperature limit of the return water.

b) Increase the efficiency of chilling; that is, increase the chiller COPs to improve the system COP. A higher COP indicates a reduction in the compressor power needed to produce chilled water, and since this compressor power is rejected with the chilling load, an improvement in COP means that, for the *same* total amount of heat rejected to return water, a chiller can reject a larger chilling load because the heat contribution from compressor power is reduced.

2.3.4 Chilling efficiency

In a single chiller, the energy rejected by condensing refrigerant, $\dot{Q}_C$, raises the temperature of the return water stream. In equation 2.5, this total rejected energy is the sum of energy removed from the chilled evaporator water stream and compression input work.

$$\dot{Q}_C = \dot{Q}_E + \dot{W}_{IN} \qquad \text{(Equation 2.5)}$$

For a multiple chiller arrangement, this may be written as

$$\sum \dot{Q}_C = \sum \dot{Q}_E + \sum \dot{W}_{IN} \qquad \text{(Equation 2.5A)}$$

and since for an individual chiller

$$\dot{Q}_C = \dot{m}_{(w)C}\, c_p \left(t_{(w)Co} - t_{(w)Ci}\right) \qquad \text{(Equation 2.6)}$$

for a multiple chiller arrangement of *n* chillers, this becomes

$$\sum_{n} \dot{Q}_C = \dot{m}_{(w)C}\, c_p \left(t_{(w)Co[max]} - t_{(w)Ci}\right) \qquad \text{(Equation 2.6A)}$$

Substituting Equation 2.6A into Equation 2.5A,

$$\dot{m}_{(w)C}\, c_p\left(t_{(w)Co[max]} - t_{(w)Ci}\right) = \sum_n \dot{Q}_E + \sum_n \dot{W}_{IN} \qquad \text{(Equation 2.6B)}$$

For the chiller installations in this study[14], Equation 2.6B shows that the number of machines n, each contributing an individual chilling load $\dot{Q}_E$, with associated individual compressor work $\dot{W}_{IN}$, cannot exceed the number that can raise the return water temperature to its specified limit $t_{(w)Co[max]}$, according to section 2.3.2, point (a).

Additionally in Equation 2.5A, the machine chilling loads $\sum \dot{Q}_E$ should make up as high a proportion of $\sum \dot{Q}_C$ as possible. This is equivalent to maximizing each machine's COP, where

$$COP = \frac{\dot{Q}_E}{\dot{W}_{IN}} \qquad \text{(Equation 2.7)}$$

The compression work term in Equation 2.7 may be substituted into Equation 2.5 to give Equation 2.8.

$$\dot{Q}_C = \dot{Q}_E \left(1 + \frac{1}{COP}\right) \qquad \text{(Equation 2.8)}$$

The higher each machine's COP, that is the more efficient the chilling process, the higher the proportion of chilling load in the rejected heat in the return water. Thus, in the process of raising the return water to its specified upper temperature limit, a higher chilling load is achieved because the temperature rise is achieved more efficiently.

[14] in which the condensers of all machines are in series in the water circuit and all handle the same, single continuously available flow of return water

2.3.5 Heat exchanger water circuit arrangements

Figure 2.4 defines several important terms and illustrates the general arrangement of chillers used in the study. Three chillers are used here to introduce the basic arrangement in all simulations from two to six chillers. The chiller that receives the evaporator water stream first, in this case chiller 3, is identified as the lead chiller. The chiller that receives the evaporator water stream last is the lag chiller. Chillers are numbered sequentially, from the lag chiller.

A representative temperature scale is shown on the left of Figure 2.4. The refrigerating lift, defined as the difference between the mean temperature of heat rejection and the mean temperature of heat extraction inside the chiller's refrigerant circuit, is shown illustratively for the lag chiller.

The water stream to be chilled passes through the three evaporators in turn, entering evaporator 3 of the lead chiller first. This water has an initial temperature t_{COOL} which decreases, shown by the chilled evaporator water temperature glide, until it leaves the lag evaporator at the final chilled water delivery temperature.

Similarly, the return water stream passes through each condenser in turn. Unlike the evaporators, the stream enters the condenser arrangement at the lag chiller, entering the *lag* condenser first with temperature t_{WARM} , which increases until the outlet of the lead condenser.

This exit temperature depends on the simulation settings and parameters in Chapter 3, and must be equal to or less than the specified maximum allowed temperature. This water circuit arrangement of evaporators and condensers is termed 'series-counterflow'.

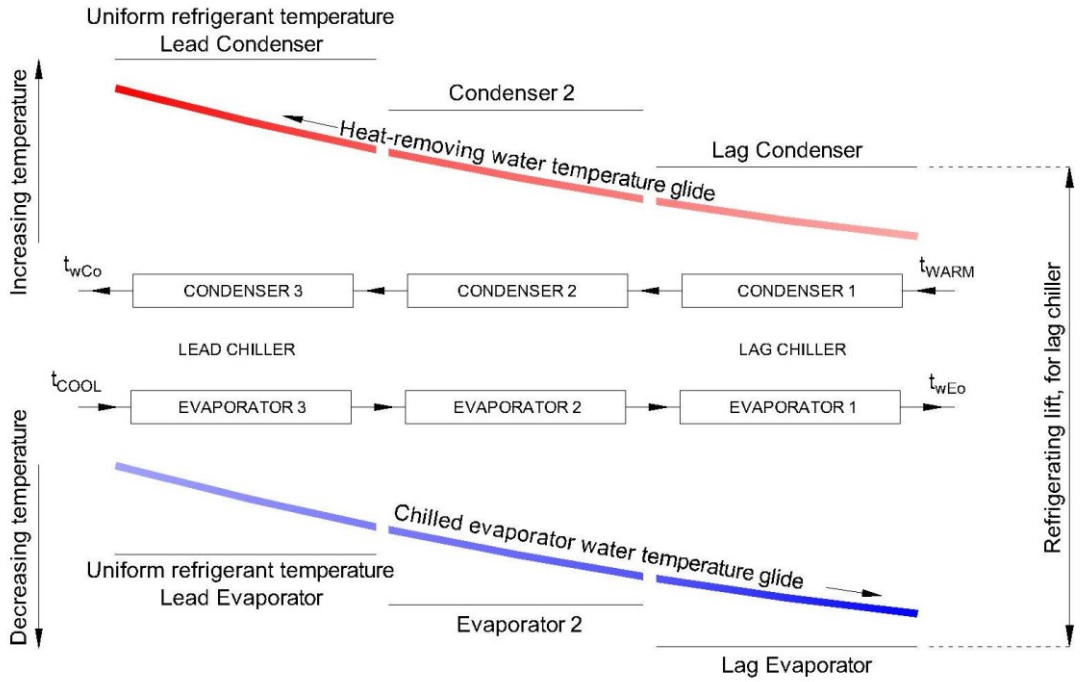

Figure 2.4 Key concepts in a series-counterflow chiller arrangement

Chilling Efficiency and Chilling Load with evaporators arranged in series in their water circuit

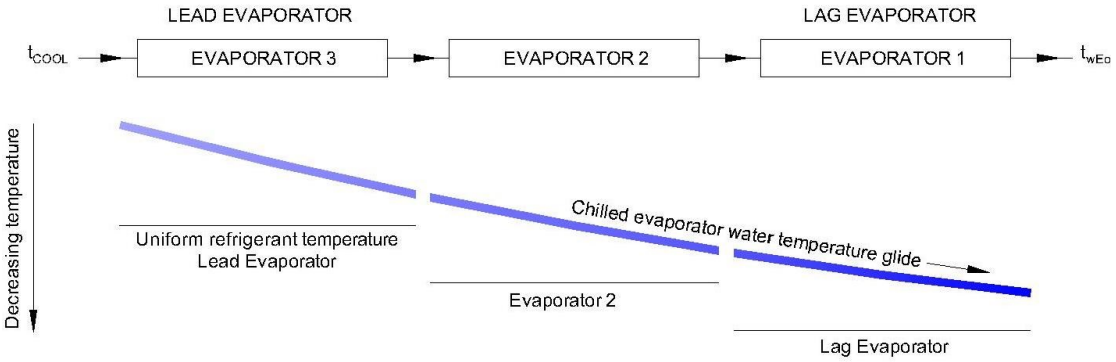

Figure 2.5 Multiple evaporators arranged in series in their water circuit

Placing evaporators in series means that all of the water being cooled passes through all machines in turn. If 400 kg/s of water require chilling, four machines in parallel each cool 100 kg/s of water.

The same four in series have the full water flowrate, i.e. 400 kg/s, flowing through their tubes. This increased water flowrate has two effects: Firstly, because the water side heat transfer coefficient $h_{[W]E}$ varies with tube water velocity according to $\nu_{(W)}{}^{0.8}$, shown in the correlation F.6 in Appendix F, the fourfold increase in the water velocity here results in the water side heat transfer coefficient increasing by a factor of three. Secondly, only the last chiller, the lag chiller, has to maintain the lowest refrigerant temperature necessary to chill the water to its desired delivery temperature.

Condensers arranged in series for a limited supply of return water

A typical underground plant might comprise two or more chillers. If a sufficient quantity of return water is available, each machine's condenser should be supplied with its own stream of cooling water. That is, the machine condensers should be arranged in parallel. This presents each machine with the lowest possible return water temperature. Lowering the log mean temperature of the cooling water passing through a condenser reduces the refrigerating lift that a compressor must provide, thereby improving the operating COP.

Where the availability of return water is limited, as in the present study, condensers should be arranged in series. This configuration provides each chiller with design flowrate of cooling water, making best use of available heat transfer area, by maximizing the water-side heat transfer coefficient.

Counterflow arrangement for heat exchanger water circuits in series

Two water-cooled condensers in series are best piped in a counterflow arrangement so that the lead machine is provided with warmer condenser and chilled water, and the lag machine is provided with colder entering condenser and chilled water. The refrigerating lift is nearly the same for each chiller. If about 55% of design cooling capacity is assigned to the lead machine and about 45% to the lag machine, identical units can be used (ASHRAE Refrigeration Handbook, p. 43.2, 2002).

A single chiller cooling water in a single step must maintain an evaporator refrigerant temperature lower than the chilled water exit temperature it delivers, and a condenser refrigerant temperature higher than its condenser water exit temperature. Maintaining these extremes of refrigerant temperature limits the performance of the machine, since the Carnot COP (Equation 2.4) for a refrigeration cycle decreases as the refrigerant lift increases.

In summary, a series-counterflow arrangement of chillers cools water in two or more steps, reducing the evaporator-condenser refrigerant temperature lift that each machine must maintain, thus improving the Carnot COP of each machine.

Thus, for a given amount of heat rejected in a machine condenser, it is the operating COP of the machine that must increase if a higher chilling load or lower compressor power input is to be realized.

2.3.6 Maximum chilling efficiency for a given operating regime

The Carnot coefficient of performance caps the maximum chilling efficiency for a chiller that maintains constant uniform refrigerant temperatures[15] in both the evaporator and condenser (Section 2.2.5). However, unlike the refrigerant temperatures, the water temperatures in the external regime are not constant (Sections 2.3.1 and 2.3.5): The return water rises in temperature in passing through the condenser and the cool water temperature decreases on its way through the evaporator.

For refrigerating duties of this type where the temperature of the external regime is not constant, the Carnot COP (using the constant refrigerant approach temperatures) is an unduly pessimistic standard of performance (Gosney, p. 41). A much better standard of performance can be aimed at, if the chiller's refrigerant temperatures can be made to follow[16] the temperature variations in the external regime as first suggested by Lorenz (Gosney, p. 41).

In calculating this better standard of performance, the limiting case is used, in which the refrigerant temperatures follow the water temperature glides in evaporator and condenser exactly[17]. This better measure of performance, representing the theoretical maximum chilling efficiency, is the Lorenz COP.

---

[15] These uniform 'approach' temperatures are the refrigerant temperatures in the internal refrigerant circuit, respectively above and below the extreme values of the water temperatures in the external water circuit. These extreme values are:
a) the return water exit temperature in the condenser $t_{(w)Co}$ (or $t_{(w)Co[max]}$, if achieved)
b) the chilled water delivery temperature in the evaporator $t_{(w)Eo}$.

[16] "One way of doing this is to use a mixture of refrigerants, the boiling point of which changes with composition as the more volatile component is boiled away. Another method is to use a gas as the refrigerant" (Gosney, p. 41)

[17] This assumption of zero temperature differences between internal refrigerant temperatures and external water temperatures in each of the two heat exchangers is of course theoretical because in reality a finite temperature difference is required for any heat transfer.

It depends *only* on the external water circuit temperatures, being the four water temperatures of the operating regime: t_{COOL} (equal to $t_{(w)Ei}$ at the lead machine), $t_{(w)Eo}$from the lag machine, t_{WARM} (equal to $t_{(w)Ci}$ at the lag machine) and $t_{(w)Co[max]}$ from the lead machine, introduced in Section 2.3.1.

$$COP_{Lorenz} = \frac{\overline{\overline{T}}_{(w)E}}{\overline{\overline{T}}_{(w)C} - \overline{\overline{T}}_{(w)E}} \qquad \text{(Equation 2.9)}$$

where $\overline{\overline{T}}_{(w)E}$ and $\overline{\overline{T}}_{(w)C}$ are the log-mean temperatures of the evaporator and return water streams.

The Lorenz COP is the maximum theoretical COP for these conditions and is valid for any single chiller or grouped arrangement of chillers, defining an upper limit for the efficiency of chilling (Section 2.3.4) for any particular operating regime. In reality, the Lorenz COP may be approached but not achieved because even for a chiller with impractically large heat exchangers as a necessary addition to the design feature of non-constant refrigerant temperatures, some temperature difference[18] would always be necessary for heat exchange in a finite time.

Because the type of chiller modelled in this study operates with constant refrigerant temperatures and does not have the capability to control these temperatures to follow the variations in the external regime, such a chiller cannot *individually* attain a better COP than the Carnot COP. But, a series-counterflow arrangement of this same type of chiller will, as the number of chillers is increased (and their individual chilling load decreased), approach the Lorenz COP[19].

[18] that is, between the internal (refrigerant circuit) temperatures and the external (water circuit) temperatures

[19] The Lorenz COP assumes no external or internal irreversibilities and would be achieved by an infinite amount of infinitesimally small chillers

This is illustrated for the arbitrary number of ten chillers in figure 2.6.

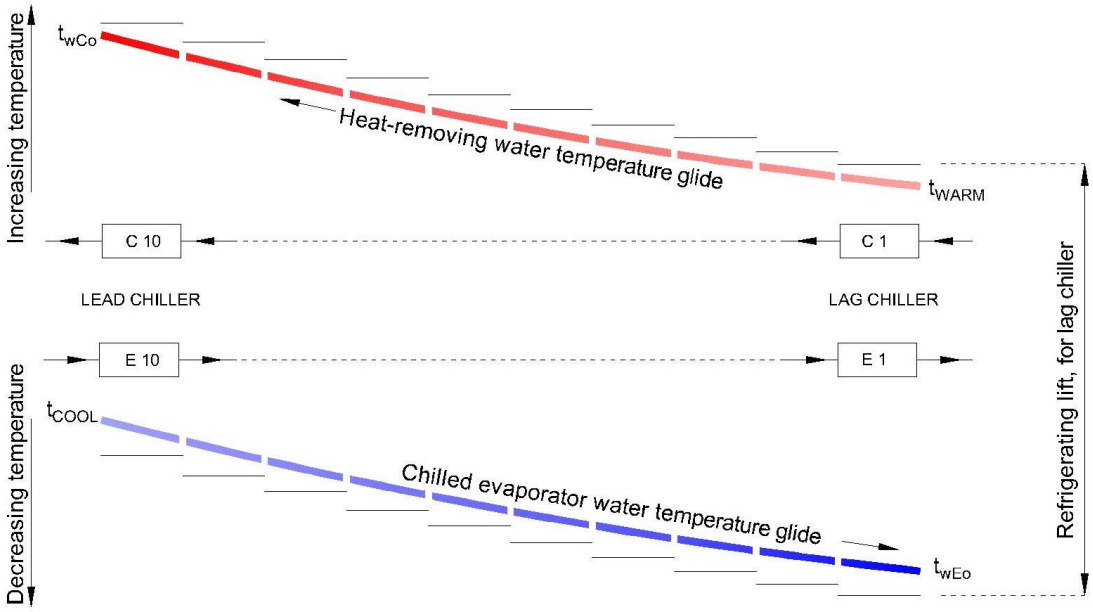

Figure 2.6 The finite Lorenz approximation using a chiller type having constant uniform refrigerant temperatures (and thus an individual maximum theoretical chilling efficiency calculated by the Carnot COP)

Figure 2.6 uses ten chillers (with constant refrigerant temperatures) to show how these temperatures may approximate the external regime water temperature glides more closely for a greater number of chillers. Such a large number of chillers is not practicable but is used in the figure to give a clearer graphical illustration. In Chapter 3, models are used to simulate such chillers[20] in the finite Lorenz approximation, to predict the ability of a realistic number of chillers to maximize the refrigerating load of underground installations. The design and operating features of these chillers are discussed further in section 3.1.1.

[20] That is, the type of chiller having constant uniform refrigerant temperatures in condenser and evaporator, finite-size heat exchangers and the assumption of a 60% cycle efficiency (Bailey-McEwan, 2002) to account for internal irreversibilities (that is, irreversibilities in the refrigerant circuit).

2.3.7 Upper temperature limit for return water

For a given operating regime, section 2.3.6 has described firstly how the maximum theoretical chilling efficiency for that regime is governed solely by its four reference water temperatures, and secondly how chillers implemented in a finite Lorenz approximation may attain to this maximum efficiency, itself quantified by the regime-specific Lorenz COP.

If an installation has an insufficient number of chillers to raise the return water stream to the specified maximum allowed temperature, there is scope to increase the chilling load simply by introducing more chillers to the installation until $t_{(w)Co[max]}$ is reached. If additional chillers are not available, the discussion in Section 2.3.6 is still valid[21] for the operating regime defined by the intermediate return water exit temperature $t_{(w)Co} < t_{(w)Co[max]}$.

Similarly, if the return water stream is allowed to exceed its specified maximum temperature and attains to some new, higher limit, then additional chillers may be added to the installation until the new, higher $t_{(w)Co[max]}$ is reached, defining a new operating regime with a new Lorenz coefficient of performance. The compressor operating points (and thus the compressor efficiencies of the chillers) are important considerations if return water is to be raised to some higher temperature. This and other aspects are considered in the simulations of Chapter 3.

[21] recalling from section 2.3.6 that the Lorenz COP depends *only* on the external water circuit temperatures, being the four water temperatures of the operating regime, introduced in Section 2.3.1.

3 SPREADSHEET MODEL SIMULATIONS

This chapter quantifies the chilling load that machines in series-counterflow might achieve in theory, for particular operating regimes.

3.1 Introduction

Appendix C describes the spreadsheet chiller model used for the simulations in this chapter. The accompanying models for heat exchangers are given separately in Appendix E.

3.1.1 The spreadsheet model

Section 2.3.6 describes the Lorenz COP, which depends on all four of the water temperatures of an operating regime. For a particular simulation, these temperatures were t_{COOL}(equal to $t_{(w)Ei}$ at the lead machine), $t_{(w)Eo}$ from the lag machine, t_{WARM} (equal to $t_{(w)Ci}$ at the lag machine) and $t_{(w)Co}$ from the lead machine. Where a simulation raised the final temperature of return water to its specified limit, then $t_{(w)Co}$ was replaced by $t_{(w)Co[max]}$.

The Lorenz COP is the maximum theoretical COP for these conditions and is valid for any single chiller or grouped arrangement of chillers. The Lorenz COP is not achievable practically for the reasons presented in Section 2.3.6., but it quantifies what may be aimed at because it is the theoretical upper limit for the efficiency of chilling (Section 2.3.4) for any particular operating regime. Because it has its basis in the Lorenz COP, the spreadsheet model is useful in showing what can be aimed at. So the spreadsheet presents the theoretical, optimal view, which is evaluated against corresponding simulations from the CHILLER program.

In Chapter 4, CHILLER is used to evaluate, at a deeper level of reality[22], how real chillers might achieve a portion of the capacity increase indicated by the 'finite Lorenz approximation' analysis of the spreadsheet model by accounting for both the external and, at a deeper level of reality, the internal irreversibilities.

The spreadsheet model, in addition to calculating the Lorenz COP for each operating regime (using $t_{(w)Co[max]}$), also calculates the Lorenz COP unique to each simulation, based on the temperature attained by the return water stream after it exits the lead chiller, $t_{(w)Co}$. Of course, if the simulated chillers do raise the return water temperature $t_{(w)Co}$ to $t_{(w)Co[max]}$, then the Lorenz COP for the simulation is the same as the Lorenz COP for the operating regime.

Key assumptions in the spreadsheet model

1. The spreadsheet model specified a constant cycle efficiency of 60%[23] for all chillers, whether simulated alone or as part of a multiple chiller arrangement. This suggested that a chiller, or any group of chillers, was infinitely flexible, maintaining a constant cycle efficiency under all circumstances.

2. Each chiller operated with a fixed evaporator heat transfer area, and a constant overall thermal conductance in the evaporator.

3. Each chiller operated with a fixed condenser heat transfer area, and a constant overall thermal conductance in the condenser.

[22] The spreadsheet, like CHILLER, does take account of internal irreversibilities. However, it does this by using a constant lumped cycle efficiency term, whereas CHILLER treats this term as variable and it emerges from first principles.

[23] Design cycle efficiency for the Tau Tona machines used in this study is 58.6% (Bailey-McEwan, 2002). This value is typical for the type of machines installed underground and analysed here. A cycle efficiency of 60% is assumed in the spreadsheet model.

4. Each Kloof or Tau Tona chiller had the same evaporator heat transfer area and overall heat transfer coefficient, and the same condenser heat transfer area and overall heat transfer coefficient.

5. Unless noted, each chiller performed an equal reduction in temperature of the evaporator water stream. For example, each chiller in a three-machine installation performed one third of the total water temperature reduction.

6. Unless noted, the chilled water flowrate was equal for all evaporators, and because of assumption 5, it followed that each chiller had an equal chilling load $\dot{Q}_E$.

7. The refrigerant temperature was uniform in any single evaporator or condenser.

8. There is a risk that water may freeze in evaporator tubes if a real installation has a low chilled water delivery temperature. To avoid this, it is common practice to prevent the evaporator refrigerant temperature from falling below some safe limit. The spreadsheet model set the lower limit at 1°C for any evaporator refrigerant temperature.

This constant cycle efficiency accounts for all internal irreversibilities of the chiller, being all irreversibilities in the refrigerant circuit. The main sources of irreversibility are compressor inefficiency and the constant enthalpy irreversible expansion through the expansion valve. The Lorenz COP is so much higher than the Carnot COP because it assumes that *all* processes (internal and external) are completely reversible.

The validity and implications of these assumptions, with regard to the expected performance of real machines, are discussed in Chapter 5. These results are compared with simulations in Section 4.2 and Section 4.3 of real machines, from the CHILLER program, to predict the extent to which real machines might deliver the potential maximum refrigerating load suggested. The CHILLER simulations use the same operating regimes as the spreadsheet models.

3.1.2 'Return water utilization' as a measure of obtainable chilling

A definition of the term 'return water utilization' provides a measurement of how well chillers use the return water available to them, individually and as a group. For example, an installation would exhibit a relatively high return water utilization if the chillers rejected enough heat to raise the return water temperature to the specified maximum upper limit and additionally operated with high operating COPs, maximising the energy removed from chilled water in the total heat rejected.

$$\text{return water utilization} = \frac{\sum \dot{Q}_E}{\dot{m}_{RW}} \quad \text{kW(R)/(kg/s)} \qquad \text{(Equation 3.1)}$$

It allows installations with different return water flow rates to be compared, or comparisons of varying flows in the same system.
An installation might reach or have the capacity to exceed the specified maximum upper return water temperature limit, but if the individual machines operate with relatively low COPs, then the efficiency of chilling is low and more of the energy raising the return water temperature will come from compressor work, resulting in a smaller numerator in Equation 3.1.

3.2 Kloof mine simulations

3.2.1 Operating regime

Kloof simulations used an operating regime from environmental constraints and criteria for a proposed return water heat rejection scheme at Number 3 sub-vertical shaft of Kloof Gold Mining Company Ltd (Biffi and Steenkamp, 1996). Table 3.1 summarizes the information.

Table 3.1 Environmental constraints and criteria for Kloof mine

Quantity	Value	Unit
Mass flowrate of return water	160	kg/s
Return water available temperature	32	°C
Cool water available temperature	25	°C
Chilled water delivery temperature	10.5	°C

3.2.2 Spreadsheet specification of full capacity for a single Kloof chiller

Chiller sizing

Table 3.2 shows the overall thermal conductance of each heat exchanger. These values are specified in Appendix E, using the machine specifications from the CHILLER program in Appendix D and comparisons with plots of the range of overall thermal conductances in the CHILLER simulations. The values in table 3.2 were constant for all Kloof chillers, following assumptions 1, 2 and 3 in Section 3.1.1.

Table 3.2 Chiller key specifications

Quantity	Value	Unit
Cycle efficiency	60	%
Evaporator overall thermal conductance	600.00	kW/°C
Condenser overall thermal conductance	800.00	kW/°C

Specification of single machine maximum chilling load

Because the equations in Appendices C and E are general and may be used to model a chiller of any duty, the size of an individual chiller in the spreadsheet was created by comparing it with its equivalent model in the CHILLER program, for the same operating regime. Setting the maximum chilling load in this way provided a simple method to 'size' the spreadsheet chillers.

Accordingly, because the CHILLER simulation of a single real machine (Appendix B: Section 9.2.1) heated the available 160 kg/s of return water to 42.28°C, the spreadsheet evaporator water flowrate was increased[24] until its condenser water outlet temperature was 42°C, almost identical to that from the CHILLER machine for the same 160 kg/s flowrate of return water. The calculated evaporator chilling load of 5,423.98 kW(R) corresponding to the final return water temperature of 42°C in Section 9.1.1 was taken as the maximum chilling load that an individual Kloof machine could provide in any spreadsheet model simulation.

[24] With the other inputs matching those in the operating regime of the CHILLER simulation:
t_{COOL} = 25 °C evaporator water inlet temperature
$t_{(w)Eo}$ = 10.5 °C outlet temperature
t_{WARM} = 32 °C return water inlet temperature
and, as stated, $\dot{m}_{(w)C}$ =160 kg/s

Simulations in Sections 9.1.1, 9.1.2, and 9.1.5 used this maximum capacity, described by category B in Table 10.1, while chillers in Sections 9.1.3, 9.1.4, and 9.1.6 were manually restricted from delivering this load, following category A in Table 10.1.

3.2.3 A specified limit of 55°C on the final return water temperature

Generally, some limit on the final temperature of return water is necessary because it influences the choice of tube material in the condenser as well as the condenser's pressure rating. The associated infrastructure of the mine must handle this hot water and minimize leakage of heat into the mine as it is pumped to surface. Accordingly, the Kloof proposal limited the return water temperature to 55°C (Butterworth, 2001). This first set of simulations analysed how much chilling capacity might be achieved when an installation heated a flow of 160 kg/s of return water from 32°C to not higher than 55°C.

Single machine

Table 3.3 Guide to Kloof results

Reference	**Description**
Appendix B: Section 9.1.1	Spreadsheet result tables
Appendix A: Section 8.1.1	Trends and comparative plots

A single machine could cool 89.34 kg/s of water from 25°C to 10.5°C, thus delivering 5423.98 kW(R) of chilling, in Figure 8.6, while raising the return water temperature from 32°C to 42°C. The obtainable chilling, as measured by the return water utilization, was 33.90 kW(R)/(kg/s).

By Equation 2.9, the four water temperatures above gave a Lorenz COP of 15.08, defining the maximum theoretical performance under these conditions. But the constant evaporating and condensing refrigerant temperatures of 6.85°C and 46.35°C, in Figures 8.4 and 8.8, meant that the chiller's Carnot COP was 7.09, by Equation 2.4. Following the first assumption in Section 3.1.1, the COP was 60% of the Carnot COP, at 4.25. This value was only 28.2% of the Lorenz COP.

Two machines

Table 3.4 Guide to Kloof results

Reference	**Description**
Appendix B: Section 9.1.2	Spreadsheet result tables
Appendix A: Section 8.1.1	Trends and comparative plots

A second chiller was now added ahead of the single machine to create a series-counterflow pair, and the chilled water flowrate manually doubled[25]. By Equation E.1, this doubling of water flow rate was needed to double the total chilling load and keep each chiller delivering the specified maximum 5423.98 kW(R) in Figure 8.6.

Accordingly, the two chillers cooled 178.68 kg/s of water between the unchanged temperatures of 25°C and 10.5°C. The chillers could be operated at this maximum load because the final temperature of the return water, at 52.36°C, in Figure 8.11, was still below the specified maximum value of 55°C. For the unchanged flowrate of 160 kg/s and the doubled chilling load, the utilization of the return water also doubled to 67.8 kW(R)/(kg/s).

[25] Recalling the explanation in Section 2.3.5, each evaporator was presented with the full flowrate of chilled water.

The higher final return water temperature of 52.36°C changed the Lorenz COP, by Equation 2.9, to 11.93, the unique maximum theoretical performance for *these* conditions. The system COP was 3.89, or 32.6% of the Lorenz COP.

Following the first assumption in section 3.1.1 again, both the lag chiller COP, at 3.97, and the lead chiller COP, at 3.80, were 60% of their respective Carnot COP. Table 3.5 compares the COPs of this simulation with the previous single machine.

Table 3.5 COP comparison of 1 chiller with the lead-lag pair

	Chiller 2 (lead)	**Chiller 1 (lag)**	**Single chiller**
Carnot COP	6.34	6.62	7.09
COP	3.80	3.97	4.25
System COP	3.89		-
Evap. water heat load	5423.98	5423.98	5423.98

Both COPs fell below the single chiller COP, the lag by 6.63% and the lead by 10.58%, illustrated in Figure 8.14 These reductions were caused by the relative magnitudes of the new refrigerant temperatures adopted by each machine, in response to the series-counterflow arrangement.

By assumption 5 in Section 3.1.1, Chiller 2 reduced the cool water temperature by half, thus providing Chiller 1 with cooler evaporator water at 17.75°C. Chiller 1, constrained in the solution to deliver the 5423.98 kW(R) chilling load, now required a lower evaporator refrigerant temperature of 4.6°C to do so, seen in Figure 8.4.

The magnitude of this refrigerant temperature reduction is explained by observing firstly that the overall thermal conductance of the evaporator remained unchanged (by assumption 2 in section 3.1.1). Equation E.2 shows that the lag evaporator LMTD therefore *also* remained unchanged to allow delivery of the same chilling load as the single chiller. Equation E.3, being the general expression for $LMTD_E$, shows that for the 50% decrease in the numerator, the denominator also had to decrease by 50% to maintain the unchanged $LMTD_E$ at 9.04°C . This describes the necessary, non-linear reduction in the evaporator refrigerant temperature needed to maintain the original chilling load for the lower evaporator water inlet temperature of 17.75°C.

Following a logically similar argument, the lead chiller received cool water at 25°C, like the single chiller previously, but now delivered this water at 17.75°C, not 10.5°C. So, in contrast to the lag chiller, its evaporator refrigerant temperature showed a non-linear increase to 11.86°C, seen in Figure 8.4.

In *isolation*, this increase in evaporator refrigerant temperature would have increased the lead COP to a value above that of the single chiller. Yet because the condenser water circuits were connected in series, the lead chiller received warmer return water at 42.13°C from the lag machine, and so experienced an accompanying increase in its condenser refrigerant temperature, seen in Figure 8.8. Thus the COP, by Equation C.7, fell below that of the single machine to 3.80.

A higher mass flowrate of return water would cause a smaller rise in its temperature through the lag condenser, thus passing cooler return water to the lead condenser. This in turn would increase the sensitivity of the lead COP to changes in the evaporator refrigerant temperature. In this simulation, the return water flowrate would have had to be increased to 192 kg/s to allow the lead chiller COP to equal the lag chiller COP.

In summary, if a pair of identical chillers was connected in series-counterflow and the water chilling load doubled over a single chiller, the penalty of using the same return water flow of 160 kg/s was a decrease in the system COP.

Three machines

Table 3.6 Guide to Kloof results

Reference	**Description**
Appendix B: Section 9.1.3	Spreadsheet result tables
Appendix A: Section 8.1.1	Trends and comparative plots

A third chiller was now added ahead of the second machine, but the chilled water flowrate could not be tripled over one machine. If three chillers had each delivered the maximum chilling load, like the single chiller and each chiller in the preceding pair, then the final temperature of the return water would have been above the specified maximum allowed temperature of 55°C.

Table 3.7 Key performance quantities

	Chiller 3	**Chiller 2**	**Chiller 1**	**Unit**
Carnot COP	6.71	7.08	7.50	-
COP	4.03	4.25	4.50	-
System COP	4.25			-
Evap. water heat load	4157.88	4157.88	4157.88	kW(R)
Cond. water heat load	5190.48	5136.01	5081.68	kW(R)
Return water utilization	25.99	25.99	25.99	kW(R)/(kg/s)
Evap. outlet water temp.	20.17	15.33	10.50	°C
Cond. outlet water temp.	55.00	47.25	39.59	°C
Evap. refrigerant temp.	15.37	10.54	5.71	°C
Cond. refrigerant temp.	58.37	50.58	42.88	°C

To avoid exceeding this temperature, each chiller was regulated to deliver a 23% reduced chilling load of 4158 kW(R), in Figure 8.6, with an associated reduction in compressor absorbed power, in Figure 8.15, to ensure that the return water left the lead condenser at 55°C.

Thus, the three chillers could cool 205.46 kg/s of water from 25°C to 10.5°C, delivering a total of 12,473.63 kW(R) of chilling, in Figure 8.12, while raising the return water temperature from 32°C to 55°C. The obtainable chilling, as measured by the return water utilization, was 77.96 kW(R)/(kg/s).

This shows how a limit on the maximum allowed return water temperature prevented the full use of the available installed chiller capacity, because three chillers at full load would have achieved a return water utilization of 101.7 kW(R)/(kg/s).

By Equation E.2, with each chiller delivering a smaller chilling load, each evaporator LMTD also decreased by 23.3% to 6.93°C, in Figure 8.5. This allowed each chiller to have relatively higher evaporator refrigerant temperature than if it had delivered the full chilling load.
Thus, the COP of each chiller increased to a value similar to the single chiller, seen in Figure 8.14. Following the trend of two chillers, and for the same reasons, the lag chiller COP was slightly higher than the other chillers, the lead chiller COP again being lowest. The system COP was 37.5% of the Lorenz COP.

Four machines

Table 3.8 Guide to Kloof results

Reference	Description
Appendix B: Section 9.1.4	Spreadsheet result tables
Appendix A: Section 8.1.1	Trends and comparative plots

The addition of a fourth machine meant that the chilling load of each machine had to be reduced by a further 18% in Figure 8.6 to hold the leaving return water at 55°C. The COP of each machine increased again in Figure 8.14, due to the decreased evaporator LMTDs required to meet the lower individual chilling.

Table 3.9 Key performance quantities

	Chiller 4	Chiller 3	Chiller 2	Chiller 1	Unit
Carnot COP	7.30	7.63	8.00	8.40	-
COP	4.38	4.58	4.80	5.04	-
System COP	4.69				-
Evap. water heat load	3174.79	3174.79	3174.79	3174.79	kW(R)
Cond. water heat load	3899.60	3867.91	3836.30	3804.76	kW(R)
Return water utilization	19.84	19.84	19.84	19.84	kW(R)/(kg/s)
Evap. outlet water temp.	21.38	17.75	14.13	10.50	°C
Cond. outlet water temp.	55.00	49.18	43.41	37.68	°C
Evap. refrigerant temp.	17.69	14.07	10.44	6.82	°C
Cond. refrigerant temp.	57.53	51.69	45.89	40.15	°C

From Equation 2.9, the Lorenz COP remained the same as the previous simulation because of the unchanging final return water temperature. The system COP, at 4.69, achieved 41.4% of this Lorenz COP. This improvement over three machines occurred because each machine chilled more efficiently, as seen by its increased COP, for the *same* return water outlet temperature. The increased efficiency of chilling yielded an increase in the obtainable chilling, shown by the small 1.8% increase in return water utilization to 79.37 kW(R)/(kg/s).

3.2.4 Increased specified limit on the final return water temperature, to 70°C

The preceding simulations for three and four machines were now repeated for an increased return water temperature limit of 70°C.

Three machines

Table 3.10 Guide to Kloof results

Reference	**Description**
Appendix B: Section 9.1.5	Spreadsheet result tables
Appendix A: Section 8.1.2	Trends and comparative plots

Three chillers operating at full capacity remained well below the final return water temperature limit of 70°C, delivering only 63.29°C in Figure 8.29. Each delivered the same chilling load as the individual machines in Sections 9.1.1 and 9.1.2, giving a total of 16,271.94 kW(R), or three times the single machine load. Accordingly, the return water utilization of each chiller picked up to the single chiller's 33.90 kW(R)/(kg/s), with the total utilization three times larger at 101.7 kW(R)/(kg/s).

Table 3.11 Key performance quantities

	Chiller 3	**Chiller 2**	**Chiller 1**	**Unit**
Carnot COP	5.25	5.79	6.44	-
COP	3.15	3.47	3.87	-
System COP	3.47			-
Evap. water heat load	5423.98	5423.98	5423.98	kW(R)
Cond. water heat load	7146.71	6985.64	6826.85	kW(R)
Return water utilization	33.90	33.90	33.90	kW(R)/(kg/s)
Evap. outlet water temp.	20.17	15.33	10.50	°C
Cond. outlet water temp.	63.29	52.62	42.19	°C
Evap. refrigerant temp.	13.33	8.50	3.66	°C
Cond. refrigerant temp.	67.92	57.15	46.62	°C

Again, the lag machine COP was the highest of the three and each machine COP was lower than the values in Section 9.1.3, meaning that the lead machine consumed approximately 67% more power than its part-load counterpart in that simulation, and the lag machine 52% more. Though compared to a single chiller at full load, the lead consumed 35% more power, and the lag 10% more.

The system COP was 3.47, and 35.4% of the Lorenz COP for this return water outlet temperature. The total return water utilization of 101.7 kW(R) per kg/s of return water was 28% higher than four chillers regulated to final return water temperature of 55°C in Section 9.1.4, and 30.45% higher than the three chillers in Section 9.1.3.

Four machines

Table 3.12 Guide to Kloof results

Reference	**Description**
Appendix B: Section 9.1.6	Spreadsheet result tables
Appendix A: Section 8.1.2	Trends and comparative plots

When a fourth machine was added, the machines had to be simulated, once again, with reduced capacity, although now much less severely, to limit the final return water temperature to 70°C.

Each machine required a chilling load reduction of only 9%. Therefore the fourth machine was able to contribute markedly to the total obtainable chilling, increasing by 21% over the previous simulation. The return water utilization increased by 55% over the four machines regulated to 55°C.

Table 3.13 Key performance quantities

	Chiller 4	Chiller 3	Chiller 2	Chiller 1	Unit
Carnot COP	4.85	5.36	5.98	6.74	-
COP	2.91	3.21	3.59	4.04	-
System COP	3.39				-
Evap. water heat load	4913.29	4913.29	4913.29	4913.29	kW(R)
Cond. water heat load	6602.66	6441.78	6283.80	6128.71	kW(R)
Return water utilization	30.71	30.71	30.71	30.71	kW(R)/(kg/s)
Evap. outlet water temp.	21.38	17.75	14.13	10.50	°C
Cond. outlet water temp.	70.00	60.14	50.53	41.15	°C
Evap. refrigerant temp.	14.87	11.24	7.62	3.99	°C
Cond. refrigerant temp.	74.28	64.32	54.61	45.12	°C

In summary, if the return water was permitted to accept more rejected heat for a higher final temperature, the spreadsheet model indicated the potential for chillers to increase the total chilling load, and thus the total return water utilization, significantly, even for a restricted, unchanging return water flowrate.

3.2.5 Summary of simulations

With a single machine raising the return water temperature to only 42 ^{o}C, there remained significant scope to produce additional refrigerating load by using more machines. For this reason, the second machine at maximum refrigerating load was added. The natural emphasis was on increasing the system refrigerating load, and not on improving chilling efficiency because a large improvement in return water utilization was achieved easily by adding the second machine.

Adding the second machine doubled the chilled water flowrate, and thus the return water utilization also, exhibiting better use of the 160 kg/s flow. Yet, this increase in utilization was not achieved particularly efficiently

because the COPs of both machines decreased. The lag machine due to the need to maintain a lower evaporator refrigerant temperature to deliver its chilling load, and the lead machine due to magnitude of the restricted, unaltered return water flowrate of 160 kg/s. This means simply that in achieving a doubling of the system refrigerating load, and hence return water utilization, more power was consumed than if the machine COPs had not decreased.

The machine COP's may have been improved or at least maintained by increasing the return water flow through the series condensers - if the water was to become available - or by increasing the machine cycle efficiency to more than 60%, or increasing the heat exchanger overall thermal conductances, being the UA_E and UA_C terms.
Of course, throughout these simulations, the series arrangement of evaporator water circuits and the counterflow series arrangement of the condensers *did minimize the reduction* in COPs by minimizing the refrigerating lift required from each chiller[26].

The two machines at maximum chilling load heated the return water to 52.36°C, a little below the 55°C limit. Now, the only available option for obtaining more chilling was to add another chiller to the arrangement.

With the addition of the third machine, all three machine capacities had to be reduced by 23%, so as not to exceed the return water 55°C limit. Although this was an undesirable situation where the available chilling capacity was not used fully, the chilling *efficiency* did increase. Because of the heat exchangers being less than fully loaded, the evaporator and condenser LMTDs of all machines decreased, hence reducing the overall refrigerant temperature lifts and improving COPs. The system COP increased by 9.3% over 2 machines.

[26] Sections 2.2.3, 2.2.4 and 2.3.5 introduce the term *refrigerating lift*.

The main issues with adding this third machine were:

a) The unused machine capacity with each machine operating at 23% below maximum chilling load

b) Assumption 1 in section 3.1.1, which runs all machines at a constant 60% cycle efficiency, regardless of the manual reduction in chilling capacity or operating regime. Real machines do not operate with constant cycle efficiency, and this aspect is investigated in Chapter 4 with the CHILLER program.

The addition of the fourth machine, while enforcing the return water temperature limit of 55°C, required a further significant capacity reduction for each machine, making even poorer use of the total available capacity. However, the system COP increased by an additional 11.3% over two machines, again illustrating the principle of increased chilling efficiency.

The simulations thus far highlight several aspects of maximising refrigerating load.

a) For a given flowrate of return water, as many machines as possible may be turned on at full capacity until the maximum specified return water temperature is either closely approached, or reached.

b) If the maximum return water temperature is reached, and additional machines are available, additional chilling may be deliverable, but it requires that all machines are able to maintain cycle efficiency at moderate to severe part load. Otherwise, if the cycle efficiency falls off significantly, then the energy which heats the return water to 55°C will come from additional compressor input power, and not from additional chilling load.

Lastly, for a higher specified maximum return water temperature, three machines were able to run at maximum capacity, and four machines required capacity reduction of only 9%. The situation for 3 machines and a return water limit of 70°C is comparable to 2 machines with return water limit of 55°C, in that the primary goal is simply to use as many machines at maximum capacity as possible, for the given environmental constraints.

3.3 Tau Tona mine simulations

3.3.1 Operating regime

Tau Tona simulations used an operating regime from environmental constraints and criteria for a chilling installation at Tau Tona mine, summarized in Table 3.14.

Table 3.14 Environmental constraints and criteria for Tau Tona mine

Quantity	Value	Unit
Mass flowrate of return water	266	kg/s
Return water available temperature	32	°C
Cool water available temperature	18.89	°C
Chilled water deliver temperature	5.50	°C

3.3.2 Spreadsheet specification of full capacity for a single Tau Tona chiller

Chiller sizing

Table 3.15 presents the heat exchanger sizes. Derivations for these quantities are given in Appendix E, using the machine specifications in Appendix D. These values were constant for all Tau Tona chillers, following assumptions 2, 3 and 4 in Section 3.1.1.

Table 3.15 Chiller key specifications

Quantity	Value	Unit
Cycle efficiency	60	%
Evaporator overall thermal conductance	750.00	kW/°C
Condenser overall thermal conductance	800.00	kW/°C

Specification of single machine maximum chilling load

The CHILLER simulation of a lead lag pair (Appendix B: Section 9.2.6) for this operating regime heated the available 266 kg/s of return water to 42.40°C. Taking this value as a reference, the spreadsheet evaporator water flowrate was varied until the lead machine outlet temperature was similar, at 41.98°C. The accompanying calculated chilling load of 4,512 kW(R) per chiller was taken as the maximum chilling load that each Tau Tona chiller could provide in a multiple chiller simulation. The chillers in all Tau Tona simulations achieved this maximum chilling load, summarized by Category B in Table 10.1 in Appendix C.

At the outset, there were two major differences between the Tau Tona simulations and those for Kloof mine. Firstly the chiller size for each scenario is different: a Kloof machine had an approximately 20% larger chilling capacity than a Tau Tona machine.

Secondly, the Tau Tona flowrate of available return water was approximately 66% larger than Kloof, at an unchanged temperature t_{COOL}= 32°C. In summary, the smaller Tau Tona machines were provided with a significantly higher flowrate of heat removing water, but at the same initial temperature.

3.3.3 A specified limit of 55°C on the final return water temperature

The temperature limit applied in the Kloof simulations was again applied here, for the larger return water flowrate of 266 kg/s.

Two machines

Table 3.16 Guide to Tau Tona results

Reference	**Description**
Appendix B: Section 9.1.7	Spreadsheet result tables
Appendix A: Section 8.2.1	Trends and comparative plots

Table 3.17 Key performance quantities

	Chiller 2	**Chiller 1**	**Unit**
Carnot COP	7.47	6.96	-
COP	4.48	4.17	-
System COP	4.32		-
Evap. water heat load	4512.00	4512.00	kW(R)
Cond. water heat load	5519.07	5592.78	kW(R)
Return water utilization	16.96	16.96	kW(R)/(kg/s)
Evap. outlet water temp.	12.20	5.50	°C
Cond. outlet water temp.	41.98	37.02	°C
Evap. refrigerant temp.	8.92	2.22	°C
Cond. refrigerant temp.	46.69	41.80	°C

A lead-lag pair could deliver a chilled water flowrate of 160.96 kg/s and a water chilling load of 9024 kW(R) when heating the return water stream from 32°C to 42°C. Each machine once again delivered half the total chilling duty, following assumptions 5 and 6 in Section 3.1.1. In contrast to the Kloof simulation for two machines from section 3.2.3 (summarized in Appendix B: Section 9.1.2), the lead machine had a higher COP than the lag machine. This reversal in COP trend depended on the magnitude of the flowrate of return water, as explained in section 3.2.3.

Here, the flowrate of return water was large enough (in proportion to the total energy delivered into the water by the lag chiller) that its temperature increase by 5.02°C through the lag machine was significantly smaller than the previous increase by 10.13°C through the Kloof lag machine. This resulted in the lead condenser receiving return water at 37°C (Figure 8.46) instead of 42°C (Figure 8.10). Thus, the lead chiller compressor needed to provide the smaller refrigerant temperature lift of 37.77°C and the lag compressor the larger 39.58°C. In contrast, the Kloof lead compressor exhibited the larger lift of the two chillers, at 44.94°C, with the lag compressor smaller at 41.93°C.

The system COP was 4.32, again 60% of the Carnot COP as shown by the cycle efficiency term, and 37.6% of the Lorenz COP for this operating regime. The obtainable chilling of each machine gave a total return water utilization of 33.92 kW(R) per kg/s of return water.

Four machines, all in series-counterflow

Table 3.18 Guide to Tau Tona results

Reference	**Description**
Appendix B: Section 9.1.8	Spreadsheet result tables
Appendix A: Section 8.2.1	Trends and comparative plots

With the addition of two more chillers, the evaporator water flowrate of the previous simulation pair was doubled manually. Decreasing in response, the lag evaporator refrigerant temperature encountered the general 1°C limit[27], with all machines operating at full capacity.

[27] Following assumption 8 in Section 3.1.1

Table 3.19 Key performance quantities

	Chiller 4	Chiller 3	Chiller 2	Chiller 1	Unit
Carnot COP	6.14	6.32	6.51	6.71	-
COP	3.69	3.79	3.91	4.03	-
System COP	3.85				-
Evap. water heat load	4512.00	4512.00	4512.00	4512.00	kW(R)
Cond. water heat load	5736.37	5701.90	5667.43	5632.98	kW(R)
Return water utilization	16.96	16.96	16.96	16.96	kW(R)/(kg/s)
Evap. outlet water temp.	15.54	12.20	8.85	5.50	°C
Cond. outlet water temp.	52.42	47.27	42.15	37.06	°C
Evap. refrigerant temp.	11.05	7.70	4.35	1.00	°C
Cond. refrigerant temp.	57.32	52.14	46.99	41.87	°C

This arrangement could chill 321.92 kg/s of water from 18.89°C to 5.5°C, thus delivering 18,048 kW(R) of chilling while raising the return water temperature from 32°C to 52.42°C. The obtainable chilling, as measured by the return water utilization, was 67.85 kW(R)/(kg/s).

After having reversed in the previous simulation, the trend of the lag machine having the highest COP and decreasing sequentially toward the lead was now re-established. In the previous simulation, the second chiller received cool water at 18.89°C because it held the lead position. However, as a third and fourth machine were added upstream, Figure 8.37 shows that the second chiller's evaporator inlet water temperature decreased rapidly, although in successively smaller steps. Indeed, this occurred for all chillers downstream of each additional lead machine. Only the chiller added in the lead position saw an increase in evaporator water *outlet* temperature, observed by tracking the lead position in Figure 8.38. The corresponding evaporator refrigerant temperatures are plotted in Figure 8.40, and exhibit similar changes.

So, although the return water flowrate was relatively large for Tau Tona, leading to small water temperature increases through the condensers with accompanying small incremental increases in condenser refrigerant temperature for successive machines, the present simulation of four machines showed the lead compressor once again delivering the largest refrigerant temperature lift, decreasing sequentially towards the lag chiller. The change back to this trend is shown to occur for three chillers in Figures 8.49 and 8.50, where the COPs are nearly equal.

3.3.4 Increased specified limit on the final return water temperature, to 70°C

Six machines

Table 3.20 Guide to Tau Tona results

Reference	**Description**
Appendix B: Section 9.1.9	Spreadsheet result tables
Appendix A: Section 8.2.1	Trends and comparative plots

To bypass the problem of the 1°C refrigerant temperature lower limit, a pair of machines with evaporators in parallel was added to the previous four machine arrangement. This arrangement, shown in figure 3.1, performed the chilled water temperature reduction in five steps.

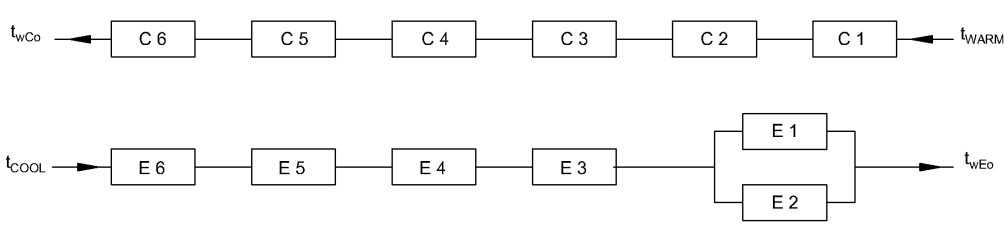

Figure 3.1 Six machine series-counterflow arrangement with parallel lag evaporator pair

Table 3.21 Key performance quantities

	Chill. 6	Chill. 5	Chill. 4	Chill. 3	Chill. 2	Chill. 1	Unit
Carnot COP	5.01	5.27	5.55	5.87	6.01	6.80	-
COP	3.01	3.16	3.33	3.52	3.61	4.08	-
Evap. w. heat load	4512.00	4512.00	4512.00	4512.00	4512.00	4512.00	kW(R)
Cond. w. heat load	6013.36	5939.24	5865.74	5792.87	5763.59	5618.47	kW(R)
Ret. w. utilization	16.96	16.96	16.96	16.96	16.96	16.96	kW(R)/(kg/s)
Evap. outlet water temp.	16.66	14.43	12.20	9.96	5.50	5.50	°C
Cond. outlet water temp.	63.42	58.02	52.69	47.42	42.22	37.04	°C
Evap. refrigerant temp.	11.69	9.46	7.23	4.99	1.44	1.44	°C
Cond. refrigerant temp.	68.56	63.09	57.70	52.37	47.14	41.84	°C

The dual lag machines both received half the total water flowrate, at temperature 9.96°C, and performed the final temperature reduction to 5.5°C. This final temperature reduction by machines 1 and 2 in the lag evaporator pair was twice that of each of the preceding four machines, resulting in all six machines delivering the same chilling load.

The lag evaporator pair received cool water at a higher temperature than the fourth machine in the previous simulation, thus each machine in this pair was able to meet the chilling load while maintaining its refrigerant temperature at 1.44°C, tabled in Section 9.1.9, Appendix B. Chiller 1 received return water at 32°C and chiller 2 at 37°C because the condensers were still arranged in series so that all machines received the specified flowrate of return water. For this reason, chiller 1 operated with a slightly higher COP than chiller 2.

The significance of this simulation is that the parallel arrangement of the first two evaporators allowed two extra machines, still at full load, to be added to the previous four chiller group. Here, the minimum allowable evaporator refrigerant temperature, instead of the specified maximum return water temperature, had limited the obtainable chilling.

3.3.5 Summary of simulations

The Tau Tona machines operated with two main advantages over the Kloof scenario:

a) A Tau Tona machine had a larger evaporator than a Kloof chiller, modelled by the 25% larger evaporator overall thermal conductance

b) The return water flowrate of 260 kg/s was 66% larger than the return water flow available to the Kloof machines.

The Tau Tona machines never required capacity reduction because the higher return water flowrate ensured that none of the simulations reached the 55°C limit other than six chillers under the increased limit of 70°C.

Table 3.22 Comparison of Kloof and Tau Tona spreadsheet model simulations

Mine	Number of Chillers	Capacity reduction at part load (%)	Return water flowrate (kg/s)	Specified upper temperature limit of return water (°C)	Lorenz COP	Combined chiller COP	Water chilling load kW(R)	Appendix B reference section
Kloof	1	0.0	160	55	15.08	4.25	5424	9.1.1
Kloof	2	0.0	160	55	11.93	3.89	10848	9.1.2
Kloof	3	23.3	160	55	11.33	4.25	12474	9.1.3
Kloof	3	0.0	160	70	9.79	3.47	16272	9.1.5
Kloof	4	41.5	160	55	11.33	4.69	12699	9.1.4
Kloof	4	9.4	160	70	8.83	3.39	19653	9.1.6
Tau Tona	2	0.0	266	55	11.49	4.32	9024	9.1.7
Tau Tona	4	0.0	266	55	9.52	3.85	18048	9.1.8
Tau Tona	6	0.0	266	70	8.08	3.42	27072	9.1.9

Table 3.22 highlights the advantage of a higher return water flowrate: For almost identical corresponding system and Lorenz COP's, six Tau Tona machines at full load delivered 38% more chilling load than four Kloof machines with 9.4% load reduction.

Of course, in delivering this higher chilling load, the Tau Tona machines consumed 36.5% more power, but individual machine power consumption was similar to the Kloof machines.

With large capacity reduction to limit the return water temperature to 55°C, Kloof simulations of 3 and 4 machines also showed higher values of system COP and Lorenz COP. However, in achieving these better values through decreasing the LMTDs, as explained in section 3.2.3, the heat exchangers were less than fully loaded meaning that the total installed capacity was not fully utilized. In contrast, the Tau Tona simulation of 2 machines shows similar COP values with the machines at full capacity, making full use of installed capacity.

4 CHILLER PROGRAM SIMULATIONS

4.1 Introduction

4.1.1 The CHILLER computer program version 1.01

The CHILLER computer program was developed by the Chamber of Mines of South Africa for the South African mining industry (Bailey-McEwan and Penman, 1987).

Appendix F describes how CHILLER, as well as using detailed models for the individual components of chillers, models the two-stage centrifugal compressors more fundamentally than the spreadsheet model.

4.1.2 Key aspects of more realistic modelling in the CHILLER program

1 a. In the CHILLER computer program, cycle efficiency is not pre-specified and is calculated from first principles. So, unlike the spreadsheet model, which uses a lumped constant cycle efficiency, a machine in the CHILLER program is not infinitely flexible. This means that it does not maintain constant cycle efficiency for all operating regimes. In fact, the cycle efficiency is dependent on the compressor stage operating points and conditions in the heat exchangers, affecting the evaporator and condenser refrigerant temperatures.

1 b. Because of these factors, the cycle efficiency thus varies for each chiller in a multiple arrangement,.

1 c. Although the spreadsheet model does not assign an explicit value to compressor stage isentropic efficiency, accounting for it within constant cycle efficiency term, it is constant. In CHILLER, this constraint is removed: As part of calculating the cycle efficiency, the isentropic efficiency of a compressor stage is dependent on its operating point.

2. Each evaporator still has a fixed heat transfer area, but varying water- and refrigerant-side heat transfer coefficients with variable, specifiable water-side fouling factors.

3. Each condenser still has a fixed heat transfer area, but varying water- and refrigerant-side heat transfer coefficients with variable, specifiable water-side fouling factors.

4. All evaporators in a multiple machine arrangement had the same heat transfer area. All condensers also had the same heat transfer area. However following from assumptions 2 and 3 here, in contrast to the spreadsheet models, the heat transfer coefficients were variable.

5. Chillers in a multiple arrangement thus performed unequal reductions in evaporator water stream temperature.

6. Hence, although the chilled water flowrate was equal for all evaporators, the evaporator water chilling loads were not equal for all chillers.

7. Refrigerant temperature was uniform in any single evaporator or condenser.

8. The CHILLER simulations followed the same 1°C water temperature limit as the spreadsheet models.

With reference to the compressor operating characteristics in section 2.2.3, the CHILLER program allows the vanes to be set in the range 0° (fully open) to −80° (−90° being the fully closed position). Although the CHILLER program is able to model prerotation vanes on both stages of a two-stage centrifugal compressor, the centrifugal compressors modelled in this study have capacity control on the *first stage only*. The second stage is unregulated.

4.2 Kloof mine simulations

4.2.1 A specified limit of 55°C on the final return water temperature

Single machine

Table 4.1 Guide to Kloof results

Reference	**Description**
Appendix B: Section 9.2.1	CHILLER result tables
Appendix A: Section 8.1.1	Trends and comparative plots

A single machine at full load[28] could cool 84.50 kg/s of water from 25°C to 10.5°C, thus delivering 5131.1 kW(R) of chilling, in Figure 8.6, while raising the return water temperature from 32°C to 42.28°C. The obtainable chilling, as measured by the return water utilization, was 32.07 kW(R)/(kg/s).

[28] Having the stage 1 compressor vanes set to 0°

Table 4.2 Key performance quantities

	Chiller 1	**Unit**
Carnot COP	7.06	-
COP	2.92	-
System COP	2.92	-
Evap. water heat load	5131.1	kW(R)
Cond. water heat load	6886.1	kW(R)
Return water utilization	32.07	kW(R)/(kg/s)
Evap. outlet water temp.	10.50	°C
Cond. outlet water temp.	42.28	°C
Evap. refrigerant temp.	7.34	°C
Cond. refrigerant temp.	47.07	°C
Compr. stage 1 efficiency	55.49	%
Compr. stage 2 efficiency	41.37	%

By Equation 2.9, the four water temperatures above gave a Lorenz COP of 14.97 defining the maximum theoretical performance under these conditions. But the constant evaporating and condensing refrigerant temperatures of 7.34°C and 47.07°C, in Figures 8.4 and 8.8, meant that the chiller's Carnot COP was 7.06, by Equation 2.4. The COP was only 41% of the Carnot COP, at 2.92. This value was only 19.5% of the Lorenz COP.

The isentropic efficiencies of the stage 1 and stage 2 compressors, at 55.49% and 41.37% respectively, were low compared to the design values of 72.5% listed in Tables 11.3 and 11.4, because with inlet volumetric flowrate of 1.79 m^3/s and developed isentropic head 11.00 kJ/kg, the stage 1 compressor operated to the right of its design point on the compressor operating curve. The stage 2 efficiency was low for similar reasons.

Two machines

Table 4.3 Guide to Kloof results

Reference	Description
Appendix B: Section 9.2.2	CHILLER result tables
Appendix A: Section 8.1.1	Trends and comparative plots

In this simulation, a lead lag pair at full load chilled 169.70 kg/s of water, approximately double that of a single machine, from 25°C to 10.5°C, delivering 10,302.2 kW(R) of chilling, in Figure 8.6, while raising the return water temperature from 32°C to 52.50°C. The obtainable chilling, as measured by the total return water utilization, was 64.39 kW(R)/(kg/s).

Table 4.4 Key performance quantities

	Chiller 2	Chiller 1	Unit
Carnot COP	6.24	6.84	-
COP	2.97	3.03	-
System COP	3.00		-
Evap. water heat load	5472.1	4830.1	kW(R)
Cond. water heat load	7312.3	6421.9	kW(R)
Return water utilization	34.20	30.19	kW(R)/(kg/s)
Evap. outlet water temp.	17.30	10.50	°C
Cond. outlet water temp.	52.50	41.59	°C
Evap. refrigerant temp.	11.81	5.31	°C
Cond. refrigerant temp.	57.48	46.01	°C
Compr. stage 1 efficiency	62.08	57.39	%
Compr. stage 2 efficiency	51.64	45.76	%

The previous single chiller simulation used an evaporator model with four water passes, following the original configuration of the real machines (Appendix D: Table 11.1), which resulted in a tube water velocity of 2.30 m/s for that chilled water flowrate.

Here, when adding the second machine, both evaporators were converted to two pass to control the increase in tube water velocity. The resulting velocity was practically identical, at 2.31 m/s because the pair cooled twice the water flowrate of the single machine.

Thus, it was the higher evaporator water inlet and outlet temperatures of the lead machine that gave it a 8.2% lower water thermal resistance (Table 9.76) than the lag machine. The higher heat flux through the lead evaporator tubes also resulted in an 8.4% lower refrigerant thermal resistance (again, in Table 9.76). In combination, these effects caused the lead evaporator overall thermal conductance to be 4.7% larger than the lag evaporator (Appendix A: Figure 8.3).

The resulting higher refrigerant vapour pressure and correspondingly lower specific volume (Equation 2.1) of refrigerant vapour caused a 18.7% larger mass flowrate of refrigerant through the lead first stage compressor, giving a chilling load 13.3% larger than the lag chiller (Appendix A: Figure 8.6). Once again, this observation corresponds to the ASHRAE Refrigeration Handbook (2002, p. 43.2) that for identical chillers, the lead machine develops more capacity than the lag.

In delivering this larger chilling load, the lead compressor also consumed 15.6% more power (Appendix A: Figure 8.15). The difference in Carnot COP between the machines was 9.6% (Appendix A: Figure 8.13), with the lead chiller having the slightly lower value. However, its COP was only 2% less than the lag COP (Appendix A: Figure 8.14) because of slightly higher isentropic efficiencies in its first and second compressor stages (Appendix A: Figures 8.16 and 8.17).

The system COP improved slightly over the single machine from 2.92 to 3.0, on the basis of higher isentropic efficiencies for both compressor stages in the lead and lag machine.

Three machines

Table 4.5 Guide to Kloof results

Reference	Description
Appendix B: Section 9.2.3	CHILLER result tables
Appendix A: Section 8.1.1	Trends and comparative plots

This simulation of three real machines required closure of -37.5°, or nearly 47%, on the first stage compressor[29] of each machine to remain within the 55°C limit.

Table 4.6 Key performance quantities

	Chiller 3	Chiller 2	Chiller 1	Unit
Carnot COP	6.66	7.18	7.76	-
COP	2.90	2.95	2.96	-
System COP	2.93			-
Evap. water heat load	4112.2	3829.6	3549.4	kW(R)
Cond. water heat load	5531.3	5128.0	4749.4	kW(R)
Return water utilization	25.70	23.94	22.18	kW(R)/(kg/s)
Evap. outlet water temp.	19.81	14.98	10.50	°C
Cond. outlet water temp.	55.00	46.75	39.09	°C
Evap. refrigerant temp.	15.26	10.56	6.22	°C
Cond. refrigerant temp.	58.57	50.10	42.24	°C
Compr. stage 1 efficiency	37.29	32.41	28.46	%
Compr. stage 2 efficiency	72.37	72.49	69.95	%

For each of the three chillers, the vane closure resulted in a reduction in chiller load and power consumption. In Figure 8.18, the cycle efficiencies decreased slightly from the two machines operating at full capacity. The system COP decreased slightly by 2.3% to 2.93, achieving 25.9% of the Lorenz COP for the final return water temperature of 55°C.

[29] As described in Section 2.2.3 under Capacity Control, the chiller models in this study have inlet prerotation guide vanes on the first compressor stage only.

The return water utilization showed an 11.5% increase to 71.82 kW(R)(kg/s). However, it must be remembered that this was accompanied by an average 25% capacity reduction *per machine*, in conforming to the 55°C limit. Similarly to the corresponding spreadsheet simulation in Section 9.3, this was an undesirable situation where the available chilling capacity was not used fully.

In contrast to the spreadsheet simulation in Section 9.1.3 however, the chillers here additionally suffered from low COPs and thus low cycle efficiencies, mainly due to the extremely poor stage 1 compressor isentropic efficiencies for all three machines in Table 9.86, listed as 37%, 32% and 28% respectively. So, unlike the spreadsheet machines, the *real* machine COPs were predicted to decrease, indicating that the chilling load was being delivered less efficiently. Four machines were not simulated in the CHILLER program for this temperature limit because the three machine performance was already poor.

4.2.2 Increased specified limit on the final return water temperature, to 70°C

Three machines

Table 4.7 Guide to Kloof results

Reference	**Description**
Appendix B: Section 9.2.4	CHILLER result tables
Appendix A: Section 8.1.2	Trends and comparative plots

The simulation for three machines was repeated, now with the machines at full capacity, for the higher return water temperature limit of 70°C.

Table 4.8 Key performance quantities

	Chiller 3	Chiller 2	Chiller 1	Unit
Carnot COP	5.46	6.06	6.81	-
COP	3.06	3.10	3.05	-
System COP	3.07			-
Evap. water heat load	5342.4	5098.4	4791.5	kW(R)
Cond. water heat load	7088.5	6743.0	6361.4	kW(R)
Return water utilization	33.39	31.87	29.94	kW(R)/(kg/s)
Evap. outlet water temp.	19.91	15.06	10.50	°C
Cond. outlet water temp.	62.14	51.56	41.50	°C
Evap. refrigerant temp.	14.19	9.44	5.04	°C
Cond. refrigerant temp.	66.82	56.10	45.87	°C
Compr. stage 1 efficiency	70.97	64.44	57.66	%
Compr. stage 2 efficiency	66.14	56.96	46.37	%

The lead machine delivered 11.5% more chilling duty than the lag machine, once again due to higher evaporator pressure with corresponding lower specific volume of refrigerant vapour at the stage 1 compressor inlet.

The energy removed from the chilled water along with the compressor absorbed power heated the return water from 32 °C to 62.14°C, chilling 250.93 kg/s, or almost triple the flowrate for one machine in Section 9.2.1, to yield 15,231.3 kW(R) with a total return water utilization of 95.20 kW(R)/(kg/s).

Because, as before, the lag machine had to chill its water to the specified delivery temperature of 10.5°C, the chilled water flowrate was less than three times that of one machine, corresponding to slightly less than three times the chilling load, due to the refrigerant properties at the temperature and pressure conditions in each evaporator. Referenced to the single machine in Section 9.2.1, higher temperatures and pressures in the lead and mid evaporators resulted in refrigerating effects that were 6.8% and 2.7% lower respectively.

The lag machine exhibited an approximately 1% higher refrigerating effect due to its evaporator temperature and pressure being lower than the single chiller. The higher refrigerant mass flowrates in the lead and mid chiller compressors did not fully compensate for these decreases, and the small increase in the lag chiller was nullified by the lower mass flowrate, thus yielding slightly less than triple the total chilling load of the single chiller earlier.

Four machines

Table 4.9 Guide to Kloof results

Reference	**Description**
Appendix B: Section 9.2.5	CHILLER result tables
Appendix A: Section 8.1.2	Trends and comparative plots

Four machines operating at full capacity achieved the 70 °C limit.

Table 4.10 Key performance quantities

	Chiller 4	**Chiller 3**	**Chiller 2**	**Chiller 1**	**Unit**
Carnot COP	5.00	5.37	5.98	6.80	-
COP	2.84	3.15	3.16	3.06	-
System COP	3.05				-
Evap. water heat load	4589.3	4984.2	4939.8	4773.2	kW(R)
Cond. water heat load	6207.2	6568.9	6505.5	6335.0	kW(R)
Return water utilization	28.68	31.15	30.87	29.83	kW(R)/(kg/s)
Evap. outlet water temp.	21.55	17.80	14.09	10.50	°C
Cond. outlet water temp.	70.24	60.97	51.17	41.46	°C
Evap. refrigerant temp.	16.28	12.16	8.43	4.92	°C
Cond. refrigerant temp.	74.17	65.26	55.52	45.81	°C
Compr. stg. 1 efficiency	71.27	72.26	65.52	57.78	%
Compr. stg. 2 efficiency	71.96	70.10	59.36	46.65	%

Adding a fourth machine increased the chilling duty to 19,286.5 kW(R), thereby increasing the return water utilization by 25 kW(R)/(kg/s), or 21%, over three machines. The lag machine chilling load deteriorated slightly from the previous value because although the overall thermal conductance of the evaporator improved due to the higher water flow rate, the decrease in cool water entry temperature lowered the evaporator pressure resulting in a slightly lower refrigerant vapour mass flowrate. The intermediate machines delivered chilling loads within 5% of the second machine in Section 9.2.4. However, the lead machine load deteriorated by 14%. Although its overall thermal conductance in the evaporator was similar to the previous lead chiller, the machine operated with a high condenser pressure due to the elevated condenser water temperature. A comparison of the lead chiller stage 1 compressor mass flowrate (between Tables 9.94 and 9.102) shows a decrease of 11.7%.

4.3 Tau Tona mine simulations

As for the spreadsheet simulations, the Tau Tona simulations used a return water flowrate 66% larger than the Kloof simulations, at the same available temperature of 32 °C.

4.3.1 A specified limit of 55°C on the final return water temperature

Tau Tona mine, from which the simulation conditions were derived, used machines connected in lead-lag pairs. The first simulation, therefore, modelled two machines.

Two machines

Table 4.11 Guide to Tau Tona results

Reference	**Description**
Appendix B: Section 9.2.6	CHILLER result tables
Appendix A: Section 8.2.1	Trends and comparative plots

Table 4.12 Key performance quantities

	Chiller 2	**Chiller 1**	**Unit**
Carnot COP	7.31	7.22	-
COP	3.06	3.25	-
System COP	3.14		-
Evap. water heat load	4740.7	4045.9	kW(R)
Cond. water heat load	6292.2	5289.8	kW(R)
Return water utilization	17.82	15.21	kW(R)/(kg/s)
Evap. outlet water temp.	11.66	5.50	°C
Cond. outlet water temp.	42.40	36.75	°C
Evap. refrigerant temp.	8.73	2.67	°C
Cond. refrigerant temp.	47.31	40.85	°C
Compr. stage 1 efficiency	50.40	51.11	%
Compr. stage 2 efficiency	48.34	52.48	%

In this simulation, a pair of series-counterflow machines running at full capacity chilled 156.71 kg/s of water to from 18.89°C to 5.5°C, producing 8,786.6 kW(R) and achieving a combined return water utilization of 33.03 kW(R)/(kg/s).

The higher evaporator water inlet and outlet temperatures of the lead machine gave it a 8.9% larger water side heat transfer coefficient (Equation F.6) than the lag machine[30].

[30] Seen differently, the smaller water side heat transfer coefficient in the lag machine caused it to have an 8.9% larger water side thermal resistance (Appendix F: First term on the right-hand side in Equation F.5) than the lead machine.

The higher heat flux through the lead evaporator tubes also resulted in an 11.7% larger coefficient of heat transfer to the evaporating refrigerant (Equation F.9). In combination, these effects caused the lead evaporator overall thermal conductance to be 7.2% larger than the lag evaporator (Appendix A: Figure 8.39).

The resulting higher refrigerant vapour pressure and correspondingly lower specific volume (Equation 2.1) of refrigerant vapour caused a 20.3% larger mass flowrate of refrigerant through the lead first stage compressor, giving a chilling load 17.2% larger than the lag chiller[31] (Appendix A: Figure 8.42). Once again, this observation corresponds to the statement in the ASHRAE Refrigeration Handbook (p. 43.2, 2002) that for identical chillers, the lead machine develops more capacity than the lag.

In delivering this larger chilling load, the lead compressor also consumed 24.7% more power (Appendix A: Figure 8.51). The difference in Carnot COP between the machines was less than 2% (Appendix A: Figure 8.49), with the lead chiller having the slightly higher value. However, its COP was only 94.2% of the lag COP (Appendix A: Figure 8.50) because of slightly lower isentropic efficiencies in its first and second compressor stages (Appendix A: Figures 8.52 and 8.53).

For the four external water circuit temperatures (refer to section 2.3.6) specific to this simulation, the Lorenz COP (Equation 2.9) was 11.4 but the system COP, at 3.14, was only 27.5% of this value.

[31] Although the mass flowrate of refrigerant was 20.3% larger in the lead compressor, the increase in chilling load over the lag machine was only 17.2% because the magnitude of the refrigerating effect term (h_1-h_8) in Equation 2.1 decreased. So the smaller magnitude of (h_1-h_8) at higher pressure in the lead evaporator partially offset the increase in refrigerant mass flowrate.

Three machines

Table 4.13 Guide to Tau Tona results

Reference	Description
Appendix B: Section 9.2.7	CHILLER result tables
Appendix A: Section 8.2.1	Trends and comparative plots

In this simulation, three series-counterflow machines running at full capacity chilled 226.2 kg/s of water to from 18.89°C to 5.5°C, producing 12,679.6 kW(R) and achieving a 44.3% higher combined return water utilization, over the previous lead lad pair, of 47.67 kW(R)/(kg/s).

Table 4.14 Key performance quantities

	Chiller 3	Chiller 2	Chiller 1	Unit
Carnot COP	6.65	6.82	6.97	-
COP	3.17	3.27	3.36	-
System COP	3.26			-
Evap. water heat load	4647.1	4207.6	3824.9	kW(R)
Cond. water heat load	6114.0	5493.4	4963.0	kW(R)
Return water utilization	17.47	15.82	14.38	kW(R)/(kg/s)
Evap. outlet water temp.	13.98	6.54	5.50	°C
Cond. outlet water temp.	46.88	41.39	36.46	°C
Evap. refrigerant temp.	9.14	4.86	0.97	°C
Cond. refrigerant temp.	51.58	45.61	40.28	°C
Compr. stage 1 efficiency	57.30	55.30	53.67	%
Compr. stage 2 efficiency	56.01	56.36	56.61	%

Gosney (1982, p. 86) explains that the objective of using several passes in a heat exchanger is to increase the velocity of the water in the tubes for the same total quantity of water, and thereby to improve the water side heat transfer coefficient.

The previous simulation used an evaporator model with three water passes, following the original configuration of the real machines (Appendix D: Table 11.5), which resulted in a tube water velocity of 2.9 m/s for that chilled water flowrate.

Here, when adding the third machine, all evaporators were converted to a single pass to minimize the increase in tube water velocity. The resulting velocity was lower, at 1.39 m/s, but still sufficient to maintain turbulent flow in the heat exchanger tubes.

Primarily[32] due to this reduction in velocity, the lead[33] evaporator water side heat transfer coefficient decreased to 56.5% of the previous value[34], resulting in a reduction of 18.6% in overall thermal conductance. The lead chilling load showed a related decrease, although only by 2% because the LMTD increased by 20.4% for the lead compressor's new operating point. The increase in lead evaporator LMTD decreased the efficiency of heat transfer in the evaporator, but this detrimental effect on cycle efficiency was offset by improvements in isentropic efficiency of 13.7% and 15.9% in the first and second compressor stages respectively (Appendix A: Figures 8.52 and 8.53), resulting in modest gains in COP and cycle efficiency of 3.6% and 14.3% (Figures 8.50 and 8.54).
Still, both lead compressor stages performed significantly below their design values of isentropic efficiency (Appendix D: Tables 11.7 and 11.8) because their refrigerant volumetric flowrates were above the design values.

---

[32] The decrease in water side heat transfer coefficient would have been slightly larger, except that the lead machine now chilled water from 18.89°C to 13.98°C, instead of 11.66°C previously, due to the higher water flowrate. This fact increased the term $[t_{(w)i} + t_{(w)o}]$ in Equation F.6 by 7.6%, slightly offsetting the decrease due to the lower water velocity.

[33] chiller 3

[34] For chiller 2, in the preceding simulation of two machines.

The second chiller, previously the lead machine, now occupied the mid position. Its evaporator too showed a large decrease in water side heat transfer coefficient to 53.3% of the previous value. Like the new lead chiller just described, this was caused by the lower water velocity after conversion to a single water pass but now additionally because it received and delivered water at lower temperatures[35] (Appendix A: Figures 8.37 and 8.38) due to its positioning after the lead chiller . An expected decrease in chilling load, at 11.2%, followed. In its new mid position, this chiller also showed increases in its first and second stage compressor isentropic efficiencies of 9.7% and 16.6% respectively, due to an increase in the overall refrigerant temperature lift[36] and small decreases in refrigerant inlet volumetric flowrate for both stages, bringing the stages closer to design isentropic efficiency.

Instead of receiving water at 11.66°C as before, the lag evaporator now cooled water from 9.54°C to the same final 5.5°C. Following the trend of the mid evaporator, and for the same reasons, its chilling load decreased by 5.5%, with small increases of 5% and 7.9% in isentropic efficiency for the first and second compressor stages. At 0.97°C, the refrigerant temperature (Appendix A: Figure 8.40) had reached the lower 1°C limit (refer to assumption 7 in Section 3.1.1).

As noted at the beginning of this subsection, the total return water utilization did improve by 44.3% from the previous simulation because of the addition of the third machine, but no single machine achieved a better utilization than either of the machines in the previous lead lag pair, and the *average* utilization per machine dropped 3.8% to 15.89 kW(R)/(kg/s).

---

[35] Here decreasing the term $[t_{(w)I} + t_{(w)O}]$ in Equation F.6 by 23%

[36] A 3.4% decrease in condenser refrigerant temperature from 47.31°C to 45.61°C, and a larger 44.3% decrease in evaporator refrigerant temperature from 8.73°C to 4.86°C demonstrate the larger refrigerant lift provided by the compressor.

Four machines

Table 4.15 Guide to Tau Tona results

Reference	Description
Appendix B: Section 9.2.8	CHILLER result tables
Appendix A: Section 8.2.1	Trends and comparative plots

In this simulation, four series-counterflow machines running at full capacity chilled 226.2 kg/s of water to from 18.89°C to 5.5°C, producing 16,946.5 kW(R) and achieving a 33.7% higher combined return water utilization, over the previous three-chiller installation, of 63.71 kW(R)/(kg/s).

Table 4.16 Key performance quantities

	Chiller 4	Chiller 3	Chiller 2	Chiller 1	Unit
Carnot COP	6.17	6.43	6.71	6.99	-
COP	3.22	3.28	3.33	3.35	-
System COP	3.29				-
Evap. water heat load	4653.1	4363.4	4091.4	3838.6	kW(R)
Cond. water heat load	6098.6	5692.7	5321.5	4983.2	kW(R)
Return water utilization	17.49	16.40	15.38	14.43	kW(R)/(kg/s)
Evap. outlet water temp.	15.21	11.77	8.53	5.50	°C
Cond. outlet water temp.	51.84	46.36	41.25	36.47	°C
Evap. refrigerant temp.	10.48	7.14	4.01	1.08	°C
Cond. refrigerant temp.	56.47	50.70	45.33	40.31	°C
Compr. stg. 1 efficiency	63.95	60.13	56.66	53.50	%
Compr. stg. 2 efficiency	62.22	60.43	58.45	56.34	%

Each new chiller (always added in the lead position) received water for cooling at 18.89°C, as shown in Figure 8.37. Figure 8.38, however, shows that the water stream exited the lead evaporator at progressively higher temperature for every additional chiller added, as the mass flowrate of cool

water was increased[37], thus raising the mean temperature of the water stream in the lead evaporator. Results in Figure 8.40 from the spreadsheet model show that this trend alone[38] was responsible for the basic *increasing* trend in the lead evaporator refrigerant temperature.

Figures 8.37 and 8.38 show that the addition of each extra chiller as lead machine also served to decrease both the inlet and outlet water temperature of the evaporators connected downstream of it, lowering the mean temperature of the water stream in each one.

Once again, the refrigerant temperature trend results in Figure 8.40 from the spreadsheet model give clear indication that this lowering of the evaporator mean water temperatures drove the trend of decreasing refrigerant temperature in the downstream evaporators.

In contrast to the generally decreasing evaporator refrigerant trends, Figure 8.40 shows that the addition of a fourth machine in the lead position caused the *lag* evaporator refrigerant temperature to *increase* from 0.97°C to 1.08°C. Another increase to 1.15°C occurred in the lag evaporator when a fifth machine was added in the lead position. The explanation for this trend begins by observing that the lag chiller always delivered water at 5.5°C[32] and thus was subjected to the smallest incremental decreases in mean evaporator water temperature of all the downstream chillers. So, as the fourth and then fifth lead chiller was added, and the cool water flowrate made larger to suit, the lag chiller exhibited the smallest decreases in the term $[t_{(w)I} + t_{(w)o}]$ in Equation F.6, and thus the largest percentage increase

[37] As presented earlier, the mass flowrate of cool water was increased with every additional chiller to keep the evaporators fully loaded. The magnitude of each increase was adjusted to maintain the final desired chilled water delivery temperature at 5.5°C.

[38] From assumption 1 in Section 3.1.1, every spreadsheet evaporator operated with a constant evaporator overall thermal conductance. This assumption isolated the evaporator refrigerant temperature trend from the influences of increased water flowrate and changing water velocity, thus showing in the spreadsheet results in Figure 8.40 that the basic shape of the lead refrigerant temperature trend is dependent on the lead evaporator water outlet temperature trend in Figure 8.38.

(relative each time to its preceding performance) in water side heat transfer coefficient, as the velocity term increased.

Thus, in contrast to the other downstream chillers, its evaporator refrigerant temperature increased, although only marginally, as stated, accompanied by a small rises in evaporator pressure each time and marginal increases in chilling load of 13.7 kW and a further 9.9 kW.

The lead chiller showed a 0.11% higher return water utilization over the previous value[39], the lag machine slightly more at 0.35%. The intermediate chillers showed small decreases in utilization, but overall, the *average* utilization per machine was 0.25% higher at 15.94 kW(R)/(kg/s). However, this slight recovery in utilization occurred because the mass flowrate of cool water had been increased, resulting in higher tube water velocity and thus a recovery to better water side heat transfer in the evaporators.

Five machines

Table 4.17 Guide to Tau Tona results

Reference	**Description**
Appendix B: Section 9.2.9	CHILLER result tables
Appendix B: Section 9.2.10	CHILLER result tables
Appendix B: Section 9.2.11	CHILLER result tables
Appendix B: Section 9.2.12	CHILLER result tables
Appendix A: Section 8.2.1	Trends and comparative plots

Because the Tau Tona chillers were approximately 17% smaller than the Kloof chillers, and yet had available to them a 66% higher flow of return water, the final temperature of the Tau Tona return water stream, after accepting all the heat rejected, was, in general, lower than a comparable

[39] For chiller 3, in the preceding simulation of three machines.

Kloof simulation[40]. Figure 8.47 shows the return water stream leaving the fourth machine at a comparatively low 51.84°C, indicating underutilization of the return water stream. Thus scope existed to increase the chilling load, and thus the return water utilization, simply by introducing a fifth chiller to the installation as put forward in Section 2.3.7.

Table 4.18 Key performance quantities for Section 9.2.9, Appendix B

	Chiller 5	**Chiller 4**	**Chiller 3**	**Chiller 2**	**Chiller 1**	**Unit**
Carnot COP	5.73	6.01	6.32	6.64	7.00	-
COP	3.27	3.32	3.35	3.36	3.35	-
System COP	3.33					-
Evap. water heat load	4562.9	4389.4	4208.4	4026.8	3848.5	kW(R)
Cond. water heat load	5958.9	5711.7	5465.5	5226.6	4997.8	kW(R)
Return water utilization	17.15	16.50	15.82	15.14	14.47	kW(R)/(kg/s)
Evap. outlet water temp.	15.99	13.19	10.51	7.95	5.50	°C
Cond. outlet water temp.	56.57	51.22	46.09	41.18	36.49	°C
Evap. refrigerant temp.	11.38	6.84	6.03	3.53	1.15	°C
Cond. refrigerant temp.	61.02	55.52	50.23	45.17	40.34	°C
Compr. stage 1 efficiency	71.24	66.50	61.85	57.45	53.38	%
Compr. stage 2 efficiency	69.06	66.15	63.01	59.65	56.15	%

Accordingly, five machines running at full capacity raised the return water temperature from 32°C to 56.6°C in Figure 8.47 and Section 9.2.9, chilling 375.32 kg/s of water from 18.89°C to 5.5°C, producing 21,036 kW(R) and achieving a 24.1% higher combined return water utilization of 79.08 kW(R)/(kg/s) over the previous four-chiller installation.

As emphasized in Section 2.3.2, the maximum allowed temperature of return water is, generally, limited by the ability of a mine's dams, dewatering pumps and piping to handle hot return water. Once this specified limit is reached, no extra chillers may be brought into the arrangement because the thermal reservoir provided by the return water

[40] Figures 8.29 and 8.47 plot these final return water temperatures.

stream has been exhausted. Additionally, reduction in the total chilling load using capacity control, as presented in Section 2.2.3, may be needed to keep the return water temperature at this limit.

Here, when the return water temperature leaving the lead chiller condenser was capped at 55°C, any further gain in return water utilization could be achieved only if the machines were caused to chill the evaporator water stream *more efficiently*. A higher chilling efficiency would change the proportions of the rejected heat, with more coming from an increased chilling load in the rejected heat in the return water, and less from the compressor input work.

Thus, having the full capacity simulation as reference, this section proceeded to investigate three methods of using the first stage compressor inlet guide vanes to limit the final return water temperature to 55°C, while attempting to maximise the chilling load for this limiting case.

- Capacity control on the lag chiller only, in Section 9.2.10
- Capacity control with restricted vane closure, in Section 9.2.11
- Equal vane closure on all five machines, in Section 9.2.12

The evaporator water flow rate was adjusted in each instance to maintain a final chilled water temperature of 5.5°C.

Firstly, in Section 9.2.10, using the capacity controls of the lag chiller only and closing its guide vanes by 60% to -47.5° reduced the final return water temperature by 1.6°C from 56.6°C to 55°C. This method was an attempt to keep the four upstream chillers at full load, sacrificing only the chilling capacity of the lag chiller. This method chilled 350.5 kg/s of water to from 18.89°C to 5.5°C, producing 19,654.6 kW(R) and dropping the combined return water utilization by 6.6% from the full capacity simulation in Section 9.2.9, to 73.89 kW(R)/(kg/s).

Table 4.19 Key performance quantities for Section 9.2.10, Appendix B

	Chiller 5	**Chiller 4**	**Chiller 3**	**Chiller 2**	**Chiller 1**	**Unit**
Carnot COP	5.86	6.14	6.44	6.75	7.78	-
COP	3.26	3.31	3.34	3.36	3.17	-
System COP	3.29					-
Evap. water heat load	4594.5	4384.4	4174.8	3970.5	2530.4	kW(R)
Cond. water heat load	6005.3	5709.0	5424.1	5153.9	3328.4	kW(R)
Return water utilization	17.27	16.48	15.69	14.93	9.51	kW(R)/(kg/s)
Evap. outlet water temp.	15.76	12.77	9.93	7.22	5.50	°C
Cond. outlet water temp.	55.01	49.61	44.49	39.62	34.99	°C
Evap. refrigerant temp.	11.08	8.17	5.40	2.77	2.11	°C
Cond. refrigerant temp.	59.59	53.99	48.68	43.62	37.48	°C
Compr. stage 1 efficiency	68.98	64.46	60.14	56.12	14.19	%
Compr. stage 2 efficiency	66.96	64.36	61.55	58.55	77.43	%

Next, in Section 9.2.11, the lag chiller was regulated to a maximum of 25%, corresponding to -20° inlet vane closure on the first stage compressor, before moving to the next machine.

Table 4.20 Key performance quantities for Section 9.2.11, Appendix B

	Chiller 5	**Chiller 4**	**Chiller 3**	**Chiller 2**	**Chiller 1**	**Unit**
Carnot COP	5.86	6.14	6.58	6.96	7.27	-
COP	3.26	3.31	3.37	3.37	3.37	-
System COP	3.33					-
Evap. water heat load	4596.0	4386.9	3846.8	3512.3	3358.1	kW(R)
Cond. water heat load	6007.5	5712.6	4988.1	4553.5	4354.2	kW(R)
Return water utilization	17.28	16.49	14.46	13.20	12.62	kW(R)/(kg/s)
Evap. outlet water temp.	15.77	12.79	10.17	7.79	5.50	°C
Cond. outlet water temp.	55.00	49.61	44.48	40.00	36.91	°C
Evap. refrigerant temp.	11.09	8.18	5.89	3.69	1.47	°C
Cond. refrigerant temp.	59.59	53.99	48.29	43.48	39.26	°C
Compr. stage 1 efficiency	68.95	64.42	45.34	35.57	32.74	%
Compr. stage 2 efficiency	66.93	64.31	67.71	69.91	67.35	%

This method was an attempt to keep as many of the upstream machines as possible at full load[41] while limiting the loss of cooling capacity on the regulated machines. The lag and second machine required vane closure to this -20° limit but the third machine needed less regulation at 17%, or -13.7°, to bring the return water final temperature down to 55°C. This method chilled 351.5 kg/s of water from 18.89°C to 5.5°C, producing 19,700.1 kW(R) and dropping the combined return water utilization slightly less by 6.3% from the unregulated simulation in Section 9.2.9, to 74.06 kW(R)/(kg/s).

Lastly, when equal vane closure was used on all five chillers, Section 9.2.12 shows that it was sufficient to close the inlet guide vanes on each machine by 13.6%, corresponding to -11°, to limit the return water temperature to 55°C.

Table 4.21 Key performance quantities for Section 9.2.12, Appendix B

	Chiller 5	**Chiller 4**	**Chiller 3**	**Chiller 2**	**Chiller 1**	**Unit**
Carnot COP	5.96	6.22	6.51	6.81	7.13	-
COP	3.29	3.34	3.37	3.38	3.38	-
System COP	3.35					-
Evap. water heat load	4316.0	4127.5	3940.6	3759.9	3584.1	kW(R)
Cond. water heat load	5627.2	5363.7	5111.2	4871.5	4645.4	kW(R)
Return water utilization	16.23	15.52	14.81	14.13	13.47	kW(R)/(kg/s)
Evap. outlet water temp.	15.96	13.16	10.49	7.94	5.50	°C
Cond. outlet water temp.	55.00	49.95	45.13	40.55	36.17	°C
Evap. refrigerant temp.	11.48	8.74	6.14	3.66	1.30	°C
Cond. refrigerant temp.	59.26	54.03	49.05	44.30	39.77	°C
Compr. stage 1 efficiency	57.23	52.80	48.75	45.07	41.76	%
Compr. stage 2 efficiency	71.14	70.01	67.57	64.90	62.03	%

[41] to take advantage of the benefit to their compressors of the higher evaporator pressures generated by receiving cool water at higher temperature

This method chilled 352 kg/s of water from 18.89°C to 5.5°C, producing 19,727.1 kW(R) and dropping the combined return water utilization by 6.2% to 74.16 kW(R)/(kg/s), a fractionally smaller reduction from full load than the previous ‘restricted vane closure’ method.

5 DISCUSSION

This chapter compares the spreadsheet model- and CHILLER program simulations to identify the main reasons for the similarities and differences between potential maximum- and expected refrigerating loads, thus addressing the practicability of maximizing total refrigerating load.

5.1 Using additional chillers to increase return water utilization

5.1.1 Single machine

This section compares the spreadsheet simulation of a single Kloof chiller to the simulation of its CHILLER counterpart.

Table 5.1 Guide to Kloof results

Reference	Description
Section 3.2.3 (Single machine)	Kloof spreadsheet model simulation
Appendix B: Section 9.1.1	Spreadsheet result tables
Section 4.2.1 (Single machine)	Kloof CHILLER program simulation
Appendix B: Section 9.2.1	CHILLER result tables
Appendix B: Section 9.3.1	Side by side comparison of results
Appendix A: Section 8.1.1	Trends and comparative plots

Table 5.2 shows that the Carnot COPs of the two chillers were similar because the absolute evaporating refrigerant temperature was 0.18% larger than the spreadsheet value, and the difference between the condensing and evaporating refrigerant temperatures increased by 0.58%. The real machine Carnot COP, being the ratio of these quantities, hardly changed. All else being equal, this similarity in Carnot COP indicated a good foundation for the real chiller to achieve a similar chilling load and return water utilization to the spreadsheet model.

Table 5.2 Key performance quantities for comparison

	CHILLER	S-sheet	
Chiller	**Chiller 1**	**Chiller 1**	**Unit**
Carnot COP	7.06	7.09	-
COP	2.92	4.25	-
System COP	2.92	4.25	-
Evap. water heat load	5131.10	5423.98	kW(R)
Cond. water heat load	6886.10	6699.13	kW(R)
Return water utilization	32.07	33.90	kW(R)/(kg/s)
Evap. outlet water temp.	10.50	10.50	°C
Cond. outlet water temp.	42.28	42.00	°C
Evap. refrigerant temp.	7.34	6.85	°C
Cond. refrigerant temp.	47.07	46.35	°C
Compr. stage 1 efficiency	55.49	-	%
Compr. stage 2 efficiency	41.37	-	%

The spreadsheet predicted that a chiller operating with 60% cycle efficiency, having evaporator and condenser overall thermal conductances of 600- and 800 kW/°C respectively, while raising the return water temperature to 42°C, could deliver a 5423.98 kW(R) chilling load and for these conditions would maintain an evaporator refrigerant temperature of 6.85°C[42]. The real chiller model, in contrast, exhibited a higher evaporator refrigerant temperature of 7.34°C and a smaller log mean temperature difference.

The real evaporator overall thermal conductance was 1.47% larger than the assumed value of 600 kW/°C but the said decrease in LMTD, caused by the higher refrigerant temperature maintained by the real compressor model, meant that the real evaporator chilling load was 5.4% less than the spreadsheet value.

[42] Even if the spreadsheet had assumed the same evaporator and condenser conductance values as the CHILLER program had predicted, that is 608.83- and 768.18 kW/°C respectively, and raised the return water temperature to 42.28°C, the evaporator refrigerant temperature would have been 6.78°C.

The simulated real machine absorbed 37.6% more compressor power than the spreadsheet, due to the poor individual stage isentropic efficiencies of 55.49% and 41.37%. These stage efficiencies were low due to operation at higher than design refrigerant inlet volumetric flowrates for lower than design values of isentropic head.

These poor compressor stage isentropic efficiencies resulted in an expected cycle efficiency of 41%, in Table 9.161, well below the constant 60% assumed by the spreadsheet.

In Table 9.160, the spreadsheet predicted that a single machine could expect to achieve only 28.2% of the Lorenz COP, but the real model achieved even less, at 19.5%, due to the lower cycle efficiency of 41%.

This comparison shows that a particular return water utilization, predicted for a machine operating at a reasonable cycle efficiency in the spreadsheet, could still be achieved even if the real machine would operate at a lower cycle efficiency. The penalty was a greater compressor absorbed power and thus a higher final return water temperature.

5.1.2 Two machines, having a specified limit of 55°C on the final return water temperature

Table 5.3 Guide to Kloof results

Reference	**Description**
Section 3.2.3 (Two machines)	Kloof spreadsheet model simulation
Appendix B: Section 9.1.2	Spreadsheet result tables
Section 4.2.1 (Two machines)	Kloof CHILLER program simulation
Appendix B: Section 9.2.2	CHILLER result tables
Appendix B: Section 9.3.2	Side by side comparison of results
Appendix A: Section 8.1.1	Trends and comparative plots

This section compares the spreadsheet simulation of a Kloof lead lag pair to the simulation of its CHILLER counterpart.

Table 5.4 Key performance quantities for comparison

	CHILLER		S-sheet		
Chiller	**Chiller 2**	**Chiller 1**	**Chiller 2**	**Chiller 1**	**Unit**
Carnot COP	6.24	6.84	6.34	6.62	-
COP	2.97	3.03	3.80	3.97	-
System COP	3.00		3.89		-
Evap. water heat load	5472.10	4830.10	5423.98	5423.98	kW(R)
Cond. water heat load	7312.30	6421.90	6849.62	6788.73	kW(R)
Return water utilization	34.20	30.19	33.90	33.90	kW(R)/(kg/s)
Evap. outlet water temp.	17.30	10.50	17.75	10.50	°C
Cond. outlet water temp.	52.50	41.59	52.36	42.13	°C
Evap. refrigerant temp.	11.81	5.31	11.86	4.61	°C
Cond. refrigerant temp.	57.48	46.01	56.80	46.54	°C
Compr. stg. 1 efficiency	62.08	57.39	-	-	%
Compr. stg. 2 efficiency	51.64	45.76	-	-	%

Summarized in table 5.4, the Kloof simulation of a real lead lag pair produced 545.76 kW(R) less, or an average of 272.88 kW(R) less per machine, than the corresponding spreadsheet simulation, for an increase of 23% in compressor absorbed power. The real *lead* machine produced slightly more chilling than predicted by the spreadsheet. The lead chiller performed better because although it maintained a 2.88% smaller evaporator LMTD than the spreadsheet machine, it exhibited a 3.85% larger overall thermal conductance. The real machine achieved this increase in chilling load at the expense of more absorbed compressor power, because although the compressor stage efficiencies had improved over a single machine to 62.08% and 51.64% respectively, they were still below the design value of 72.5%.

Although the simulation of a real lead lag pair delivered less chilling than the corresponding spreadsheet simulation, in moving from one simulated real machine in Section 9.2.1, the return water utilization of this pair effectively doubled.

Next, the spreadsheet simulation of a Tau Tona lead lag pair is compared in table 5.6 with the simulation of *its* CHILLER counterpart.

Table 5.5 Guide to Tau Tona results

Reference	**Description**
Section 3.3.3 (Two machines)	Tau Tona spreadsheet model simulation
Appendix B: Section 9.1.7	Spreadsheet result tables
Section 4.3.1 (Two machines)	Tau Tona CHILLER program simulation
Appendix B: Section 9.2.6	CHILLER result tables
Appendix B: Section 9.3.3	Side by side comparison of results
Appendix A: Section 8.2.1	Trends and comparative plots

Table 5.6 Key performance quantities for comparison

	CHILLER		**S-sheet**		
Chiller	**Chiller 2**	**Chiller 1**	**Chiller 2**	**Chiller 1**	**Unit**
Carnot COP	7.31	7.22	7.47	6.96	-
COP	3.06	3.25	4.48	4.17	-
System COP	3.14		4.32		-
Evap. water heat load	4740.7	4045.9	4512.00	4512.00	kW(R)
Cond. water heat load	6292.2	5289.8	5519.07	5592.78	kW(R)
Return water utilization	17.82	15.21	16.96	16.96	kW(R)/(kg/s)
Evap. outlet water temp.	11.66	5.50	12.20	5.50	°C
Cond. outlet water temp.	42.40	36.75	41.98	37.02	°C
Evap. refrigerant temp.	8.73	2.67	8.92	2.22	°C
Cond. refrigerant temp.	47.31	40.85	46.69	41.80	°C
Compr. stg. 1 efficiency	50.40	51.11	-	-	%
Compr. stg. 2 efficiency	48.34	42.48	-	-	%

The Tau Tona CHILLER simulation and its spreadsheet counterpart produced similar trends to the Kloof comparison. Once again, the simulated real machines required more compressor input power, now 33.9% more, to produce 2.62% less chilling load, thus achieving a 2.62% lower return water utilization than the spreadsheet simulation, which operated with a higher cycle efficiency.

Although the Kloof and Tau Tona pairs of simulated real machines operated with cycle efficiencies well below 60%, each pair obtained quantities of chilling similar to the spreadsheet machines but with higher compressor power inputs and thus higher final return water temperatures.

This emphasized that a group of chillers operating at poor cycle efficiency could still make *partial* use of return water by being arranged in series-counterflow, as long as the specified maximum temperature, here 55°C, was not reached. This approach did not, however, *maximize* the use of return water indicated by the spreadsheet simulations. Rather, the use of a series-counterflow arrangement minimized the reduction in chilling load caused by poor cycle efficiencies. This is brought out by comparing the cycle efficiency in Table 9.161 with those in Table 9.169.

5.1.3 An increase to three machines, maintaining the specified limit of 55°C on the final return water temperature

This section begins by comparing the spreadsheet simulation of a 3-chiller Kloof installation to the simulation of its CHILLER counterpart. Both simulations operated at part load, to conform to the return water temperature limit of 55°C. Then, comparison is made with the CHILLER simulation of a 3-chiller Tau Tona installation, where, because of the higher return water flowrate, it was possible to operate the machines at full load without approaching the 55°C limit.

Table 5.7 Guide to Kloof results

Reference	**Description**
Section 3.2.3 (Three machines)	Kloof spreadsheet model simulation
Appendix B: Section 9.1.3	Spreadsheet result tables
Section 4.2.1 (Three machines)	Kloof CHILLER program simulation
Appendix B: Section 9.2.3	CHILLER result tables
Appendix B: Section 9.3.4	Side by side comparison of results
Appendix A: Section 8.1.1	Trends and comparative plots

The CHILLER simulation predicted a total chilling load 7.9% smaller than the spreadsheet, for exactly the same environmental conditions. Since the initial and final water temperatures in the evaporator and condenser water circuits were identical, as listed in Table 9.184, the Lorenz COP for each simulation was also identical.

Table 5.8 Key performance quantities for comparison

	CHILLER			**S-sheet**			
Chiller	**Chiller 3**	**Chiller 2**	**Chiller 1**	**Chiller 3**	**Chiller 2**	**Chiller 1**	**Unit**
Carnot COP	6.66	7.18	7.76	6.71	7.08	7.50	-
COP	2.90	2.95	2.96	4.03	4.25	4.50	-
System COP	2.93			4.25			-
Evap. water heat load	4112.2	3829.6	3549.4	4157.88	4157.88	4157.88	kW(R)
Cond. water heat load	5531.3	5128.0	4749.4	5190.48	5136.01	5081.68	kW(R)
Return water utilization	25.70	23.94	22.18	25.99	25.99	25.99	kW(R) /(kg/s)
Evap. outlet water temp.	19.81	14.98	10.50	20.17	15.33	10.50	°C
Cond. outlet water temp.	55.00	46.75	39.09	55.00	47.25	36.59	°C
Evap. refrigerant temp.	15.26	10.56	6.22	15.37	10.54	5.71	°C
Cond. refrigerant temp.	58.57	50.10	42.24	58.37	50.58	42.88	°C
Compr. stg. 1 efficiency	37.29	32.41	28.46	-	-	-	%
Compr. stg. 2 efficiency	72.37	72.49	69.95	-	-	-	%

Tables 9.188 and 9.188 show similar values of refrigerant temperature in the evaporator, and condenser, of each corresponding chiller, and thus similar positional Carnot COPs in Table 9.185. The first major discrepancy occurs in the CHILLER simulation cycle efficiencies, which were between 26.7% and 36.7% lower than the constant assigned value in the spreadsheet. The vane angle position of -37.52°, or nearly 47% closed, on each stage 1 compressor caused the lead, mid and lag stages to operate with isentropic efficiencies of 37.29%, 32.41% and 28.46% respectively. In fact, these stage 1 performances would have caused even lower cycle efficiencies than those obtained, except that the stage 2 compressors on all three chillers operated very close to design conditions, with the mid stage 2 compressor practically at design load. The much higher isentropic efficiencies for the stage 2 compressors were 72.37%, 72.49% and 69.95% respectively, as listed in Table 9.191.

Given the aim of maximising chiller load (supported by the aim to maximise chilling efficiency), it is difficult not to disregard such poor results. But the increase in total chilling load predicted when moving from two to three spreadsheet chillers (Sections 9.1.2 and 9.1.3), where the constant cycle efficiency was set at 60%, was 14.99%. In comparison, the increase in total chilling load moving from two to three CHILLER machines here (Sections 9.2.2 and 9.2.3), even with poor part load efficiencies, was still a useful 11.54%.

Lastly, the higher return water flowrate at Tau Tona allowed three chillers to operate at full load, even though the chillers heated the final return water to a higher temperature, 46.88°C, than if the compressors had operated with better cycle efficiencies. The boost of the return water outlet temperature due to a larger amount of absorbed compressor power was irrelevant in this case because the limit of 55°C was not reached.

Table 5.9 Guide to Tau Tona results

Reference	**Description**
Section 4.3.1 (Three machines)	Tau Tona CHILLER program simulation
Appendix B: Section 9.2.7	CHILLER result tables
Appendix A: Section 8.2.1	Trends and comparative plots

Summarized by table 5.10, a higher return water flowrate is particularly useful because even with poor chilling efficiency, which raises the final return water temperature higher than it would otherwise have been, the return water temperature limit is not reached. Also, poor cycle efficiency, while not serving the highest aim of maximising chilling load, does not prevent incremental increases in return water utilization as further machines are added.

Table 5.10 Key performance quantities

	Chiller 3	**Chiller 2**	**Chiller 1**	**Unit**
Carnot COP	6.65	6.82	6.97	-
COP	3.17	3.27	3.36	-
System COP	3.26			-
Evap. water heat load	4647.1	4207.6	3824.9	kW(R)
Cond. water heat load	6114.0	5493.4	4963.0	kW(R)
Return water utilization	17.47	15.82	14.38	kW(R)/(kg/s)
Evap. outlet water temp.	13.98	6.54	5.50	°C
Cond. outlet water temp.	46.88	41.39	36.46	°C
Evap. refrigerant temp.	9.14	4.86	0.97	°C
Cond. refrigerant temp.	51.58	45.61	40.28	°C
Compr. stage 1 efficiency	57.30	55.30	53.67	%
Compr. stage 2 efficiency	56.01	56.36	56.61	%

5.1.4 Three machines, increasing the specified limit on the final return water temperature to 70°C

This section compares, once again, the spreadsheet simulation of a 3-chiller Kloof installation to the simulation of its CHILLER counterpart. The difference from the previous simulation, however, was that the specified limit on the final return water temperature was increased from 55°C to 70°C, allowing the chillers to operate at full load.

Table 5.11 Guide to Kloof results

Reference	**Description**
Section 3.2.4 (Three machines)	Kloof spreadsheet model simulation
Appendix B: Section 9.1.5	Spreadsheet result tables
Section 4.2.2 (Three machines)	Kloof CHILLER program simulation
Appendix B: Section 9.2.4	CHILLER result tables
Appendix B: Section 9.3.5	Side by side comparison of results
Appendix A: Section 8.1.2	Trends and comparative plots

Table 5.12 Key performance quantities for comparison

	CHILLER			**S-sheet**			
Chiller	**Chiller 3**	**Chiller 2**	**Chiller 1**	**Chiller 3**	**Chiller 2**	**Chiller 1**	**Unit**
Carnot COP	5.46	6.06	6.81	5.25	5.79	6.44	-
COP	3.06	3.10	3.05	3.15	3.47	3.87	-
System COP	3.07			3.47			-
Evap. water heat load	5342.4	5098.4	4790.5	5423.98	5423.98	5423.98	kW(R)
Cond. water heat load	7088.5	6743.0	6361.4	7146.71	6985.64	6826.85	kW(R)
Return water utilization	33.39	31.87	29.94	33.90	33.90	33.90	kW(R)/(kg/s)
Evap. outlet water temp.	19.91	15.06	10.50	20.17	15.33	10.50	°C
Cond. outlet water temp.	62.14	51.56	41.50	63.29	52.62	42.19	°C
Evap. refrigerant temp.	14.19	9.44	5.04	13.33	8.50	3.66	°C
Cond. refrigerant temp.	66.82	56.10	45.87	67.92	57.15	46.62	°C
Compr. stg. 1 efficiency	70.97	64.44	57.66	-	-	-	%
Compr. stg. 2 efficiency	66.14	56.96	46.37	-	-	-	%

When the return water outlet temperature limit was increased to 70°C, Section 9.1.5 and the summary table 5.12 shows that three spreadsheet machines operating at full capacity could achieve a return water utilization of 101.7 kW(R)/(kg/s) of return water. The CHILLER program predicted that the return water utilization would be 6.4% lower at 95.2 kW(R)/(kg/s).

The real machine models all presented evaporator overall thermal conductances above the 600 kW/°C assumed value, at 11.30%, 8.98% and 6.30% respectively, leading to the real machines maintaining higher evaporator refrigerant temperatures than their spreadsheet equivalents. The accompanying higher pressures in the evaporators also improved the operating points of all three stage 1 compressors, having isentropic efficiencies in table 9.198 of 70.97%, 64.44% and 57.66% respectively. Thus, with the CHILLER Carnot COPs in fact *higher* than the spreadsheet prediction, and the improved compressor stage efficiencies, the expected COPs of real machines were not far off the spreadsheet predictions.

5.1.5 Four machines, having a specified limit of 70°C on the final return water temperature

This section begins by comparing the spreadsheet simulation of a 4-chiller Kloof installation to the simulation of its CHILLER counterpart. The higher return water temperature limit of 70°C allowed the four chiller models of the spreadsheet to operate near full load. The CHILLER machines, run at full load, raised the return water temperature to 70.24°C.

Table 5.13 Guide to Kloof results

Reference	**Description**
Section 3.2.4 (Four machines)	Kloof spreadsheet model simulation
Appendix B: Section 9.1.6	Spreadsheet result tables
Section 4.2.2 (Four machines)	Kloof CHILLER program simulation
Appendix B: Section 9.2.5	CHILLER result tables
Appendix B: Section 9.3.6	Side by side comparison of results
Appendix A: Section 8.1.2	Trends and comparative plots

Table 5.14 Key performance quantities for comparison

	CHILLER				**S-sheet**				
Chiller	**Chill.4**	**Chill.3**	**Chill. 2**	**Chill. 1**	**Chill.4**	**Chill.3**	**Chill.2**	**Chill.1**	**Unit**
Carnot COP	5.00	5.37	5.98	6.80	4.85	5.36	5.98	6.74	-
COP	2.84	3.15	3.16	3.06	2.91	3.21	3.59	4.04	-
System COP	3.05				3.39				-
Evap. water heat load	4589.3	4984.2	4939.8	4773.2	4913.29	4913.29	4913.29	4913.29	kW(R)
Cond. water heat load	6207.2	6568.9	6505.5	6335.0	6602.66	6441.78	6283.80	6128.71	kW(R)
Return water utilization	28.68	31.15	30.87	29.83	30.71	30.71	30.71	30.71	kW(R)/ (kg/s)
Evap. outlet water temp.	21.55	17.80	14.09	10.50	21.38	17.75	14.13	10.50	°C
Cond. outlet water temp.	70.24	60.97	51.17	41.46	70.00	60.14	50.53	41.15	°C
Evap. refrigerant temp.	16.28	12.16	8.43	4.92	14.87	11.24	7.62	3.99	°C
Cond. refr. temp.	74.17	65.26	55.52	45.81	74.28	64.32	54.61	45.12	°C
Comp. stg. 1 eff.	71.27	72.26	65.52	57.78	-	-	-	-	%
Comp. stg. 2 eff.	71.96	70.10	59.36	46.65	-	-	-	-	%

Each spreadsheet machine required a chilling capacity reduction of only 9% to keep the return water final temperature at 70°C. Therefore, unlike the fourth machine in Section 9.1.4, which was heavily regulated to prevent the return water temperature from rising above 55°C, the addition of the fourth machine here contributed significantly to an increase in total obtainable chilling giving 122.83 kW(R)(kg/s), increasing 20.8% over the 101.72 kW(R)(kg/s) from three machines.

In a similar and improved manner to the three machines in the previous section, these four machines very nearly equalled the chilling load and effectiveness predicted by the spreadsheet. In fact, the delivered load was just 366.68 kW(R), or 1.9%, less.

Even though the evaporators had been converted to two water passes earlier to control the tube water velocity, Table 9.202 records that the value here was too high at 4.33 m/s[43] because of the high evaporator water flowrate of 317.75 kg/s. Thus the values of water thermal resistance were relatively low in all evaporators, on average 42.1% lower than two machines at full load in Section 9.2.2. These changes brought about significant increases in the evaporator overall thermal conductance values, on average now 11.6% higher than the spreadsheet assumption of 600 kW/°C.

[43] Both the Kloof and Tau Tona chillers in this study are fitted with cupro-nickel (Cu-Ni) heat exchanger tubes. Water velocities that are too high cause erosion in this material and van der Walt (1979, p. 361) recommends that heat exchangers should be dimensioned to provide *design* water velocities in evaporator tubes in the range 2 m/s to 2.3 m/s, primarily to reserve some margin, albeit restricted, for increasing the water flow rate through the evaporators should this prove necessary. For example, some increase in water velocity might be used to provide adequate compensation for tube fouling by increasing the water side heat transfer coefficient.

Gosney (1982, p. 88) states that higher water velocities may, in general, be specified for particular applications, provided that appropriate tube material, being more resistant to erosion at such velocities, is used.

The second and lag chiller compressor isentropic efficiencies were similar to the lead lag pair in Section 9.2.2 but in this simulation, the third and lead chiller benefitted greatly from higher evaporator pressures (and the accompanying decreases in refrigerant specific volume) at their stage 1 compressor inlets. Coupled with the larger refrigerant lifts required from the compressors for the higher condensing temperatures, the third and lead compressors exhibited refrigerant inlet volumetric flowrates and isentropic head values that yielded higher isentropic efficiencies[44].

5.2 The influence of cycle efficiency at part load

5.2.1 Four machines, having a specified limit of 55°C on the final return water temperature

In Section 5.1.3, operation at part load was already needed for a Kloof installation of *three* machines to remain at the return water temperature limit of 55°C. This section discusses the spreadsheet simulation performance of a 4-chiller Kloof installation placed on severe part load for the same temperature limit.

Table 5.15 Guide to Kloof results

Reference	**Description**
Section 3.2.3 (Four machines)	Kloof spreadsheet model simulation
Appendix B: Section 9.1.4	Spreadsheet result tables
Appendix A: Section 8.1.1	Trends and comparative plots

[44] The values of compressor inlet volumetric flowrate and isentropic head were not always numerically closer to the respective stage design values in Tables 11.3 and 11.4, but nevertheless yielded higher isentropic efficiencies due to the general shape of the regions of efficiency for a centrifugal compressor, illustrated in Figure 2.3

In Section 9.1.3, three Kloof machines had already reached the return water temperature limit of 55°C. So, when a fourth machine was added in a spreadsheet simulation, and every machine placed on severe part duty to keep the final temperature at 55°C, the return water utilization still improved by 1.8% over three machines. This increase was due exclusively to an improvement in the efficiency of chilling, shown by the higher Carnot COPs (and thus higher COPs) brought about by the decreased LMTDs in evaporators and condensers to match the reduced chiller loads.

Table 5.16 Key performance quantities

	Chiller 4	**Chiller 3**	**Chiller 2**	**Chiller 1**	**Unit**
Carnot COP	7.30	7.63	8.00	8.40	-
COP	4.38	4.58	4.80	5.04	-
System COP	4.69				-
Evap. water heat load	3174.79	3174.79	3174.79	3174.79	kW(R)
Cond. water heat load	3899.60	3867.91	3836.30	3804.76	kW(R)
Return water utilization	19.84	19.84	19.84	19.84	kW(R)/(kg/s)
Evap. outlet water temp.	21.38	17.75	14.13	10.50	°C
Cond. outlet water temp.	55.00	49.18	43.41	37.68	°C
Evap. refrigerant temp.	17.69	14.07	10.44	6.82	°C
Cond. refrigerant temp.	57.53	51.69	45.89	40.15	°C

In the CHILLER program, a fourth machine could not be added to the three machines in Section 9.2.3, because to keep the return water final temperature at 55°C, the extra capacity reduction required on all machines would have caused the lead machine compressor to enter the surge region.

5.2.2 Five machines, maintaining the specified limit of 55°C on the final return water temperature

Table 5.17 Guide to Tau Tona results

Reference	**Description**
Section 4.3.1 (Five machines)	Tau Tona CHILLER program simulations
Appendix B: Section 9.2.9	CHILLER result tables
Appendix B: Section 9.2.10	CHILLER result tables
Appendix B: Section 9.2.11	CHILLER result tables
Appendix B: Section 9.2.12	CHILLER result tables
Appendix A: Section 8.2.1	Trends and comparative plots

The relatively high return water flowrate of 266 kg/s for the Tau Tona environment meant that five machines operating at full capacity heated the return water to only 56.6°C, in Section 9.2.9. This provided an opportunity to investigate the use of small amounts of compressor capacity control to limit the return water outlet temperature to 55°C, whilst attempting to increase the chilling efficiency of the process. Table 5.18 provides a summary of this 5-machine investigation. If regulated alone, in Section 9.2.10, the lag machine first stage compressor guide vanes would have required closing to -47.5°, or 60%, to achieve the desired 1.6°C return water temperature reduction to 55°C.

Instead, each machine beginning with the lag machine was regulated to a maximum of -20°, or 25%, inlet vane closure in Section 9.2.11 before moving to the next machine. The lag and fourth machine both reached this vane setting limit, and the third machine needed regulation to -13.7°, or 17%. This method increased the average machine cycle efficiency to 51%, and the total return water utilization from 73.87 kW(R)/(kg/s) to 74.06 kW(R)/(kg/s), showing a slight increase in obtainable chilling when three machines were used to control the return water outlet temperature.

Table 5.18 Key performance quantities for comparison

		Chiller 5	Chiller 4	Chiller 3	Chiller 2	Chiller 1	Unit
Carnot COP	all full capacity	5.73	6.01	6.32	6.64	7.00	-
	lag only regulated	5.86	6.14	6.44	6.75	7.78	
	max. -20° reg.	5.86	6.14	6.58	6.96	7.27	
	all equal reg.	5.96	6.22	6.51	6.81	7.13	
COP	all full capacity	3.27	3.32	3.35	3.36	3.35	-
	lag only regulated	3.26	3.31	3.34	3.36	3.17	
	max. -20° reg.	3.26	3.31	3.37	3.37	3.37	
	all equal reg.	3.29	3.34	3.37	3.38	3.38	
System COP	all full capacity	3.33					-
	lag only regulated	3.29					
	max. -20° reg.	3.33					
	all equal reg.	3.35					
Evaporator water heat load	all full capacity	4562.9	4389.4	4208.4	4026.8	3848.5	kW(R)
	lag only regulated	4594.5	4384.4	4174.8	3970.5	2530.4	
	max. -20° reg.	4596.0	4386.9	3846.8	3512.3	3358.1	
	all equal reg.	4316.0	4127.5	3940.6	3759.9	3584.1	
Condenser water heat load	all full capacity	5958.9	5711.7	5465.5	5226.6	4997.8	kW(R)
	lag only regulated	6005.3	5709.0	5424.1	5153.9	3328.4	
	max. -20° reg.	6007.5	5712.6	4988.1	4553.5	4354.2	
	all equal reg.	5627.2	5363.7	5111.2	4871.5	4645.4	
Return water utilization	all full capacity	17.15	16.50	15.82	15.14	14.47	kW(R)/(kg/s)
	lag only regulated	17.27	16.48	15.69	14.93	9.51	
	max. -20° reg.	17.28	16.49	14.46	13.20	12.62	
	all equal reg.	16.23	15.52	14.81	14.13	13.47	
Evaporator outlet water temperature	all full capacity	15.99	13.19	10.51	7.95	5.50	°C
	lag only regulated	15.76	12.77	9.93	7.22	5.50	
	max. -20° reg.	15.77	12.79	10.17	7.79	5.50	
	all equal reg.	15.96	13.16	10.49	7.94	5.50	
Condenser outlet water temperature	all full capacity	56.57	51.22	46.09	41.18	36.49	°C
	lag only regulated	55.01	49.61	44.49	39.62	34.99	
	max. -20° reg.	55.00	49.61	44.48	40.00	36.91	
	all equal reg.	55.00	49.95	45.13	40.55	36.17	
Evaporator refrigerant temperature	all full capacity	11.38	6.84	6.03	3.53	1.15	°C
	lag only regulated	11.08	8.17	5.40	2.77	2.11	
	max. -20° reg.	11.09	8.18	5.89	3.69	1.47	
	all equal reg.	11.48	8.74	6.14	3.66	1.30	
Condenser refrigerant temperature	all full capacity	61.02	55.52	50.23	45.17	40.34	°C
	lag only regulated	59.59	53.99	48.68	43.62	37.48	
	max. -20° reg.	59.59	53.99	48.29	43.48	39.26	
	all equal reg.	59.26	54.03	49.05	44.30	39.77	
Compressor stage 1 efficiency	all full capacity	71.24	66.50	61.85	57.45	53.38	%
	lag only regulated	68.98	64.46	60.14	56.12	14.19	
	max. -20° reg.	68.95	64.42	45.34	35.57	32.74	
	all equal reg.	57.23	52.80	48.75	45.07	41.76	
Compressor stage 2 efficiency	all full capacity	69.06	66.15	63.01	59.65	56.15	%
	lag only regulated	66.96	64.36	61.55	58.55	77.43	
	max. -20° reg.	66.93	64.31	67.71	69.91	67.35	
	all equal reg.	71.14	70.01	67.57	64.90	62.03	

Lastly, when the compressor inlet guide vanes were closed equally by -11° on the stage 1 compressor of all five machines, there was an increase in average cycle efficiency to 51.6%. This was manifested as an increase in obtainable chilling to 74.16 kW(R)/(kg/s) with a small decrease in compressor input power relative to the previous method.

5.3 Summary of return water utilization

From the spreadsheet model results in Figure 5.1, a single chiller in the Kloof environment, operating with a specified, fixed cycle efficiency of 60%, could perform with a return water utilization of 33.90 kW(R)/(kg/s), raising the return water to a final temperature of 42°C.

A real single machine, modelled by the CHILLER program, also heated water to 42.28°C, but its compressor stages operated with relatively low isentropic efficiencies, compared to their design values, because the compressor developed lower-than-design isentropic head in both stages due to the machine condenser receiving relatively cool return water at 32°C. Thus, the compressor absorbed power was higher than predicted by the spreadsheet.

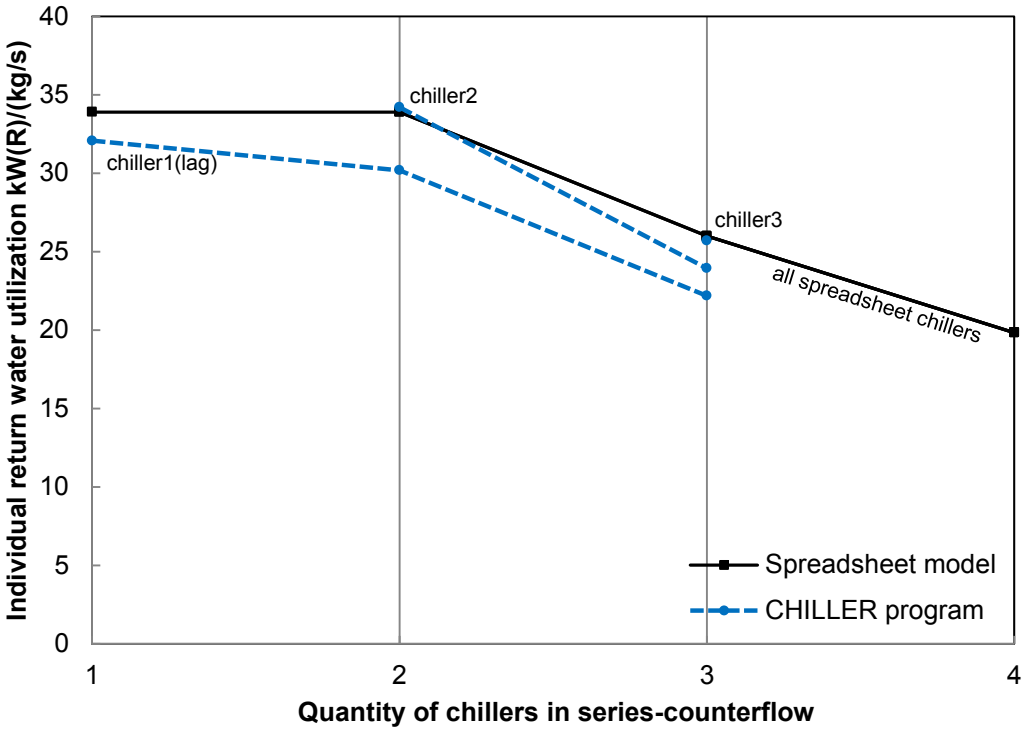

Figure 5.1 Effect of a maximum return water temperature of 55°C on the predicted return water utilization of Kloof chillers

The poor compressor stage efficiencies indicated a larger proportion of absorbed compressor power, and a smaller proportion of chilling load, in the heated return water. This was indeed the case, with the expected chilling load being 5.4% less than the spreadsheet. Hence, the return water utilization was also 5.4% lower at 32.07 kW(R)/(kg/s).

In moving to the simulation of two real machines, the evaporator chilled water flowrate was doubled to keep both chillers fully loaded and the final chilled water temperature at 10.5°C, but this increase did not aid heat transfer in the evaporators due to the conversion from four to two passes and the resulting unchanged tube water velocity. When chiller 1 occupied the lag position, its evaporator refrigerant temperature and pressure dropped, increasing the specific volume of refrigerant vapour and thus lowering the mass flowrate of refrigerant in the stage 1 compressor.

Chiller 1's utilization of return water consequently decreased to 30.19 kW(R)/(kg/s).

The lead chiller, however, exhibited a return water utilization comparable to the spreadsheet prediction. Higher refrigerant vapour pressure and a correspondingly lower vapour specific volume in the evaporator resulted in a larger chilling load than the lag machine. The lead compressor stages developed closer-to-design isentropic heads and so operated with improved isentropic efficiencies.

In moving to a lead lag pair, both spreadsheet chillers exhibited the same utilization as the single spreadsheet machine[45].

The decrease in return water utilization when moving to three chillers was due, for both sets of simulations, to the capacity control required to prevent the final return water temperature from exceeding 55°C. Importantly, the spreadsheet chillers were modelled to retain a cycle efficiency of 60% at all part load. Once again, higher evaporator pressure aided the real lead chiller, now Chiller 3, to deliver a utilization comparable to the spreadsheet. Four real machines with a further controlled capacity reduction were not simulated because the performance of three machines was already poor.

Figure 5.2 illustrates the total return water utilization achieved by each configuration, with the individual values from Figure 5.1 reproduced for reference.

[45] The data points for the spreadsheet chillers, and thus the lines linking these points, overlay one another directly for each quantity of chillers in Figures 5.1 through 5.6. This is due simply to the assumption of equal chilling load for all machines in a spreadsheet simulation. By Equation 3.1 the return water utilization values, being the ratio of chilling load to constant return water flowrate, were also equal.

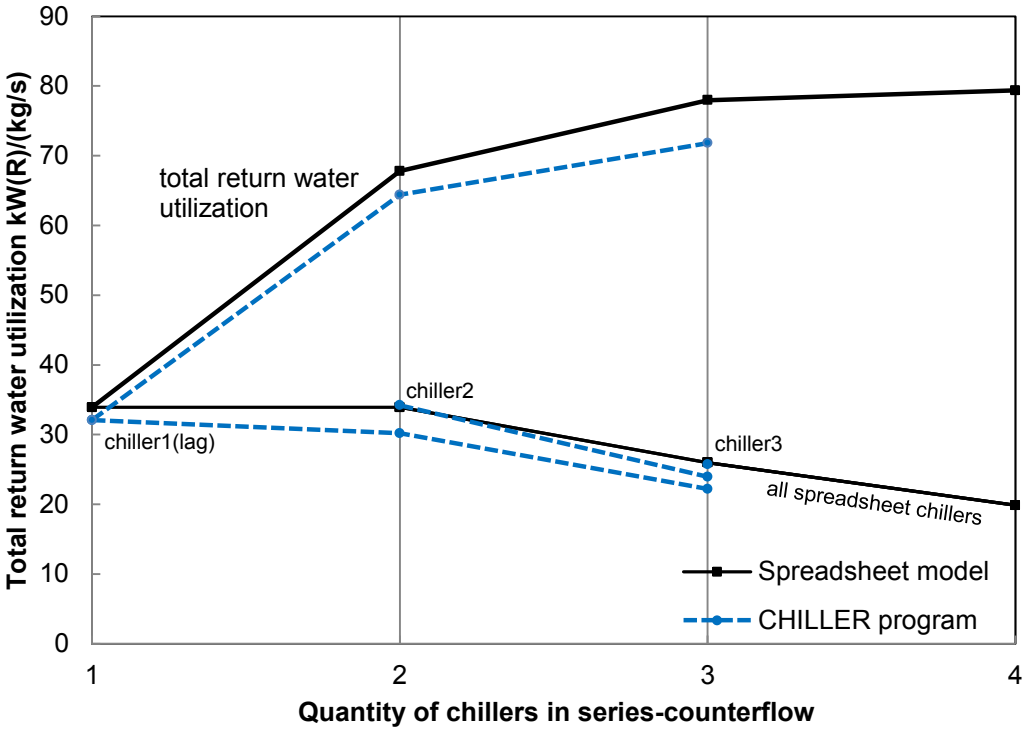

Figure 5.2 Effect of a maximum return water temperature of 55°C on the predicted return water utilization of Kloof chilling installations

The utilization trends for the spreadsheet and CHILLER simulations showed rapidly diminishing increases for three chillers and four chillers due to controlled operation at part load to remain a the specified maximum allowed return water temperature of 55°C. Multiple-chiller installations of real machines were predicted to follow the same general trend as chillers with a constant cycle efficiency of 60%, but at lower values of return water utilization.

When the maximum allowed return water temperature was increased from 55°C to 70°C, this change allowed all the chillers in both simulation groups to operate at full load. The resulting return water utilization by individual machines after the removal of this restriction is shown in Figure 5.3.

The only exception was the spreadsheet simulation of four chillers, which still required a small amount of capacity control to restrict the return water temperature to 70°C.

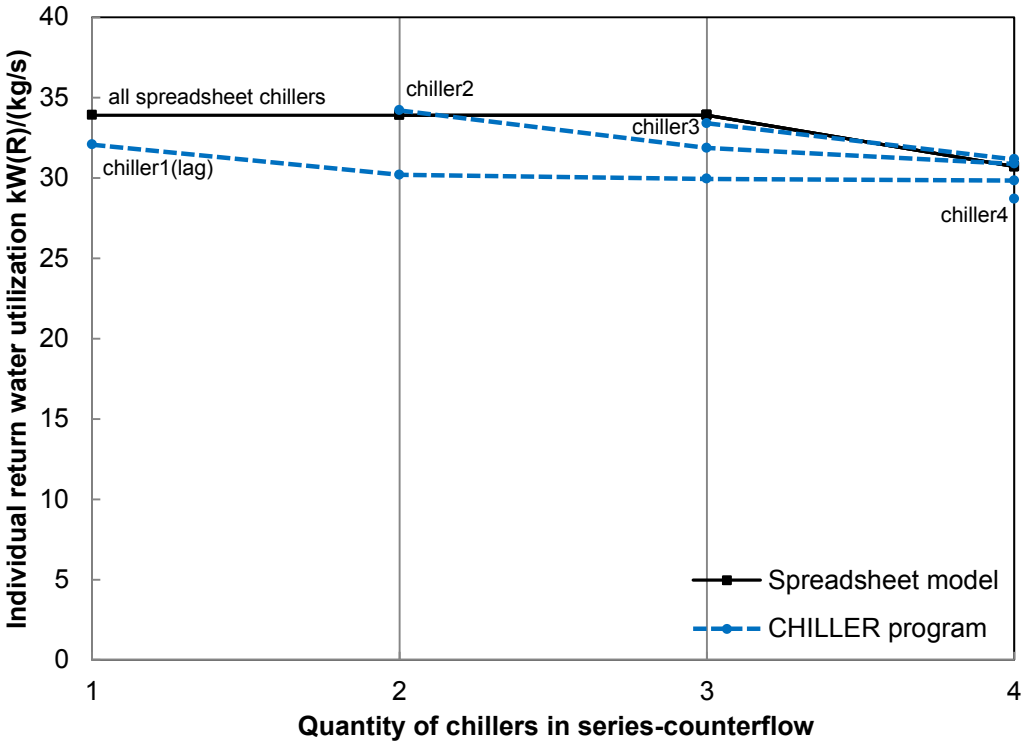

Figure 5.3 Effect of a maximum return water temperature of 70°C on the predicted return water utilization of Kloof chillers

The results for one and two machine configurations in Figure 5.3 are identical to those in Figure 5.1 because those simulations were also permitted to operate at full load, not reaching the return water temperature of 55°C. In Figure 5.3, for a 3 chiller configuration, the lead machine very nearly matched the return water utilization of its spreadsheet counterpart, due to higher evaporator pressure accompanied by a lower specific volume of refrigerant vapour.

In a four-machine configuration Chiller 4, in the lead position, operated with a high condenser pressure due to the elevated return water temperature, restricting its chilling load and hence its return water utilization.

For three and four machines at full load, the higher tube water velocity improved the evaporator water side heat transfer coefficients and hence the overall thermal conductance values, offsetting the negative effect of lower evaporator pressure in the lag chiller.

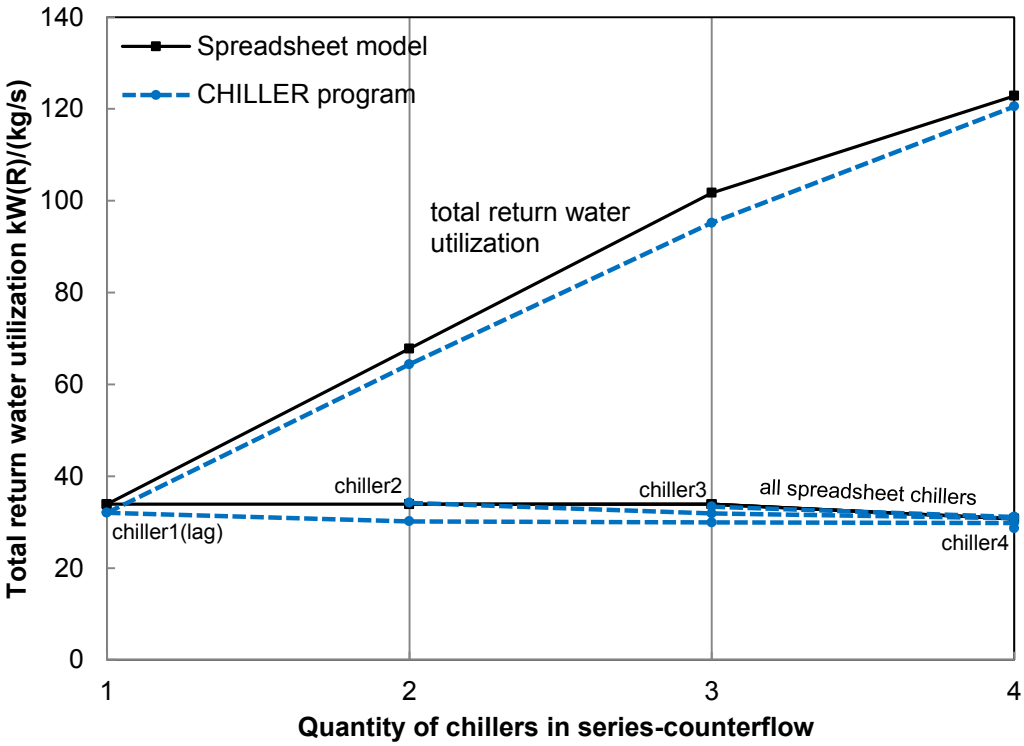

Figure 5.4 Effect of a maximum return water temperature of 70°C on the predicted return water utilization of Kloof chilling installations

Figure 5.4 illustrates the total return water utilization achieved by each configuration, with the individual values from Figure 5.3 reproduced for reference. With the 55°C return water temperature limit lifted to 70°C, the real machine configurations operated at full load, approaching the total return water utilization values predicted by the spreadsheet.

6 CONCLUSION

In review, the study aimed to assess how the refrigerating load of older, already installed chillers rejecting heat into a limited supply of return water could be maximized, by configuration of their water circuits and control of their compressors.

The first objective found that the condenser water circuits of chillers would have to be connected in series, this being the only practicable configuration of condensers that would permit a limited supply of return water to be used for heat rejection. Then, connecting an installation's evaporator water circuits in series as well, and supplying return water to the lag condenser first and water for chilling to the lead evaporator first, would enable the installation to run as a series-counterflow arrangement, thus minimizing the refrigerant temperature lift required of each chiller, and so encouraging an improvement of its COP.

The second objective framed the investigation in the theoretical context of the Lorenz concept, which is quantified by the Lorenz COP, thus providing the means to describe any installation's theoretical maximum chilling efficiency, based only on the initial and final water temperatures of the return- and evaporator water streams.

The third and fourth objectives compared the refrigerating loads and associated parameters from two types of simulations to assess the practicability of maximizing total refrigerating load in multiple-chiller installations. The first type of simulation used a spreadsheet model to quantify the potential maximum refrigerating loads that installations might achieve at best, creating the reference to which simulations of real chillers could be compared. The second type of simulation used the CHILLER program to model real chillers at a higher level of detail, and so quantify the expected refrigerating loads that real chillers should achieve.

The more realistic CHILLER simulations indicated that real machines would not conform to the assumptions of the spreadsheet model. Real machines would not operate with fixed, or equal, cycle efficiencies for several related reasons.

a) The isentropic efficiencies of the compressor stages varied with their operating points

b) Efficiency of the heat transfer in evaporator and condenser was not constant, decreasing for a larger log mean temperature difference between water and refrigerant, impacting cycle efficiency directly.

c) The water heat transfer coefficients increased with increasing tube water velocity, brought about by the changes in cool water flow rate through the evaporators as additional machines were added. Also, conversions from three to one pass, and from four to two passes in the evaporators decreased the water flowrate in several cases to a below optimal tube water velocity. Increases in the overall heat transfer coefficients tended to lower the heat exchanger LMTD, and vice versa.

Real machines would not perform equal temperature reduction steps as assumed, because the higher the evaporator pressure, the higher is the vapour density entering the compressor, and hence the higher are the refrigerant mass flowrate and chilling load. A real lead machine would be expected to deliver a higher chilling load and evaporator water temperature reduction than the downstream machines.

The first CHILLER simulation of a single Kloof machine achieved only 24% of its Lorenz COP due to low isentropic efficiencies in its compressor stages and a subsequent cycle efficiency of 41%. However, it still closely approached the return water utilization delivered by its more efficient

spreadsheet counterpart, indicating that a poorly performing chiller might match predictions, although for the penalties of a greater compressor absorbed power and thus a higher final return water temperature.

Similarly, Kloof and Tau Tona pairs of simulated real machines operated with cycle efficiencies well below 60%, but each pair again achieved return water utilization similar to that delivered by the higher efficiency models in the spreadsheet, though again for higher compressor power consumption and a higher final temperature of the return water. This emphasized that a group of chillers operating at maximum load but poor cycle efficiency might still make good use of return water by virtue of their arrangement in series-counterflow. As noted in Chapter 5 however, this approach does not maximize the use of return water. Rather, the use of the series-counterflow arrangement would minimize the reduction in chilling load caused by poor cycle efficiencies.

The fifth objective of the study showed that if the maximum return water temperature is reached by an installation, and capacity control is required to prevent the return water temperature from increasing any further, the ability of the machines to maintain acceptable cycle efficiency at moderate to severe part load becomes very important. A CHILLER simulation of three Kloof machines, when regulated to remain at a return water temperature of 55°C, predicted a total return water utilization 7.9% less than the spreadsheet model, for identical environmental conditions. For vane closure of 47%, the stage 1 compressor efficiencies of all three machines were extremely low, of the order of 30%. The return water utilization decreased by a lesser amount than this, because the stage 2 compressors on all three machines operated very close to design conditions, thus partially compensating for the poor stage 1 compressor efficiencies.

The preceding simulation also exhibited an 11.54% increase in return water utilization over a simulated lead lag pair. The same move to three machines in the spreadsheet equivalent increased the utilization by 14.99%. So, the incremental improvements offered by using more machines in series-counterflow does appear to be worthwhile, even though the baseline for return water utilization is lower than suggested by the higher efficiency models.

In general, a larger-than-design return water flowrate is particularly useful given the poor part load efficiencies of the machines studied. Even with poor chilling efficiency, which raises the final return water higher than it would otherwise would have been, the larger flowrate ensures that the return water temperature limit is not reached, removing the possibility of any further efficiency reduction that would be caused by additional capacity control.

The case of three machines operating at full load under an increased maximum return water temperature of 70°C indicated that real chillers may approach the spreadsheet predictions for return water utilization and COP, if the compressor operating points were near the design values of inlet volumetric flow rate and isentropic head. In fact, when a fourth chiller was simulated, the installation closely approached the spreadsheet predictions, with a delivered chilling load (and thus return water utilization) only 1.9% lower.

Part duty operation with up to 50% vane closure may provide acceptable thermodynamic efficiency, but doing so wastes the capacity of an installation. If the return water could be rejected at some higher temperature, then a four, five or even six series-counterflow arrangement might require only minimal capacity control, achieving a higher utilization of the machine capacity.

Adding more machines while limiting the return water final temperature approaches the Lorenz COP more closely if the machines are able to maintain higher efficiency at part duty. However, with the drive to produce more refrigeration underground, the only reason for placing machines on part duty would be if the amount of return water available for heat rejection decreases.

This analysis suggests that existing multiple-machine installations may be configured in series-counterflow arrangements to increase obtainable chilling for a limited supply of return water. The *maximization* of obtainable chilling (suggested by an improvement in chilling *efficiency*) does not appear achievable with the centrifugal machines modelled in this study when the machines are regulated to limit the condenser water delivery temperature. This is because existing compressor isentropic efficiency falls significantly below the design value when regulated with inlet guide vanes on the first stage compressor.

Nonetheless, underground installations are able to deliver more chilling load by arranging a larger number of standard machines in series-counterflow, if the subsequently higher return water final temperature can be accommodated by the mine's infrastructure. This increase in obtainable chilling comes at an increase in input compressor power.

6.1 Opportunities for further research

The findings of this study would benefit from comparison with, and application to, real installations to see if real chillers would exhibit the expected refrigerating loads, trends and supporting parameter values modelled and calculated with the CHILLER program.

For soundly based appreciation of the accuracies and limitations of the CHILLER program's simulations over the range of compressor capacity regulation by inlet guide vanes on one or both stages of a two-stage centrifugal compressor, such simulations should be verified, wherever possible, by comparison with actual, accurate performance data obtained in the field[46].

Machines that are able to operate with higher efficiency, and maintain this efficiency at part duty, might be able to achieve the increases in return water utilization presented. A survey of current compressor, heat exchanger and refrigeration control technology to suit the environmental constraints and criteria modelled in this analysis would be useful. Installing modern or retrofitted chilling equipment might create opportunities to increase refrigerating loads beyond the expected loads indicated by the CHILLER program, towards the potential maximum performance simulated by the spreadsheet model. On such a foundation, the design and testing of multivariable feedback control algorithms, customised for underground environmental constraints, to optimize return water (or, more generally, available heat sink) utilization may prove useful.

The amount of return water in deeper mines may increase significantly due to the larger amounts of fissure water that are sometimes encountered at greater depth. This water may arrive with a temperature higher than 40°C and have an increased level of entrained and dissolved solids, requiring larger and more resilient underground water treatment facilities, coupled with appropriate heat exchanger tube materials in the chillers, to enable machines to use such return water. If this water is heated to a much higher temperature as well, then upgrades to

[46] An updated version of the program, FMChiller, was produced in 2004 (FutureMine Collaborative Research Programme, 2004), with improved modelling of components of water chilling machines with centrifugal compressors. However, this version can simulate only single machines, not multiple machines interconnected in their water circuits.

infrastructure to cope therewith would present additional costs[47].

Thom et al (2002) state that a mine must be evaluated individually if its existing cooling infrastructure is to be optimized for return water, and that, as far as possible, new or upgraded refrigeration capacity should be installed underground, utilizing all available return water for heat rejection.

Thus, if mines are to maximize the amount of chilling generated underground, the need for significant investment in upgrading infrastructure will be an important consideration. Real world parameters such as cost of new equipment and upgrades to existing equipment and infrastructure, underground space for installation, additional water pumping requirements, return water availability, payback period and optimal plant location need to be analysed collectively using a systematic method, possibly in the form of a customized software tool, to estimate lifetime costs for such systems, and thus evaluate the feasibility of any proposal to maximize the refrigerating load of underground machines.

[47] Although expenses such as the capital- and operating costs of de-watering pumps in a new installation might not be allocated to the return water heat rejection scheme, because the return water must be pumped to surface in any case. Of course, the return water being hotter may require the specification of more costly de-watering pumps to handle the higher water temperatures.

7 REFERENCES

ASHRAE (2000) Multistage vapour compression refrigeration cycles, *Fundamentals handbook*, pp. 1.1-1.35

ASHRAE (2002) Centrifugal liquid chillers, *Refrigeration handbook*, pp. 43.8-43.10

ASHRAE (2012) Handbook-HVAC Systems and Equipment, pp.43.1-43.16

Bailey-McEwan, M. (1998) Assessing Performance of Large Mine Water Chilling Machines Using Refrigerant-Circuit Measurements and Machine Modelling. PhD Thesis, 1998, University of the Witwatersrand, Johannesburg, South Africa.

Bailey-McEwan, M., *Design Performance of Machines on 100 Level, Western Deep Levels 2#*, Private Communication, 2002.

Bailey-McEwan, M., *Derivation of COP of a water chilling machine when the condenser outlet water temperature is unknown*, Private Communication, 2004.

Bailey-McEwan, M. and Burrows, J. H. J. (2014) Refrigeration Theory and Equipment, to be published in: *Occupational Environmental Engineering Handbook,* The Mine Ventilation Society of South Africa, 2014.

Bailey-McEwan, M. and Penman J. C. (1987) An Interactive Computer Program for Simulating the Performance of Water Installations on Mines, APCOM 87, Proceedings of the Twentieth International Symposium on the Application of Computer and Mathematics in the Mineral Industries Volume 1: *Mining.* Johannesburg, SAIMM, pp. 191-305.

Biffi, M. and Steenkamp, A. (1996) The use of clear water as a heat rejection medium at 3 sub vertical shaft, Kloof – A division of Kloof G. M. Co. Ltd, *Proceedings, FRIGAIR '96,* Johannesburg, South Africa, 11 p.

Bluhm, S. J., Hattingh, R., Funnell, R. C., Butterworth, M., Sheer, T. J. and Hemp, R. (2000) Generation and Distribution of Refrigeration for Ultra-Deep Mining: New Challenges and Insights, *Proceedings ASHRAE-FRIGAIR 2000 Congress*, Johannesburg, 8-10 March 2000.

Burrows, J. (1982) Refrigeration – Theory and operation, *Environmental Engineering in South African Mines*, The Mine Ventilation Society of South Africa, pp. 613-652.

Butterworth, M., Private Communication, 2001, Division of Mining Technology, CSIR, South Africa.

Dixon, J. R. (1998) Presidential Address: Witwatersrand gold - quo vadis?, *Journal of the South African Institute of Mining and Metallurgy*, Vol. 98, No. 5, pp. 213-219.

Facts and Figures 2004, Chamber of Mines of South Africa. INTERNET. No address available at 29 January 2015. Cited 11 March 2006.

Facts and Figures 2012, Chamber of Mines of South Africa INTERNET.https://commondatastorage.googleapis.com/comsa/facts-and-figures-2012.pdf. Cited 8 September 2013.

FutureMine Collaborative Research Programme (CSIR Miningtek, Bluhm Burton Engineering, University of the Witwatersrand), 2004: FMChiller Refrigeration Plant Simulation Software. *This software is restricted to the agencies participating in this Collaborative Research Programme*.

Gosney, W. B. (1982) Principles of Refrigeration, Cambridge University Press, Cambridge, United Kingdom.

Hattingh, R., Butterworth, M. and Thom, M. (2000) Evaluation of cooling generation systems for ultra-deep level mining. Deepmine Project Report 6.4.1, Division of Mining Technology, CSIR, pp. 1-40.

Marx, W., Butterworth, M. and Bluhm, S. (2001) Controlling the Environment: Refrigeration and Ventilation, *DEEPMINE Colloquium 2001*, pp. 33-38.

Pulles W. (1992) Water Pollution: Its Management and Control in the South African Gold Mining Industry, *Journal of the Mine Ventilation Society of South Africa,* Vol. 45, No. 2, February 1992, pp. 18-36.

Ramokgopa, S. J., (2002) Presidential Address: The political economy of mining and metallurgy, *Journal of The South African Institute of Mining and Metallurgy*, Vol. 102, No. 6, pp. 321-328.

Ramsden, R., Sheer, T. J. and Butterworth, M. (2001) Design and simulation of ultra-deep mine cooling systems, *Proceedings of the 7th international mine ventilation congress*, Krakow, Poland, pp. 756-760.

Stoddard and Lakmidas (2013). INTERNET.http://www.bdlive.co.za/business/mining/2013/07/08/news-analysis-as-golds-bubble-bursts-sas-mines-look-sure-to-be-the-worst-hit). Cited 12 December 2013.

Stroh, R M. (1982) Chilled Water Reticulation, in: Environmental Engineering in South African Mines, the Mine Ventilation Society of South Africa, pp. 653-683.

Tedder, H. A. (1982) Water Management in Mining, Environmental Engineering in South African Mines, The Mine Ventilation Society of South Africa, pp. 893-910.

Thom, M., Butterworth, M., Bailey-McEwan, M. and Wright, C. (2003) FutureMine Research Task 7.1.3: Final Report (Year 2) Improved Heat Rejection for Underground Refrigeration Machines, Report Number: EC 03-0093, Division of Mining Technology, CSIR, 85p. *This report is not an open publication, but is restricted to the agencies participating in this Co-Operative Research Programme*.

Thom, M., Butterworth, M., Ox, I., Bailey-McEwan, M. and Wright, C. (2002) FutureMine Research Task 7.1.3: Final Report (Year 1) Improved Underground Heat Rejection, Report Number: EC 02-0253, Division of Mining Technology, CSIR, 50 p. *This report is not an open publication, but is restricted to the agencies participating in this Co-Operative Research Programme*.

Thomson Reuters GFMS (2013) *Gold Survey 2013*. INTERNET. https://forms.thomsonreuters.com/gfms/. Cited 9 May 2014.

Van der Walt, J. (1979) Engineering of refrigeration installations for cooling mines, *The South African Mechanical Engineer*, Vol. 29, October, pp. 360 - 372.

Van der Walt, J. and de Kock, E. M. (1984) Developments in the engineering of refrigeration installations for cooling mines*, International Journal of Refrigeration*, Vol. 7 No. 1, January, pp. 27-40.

Wilson, R., Bluhm, S. and Van Den Berg, L. (2012) Energy Management of Refrigeration Systems within Deep Mines in South Africa, Deep Mining 2012, *Proceedings of the Sixth International Seminar on Deep and High Stress Mining*, 28-30 March 2012, Perth, Australia, pp. 453-462.

8 APPENDIX A SPREADSHEET MODEL AND CHILLER PROGRAM COMPARATIVE PLOTS

This appendix presents comparative plots for simulation results of the spreadsheet model and CHILLER computer program. The lines which link data points are used to identify general trends and present a linear interpolation between any two consecutive points.

8.1 Kloof mine

8.1.1 A specified limit of 55°C on the final return water temperature

This section plots selected results from Appendix B: Sections 9.1.1, 9.1.2, 9.1.3, 9.1.4, 9.2.1, 9.2.2, and 9.2.3.

Evaporator water inlet temperatures

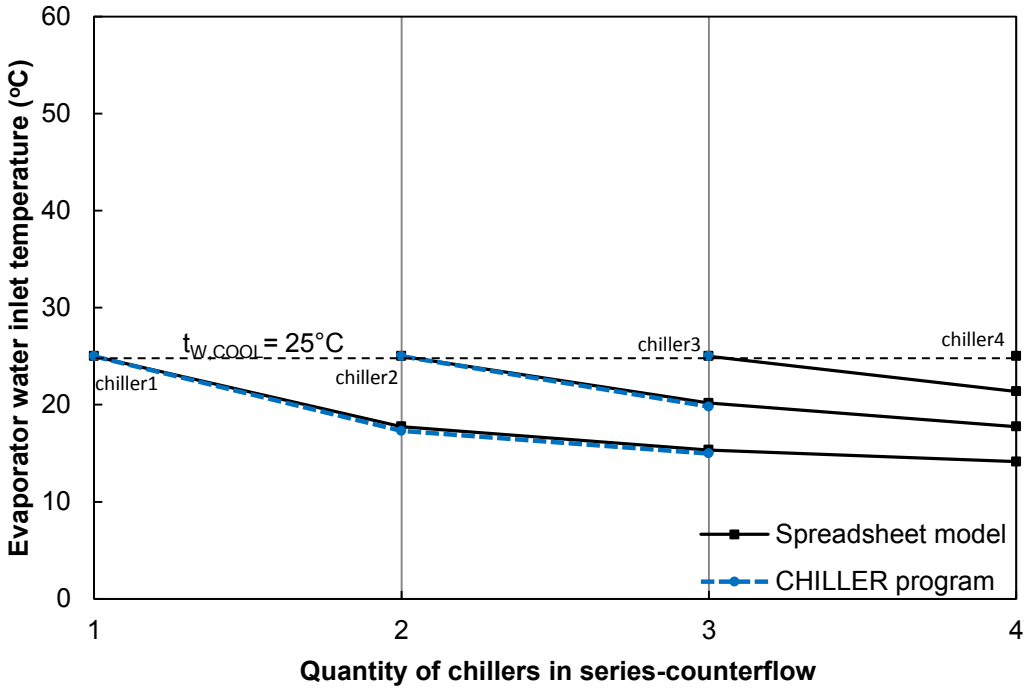

Figure 8.1 Variation of evaporator water inlet temperatures with chiller quantity

The machine labelled ‘Chiller 1’ in figure 8.1 begins alone and then retains the position of lag chiller in subsequent simulations, as additional machines are added ahead of it. The second chiller added is initially in the lead position, but is then displaced from this position by the addition of the third chiller. This pattern continues as further chillers are added, and is applicable for all of the figures in Appendix A. The definitions of lead and lag chiller, along with condenser and evaporator configurations, are given in Section 2.3.5.

Evaporator water outlet temperatures

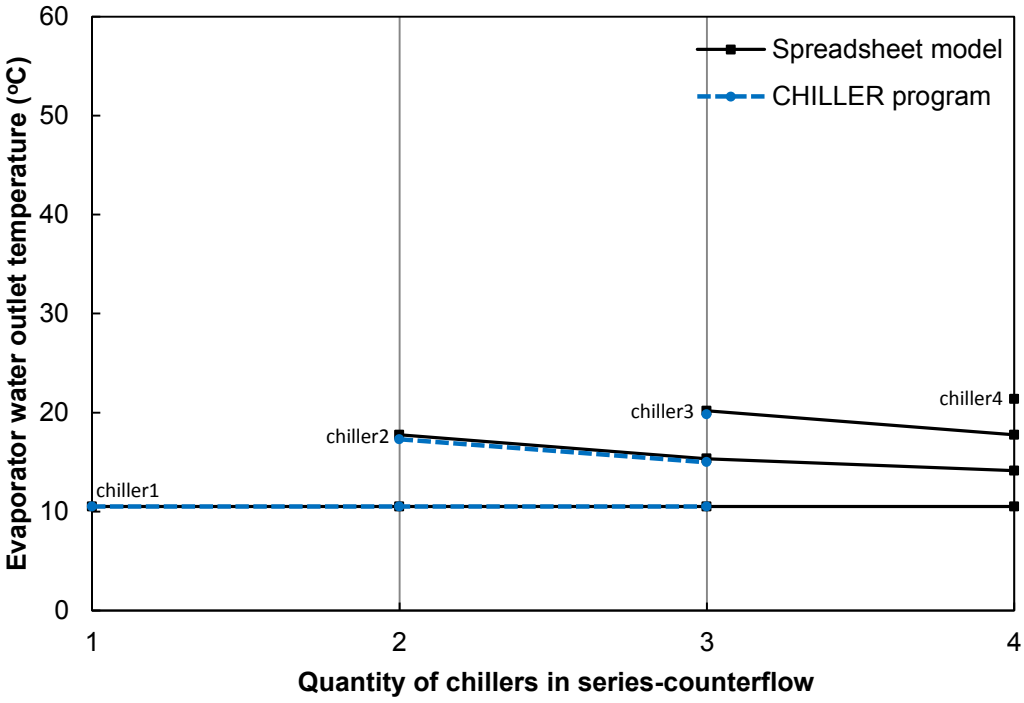

Figure 8.2 Variation of evaporator water outlet temperatures with chiller quantity

Evaporator overall thermal conductance

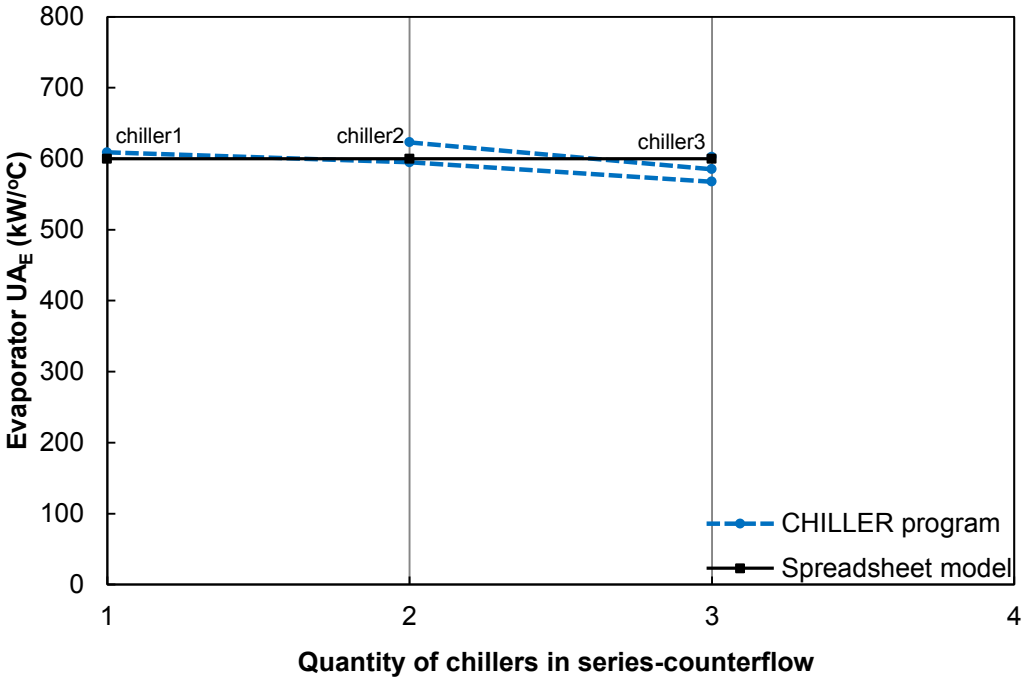

Figure 8.3 Evaporator UA variation with chiller quantity

Evaporator refrigerant temperatures

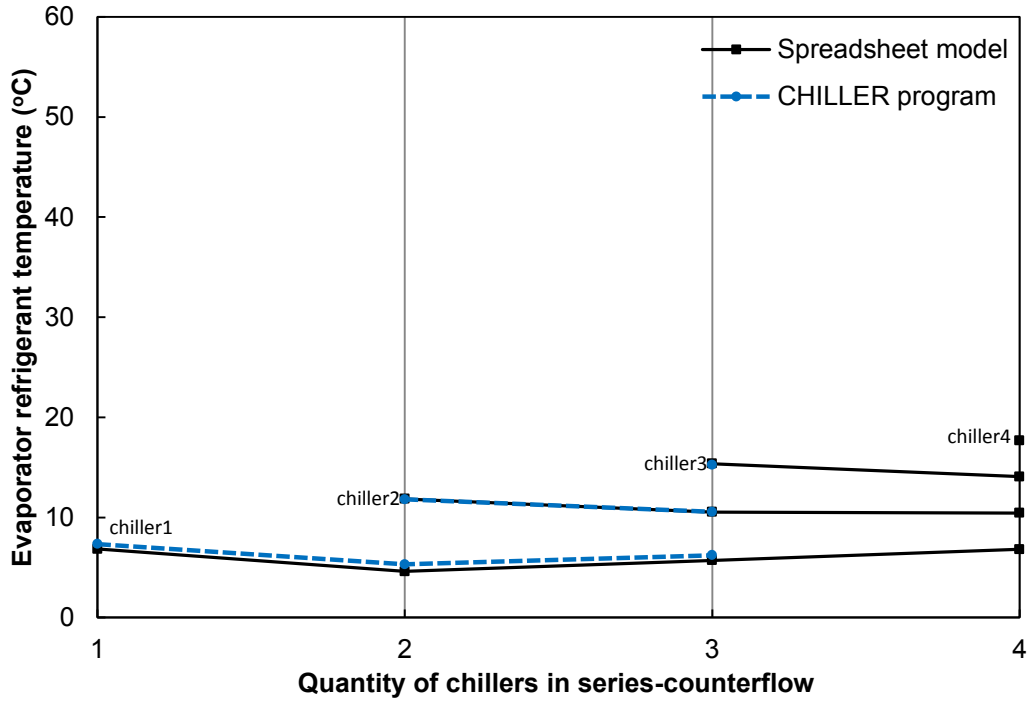

Figure 8.4 Variation of evaporator refrigerant temperatures with chiller quantity

Evaporator log-mean temperature difference (LMTD)

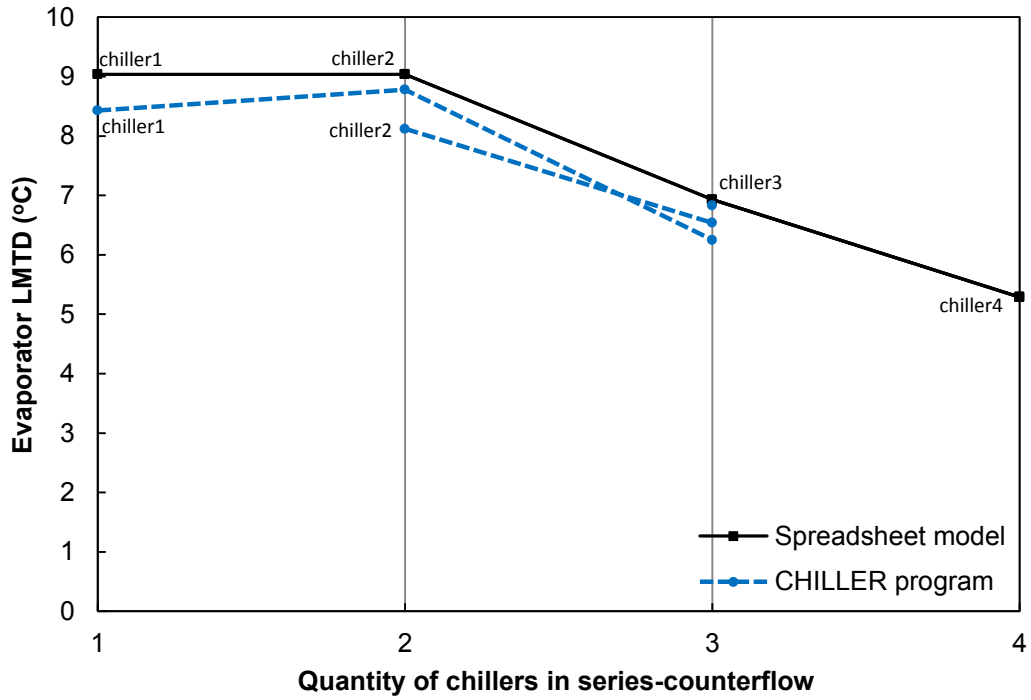

Figure 8.5 Variation of evaporator LMTD with chiller quantity

Evaporator chilling load

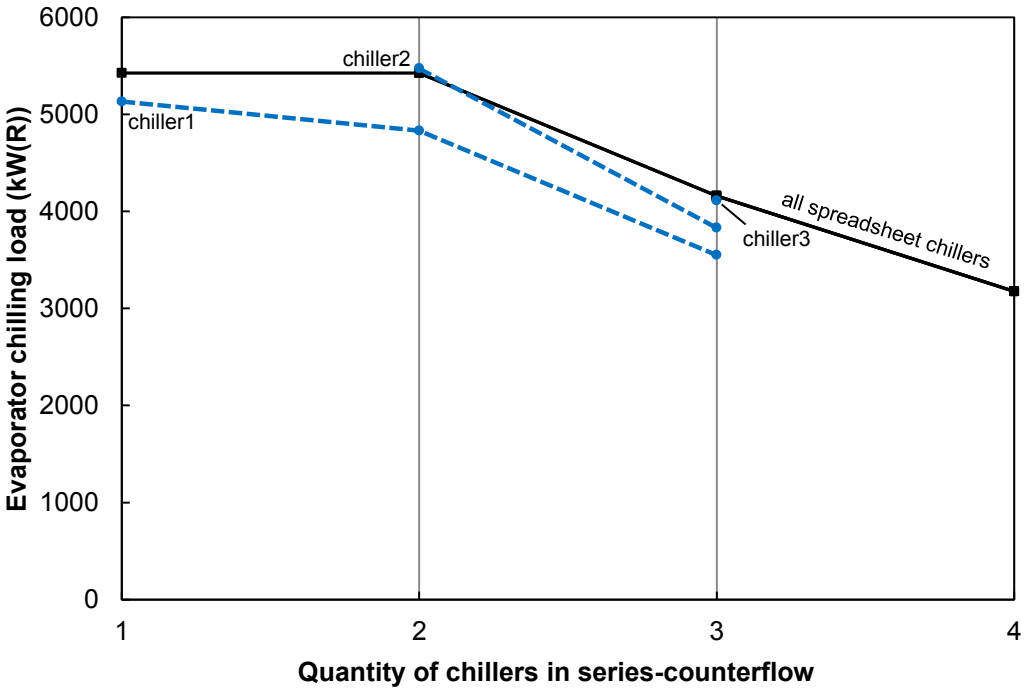

Figure 8.6 Variation of evaporator chilling load with chiller quantity

Condenser overall thermal conductance

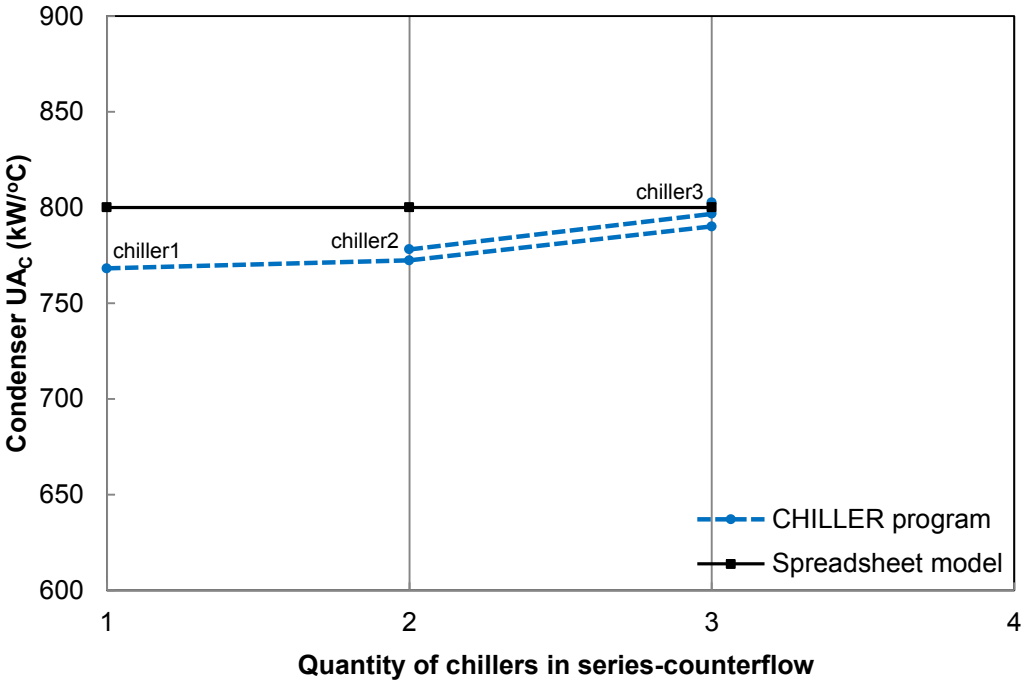

Figure 8.7 Condenser overall thermal conductance variation with chiller quantity

Condenser refrigerant temperature

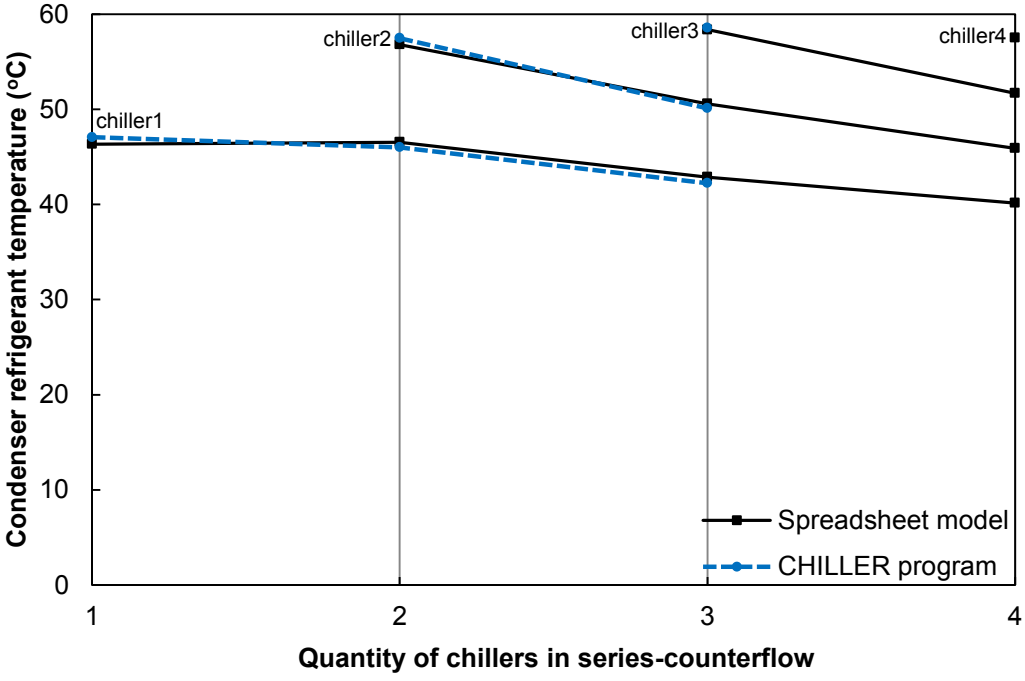

Figure 8.8 Variation of condenser refrigerant temperature with quantity of chillers

Condenser log-mean temperature difference (LMTD)

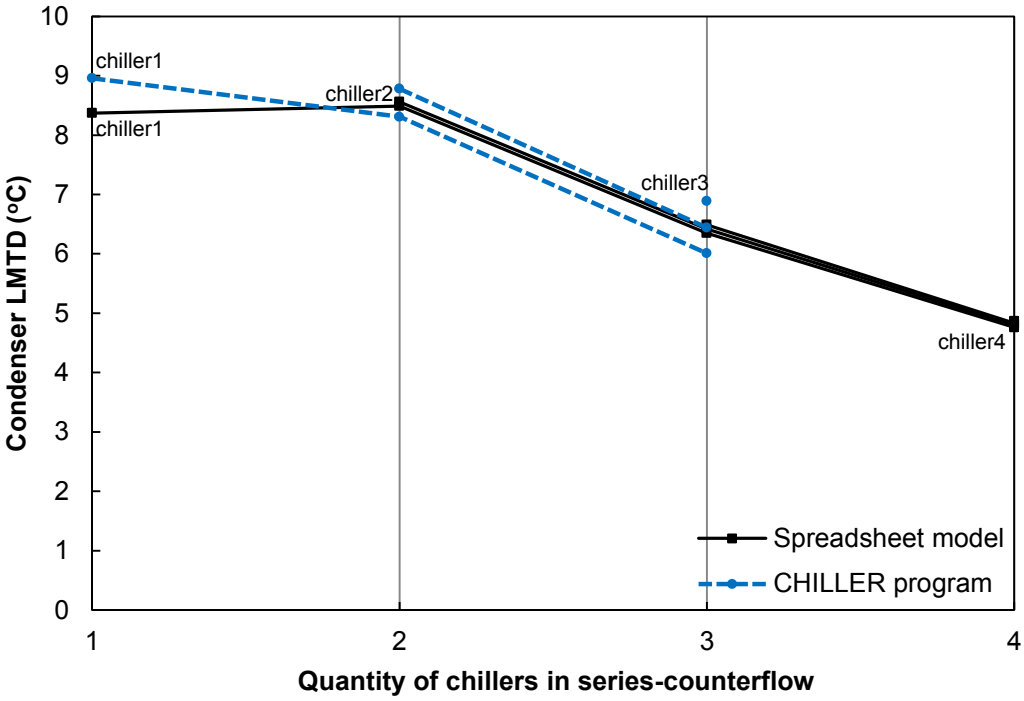

Figure 8.9 Variation of condenser log-mean temperature difference (LMTD)

Condenser water inlet temperatures

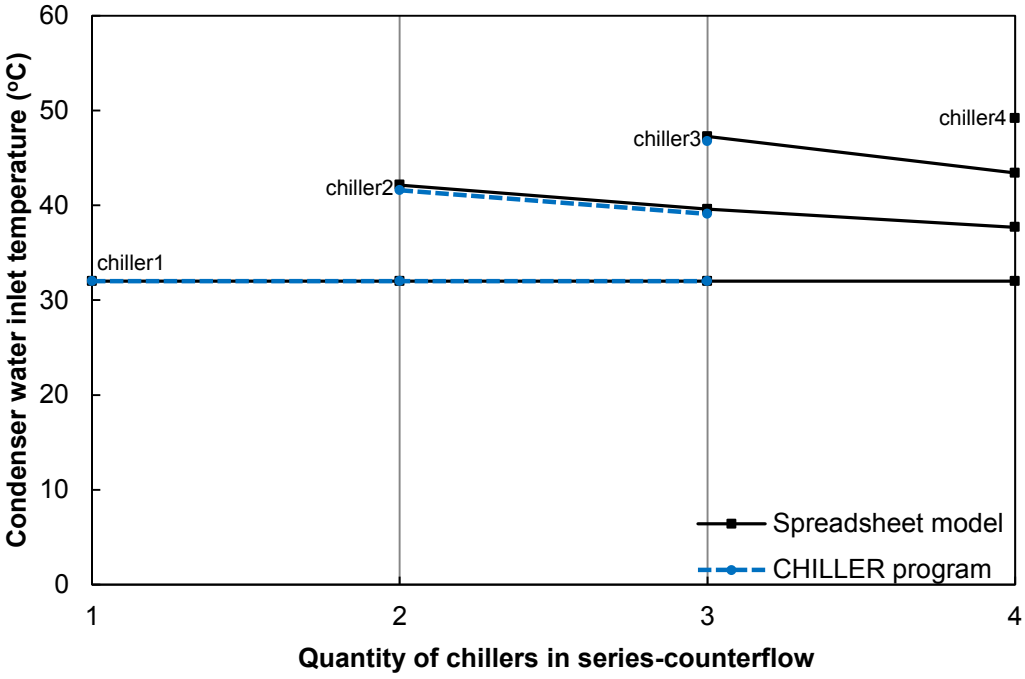

Figure 8.10 Variation of condenser water inlet temperatures with chiller quantity

Condenser water outlet temperatures

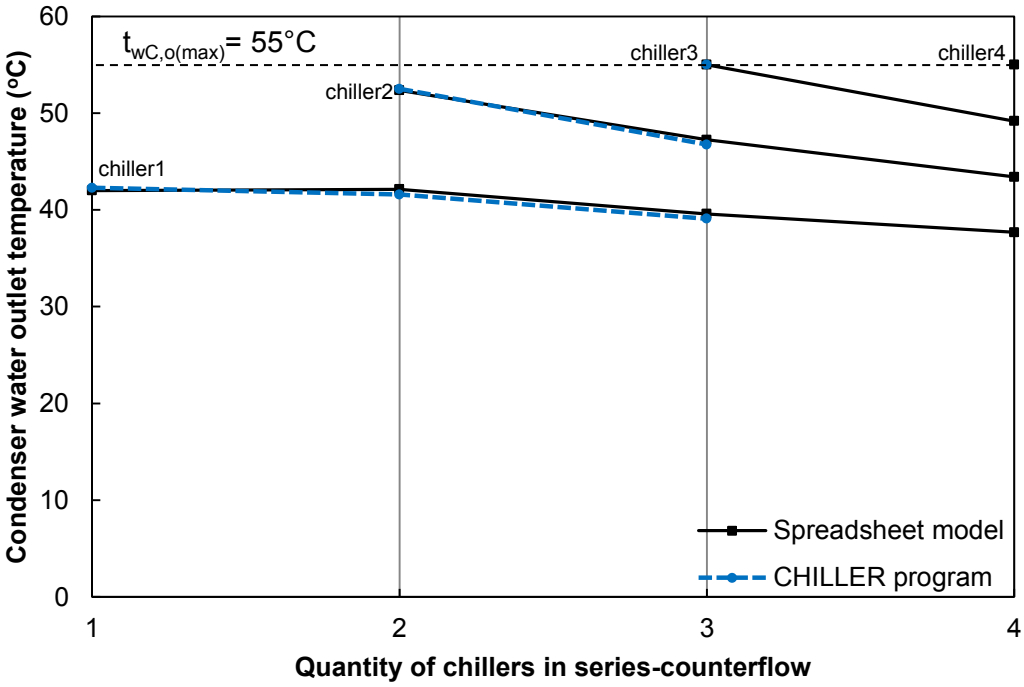

Figure 8.11 Variation of condenser water outlet temperatures with chiller quantity

System chilling load

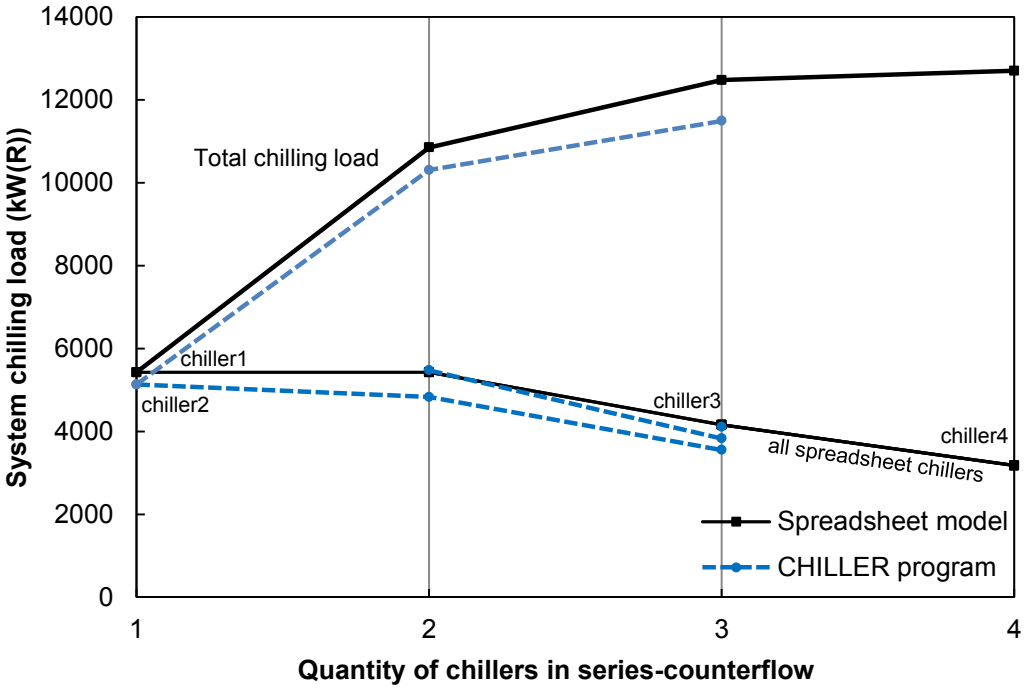

Figure 8.12 Variation of evaporator chilling load with chiller quantity

Carnot coefficient of performance

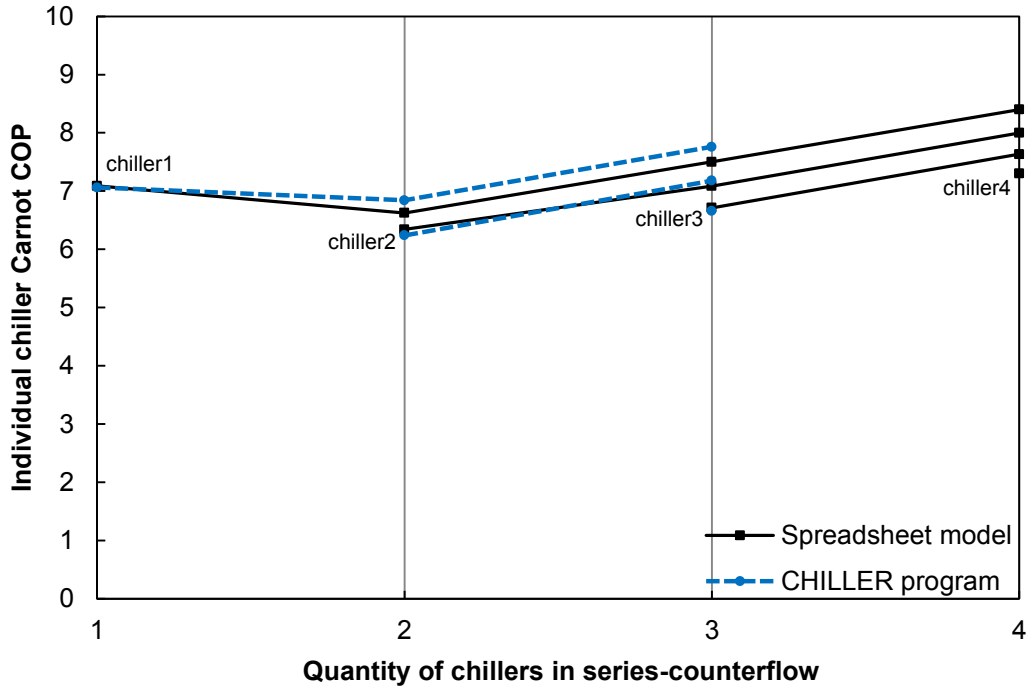

Figure 8.13 Variation of individual chiller Carnot COP with chiller quantity

Coefficient of performance

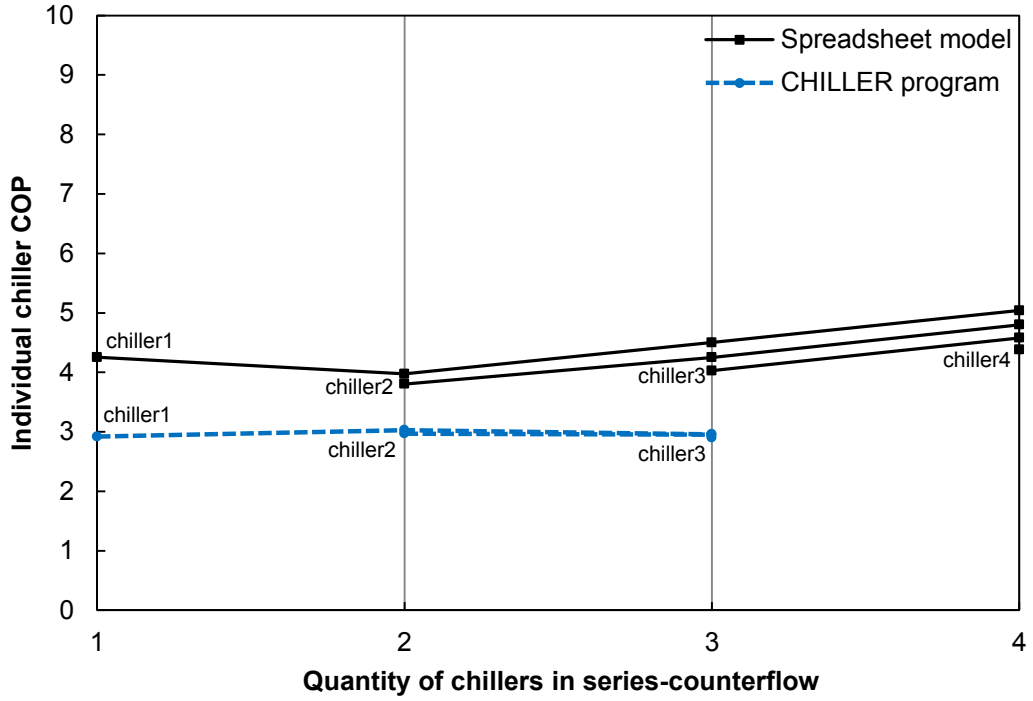

Figure 8.14 Variation of chiller COP with chiller quantity

Compressor input power

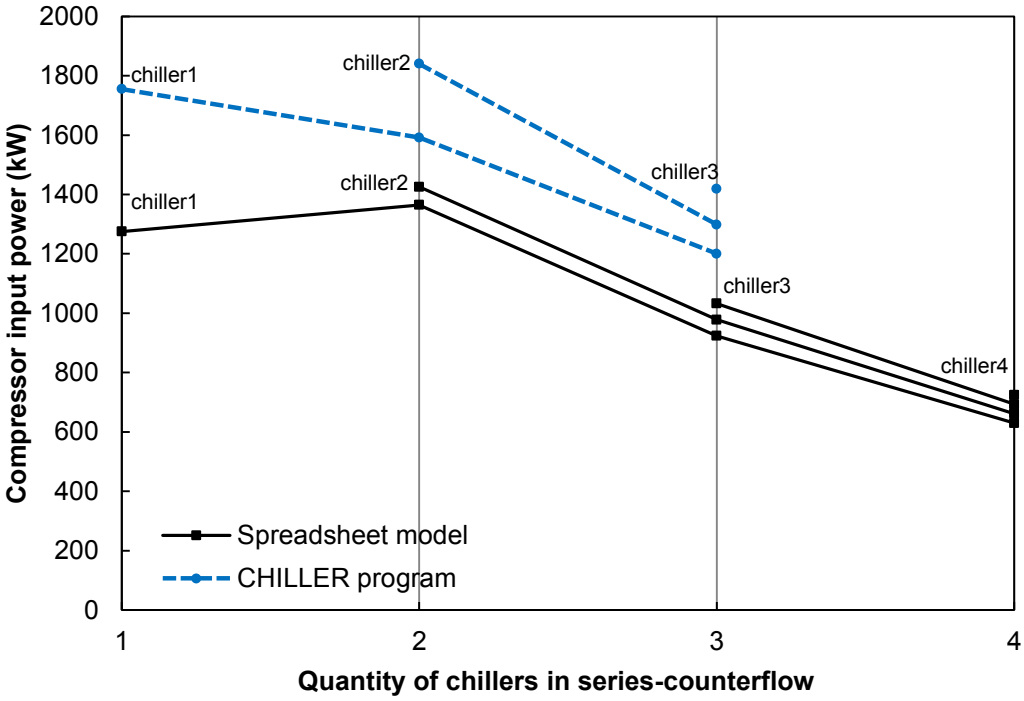

Figure 8.15 Variation of compressor (combined stages 1 & 2) input power with chiller quantity

Stage 2 compressor isentropic efficiency

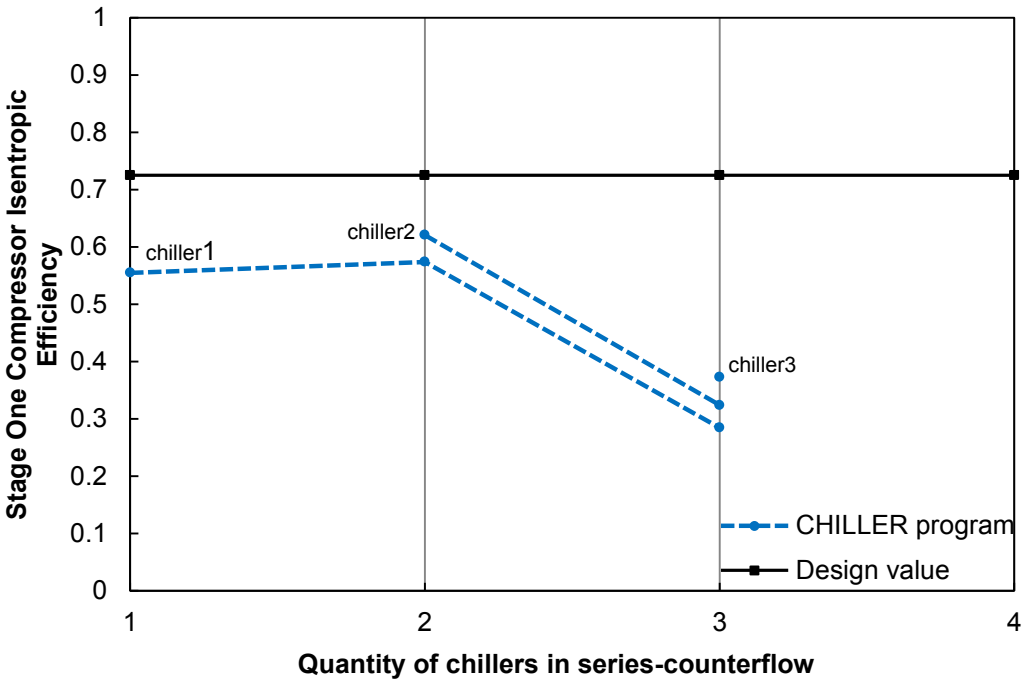

Figure 8.16 First stage compressor isentropic efficiency - CHILLER program

Stage 2 compressor isentropic efficiency

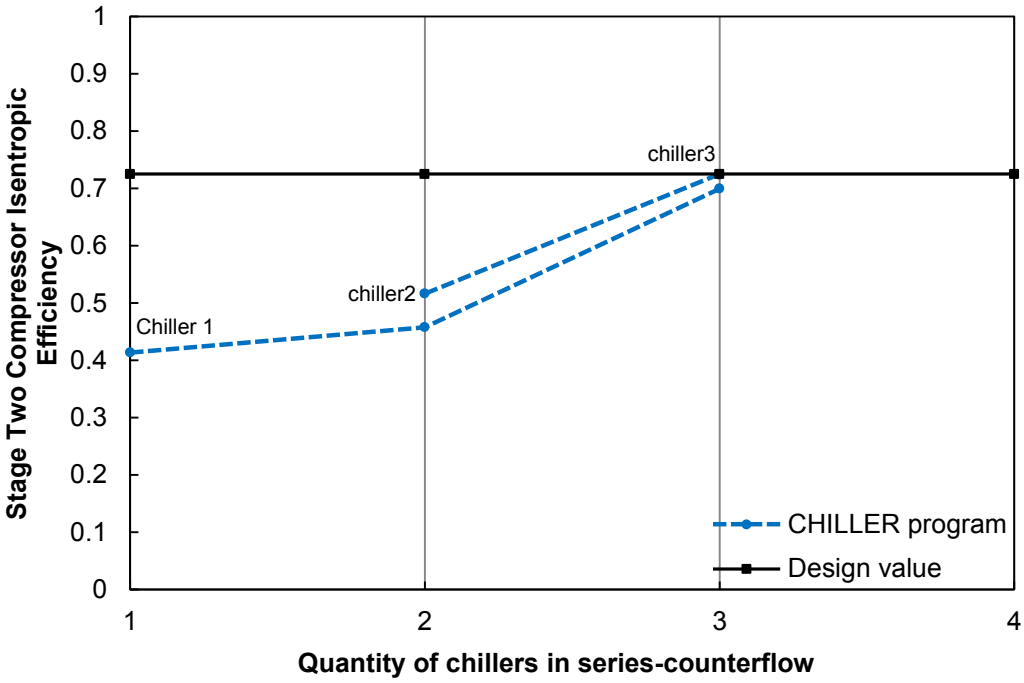

Figure 8.17 Second stage compressor isentropic efficiency - CHILLER program

Cycle efficiency

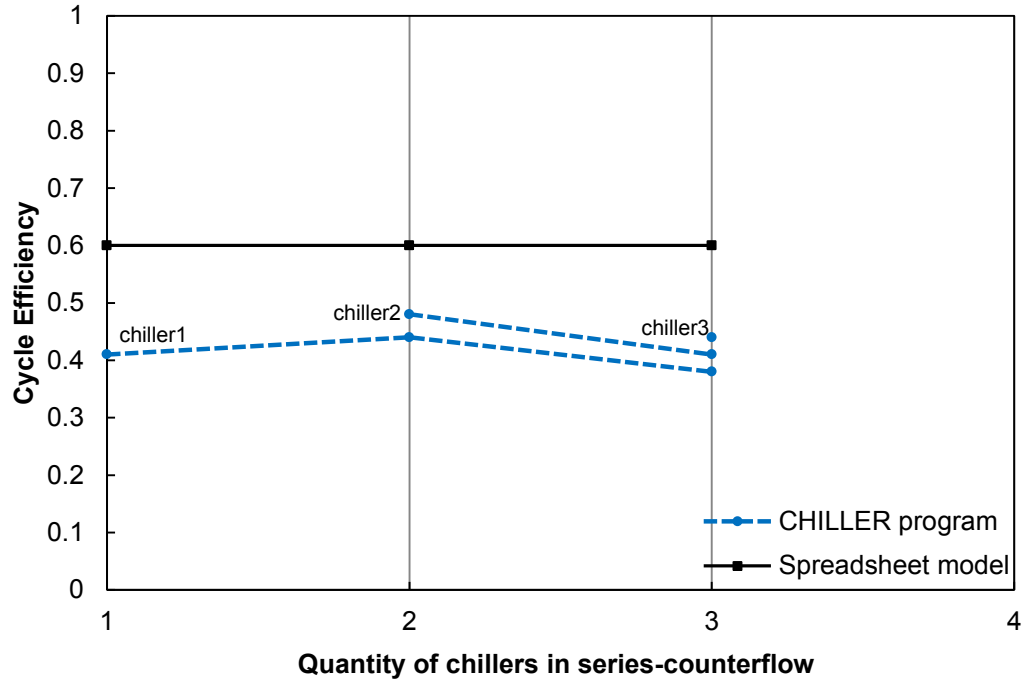

Figure 8.18 Variation of machine cycle efficiency with chiller quantity

8.1.2 Increased specified limit on the final return water temperature, to 70°C

This section plots selected results from Appendix B: Sections 9.1.5, 9.1.6, 9.2.4, and 9.2.5. It also repeats the results from Appendix B: 9.1.1, 9.1.2, 9.2.1, and 9.2.2 plotted in Section 8.1.1.

Evaporator water inlet temperature

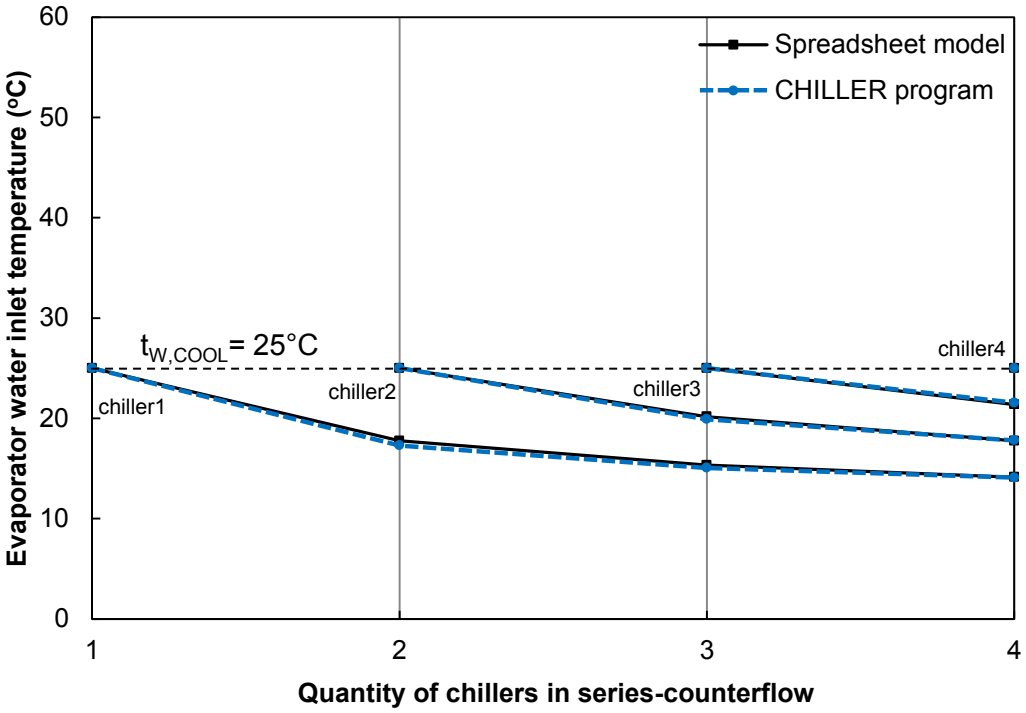

Figure 8.19 Variation of specified evaporator water inlet temperatures with chiller quantity

Evaporator water outlet temperatures

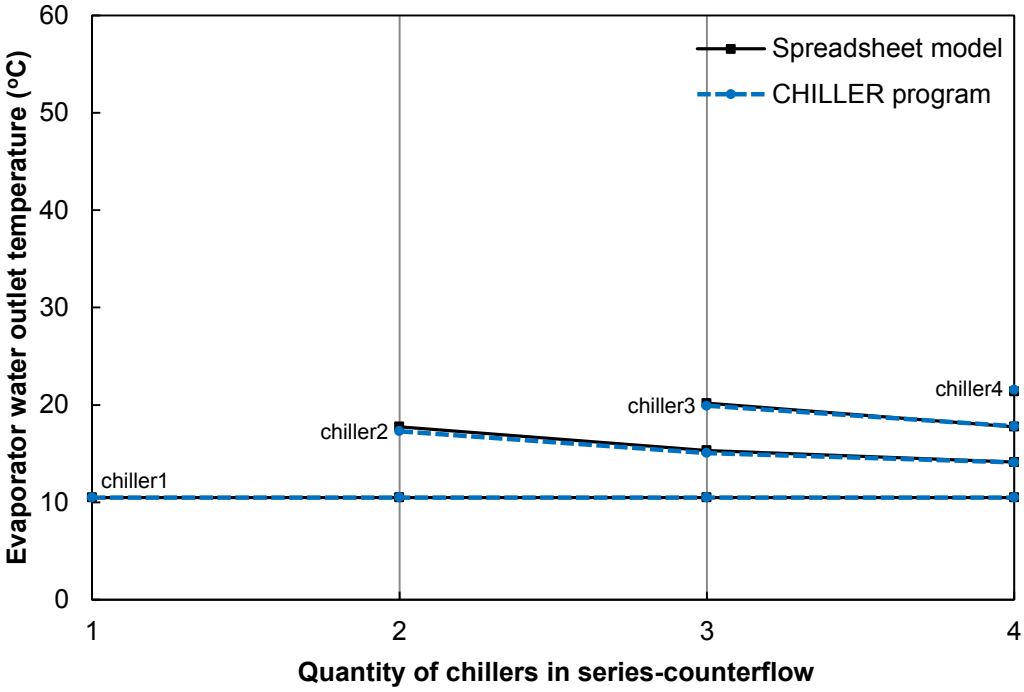

Figure 8.20 Variation of evaporator water outlet temperatures with chiller quantity

Evaporator overall thermal conductance

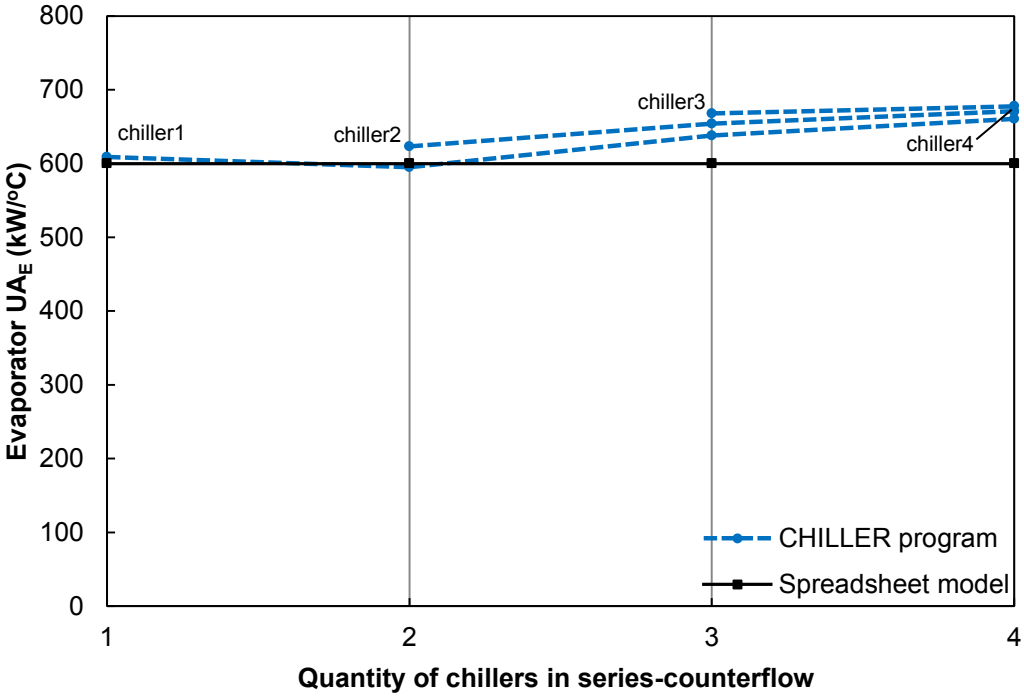

Figure 8.21 Variation of evaporator overall thermal conductance with chiller quantity

Evaporator refrigerant temperature

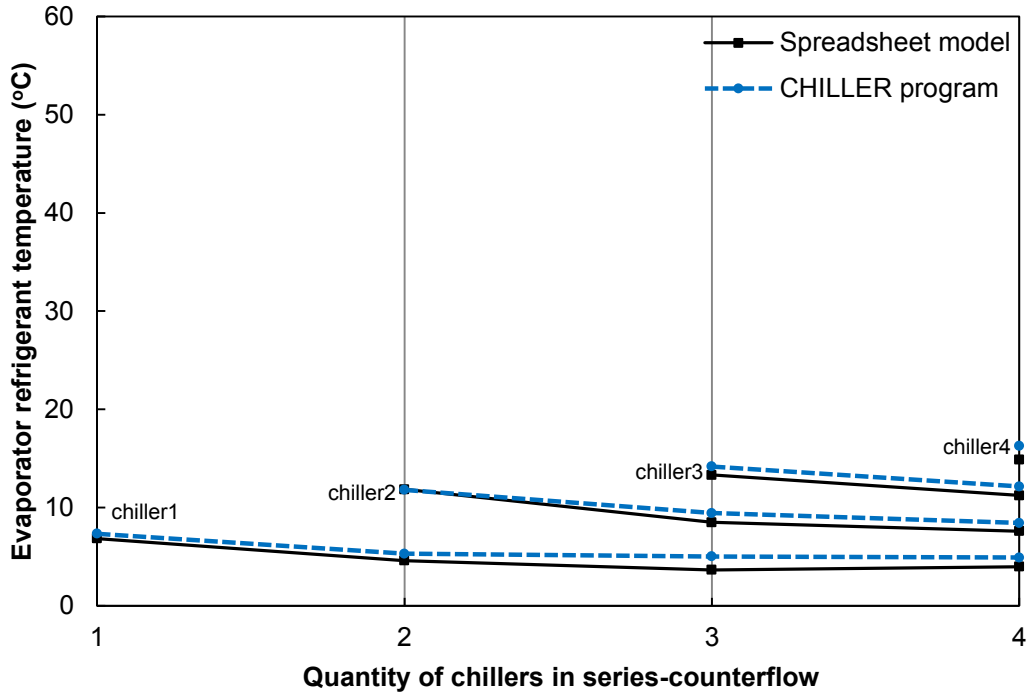

Figure 8.22 Variation of evaporator refrigerant temperatures with chiller quantity

Evaporator log-mean temperature difference

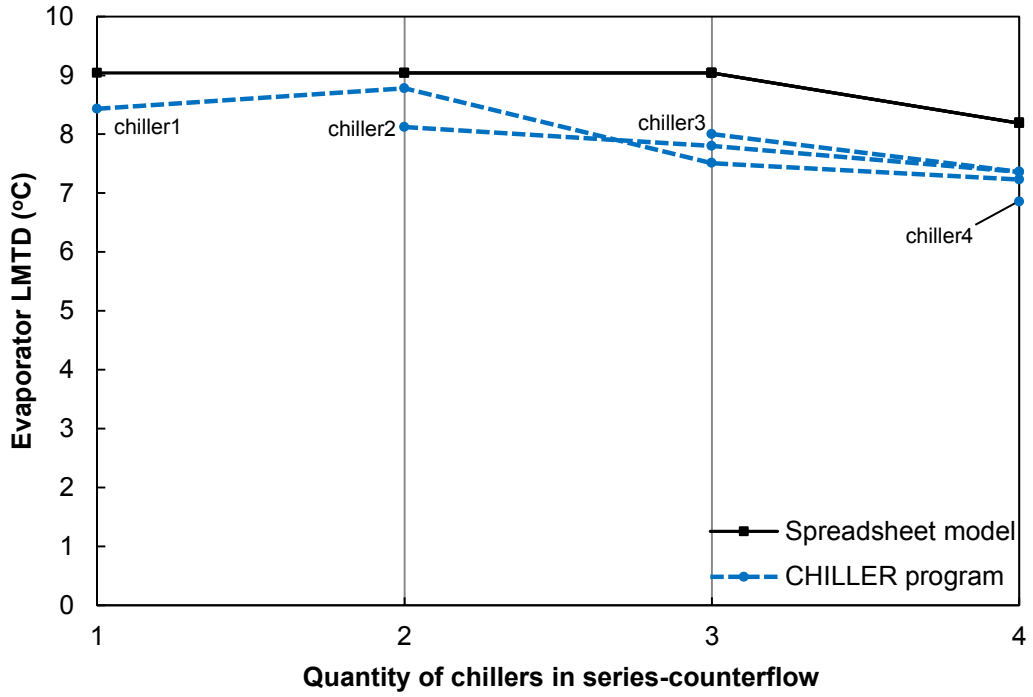

Figure 8.23 Variation of evaporator LMTD with quantity of chillers

Evaporator chilling load

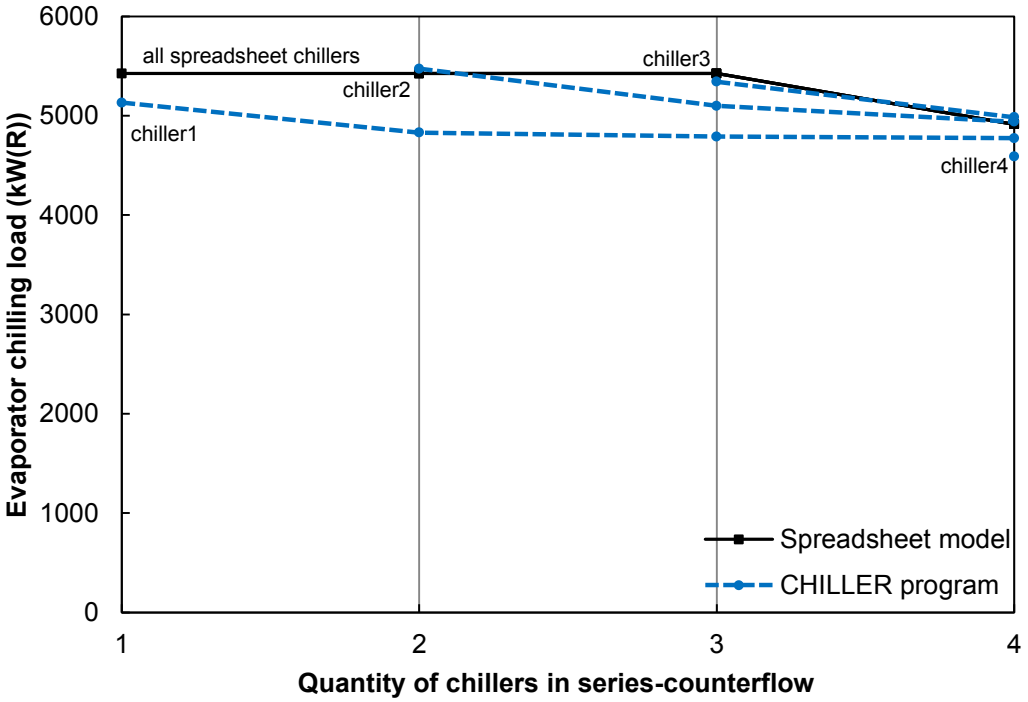

Figure 8.24 Variation of evaporator chilling load with quantity of chillers

Condenser overall thermal conductance

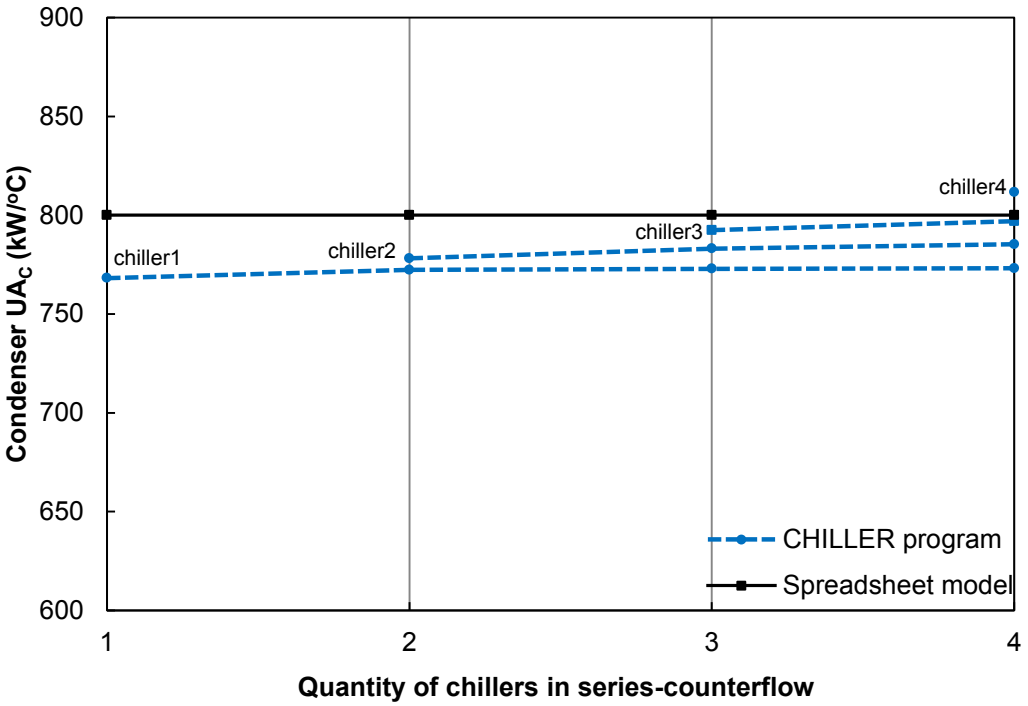

Figure 8.25 Variation of condenser overall thermal conductance with quantity of chillers

Condenser refrigerant temperature

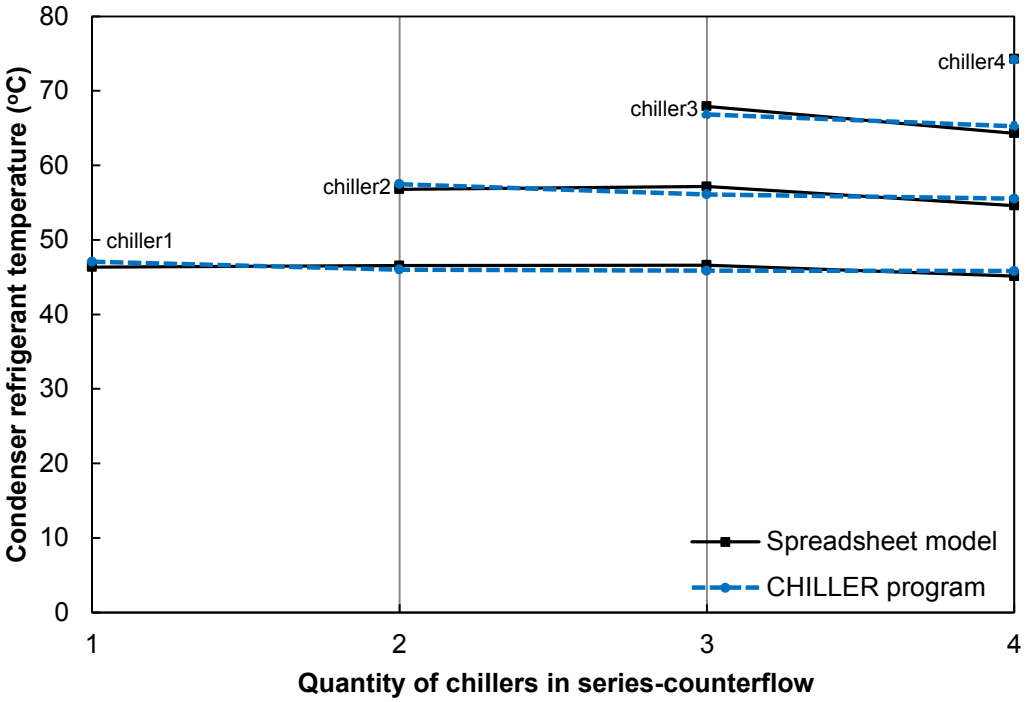

Figure 8.26 Variation of condenser refrigerant temperatures with chiller quantity

Condenser log-mean temperature difference

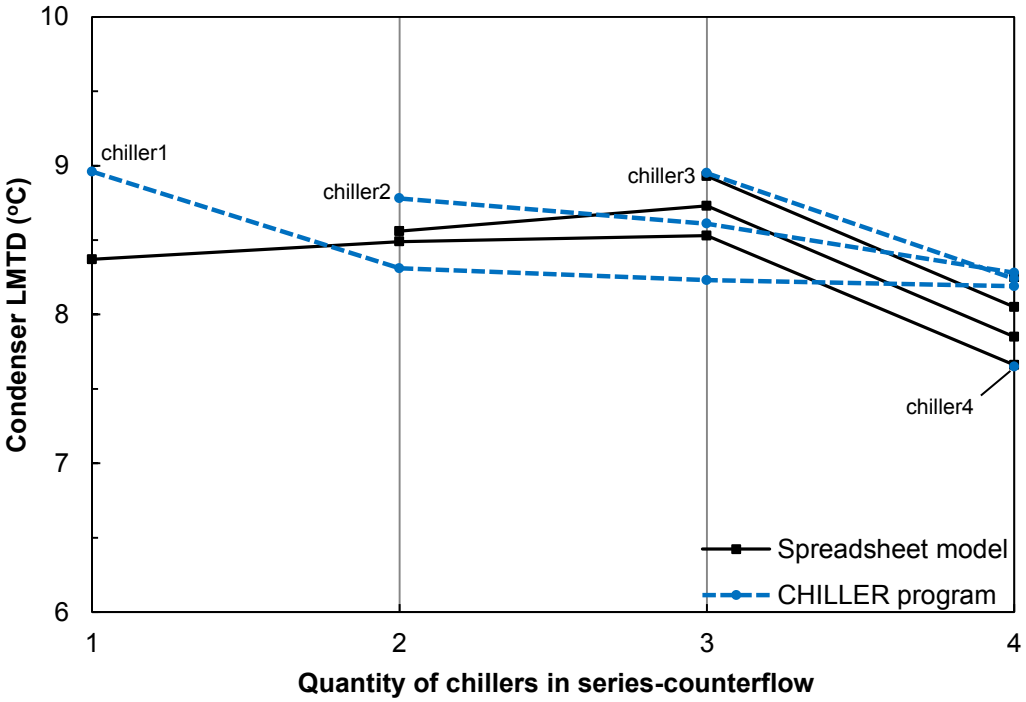

Figure 8.27 Variation of condenser LMTD with quantity of chillers

Condenser water inlet temperature

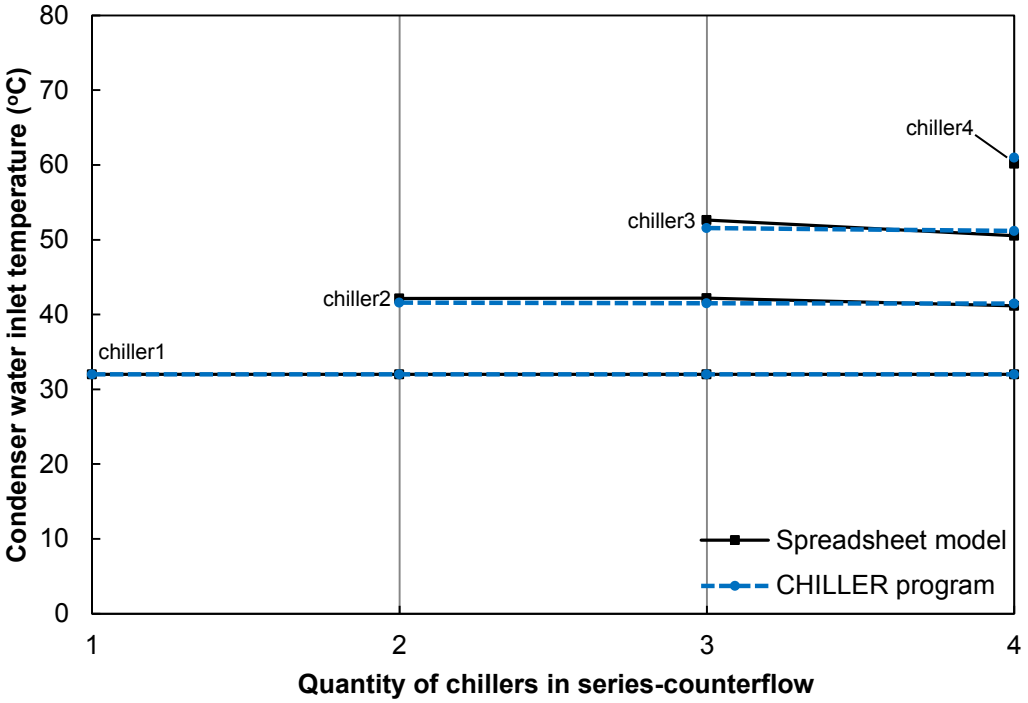

Figure 8.28 Variation of condenser water inlet temperature with quantity of chillers

Condenser water outlet temperature

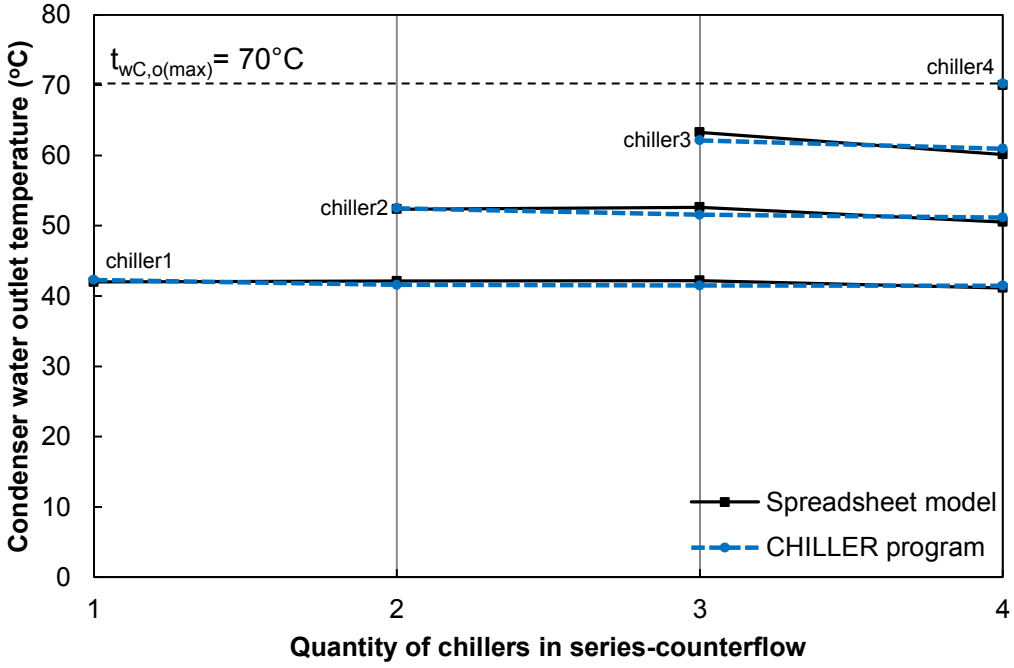

Figure 8.29 Variation of condenser water outlet temperatures with chiller quantity

System chilling load

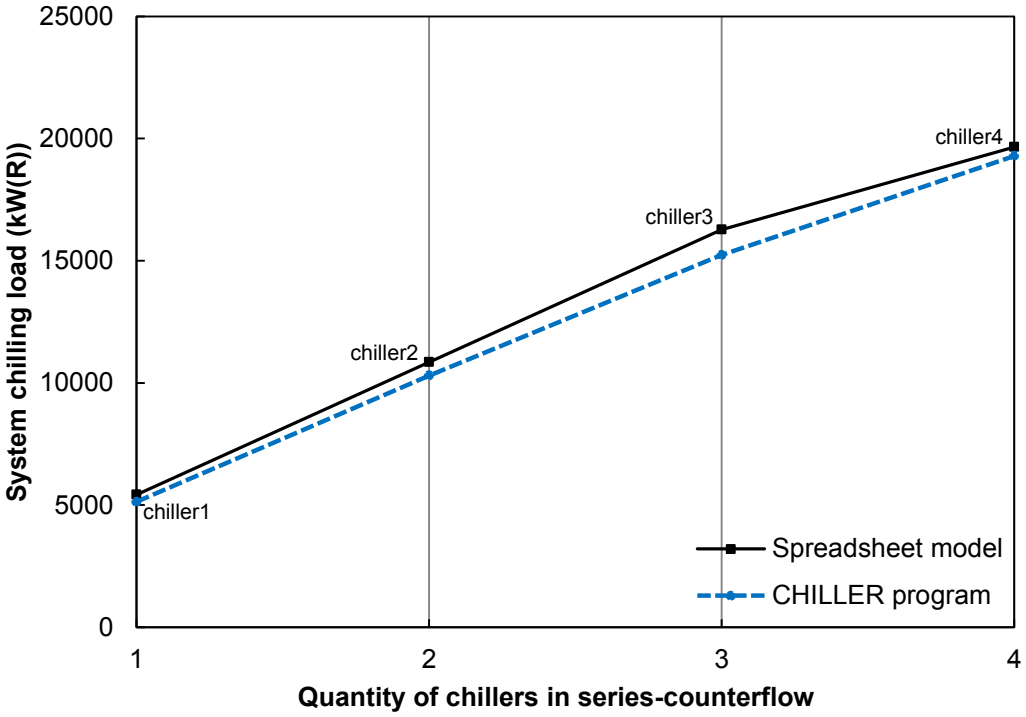

Figure 8.30 Variation of system chilling load with quantity of chillers

Carnot coefficient of performance

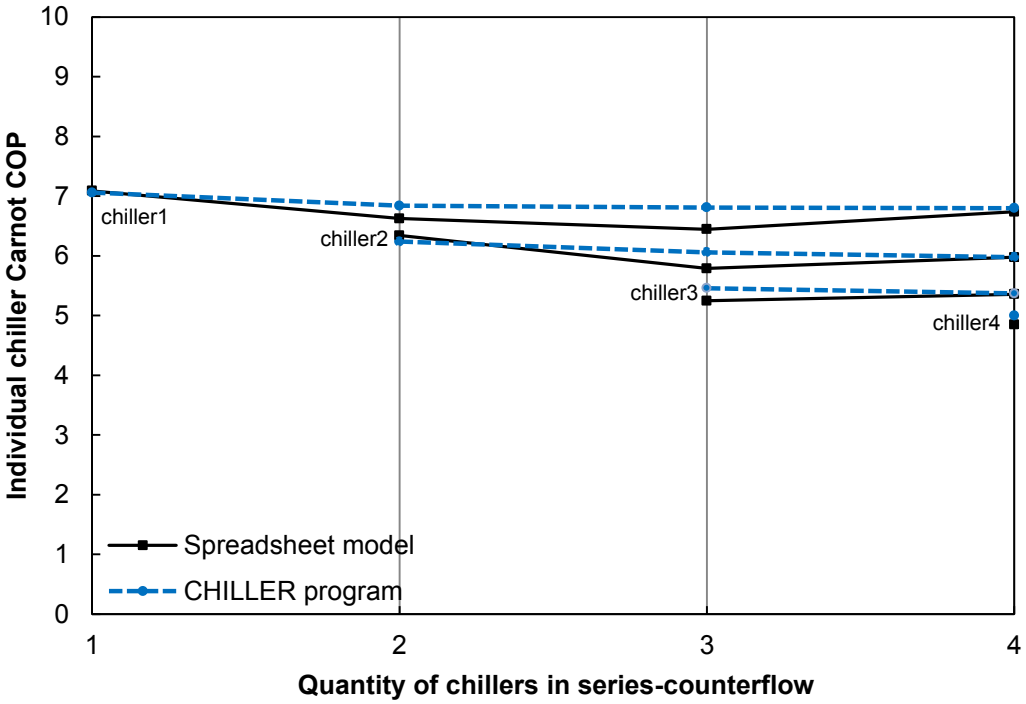

Figure 8.31 Variation of individual chiller Carnot COPs with chiller quantity

Coefficient of performance

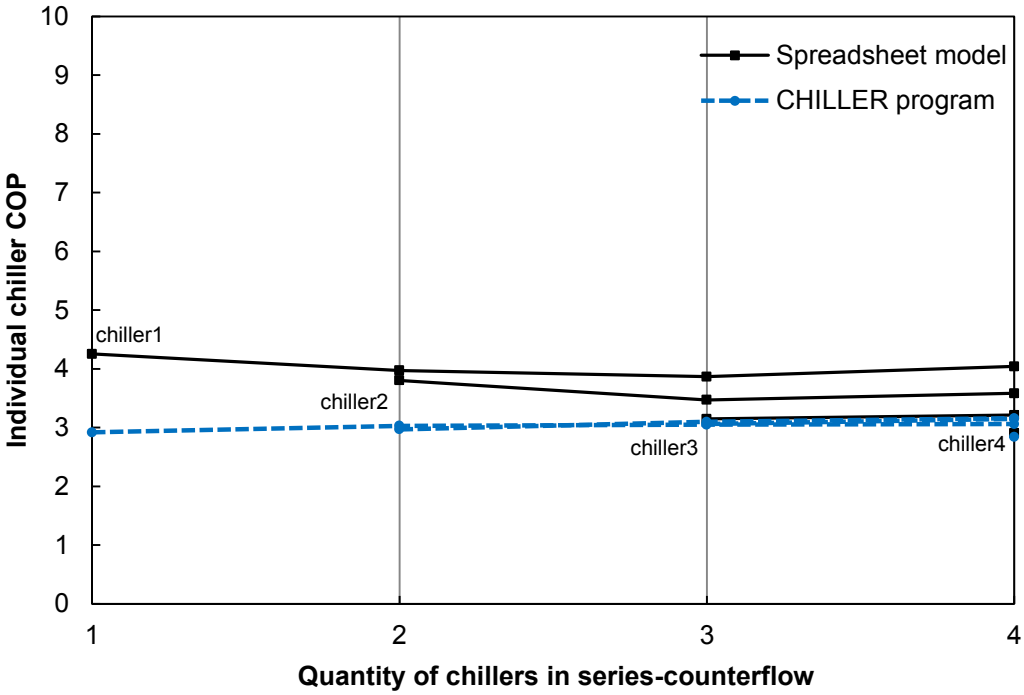

Figure 8.32 Variation of individual chiller COPs with chiller quantity

Compressor total input power

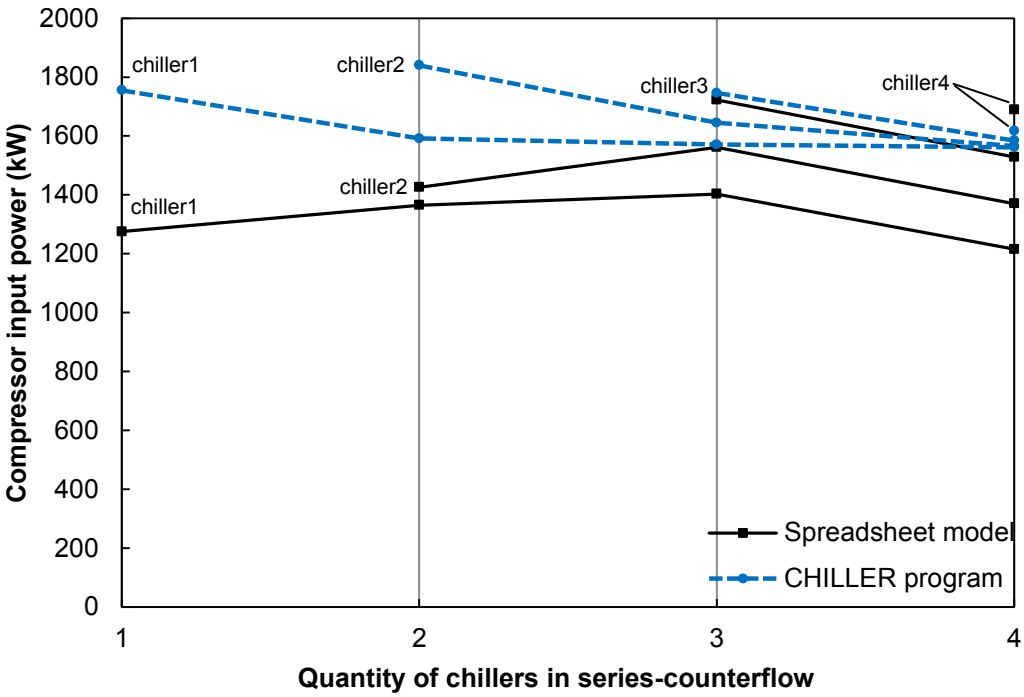

Figure 8.33 Variation of compressor input power (combined stages 1&2) with quantity of chillers

Stage 1 compressor isentropic efficiency

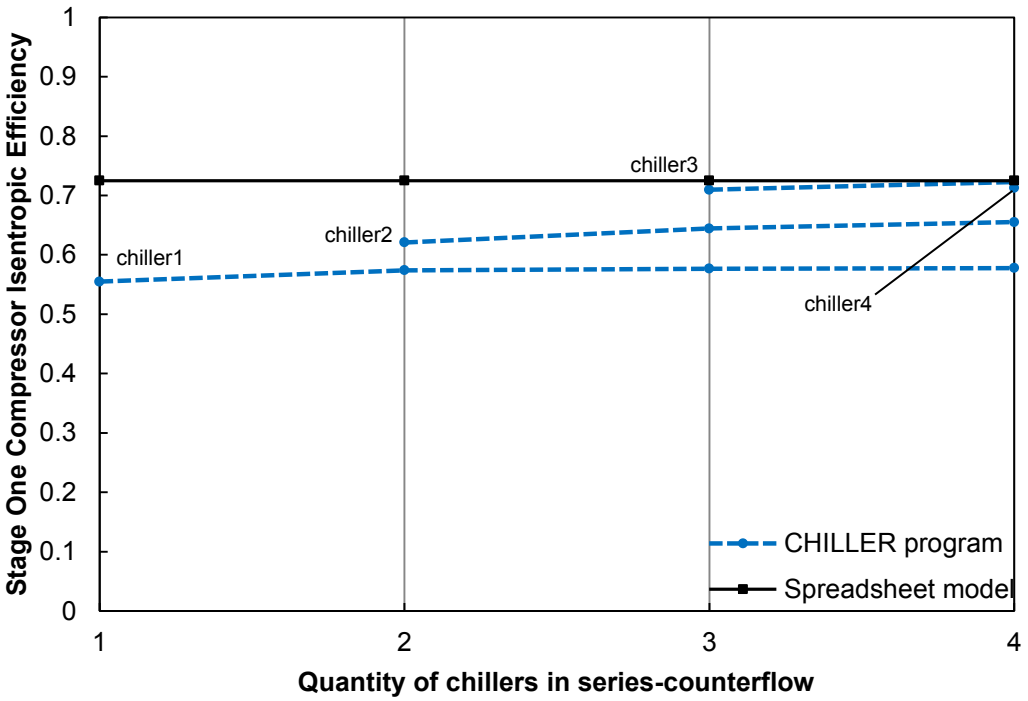

Figure 8.34 Variation of stage 1 compressor isentropic efficiency with quantity of chillers

Stage 2 compressor isentropic efficiency

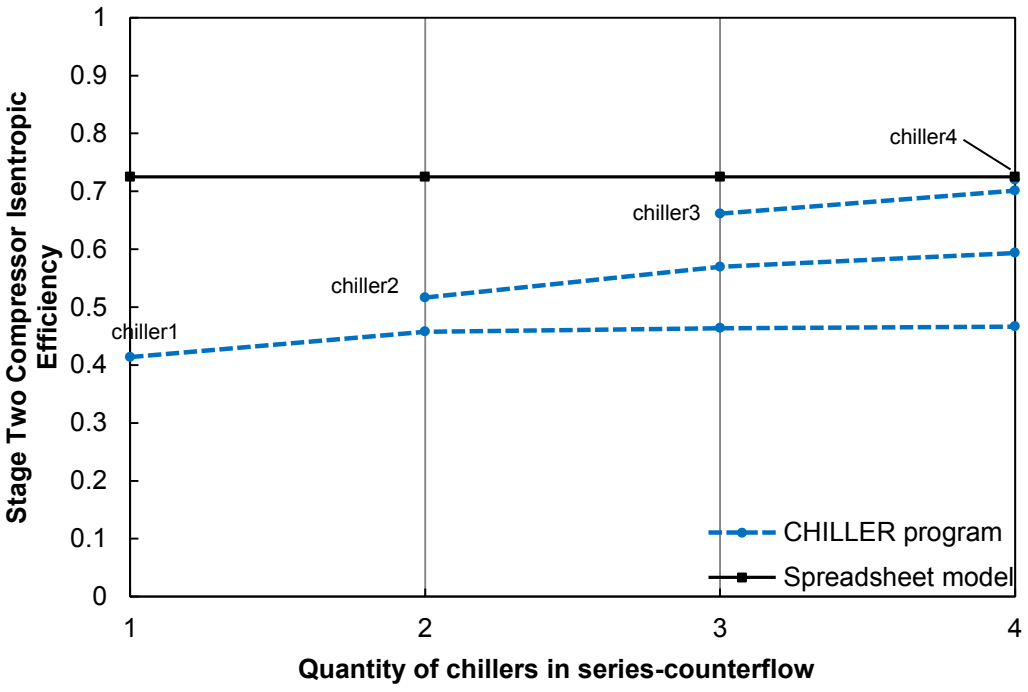

Figure 8.35 Variation of stage 2 compressor isentropic efficiency with quantity of chillers

Cycle efficiency

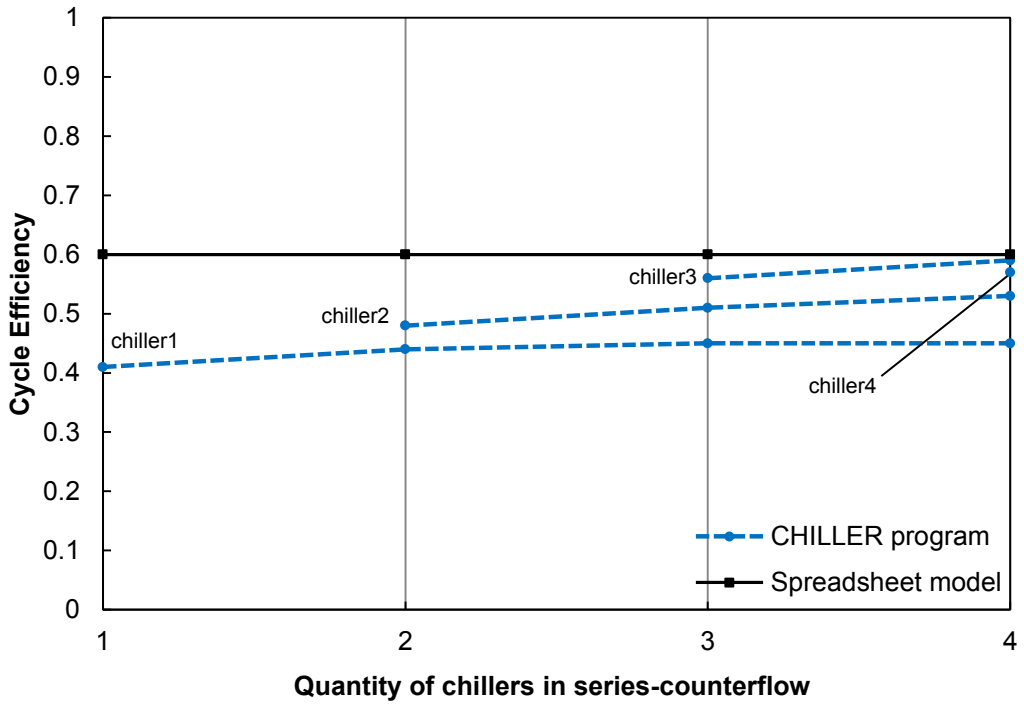

Figure 8.36 Variation of cycle efficiency with quantity of chillers

8.2 Tau Tona mine

8.2.1 Specified limits of 55°C and 70°C on the final return water temperature

This section plots selected results from Appendix B: Sections 9.1.7, 9.1.8, 9.1.9, 9.2.6, 9.2.7, 9.2.8, and 9.2.9.

Evaporator water inlet temperatures

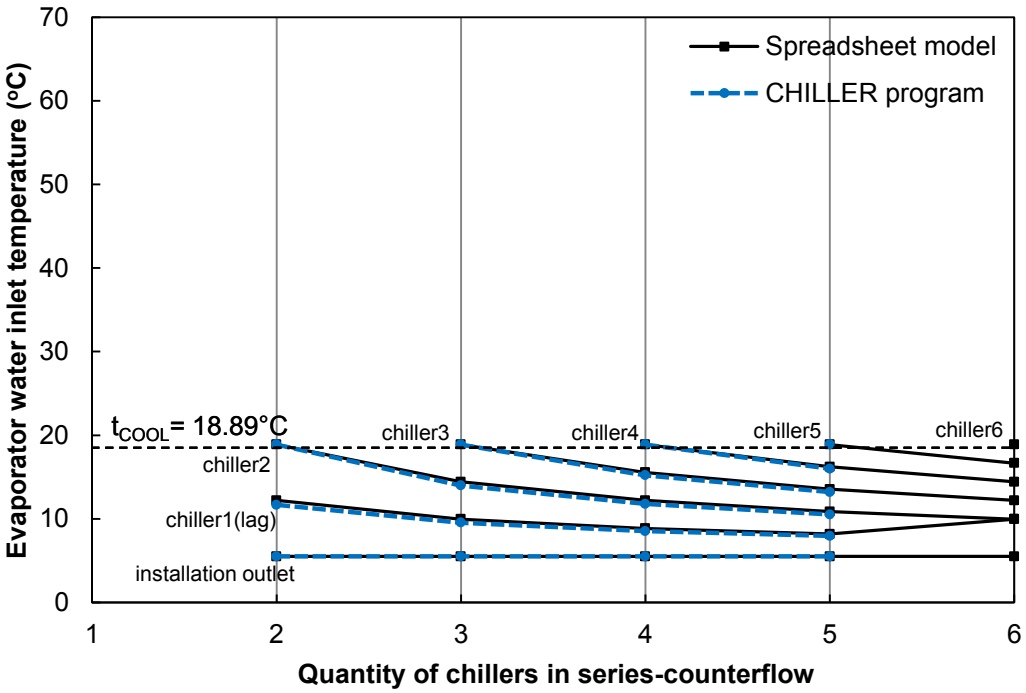

Figure 8.37 Variation of specified evaporator water inlet temperatures with chiller quantity

Evaporator water outlet temperatures

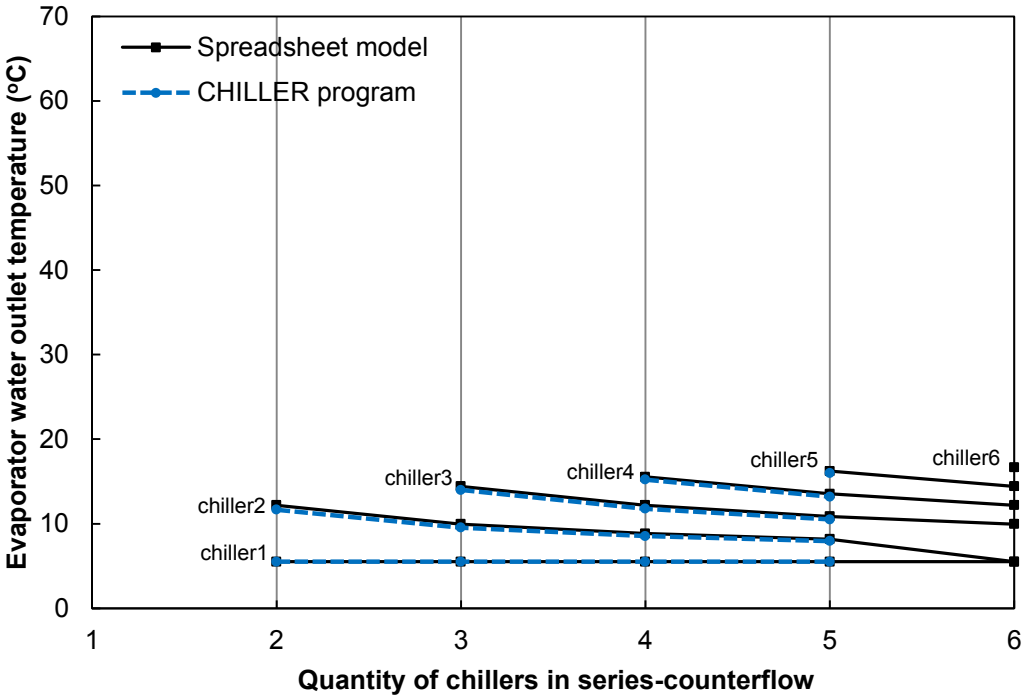

Figure 8.38 Variation of specified evaporator water outlet temperatures with chiller quantity

Evaporator overall thermal conductance

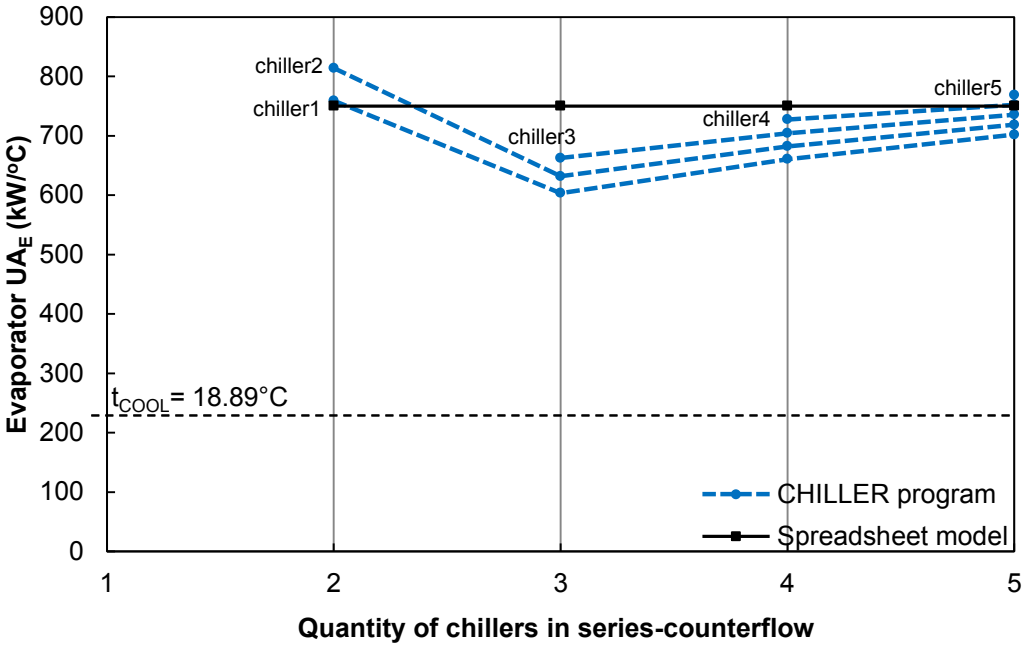

Figure 8.39 Variation of evaporator overall thermal conductance with chiller quantity

Evaporator refrigerant temperatures

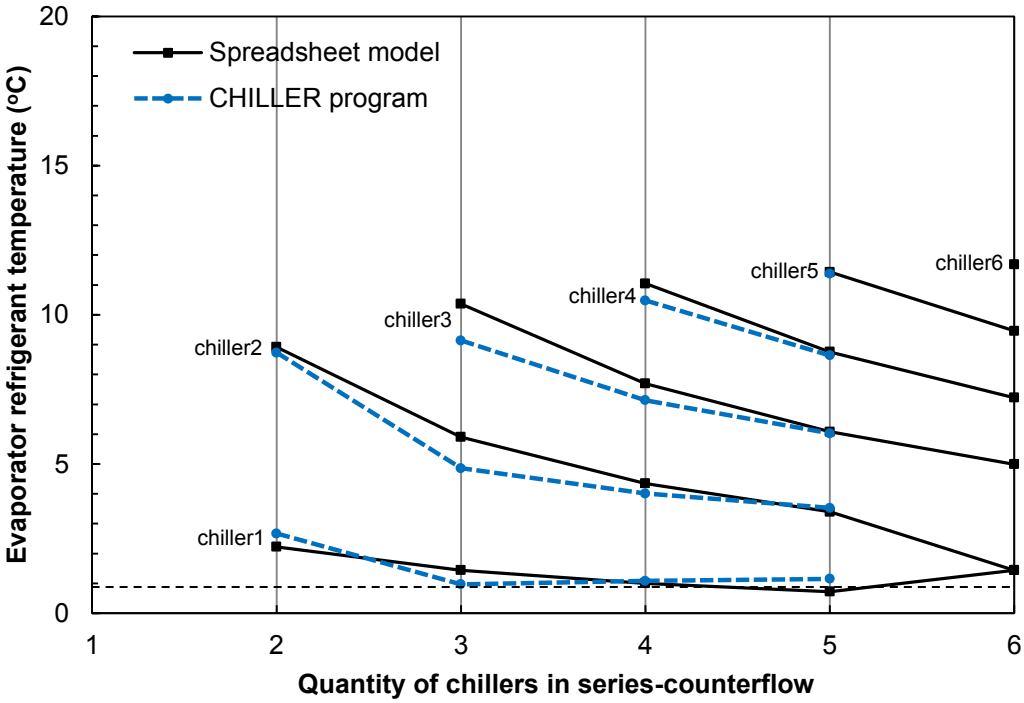

Figure 8.40 Variation of evaporator refrigerant temperatures with chiller quantity

Evaporator log mean temperature difference (LMTD)

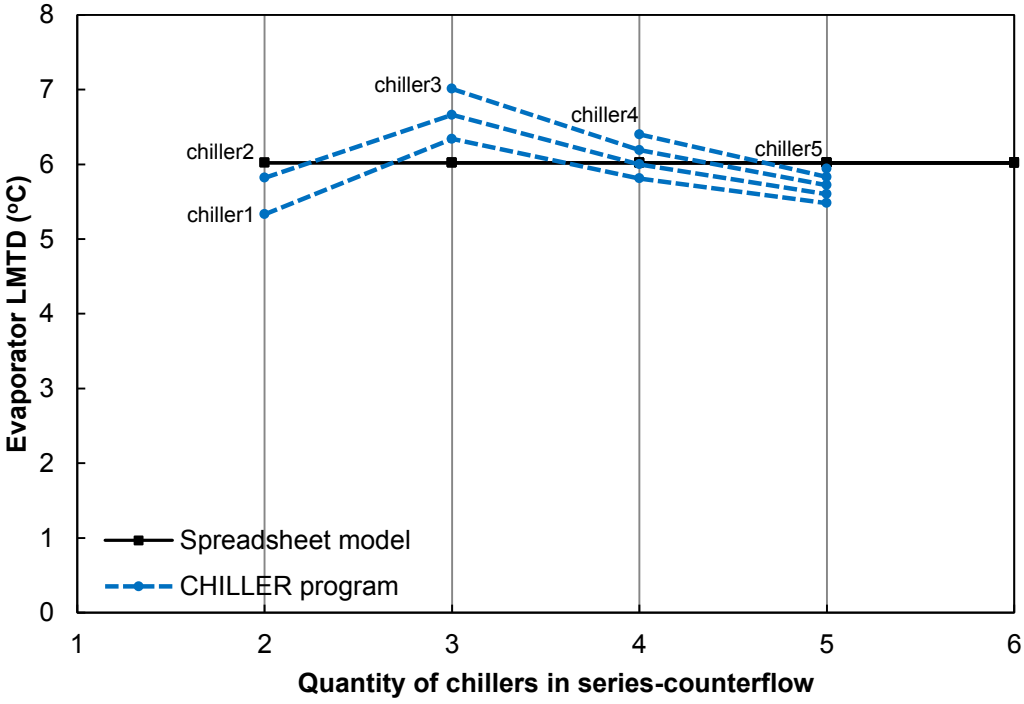

Figure 8.41 Variation of evaporator LMTD with chiller quantity

Evaporator chilling load

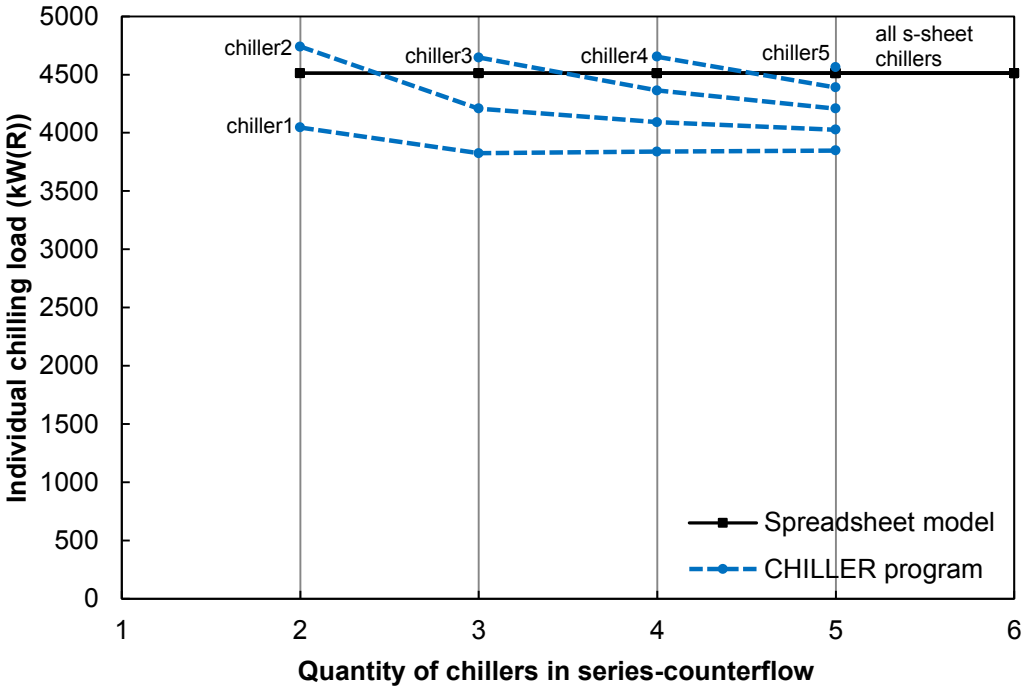

Figure 8.42 Variation of individual chilling load with chiller quantity

Condenser overall thermal conductance

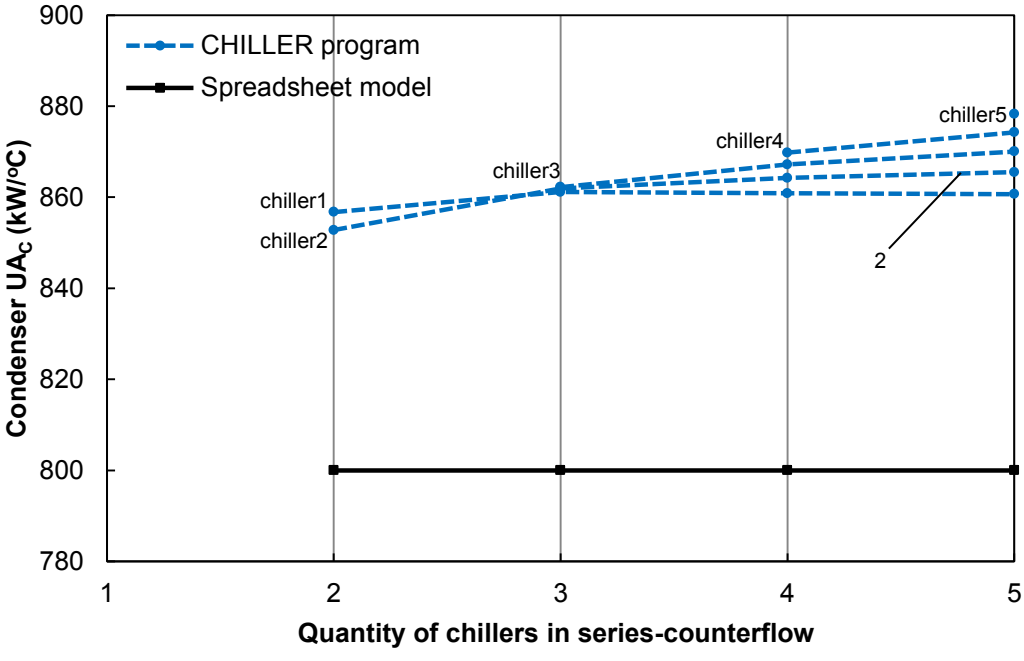

Figure 8.43 Variation of condenser overall thermal conductance with chiller quantity

Condenser refrigerant temperature

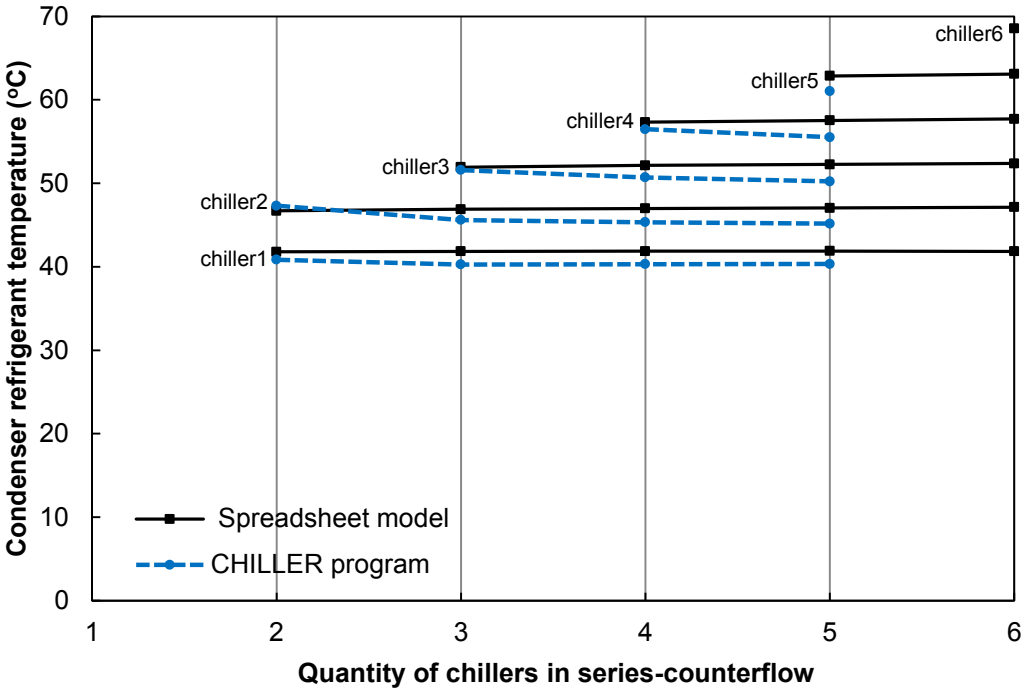

Figure 8.44 Variation of condenser refrigerant temperature with chiller quantity

Condenser log-mean temperature difference (LMTD)

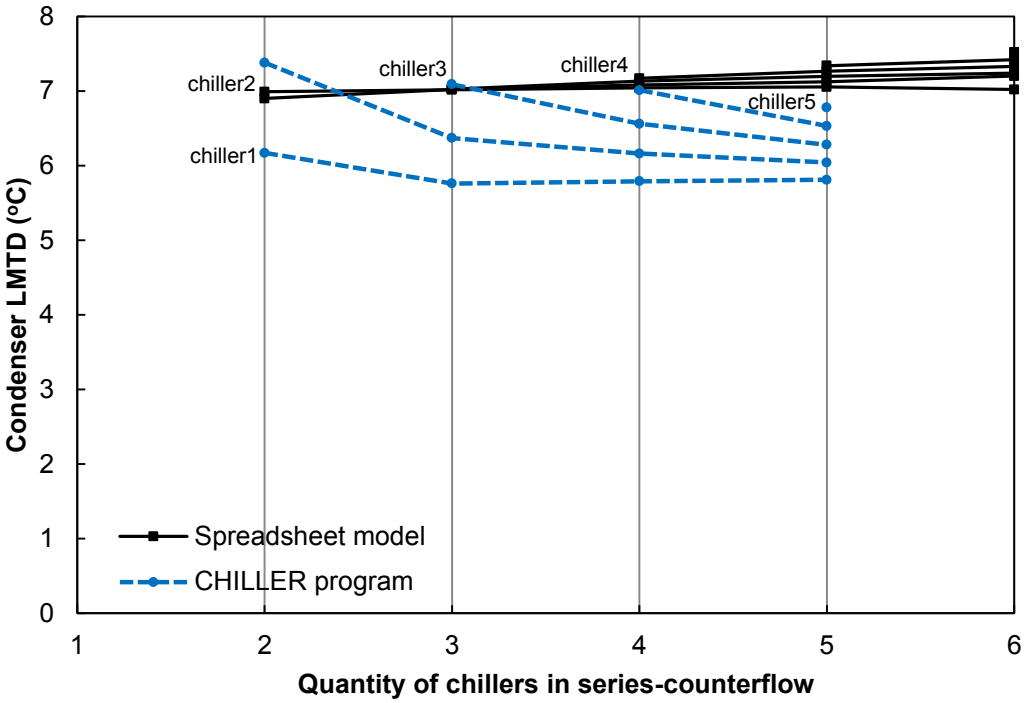

Figure 8.45 Variation of condenser LMTD with chiller quantity

Condenser water inlet temperature

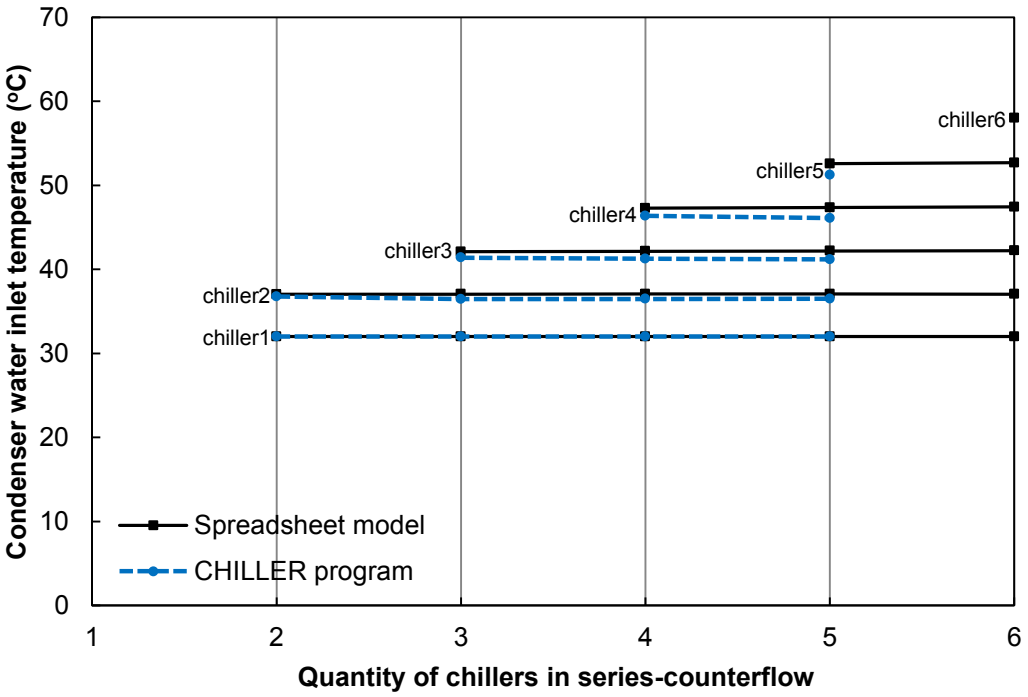

Figure 8.46 Variation of condenser water inlet temperature with quantity of chillers

Condenser water outlet temperature

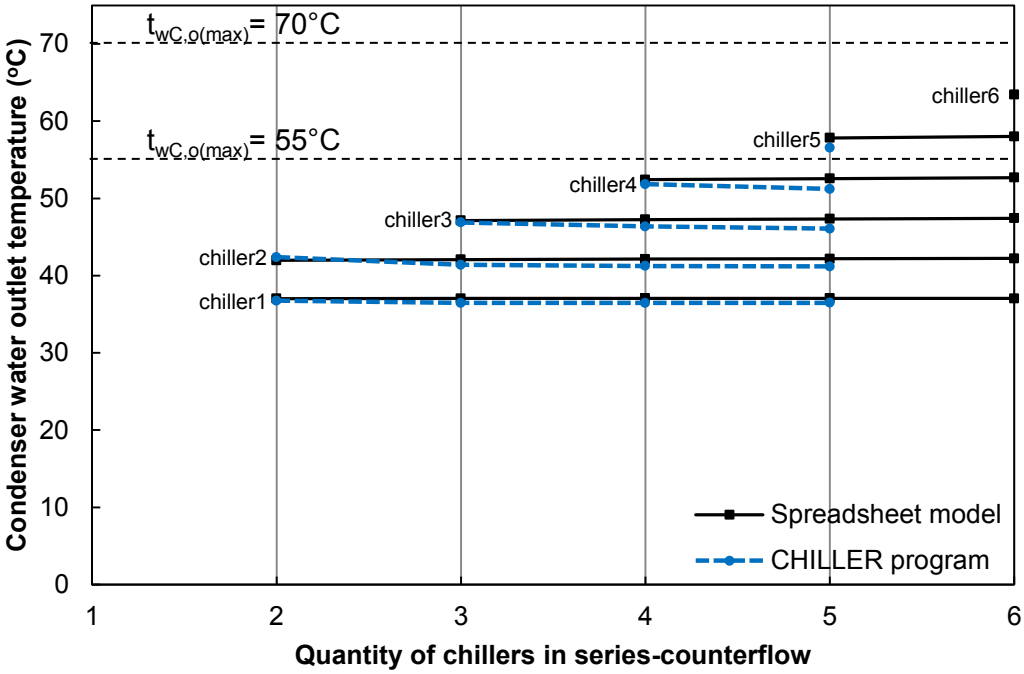

Figure 8.47 Variation of condenser water outlet temperature with quantity of chillers

System chilling load

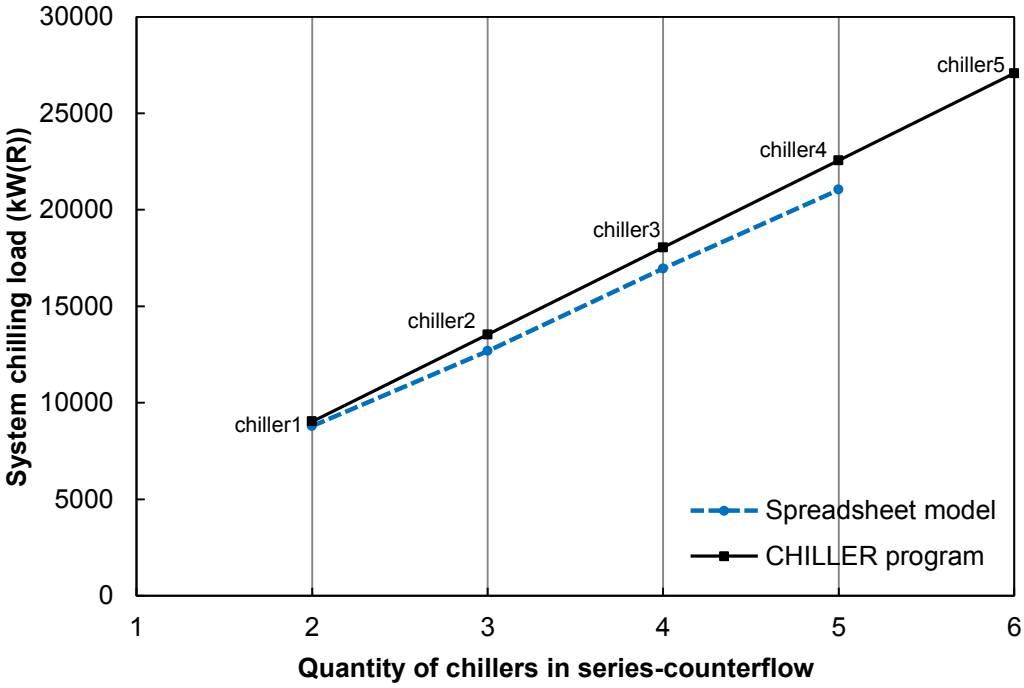

Figure 8.48 Variation of system chilling load with quantity of chillers

Carnot coefficient of performance

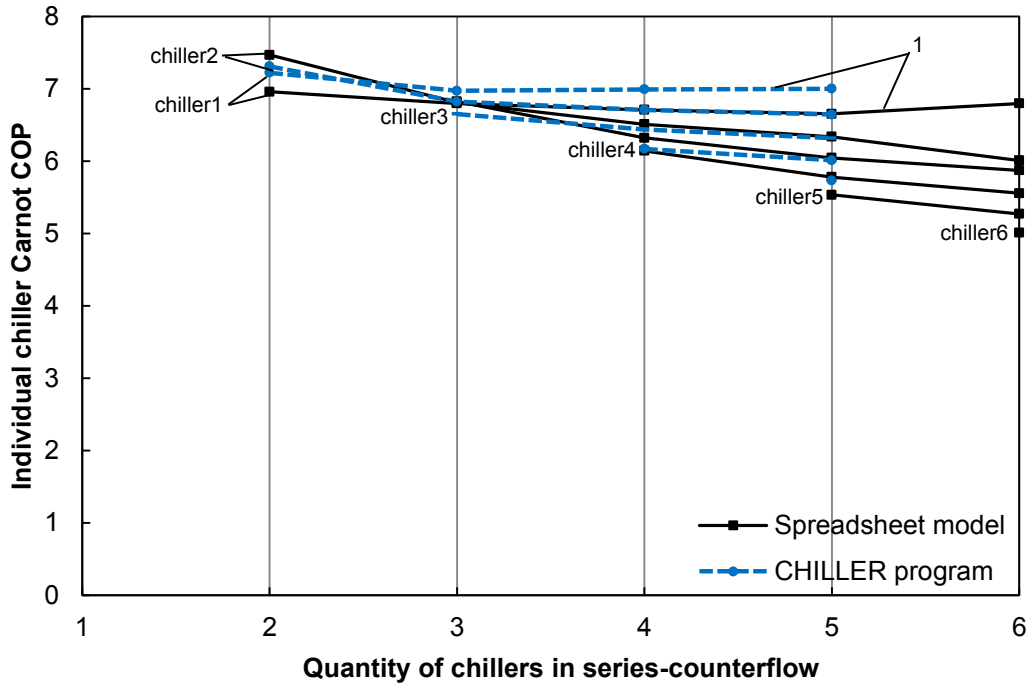

Figure 8.49 Variation of Carnot coefficient of performance with quantity of chillers

Coefficient of performance

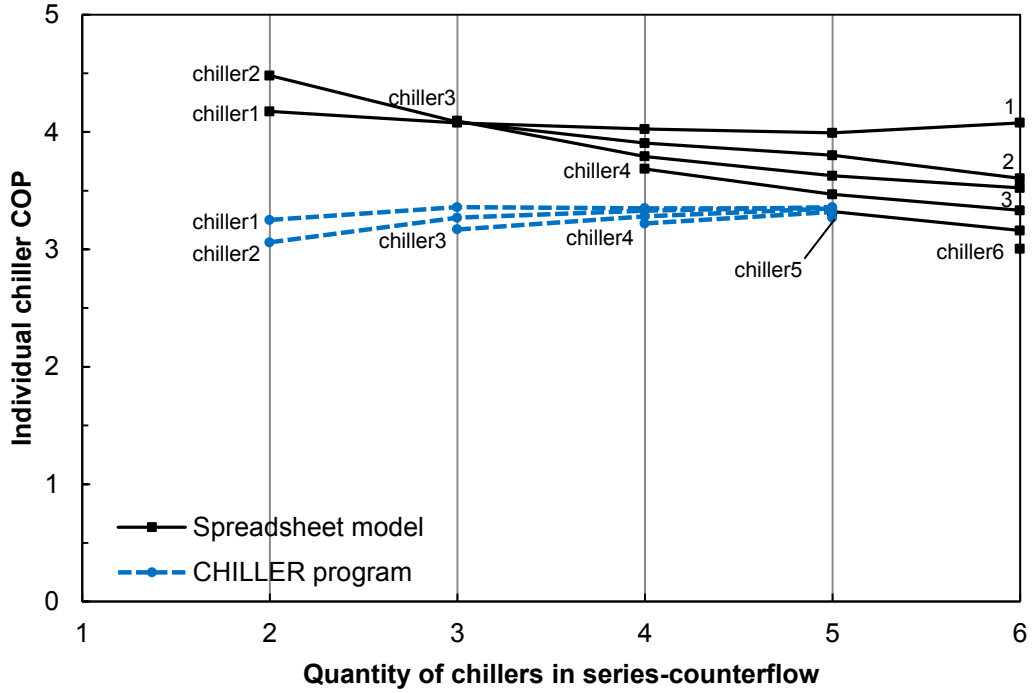

Figure 8.50 Variation of chiller coefficient of performance with quantity of chillers

Compressor total input power

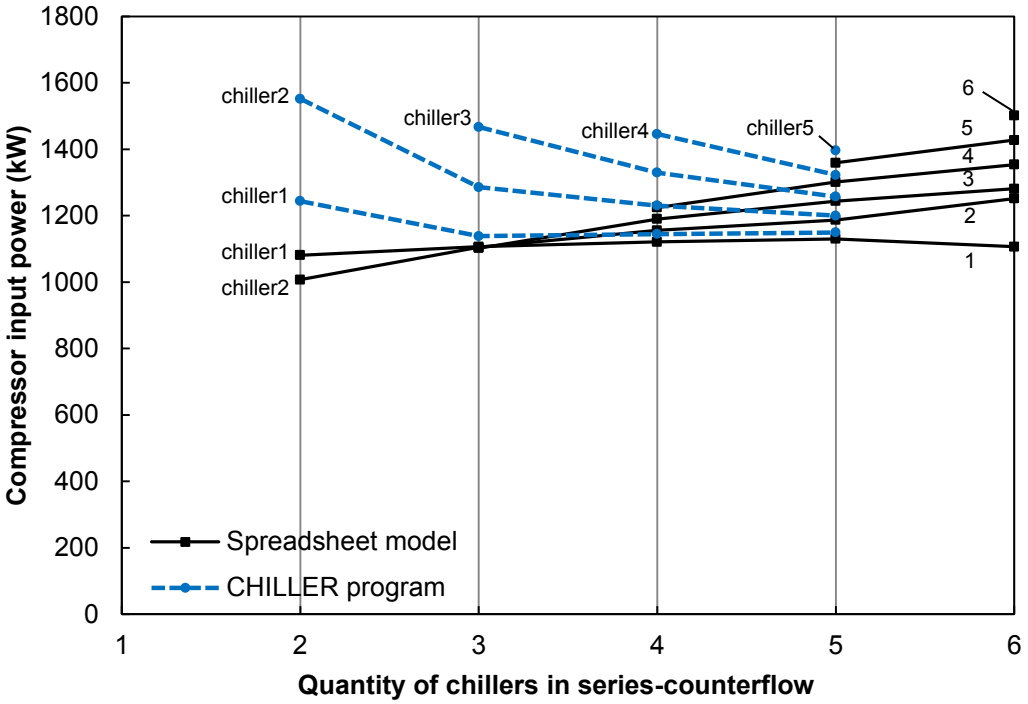

Figure 8.51 Variation of compressor input power (combined stages 1&2) with quantity of chillers

Stage 1 compressor isentropic efficiency

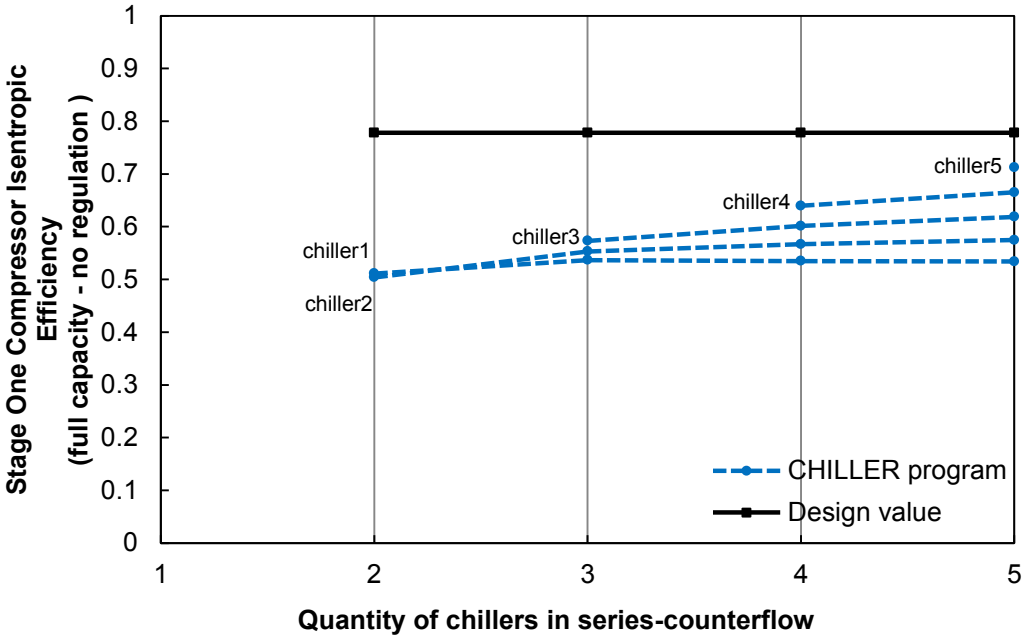

Figure 8.52 Variation of stage 1 compressor isentropic efficiency (at full capacity) with quantity of chillers

Stage 2 compressor isentropic efficiency

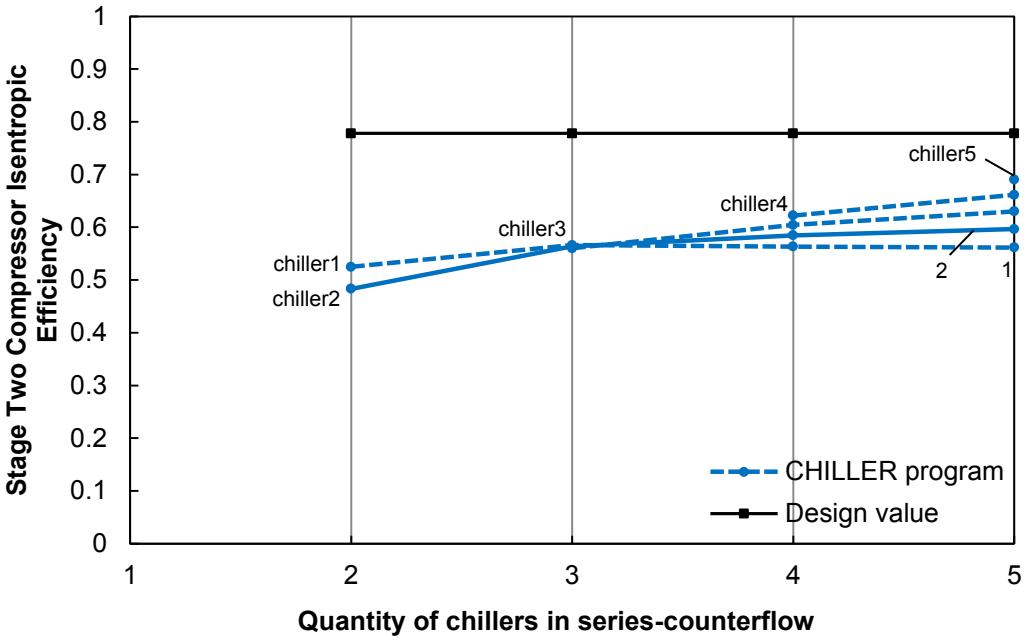

Figure 8.53 Variation of stage 2 compressor isentropic efficiency with quantity of chillers

Cycle efficiency

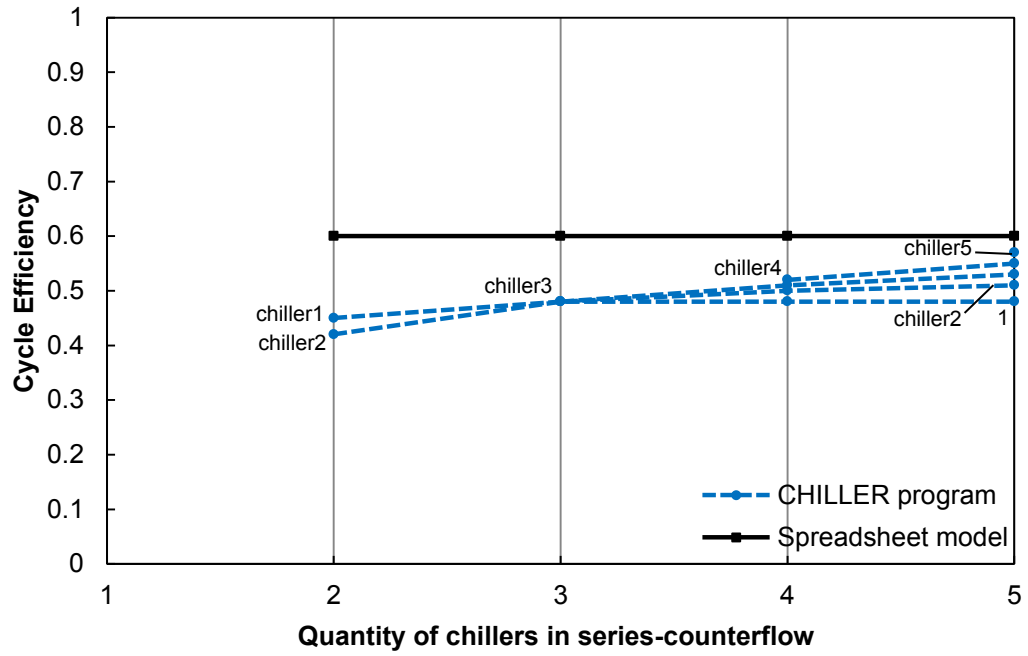

Figure 8.54 Variation of cycle efficiency with quantity of chillers

9 APPENDIX B SPREADSHEET MODEL AND CHILLER PROGRAM SIMULATION RESULTS

9.1 Spreadsheet model simulation results

9.1.1 Kloof mine, 1 chiller operating at full load

Table 9.1 Installation performance, with $t_{(w)Co[max]}$ = 55°C

Installation	Value	Unit
Return water available temperature	32.00	°C
Return water final temperature	42.00	°C
Cool water available temperature	25.00	°C
Chilled water final temperature	10.50	°C
Lorenz COP	15.08	-
System COP	4.25	-
Mass flowrate of return water	160.00	kg/s
Total evaporator water heat load	5423.98	kW(R)
Total return water utilization	33.90	kW(R)/(kg/s)

Table 9.2 Chiller performance

Chiller	Chiller 1	Unit
Carnot COP	7.09	-
COP	4.25	-
Cycle efficiency	60	%
Return water utilization	33.90	kW(R)/(kg/s)

Table 9.3 Evaporator water circuit

Evaporator	**Evap. 1**	**Unit**
Water flowrate	89.34	kg/s
Inlet water temp.	25.00	°C
Outlet water temp.	10.50	°C
Water heat load	5423.98	kW(R)

Table 9.4 Condenser water circuit

Condenser	**Cond. 1**	**Unit**
Water flowrate	160.00	kg/s
Inlet water temperature	32.00	°C
Outlet water temperature	42.00	°C
Water heat load	6699.13	kW(R)

Table 9.5 Evaporator refrigerant circuit

Evaporator	**Evap. 1**	**Unit**
Refrigerant temperature	6.85	°C
Overall UA	600.00	kW/°C
Refrigerant heat load	5423.98	kW(R)

Table 9.6 Condenser refrigerant circuit

Condenser	**Cond. 1**	**Unit**
Refrigerant temperature	46.35	°C
Overall UA	800.00	kW/°C
Refrigerant heat load	6699.13	kW(R)

Table 9.7 Compressor performance

Compressor (combined)	**Chiller 1**	**Unit**
Absorbed power	1275.15	kW(M)

9.1.2 Kloof mine, 2 chillers operating at full load

Table 9.8 Installation performance, with $t_{(w)Co[max]}$ = 55°C

Installation	Value	Unit
Return water available temperature	32.00	°C
Return water final temperature	52.36	°C
Cool water available temperature	25.00	°C
Chilled water final temperature	10.50	°C
Lorenz COP	11.93	-
System COP	3.89	-
Mass flowrate of return water	160.00	kg/s
Total evaporator water heat load	10847.96	kW(R)
Total return water utilization	67.80	kW(R)/(kg/s)

Table 9.9 Chiller performance

Chiller	Chiller 2	Chiller 1	Unit
Carnot COP	6.34	6.62	-
COP	3.80	3.97	-
Cycle efficiency	60	60	%
Return water utilization	33.90	33.90	kW(R)/(kg/s)

Table 9.10 Evaporator water circuit

Evaporator	**Evap. 2**	**Evap. 1**	**Unit**
Water flowrate	178.68	178.68	kg/s
Inlet water temp.	25.00	17.75	°C
Outlet water temp.	17.75	10.50	°C
Water heat load	5423.98	5423.98	kW(R)

Table 9.11 Condenser water circuit

Condenser	**Cond. 2**	**Cond. 1**	**Unit**
Water flowrate	160.00	160.00	kg/s
Inlet water temperature	42.13	32.00	°C
Outlet water temperature	52.36	42.13	°C
Water heat load	6849.62	6788.73	kW(R)

Table 9.12 Evaporator refrigerant circuit

Evaporator	**Evap. 2**	**Evap. 1**	**Unit**
Refrigerant temperature	11.86	4.61	°C
Overall UA	600.00	600.00	kW/°C
Refrigerant heat load	5423.98	5423.98	kW(R)

Table 9.13 Condenser refrigerant circuit

Condenser	**Cond. 2**	**Cond. 1**	**Unit**
Refrigerant temperature	56.80	46.54	°C
Overall UA	800.00	800.00	kW/°C
Refrigerant heat load	6849.62	6788.73	kW(R)

Table 9.14 Compressor performance

Compressor (combined)	**Chiller 2**	**Chiller 1**	**Unit**
Absorbed power	1425.64	1364.75	kW(M)

9.1.3 Kloof mine, 3 chillers operating at equal part load

Table 9.15 Installation performance, with $t_{(w)Co[max]}$ = 55°C

Installation	Value	Unit
Return water available temperature	32.00	°C
Return water final temperature	55.00	°C
Cool water available temperature	25.00	°C
Chilled water final temperature	10.50	°C
Lorenz COP	11.33	-
System COP	4.25	-
Mass flowrate of return water	160.00	kg/s
Total evaporator water heat load	12473.63	kW(R)
Total return water utilization	77.96	kW(R)/(kg/s)

Table 9.16 Chiller performance

Chiller	Chiller 3	Chiller 2	Chiller 1	Unit
Carnot COP	6.71	7.08	7.50	-
COP	4.03	4.25	4.50	-
Cycle efficiency	60	60	60	%
Return water utilization	25.99	25.99	25.99	kW(R)/(kg/s)

Table 9.17 Evaporator water circuit

Evaporator	**Evap. 3**	**Evap. 2**	**Evap. 1**	**Unit**
Water flowrate	205.46	205.46	205.46	kg/s
Inlet water temp.	25.00	20.17	15.33	°C
Outlet water temp.	20.17	15.33	10.50	°C
Water heat load	4157.88	4157.88	4157.88	kW(R)

Table 9.18 Condenser water circuit

Condenser	**Cond. 3**	**Cond. 2**	**Cond. 1**	**Unit**
Water flowrate	160.00	160.00	160.00	kg/s
Inlet water temperature	47.25	39.59	32.00	°C
Outlet water temperature	55.00	47.25	39.59	°C
Water heat load	5190.48	5136.01	5081.68	kW(R)

Table 9.19 Evaporator refrigerant circuit

Evaporator	**Evap. 3**	**Evap. 2**	**Evap. 1**	**Unit**
Refrigerant temperature	15.37	10.54	5.71	°C
Overall UA	600.00	600.00	600.00	kW/°C
Refrigerant heat load	4157.88	4157.88	4157.88	kW(R)

Table 9.20 Condenser refrigerant circuit

Condenser	**Cond. 3**	**Cond. 2**	**Cond. 1**	**Unit**
Refrigerant temperature	58.37	50.58	42.88	°C
Overall UA	800.00	800.00	800.00	kW/°C
Refrigerant heat load	5190.48	5136.01	5081.68	kW(R)

Table 9.21 Compressor performance

Compressor (combined)	**Chiller 3**	**Chiller 2**	**Chiller 1**	**Unit**
Absorbed power	1032.60	978.13	923.80	kW(M)

9.1.4 Kloof mine, 4 chillers operating at part load

Table 9.22 Installation performance, with $t_{(w)Co[max]}$= 55°C

Installation	Value	Unit
Return water available temperature	32.00	°C
Return water final temperature	55.00	°C
Cool water available temperature	25.00	°C
Chilled water final temperature	10.50	°C
Lorenz COP	11.33	-
System COP	4.69	-
Mass flowrate of return water	160.00	kg/s
Total evaporator water heat load	12699.14	kW(R)
Total return water utilization	79.37	kW(R)/(kg/s)

Table 9.23 Chiller performance

Chiller	Chiller 4	Chiller 3	Chiller 2	Chiller 1	Unit
Carnot COP	7.30	7.63	8.00	8.40	-
COP	4.38	4.58	4.80	5.04	-
Cycle efficiency	60	60	60	60	%
Return water utilization	19.84	19.84	19.84	19.84	kW(R)/(kg/s)

Table 9.24 Evaporator water circuit

Evaporator	**Evap. 4**	**Evap. 3**	**Evap. 2**	**Evap. 1**	**Unit**
Water flowrate	209.17	209.17	209.17	209.17	kg/s
Inlet water temp.	25.00	21.38	17.75	14.13	°C
Outlet water temp.	21.38	17.75	14.13	10.50	°C
Water heat load	3174.79	3174.79	3174.79	3174.79	kW(R)

Table 9.25 Condenser water circuit

Condenser	**Cond. 4**	**Cond. 3**	**Cond. 2**	**Cond. 1**	**Unit**
Water flowrate	160.00	160.00	160.00	160.00	kg/s
Inlet water temperature	49.18	43.41	37.68	32.00	°C
Outlet water temperature	55.00	49.18	43.41	37.68	°C
Water heat load	3899.60	3867.91	3836.30	3804.76	kW(R)

Table 9.26 Evaporator refrigerant circuit

Evaporator	**Evap. 4**	**Evap. 3**	**Evap. 2**	**Evap. 1**	**Unit**
Refrigerant temperature	17.69	14.07	10.44	6.82	°C
Overall UA	600.00	600.00	600.00	600.00	kW/°C
Refrigerant heat load	3174.79	3174.79	3174.79	3174.79	kW(R)

Table 9.27 Condenser refrigerant circuit

Condenser	**Cond. 4**	**Cond. 3**	**Cond. 2**	**Cond. 1**	**Unit**
Refrigerant temperature	57.53	51.69	45.89	40.15	°C
Overall UA	800.00	800.00	800.00	800.00	kW/°C
Refrigerant heat load	3899.60	3867.91	3836.3	3804.76	kW(R)

Table 9.28 Compressor performance

Compressor (combined)	**Chiller 4**	**Chiller 3**	**Chiller 2**	**Chiller 1**	**Unit**
Absorbed power	724.81	693.12	661.51	629.97	kW(M)

9.1.5 Kloof mine, 3 chillers operating at full load

Table 9.29 Installation performance, with $t_{(w)Co[max]}$= 70°C

Installation	Value	Unit
Return water available temperature	32.00	°C
Return water final temperature	63.29	°C
Cool water available temperature	25.00	°C
Chilled water final temperature	10.50	°C
Lorenz COP	9.79	-
System COP	3.47	-
Mass flowrate of return water	160.00	kg/s
Total evaporator water heat load	16271.94	kW(R)
Total return water utilization	101.70	kW(R)/(kg/s)

Table 9.30 Chiller performance

Chiller	Chiller 3	Chiller 2	Chiller 1	Unit
Carnot COP	5.25	5.79	6.44	-
COP	3.15	3.47	3.87	-
Cycle efficiency	60	60	60	%
Return water utilization	33.90	33.90	33.90	kW(R)/(kg/s)

Table 9.31 Evaporator water circuit

Evaporator	**Evap. 3**	**Evap. 2**	**Evap. 1**	**Unit**
Water flowrate	268.02	268.02	268.02	kg/s
Inlet water temp.	25.00	20.17	15.33	°C
Outlet water temp.	20.17	15.33	10.50	°C
Water heat load	5423.98	5423.98	5423.98	kW(R)

Table 9.32 Condenser water circuit

Condenser	**Cond. 3**	**Cond. 2**	**Cond. 1**	**Unit**
Water flowrate	160.00	160.00	160.00	kg/s
Inlet water temperature	52.62	42.19	32.00	°C
Outlet water temperature	63.29	52.62	42.19	°C
Water heat load	7146.71	6985.64	6826.85	kW(R)

Table 9.33 Evaporator refrigerant circuit

Evaporator	**Evap. 3**	**Evap. 2**	**Evap. 1**	**Unit**
Refrigerant temperature	13.33	8.50	3.66	°C
Overall UA	600.00	600.00	600.00	kW/°C
Refrigerant heat load	5423.98	5423.98	5423.98	kW(R)

Table 9.34 Condenser refrigerant circuit

Condenser	**Cond. 3**	**Cond. 2**	**Cond. 1**	**Unit**
Refrigerant temperature	67.92	57.15	46.62	°C
Overall UA	800.00	800.00	800.00	kW/°C
Refrigerant heat load	7146.71	6985.64	6826.85	kW(R)

Table 9.35 Compressor performance

Compressor (combined)	**Chiller 3**	**Chiller 2**	**Chiller 1**	**Unit**
Absorbed power	1722.73	1561.66	1402.87	kW(M)

9.1.6 Kloof mine, 4 chillers operating at part load

Table 9.36 Installation performance, with $t_{(w)Co[max]}$= 70°C

Installation	Value	Unit
Return water available temperature	32.00	°C
Return water final temperature	70.00	°C
Cool water available temperature	25.00	°C
Chilled water final temperature	10.50	°C
Lorenz COP	8.83	-
System COP	3.39	-
Mass flowrate of return water	160.00	kg/s
Total evaporator water heat load	19653.18	kW(R)
Total return water utilization	122.83	kW(R)/(kg/s)

Table 9.37 Chiller performance

Chiller	Chiller 4	Chiller 3	Chiller 2	Chiller 1	Unit
Carnot COP	4.85	5.36	5.98	6.74	-
COP	2.91	3.21	3.59	4.04	-
Cycle efficiency	60	60	60	60	%
Return water utilization	30.71	30.71	30.71	30.71	kW(R)/(kg/s)

Table 9.38 Evaporator water circuit

Evaporator	Evap. 4	Evap. 3	Evap. 2	Evap. 1	Unit
Water flowrate	323.71	323.71	323.71	323.71	kg/s
Inlet water temp.	25.00	21.38	17.75	14.13	°C
Outlet water temp.	21.38	17.75	14.13	10.50	°C
Water heat load	4913.29	4913.29	4913.29	4913.29	kW(R)

Table 9.39 Condenser water circuit

Condenser	Cond. 4	Cond. 3	Cond. 2	Cond. 1	Unit
Water flowrate	160.00	160.00	160.00	160.00	kg/s
Inlet water temperature	60.14	50.53	41.15	32.00	°C
Outlet water temperature	70.00	60.14	50.53	41.15	°C
Water heat load	6602.66	6441.78	6283.80	6128.71	kW(R)

Table 9.40 Evaporator refrigerant circuit

Evaporator	Evap. 4	Evap. 3	Evap. 2	Evap. 1	Unit
Refrigerant temperature	14.87	11.24	7.62	3.99	°C
Overall UA	600.00	600.00	600.00	600.00	kW/°C
Refrigerant heat load	4913.29	4913.29	4913.29	4913.29	kW(R)

Table 9.41 Condenser refrigerant circuit

Condenser	Cond. 4	Cond. 3	Cond. 2	Cond. 1	Unit
Refrigerant temperature	74.28	64.32	54.61	45.12	°C
Overall UA	800.00	800.00	800.00	800.00	kW/°C
Refrigerant heat load	6602.66	6441.78	6283.80	6128.71	kW(R)

Table 9.42 Compressor performance

Compressor (combined)	Chiller 4	Chiller 3	Chiller 2	Chiller 1	Unit
Absorbed power	1689.37	1528.49	1370.51	1215.42	kW(M)

9.1.7 Tau Tona mine, 2 chillers operating at full load

Table 9.43 Installation performance, with $t_{(w)Co[max]}$= 55°C

Installation	Value	Unit
Return water available temperature	32.00	°C
Return water final temperature	41.98	°C
Cool water available temperature	18.89	°C
Chilled water final temperature	5.50	°C
Lorenz COP	11.49	-
System COP	4.32	-
Mass flowrate of return water	266.00	kg/s
Total evaporator water heat load	9024.00	kW(R)
Total return water utilization	33.92	kW(R)/(kg/s)

Table 9.44 Chiller performance

Chiller	Chiller 2	Chiller 1	Unit
Carnot COP	7.47	6.96	-
COP	4.48	4.17	-
Cycle efficiency	60	60	%
Return water utilization	16.96	16.96	kW(R)/(kg/s)

Table 9.45 Evaporator water circuit

Evaporator	Evap. 2	Evap. 1	Unit
Water flowrate	160.96	160.96	kg/s
Inlet water temp.	18.89	12.20	°C
Outlet water temp.	12.20	5.50	°C
Water heat load	4512.00	4512.00	kW(R)

Table 9.46 Condenser water circuit

Condenser	Cond. 2	Cond. 1	Unit
Water flowrate	266.00	266.00	kg/s
Inlet water temperature	37.02	32.00	°C
Outlet water temperature	41.98	37.02	°C
Water heat load	5519.07	5592.78	kW(R)

Table 9.47 Evaporator refrigerant circuit

Evaporator	Evap. 2	Evap. 1	Unit
Refrigerant temperature	8.92	2.22	°C
Overall UA	750.00	750.00	kW/°C
Refrigerant heat load	4512.00	4512.00	kW(R)

Table 9.48 Condenser refrigerant circuit

Condenser	Cond. 2	Cond. 1	Unit
Refrigerant temperature	46.69	41.80	°C
Overall UA	800.00	800.00	kW/°C
Refrigerant heat load	5519.07	5592.78	kW(R)

Table 9.49 Compressor performance

Compressor (combined)	Chiller 2	Chiller 1	Unit
Absorbed power	1007.07	1080.78	kW(M)

9.1.8 Tau Tona mine, 4 chillers operating at full load

Table 9.50 Installation performance, with $t_{(w)Co[max]}$ = 55°C

Installation	Value	Unit
Return water available temperature	32.00	°C
Return water final temperature	52.42	°C
Cool water available temperature	18.89	°C
Chilled water final temperature	5.50	°C
Lorenz COP	9.52	-
System COP	3.85	-
Mass flowrate of return water	266.00	kg/s
Total evaporator water heat load	18048.00	kW(R)
Total return water utilization	67.85	kW(R)/(kg/s)

Table 9.51 Chiller performance

Chiller	Chiller 4	Chiller 3	Chiller 2	Chiller 1	Unit
Carnot COP	6.14	6.32	6.51	6.71	-
COP	3.69	3.79	3.91	4.03	-
Cycle efficiency	60	60	60	60	%
Return water utilization	16.96	16.96	16.96	16.96	kW(R)/(kg/s)

Table 9.52 Evaporator water circuit

Evaporator	Evap. 4	Evap. 3	Evap. 2	Evap. 1	Unit
Water flowrate	321.92	321.92	321.92	321.92	kg/s
Inlet water temp.	18.89	15.54	12.20	8.85	°C
Outlet water temp.	15.54	12.20	8.85	5.50	°C
Water heat load	4512.00	4512.00	4512.00	4512.00	kW(R)

Table 9.53 Condenser water circuit

Condenser	Cond. 4	Cond. 3	Cond. 2	Cond. 1	Unit
Water flowrate	266.00	266.00	266.00	266.00	kg/s
Inlet water temperature	47.27	42.15	37.06	32.00	°C
Outlet water temperature	52.42	47.27	42.15	37.06	°C
Water heat load	5736.37	5701.90	5667.43	5632.98	kW(R)

Table 9.54 Evaporator refrigerant circuit

Evaporator	Evap. 4	Evap. 3	Evap. 2	Evap. 1	Unit
Refrigerant temperature	11.05	7.70	4.35	1.00	°C
Overall UA	750.00	750.00	750.00	750.00	kW/°C
Refrigerant heat load	4512.00	4512.00	4512.00	4512.00	kW(R)

Table 9.55 Condenser refrigerant circuit

Condenser	Cond. 4	Cond. 3	Cond. 2	Cond. 1	Unit
Refrigerant temperature	57.32	52.14	46.99	41.87	°C
Overall UA	800.00	800.00	800.00	800.00	kW/°C
Refrigerant heat load	5736.37	5701.90	5667.43	5632.98	kW(R)

Table 9.56 Compressor performance

Compressor (combined)	Chiller 4	Chiller 3	Chiller 2	Chiller 1	Unit
Absorbed power	1224.37	1189.90	1155.43	1120.98	kW(M)

9.1.9 Tau Tona mine, 6 chillers operating at full load

Table 9.57 Installation performance, with $t_{(w)Co[max]}$ = 70°C

Installation	Value	Unit
Return water available temperature	32.00	°C
Return water final temperature	63.42	°C
Cool water available temperature	18.89	°C
Chilled water final temperature	5.50	°C
Lorenz COP	8.08	-
System COP	3.42	-
Mass flowrate of return water	266.00	kg/s
Total evaporator water heat load	27072.00	kW(R)
Total return water utilization	101.77	kW(R)/(kg/s)

Table 9.58 Chiller performance

Chiller	Chiller 6	Chiller 5	Chiller 4	Chiller 3	Chiller 2	Chiller 1	Unit
Carnot COP	5.01	5.27	5.55	5.87	6.01	6.80	-
COP	3.01	3.16	3.33	3.52	3.61	4.08	-
Cycle efficiency	60	60	60	60	60	60	%
Return w. utilization	16.96	16.96	16.96	16.96	16.96	16.96	kW(R)/(kg/s)

Table 9.59 Evaporator water circuit

Evaporator	Evap. 6	Evap. 5	Evap. 4	Evap. 3	Evap. 2	Evap. 1	Unit
Water flowrate	482.88	482.88	482.88	482.88	241.44	241.44	kg/s
Inlet water temp.	18.89	16.66	14.43	12.20	9.96	9.96	°C
Outlet water temp.	16.66	14.43	12.20	9.96	5.50	5.50	°C
Water heat load	4512.00	4512.00	4512.00	4512.00	4512.00	4512.00	kW(R)

Table 9.60 Condenser water circuit

Condenser	Cond. 6	Cond. 5	Cond. 4	Cond. 3	Cond. 2	Cond. 1	Unit
Water flowrate	266.00	266.00	266.00	266.00	266.00	266.00	kg/s
Inlet water temp.	58.02	52.69	47.42	42.22	37.04	32.00	°C
Outlet water temp.	63.42	58.02	52.69	47.42	42.22	37.04	°C
Water heat load	6013.36	5939.24	5865.74	5792.87	5763.59	5618.47	kW(R)

Table 9.61 Evaporator refrigerant circuit

Evaporator	Evap. 6	Evap. 5	Evap. 4	Evap. 3	Evap. 2	Evap. 1	Unit
Refrigerant temp.	11.69	9.46	7.23	4.99	1.44	1.44	°C
Overall UA	750.00	750.00	750.00	750.00	750.00	750.00	kW/°C
Ref. heat load	4512.00	4512.00	4512.00	4512.00	4512.00	4512.00	kW(R)

Table 9.62 Condenser refrigerant circuit

Condenser	Cond. 6	Cond,5	Cond. 4	Cond. 3	Cond. 2	Cond. 1	Unit
Refrigerant temp.	68.56	63.09	57.70	52.37	47.14	41.84	°C
Overall UA	800.00	800.00	800.00	800.00	800.00	800.00	kW/°C
Ref. heat load	6013.36	5939.24	5865.74	5792.87	5763.59	5618.47	kW(R)

Table 9.63 Compressor performance

Compressor (comb.)	Chiller 6	Chiller 5	Chiller 4	Chiller 3	Chiller 2	Chiller 1	Unit
Absorbed power	1501.36	1427.24	1353.74	1280.87	1251.59	1106.47	kW(M)

9.2 CHILLER program simulation results

9.2.1 Kloof mine, 1 chiller operating at full load

Table 9.64 Installation performance, with $t_{(w)Co[max]}$ = 55°C

Installation	Value	Unit
Return water available temperature	32.00	°C
Return water final temperature	42.28	°C
Cool water available temperature	25.00	°C
Chilled water final temperature	10.50	°C
Lorenz COP	14.97	-
System COP	2.92	-
Mass flowrate of return water	160.00	kg/s
Total evaporator water heat load	5131.10	kW(R)
Total return water utilization	32.07	kW(R)/(kg/s)

Table 9.65 Chiller performance

Chiller	Chiller 1	Unit
Carnot COP	7.06	-
COP	2.92	-
Cycle efficiency	41	%
Return water utilization	32.07	kW(R)/(kg/s)

Table 9.66 Evaporator water circuit

Evaporator	**Evap. 1**	**Unit**
Fouling factor	0.00020	m^2 °C/W
Water flowrate	84.50	kg/s
Tube water velocity	2.30	m/s
Inlet water temp.	25.00	°C
Outlet water temp.	10.50	°C
Water heat load	5131.1	kW(R)

Table 9.67 Condenser water circuit

Condenser	**Cond. 1**	**Unit**
Fouling factor	0.00020	m^2 °C/W
Water flowrate	160.00	kg/s
Tube water velocity	2.65	m/s
Inlet water temperature	32.00	°C
Outlet water temperature	42.28	°C
Water heat load	6886.1	kW(R)

Table 9.68 Evaporator refrigerant circuit

Evaporator	**Evap. 1**	**Unit**
Refrigerant flowrate	40.45	kg/s
Refrigerant temperature	7.34	°C
Refrigerant pressure	389.86	kPa
Inlet refrigerant enthalpy	63.77	kJ/kg
Outlet refrigerant enthalpy	7.34	kJ/kg
Tube thermal resistance	0.0521	°C/MW
Fouling thermal resistance	0.7150	°C/MW
Water thermal resistance	0.4283	°C/MW
Refrigerant thermal resistance	0.4471	°C/MW
Overall UA	608.83	kW/°C
Refrigerant heat load	5131.10	kW(R)

Table 9.69 Condenser refrigerant circuit

Condenser	**Cond. 1**	**Unit**
Refrigerant flowrate	46.67	kg/s
Refrigerant temperature	47.07	°C
Refrigerant pressure	1138.22	kPa
Inlet refrigerant enthalpy	229.39	kJ/kg
Outlet refrigerant enthalpy	81.84	kJ/kg
Tube thermal resistance	0.0422	°C/MW
Fouling thermal resistance	0.5801	°C/MW
Water thermal resistance	0.2523	°C/MW
Refrigerant thermal resistance	0.4271	°C/MW
Overall UA	768.18	kW/°C
Refrigerant heat load	6886.1	kW(R)

Table 9.70 Stage 1 compressor performance

Compressor 1	**Chiller 1**	**Unit**
Vane angle	0.00	degrees
Refrigerant flowrate	40.45	kg/s
Inlet volumetric flowrate	1.79	m^3/s
Inlet refrigerant temperature	7.34	°C
Inlet refrigerant pressure	389.86	kPa
Inlet specific volume	0.04429	m^3/kg
Inlet enthalpy	190.63	kJ/kg
Outlet refrigerant temperature	44.40	°C
Outlet refrigerant pressure	728.68	kPa
Outlet specific volume	0.02611	m^3/kg
Outlet enthalpy	210.44	kJ/kg
Isentropic head	11.00	kJ/kg
Isentropic efficiency	55.49	%
Absorbed power	801.6	kW(M)
Operating region	STABLE	-

Table 9.71 Stage 2 compressor performance

Compressor 2	**Chiller 1**	**Unit**
Vane angle	0.00	degrees
Refrigerant flowrate	46.67	kg/s
Inlet volumetric flowrate	1.21	m^3/s
Inlet refrigerant temperature	42.35	°C
Inlet refrigerant pressure	728.68	kPa
Inlet specific volume	0.02584	m^3/kg
Inlet enthalpy	208.96	kJ/kg
Outlet refrigerant temperature	77.49	°C
Outlet refrigerant pressure	1138.22	kPa
Outlet specific volume	0.01812	m^3/kg
Outlet enthalpy	229.39	kJ/kg
Isentropic head	8.45	kJ/kg
Isentropic efficiency	41.37	%
Absorbed power	953.5	kW(M)
Operating region	STABLE	-

9.2.2 Kloof mine, 2 chillers operating at full load

Table 9.72 Installation performance, with $t_{(w)Co[max]}$ = 55°C

Installation	Value	Unit
Return water available temperature	32.00	°C
Return water final temperature	52.50	°C
Cool water available temperature	25.00	°C
Chilled water final temperature	10.50	°C
Lorenz COP	11.90	-
System COP	3.00	-
Mass flowrate of return water	160.00	kg/s
Total evaporator water heat load	10302.20	kW(R)
Total return water utilization	64.39	kW(R)/(kg/s)

Table 9.73 Chiller performance

Chiller	Chiller 2	Chiller 1	Unit
Carnot COP	6.24	6.84	-
COP	2.97	3.03	-
Cycle efficiency	48	44	%
Return water utilization	34.20	30.19	kW(R)/(kg/s)

Table 9.74 Evaporator water circuit

Evaporator	**Evap. 2**	**Evap. 1**	**Unit**
Fouling factor	0.00020	0.00020	m^2 °C/W
Water flowrate	169.70	169.70	kg/s
Tube water velocity	2.31	2.31	m/s
Inlet water temp.	25.00	17.30	°C
Outlet water temp.	17.30	10.50	°C
Water heat load	5472.1	4830.1	kW(R)

Table 9.75 Condenser water circuit

Condenser	**Cond. 2**	**Cond. 1**	**Unit**
Fouling factor	0.00020	0.00020	m^2 °C/W
Water flowrate	160.00	160.00	kg/s
Tube water velocity	2.65	2.65	m/s
Inlet water temperature	41.59	32.00	°C
Outlet water temperature	52.50	41.59	°C
Water heat load	7312.3	6421.9	kW(R)

Table 9.76 Evaporator refrigerant circuit

Evaporator	**Evap. 2**	**Evap. 1**	**Unit**
Refrigerant flowrate	44.81	37.76	kg/s
Refrigerant temperature	11.81	5.31	°C
Refrigerant pressure	446.86	365.94	kPa
Inlet refrigerant enthalpy	70.36	61.88	kJ/kg
Outlet refrigerant enthalpy	192.48	189.78	kJ/kg
Tube thermal resistance	0.0521	0.0521	°C/MW
Fouling thermal resistance	0.7150	0.7150	°C/MW
Water thermal resistance	0.4104	0.4473	°C/MW
Refrigerant thermal resistance	0.4274	0.4664	°C/MW
Overall UA	623.11	594.96	kW/°C
Refrigerant heat load	5472.1	4830.1	kW(R)

Table 9.77 Condenser refrigerant circuit

Condenser	**Cond. 2**	**Cond. 1**	**Unit**
Refrigerant flowrate	54.11	43.81	kg/s
Refrigerant temperature	57.48	46.01	°C
Refrigerant pressure	1443.17	1110.20	kPa
Inlet refrigerant enthalpy	228.08	227.33	kJ/kg
Outlet refrigerant enthalpy	92.95	80.74	kJ/kg
Tube thermal resistance	0.0422	0.0422	°C/MW
Fouling thermal resistance	0.5801	0.5801	°C/MW
Water thermal resistance	0.2304	0.2532	°C/MW
Refrigerant thermal resistance	0.4324	0.4192	°C/MW
Overall UA	778.13	772.33	kW/°C
Refrigerant heat load	7312.3	6421.9	kW(R)

Table 9.78 Stage 1 compressor performance

Compressor 1	**Chiller 2**	**Chiller 1**	**Unit**
Vane angle	0.00	0.00	degrees
Refrigerant flowrate	44.81	37.76	kg/s
Inlet volumetric flowrate	1.74	1.78	m^3/s
Inlet refrigerant temperature	11.81	5.31	°C
Inlet refrigerant pressure	446.86	365.94	kPa
Inlet specific volume	0.03883	0.04706	m^3/kg
Inlet enthalpy	192.48	189.78	kJ/kg
Outlet refrigerant temperature	48.40	41.99	°C
Outlet refrigerant pressure	865.35	692.08	kPa
Outlet specific volume	0.02174	0.02739	m^3/kg
Outlet enthalpy	211.25	209.28	kJ/kg
Isentropic head	11.65	11.19	kJ/kg
Isentropic efficiency	62.08	57.39	%
Absorbed power	841.2	736.3	kW(M)
Operating region	STABLE	STABLE	-

Table 9.79 Stage 2 compressor performance

Compressor 2	**Chiller 2**	**Chiller 1**	**Unit**
Vane angle	0.00	0.00	degrees
Refrigerant flowrate	54.11	43.81	kg/s
Inlet volumetric flowrate	1.16	1.19	m^3/s
Inlet refrigerant temperature	46.21	39.93	°C
Inlet refrigerant pressure	865.35	692.08	kPa
Inlet specific volume	0.02148	0.02711	m^3/kg
Inlet enthalpy	209.61	207.80	kJ/kg
Outlet refrigerant temperature	80.74	74.31	°C
Outlet refrigerant pressure	1443.17	1110.20	kPa
Outlet specific volume	0.01376	0.01839	m^3/kg
Outlet enthalpy	228.08	227.33	kJ/kg
Isentropic head	9.53	8.94	kJ/kg
Isentropic efficiency	51.64	45.76	%
Absorbed power	999.0	855.5	kW(M)
Operating region	STABLE	STABLE	-

9.2.3 Kloof mine, 3 chillers operating at unequal part load

Table 9.80 Installation performance, with $t_{(w)Co[max]}$ = 55°C

Installation	Value	Unit
Return water available temperature	32.00	°C
Return water final temperature	55.00	°C
Cool water available temperature	25.00	°C
Chilled water final temperature	10.50	°C
Lorenz COP	11.33	-
System COP	2.93	-
Mass flowrate of return water	160.00	kg/s
Total evaporator water heat load	11491.20	kW(R)
Total return water utilization	71.82	kW(R)/(kg/s)

Table 9.81 Chiller performance

Chiller	Chiller 3	Chiller 2	Chiller 1	Unit
Carnot COP	6.66	7.18	7.76	-
COP	2.90	2.95	2.96	-
Cycle efficiency	44	41	38	%
Return water utilization	25.70	23.94	22.18	kW(R)/(kg/s)

Table 9.82 Evaporator water circuit

Evaporator	**Evap. 3**	**Evap. 2**	**Evap. 1**	**Unit**
Fouling factor	0.00020	0.00020	0.00020	m^2 °C/W
Water flowrate	189.33	189.33	189.33	kg/s
Tube water velocity	2.58	2.58	2.58	m/s
Inlet water temp.	25.00	19.81	14.98	°C
Outlet water temp.	19.81	14.98	10.50	°C
Water heat load	4112.2	3829.6	3549.4	kW(R)

Table 9.83 Condenser water circuit

Condenser	**Cond. 3**	**Cond. 2**	**Cond. 1**	**Unit**
Fouling factor	0.00020	0.00020	0.00020	m^2 °C/W
Water flowrate	160.00	160.00	160.00	kg/s
Tube water velocity	2.65	2.65	2.65	m/s
Inlet water temperature	46.75	39.09	32.00	°C
Outlet water temperature	55.00	46.75	39.09	°C
Water heat load	5531.3	5128.0	4749.4	kW(R)

Table 9.84 Evaporator refrigerant circuit

Evaporator	Evap. 3	Evap. 2	Evap. 1	Unit
Refrigerant flowrate	32.66	29.35	26.40	kg/s
Refrigerant temperature	15.26	10.56	6.22	°C
Refrigerant pressure	494.81	430.31	376.58	kPa
Inlet refrigerant enthalpy	67.96	61.48	55.70	kJ/kg
Outlet refrigerant enthalpy	193.88	191.96	190.16	kJ/kg
Tube thermal resistance	0.0521	0.0521	0.0521	°C/MW
Fouling thermal resistance	0.7150	0.7150	0.7150	°C/MW
Water thermal resistance	0.3707	0.3928	0.4158	°C/MW
Refrigerant thermal resistance	0.5220	0.5487	0.5786	°C/MW
Overall UA	602.50	585.30	567.69	kW/°C
Refrigerant heat load	4112.2	3829.6	3549.4	kW(R)

Table 9.85 Condenser refrigerant circuit

Condenser	Cond. 3	Cond. 2	Cond. 1	Unit
Refrigerant flowrate	40.67	35.44	31.08	kg/s
Refrigerant temperature	58.57	50.10	42.24	°C
Refrigerant pressure	1478.44	1221.54	1014.21	kPa
Inlet refrigerant enthalpy	230.15	229.71	229.67	kJ/kg
Outlet refrigerant enthalpy	94.15	85.02	76.85	kJ/kg
Tube thermal resistance	0.0422	0.0422	0.0422	°C/MW
Fouling thermal resistance	0.5801	0.5801	0.5801	°C/MW
Water thermal resistance	0.2229	0.2390	0.2563	°C/MW
Refrigerant thermal resistance	0.4008	0.3938	0.3870	°C/MW
Overall UA	802.57	796.66	790.12	kW/°C
Refrigerant heat load	5531.3	5128.0	4749.4	kW(R)

Table 9.86 Stage 1 compressor performance

Compressor 1	**Chiller 3**	**Chiller 2**	**Chiller 1**	**Unit**
Vane angle	-37.52	-37.52	-37.52	degrees
Refrigerant flowrate	32.66	29.35	26.40	kg/s
Inlet volumetric flowrate	1.15	1.18	1.21	m^3/s
Inlet refrigerant temperature	15.26	10.56	6.22	°C
Inlet refrigerant pressure	494.81	430.31	376.58	kPa
Inlet specific volume	0.03517	0.04027	0.04579	m^3/kg
Inlet enthalpy	193.88	191.96	190.16	kJ/kg
Outlet refrigerant temperature	55.65	52.82	50.39	°C
Outlet refrigerant pressure	813.75	684.66	581.16	kPa
Outlet specific volume	0.02425	0.02919	0.03472	m^3/kg
Outlet enthalpy	217.36	217.11	216.81	kJ/kg
Isentropic head	8.76	8.15	7.59	kJ/kg
Isentropic efficiency	37.29	32.41	28.46	%
Absorbed power	766.9	738.1	703.6	kW(M)
Operating region	STABLE	STABLE	STABLE	-

Table 9.87 Stage 2 compressor performance

Compressor 2	**Chiller 3**	**Chiller 2**	**Chiller 1**	**Unit**
Vane angle	0.00	0.00	0.00	degrees
Refrigerant flowrate	40.67	35.44	31.08	kg/s
Inlet volumetric flowrate	0.97	1.01	1.06	m^3/s
Inlet refrigerant temperature	51.21	48.30	45.91	°C
Inlet refrigerant pressure	813.75	684.66	581.16	kPa
Inlet specific volume	0.02373	0.02859	0.03404	m^3/kg
Inlet enthalpy	214.11	213.90	213.70	kJ/kg
Outlet refrigerant temperature	83.90	79.24	75.87	°C
Outlet refrigerant pressure	1478.44	1221.54	1014.21	kPa
Outlet specific volume	0.01358	0.01679	0.02061	m^3/kg
Outlet enthalpy	230.15	229.71	229.67	kJ/kg
Isentropic head	11.61	11.46	11.17	kJ/kg
Isentropic efficiency	72.37	72.49	69.95	%
Absorbed power	652.2	560.2	496.4	kW(M)
Operating region	STABLE	STABLE	STABLE	-

9.2.4 Kloof mine, 3 chillers operating at full load

Table 9.88 Installation performance, with $t_{(w)Co[max]}$= 70°C

Installation	Value	Unit
Return water available temperature	32.00	°C
Return water final temperature	62.14	°C
Cool water available temperature	25.00	°C
Chilled water final temperature	10.50	°C
Lorenz COP	9.98	-
System COP	3.07	-
Mass flowrate of return water	160.00	kg/s
Total evaporator water heat load	15231.30	kW(R)
Total return water utilization	95.20	kW(R)/(kg/s)

Table 9.89 Chiller performance

Chiller	Chiller 3	Chiller 2	Chiller 1	Unit
Carnot COP	5.46	6.06	6.81	-
COP	3.06	3.10	3.05	-
Cycle efficiency	56	51	45	%
Return water utilization	33.39	31.87	29.94	kW(R)/(kg/s)

Table 9.90 Evaporator water circuit

Evaporator	**Evap. 3**	**Evap. 2**	**Evap. 1**	**Unit**
Fouling factor	0.00020	0.00020	0.00020	m^2 °C/W
Water flowrate	250.93	250.93	250.93	kg/s
Tube water velocity	3.42	3.42	3.42	m/s
Inlet water temp.	25.00	19.91	15.06	°C
Outlet water temp.	19.91	15.06	10.50	°C
Water heat load	5342.4	5098.4	4790.5	kW(R)

Refer to footnote 43, p.117 with regard to the evaporator tube water velocity of 3.42 m/s, which is too high.

Table 9.91 Condenser water circuit

Condenser	**Cond. 3**	**Cond. 2**	**Cond. 1**	**Unit**
Fouling factor	0.00020	0.00020	0.00020	m^2 °C/W
Water flowrate	160.00	160.00	160.00	kg/s
Tube water velocity	2.65	2.65	2.65	m/s
Inlet water temperature	51.56	41.50	32.00	°C
Outlet water temperature	62.14	51.56	41.50	°C
Water heat load	7088.5	6743.0	6361.4	kW(R)

Table 9.92 Evaporator refrigerant circuit

Evaporator	Evap. 3	Evap. 2	Evap. 1	Unit
Refrigerant flowrate	45.17	41.31	37.41	kg/s
Refrigerant temperature	14.19	9.44	5.04	°C
Refrigerant pressure	479.59	415.95	362.84	kPa
Inlet refrigerant enthalpy	75.17	68.08	61.62	kJ/kg
Outlet refrigerant enthalpy	193.45	191.50	189.66	kJ/kg
Tube thermal resistance	0.0521	0.0521	0.0521	°C/MW
Fouling thermal resistance	0.7150	0.7150	0.7150	°C/MW
Water thermal resistance	0.2957	0.3132	0.3317	°C/MW
Refrigerant thermal resistance	0.4346	0.4491	0.4691	°C/MW
Overall UA	667.81	653.88	637.79	kW/°C
Refrigerant heat load	5342.4	8098.4	4790.5	kW(R)

Table 9.93 Condenser refrigerant circuit

Condenser	Cond. 3	Cond. 2	Cond. 1	Unit
Refrigerant flowrate	57.93	50.13	43.44	kg/s
Refrigerant temperature	66.82	56.10	45.87	°C
Refrigerant pressure	1764.53	1399.75	1106.59	kPa
Inlet refrigerant enthalpy	225.78	225.97	227.05	kJ/kg
Outlet refrigerant enthalpy	103.43	91.45	80.60	kJ/kg
Tube thermal resistance	0.0422	0.0422	0.0422	°C/MW
Fouling thermal resistance	0.5801	0.5801	0.5801	°C/MW
Water thermal resistance	0.2121	0.2314	0.2533	°C/MW
Refrigerant thermal resistance	0.4275	0.4232	0.4182	°C/MW
Overall UA	792.44	783.11	772.89	kW/°C
Refrigerant heat load	7088.5	6743.0	6361.4	kW(R)

Table 9.94 Stage 1 compressor performance

Compressor 1	**Chiller 3**	**Chiller 2**	**Chiller 1**	**Unit**
Vane angle	0.00	0.00	0.00	degrees
Refrigerant flowrate	45.17	41.31	37.41	kg/s
Inlet volumetric flowrate	1.64	1.72	1.78	m^3/s
Inlet refrigerant temperature	14.19	9.44	5.04	°C
Inlet refrigerant pressure	479.59	415.95	362.84	kPa
Inlet specific volume	0.03626	0.04161	0.04745	m^3/kg
Inlet enthalpy	193.45	191.50	189.66	kJ/kg
Outlet refrigerant temperature	50.47	45.59	41.67	°C
Outlet refrigerant pressure	974.34	816.27	687.34	kPa
Outlet specific volume	0.01902	0.02297	0.02757	m^3/kg
Outlet enthalpy	211.08	209.94	209.12	kJ/kg
Isentropic head	12.51	11.88	11.22	kJ/kg
Isentropic efficiency	70.97	64.44	57.66	%
Absorbed power	796.5	761.5	727.9	kW(M)
Operating region	STABLE	STABLE	STABLE	-

Table 9.95 Stage 2 compressor performance

Compressor 2	**Chiller 3**	**Chiller 2**	**Chiller 1**	**Unit**
Vane angle	0.00	0.00	0.00	degrees
Refrigerant flowrate	57.93	50.13	43.44	kg/s
Inlet volumetric flowrate	1.09	1.14	1.19	m^3/s
Inlet refrigerant temperature	48.27	43.44	36.61	°C
Inlet refrigerant pressure	974.34	816.27	687.34	kPa
Inlet specific volume	0.01878	0.02271	0.02728	m^3/kg
Inlet enthalpy	209.39	208.35	207.64	kJ/kg
Outlet refrigerant temperature	83.32	77.40	73.89	°C
Outlet refrigerant pressure	1764.53	1399.75	1106.59	kPa
Outlet specific volume	0.01072	0.01405	0.01842	m^3/kg
Outlet enthalpy	225.78	225.97	227.05	kJ/kg
Isentropic head	10.84	10.04	9.00	kJ/kg
Isentropic efficiency	66.14	56.96	46.37	%
Absorbed power	949.6	883.1	843.0	kW(M)
Operating region	STABLE	STABLE	STABLE	-

9.2.5 Kloof mine, 4 chillers operating at full load

Table 9.96 Installation performance, with $t_{(w)Co[max]}$ = 70°C

Installation	Value	Unit
Return water available temperature	32.00	°C
Return water final temperature	70.24	°C
Cool water available temperature	25.00	°C
Chilled water final temperature	10.50	°C
Lorenz COP	8.80	-
System COP	3.05	-
Mass flowrate of return water	160.00	kg/s
Total evaporator water heat load	19286.50	kW(R)
Total return water utilization	120.54	kW(R)/(kg/s)

Table 9.97 Chiller performance

Chiller	Chiller 4	Chiller 3	Chiller 2	Chiller 1	Unit
Carnot COP	5.00	5.37	5.98	6.80	-
COP	2.84	3.15	3.16	3.06	-
Cycle efficiency	0.57	0.59	0.53	0.45	%
Return water utilization	28.68	31.15	30.87	29.83	kW(R)/(kg/s)

Table 9.98 Evaporator water circuit

Evaporator	**Evap. 4**	**Evap. 3**	**Evap. 2**	**Evap. 1**	**Unit**
Fouling factor	0.00020	0.00020	0.00020	0.00020	m^2 °C/W
Water flowrate	317.75	317.75	317.75	317.75	kg/s
Tube water velocity	4.33	4.33	4.33	4.33	m/s
Inlet water temp.	25.00	21.55	17.80	14.09	°C
Outlet water temp.	21.55	17.80	14.09	10.50	°C
Water heat load	4589.3	4984.2	4939.8	4773.2	kW(R)

Refer to footnote 43, p.117 with regard to the evaporator tube water velocity of 4.33 m/s, which is too high.

Table 9.99 Condenser water circuit

Condenser	**Cond. 4**	**Cond. 3**	**Cond. 2**	**Cond. 1**	**Unit**
Fouling factor	0.00020	0.00020	0.00020	0.00020	m^2 °C/W
Water flowrate	160.00	160.00	160.00	160.00	kg/s
Tube water velocity	2.65	2.65	2.65	2.65	m/s
Inlet water temperature	60.27	51.17	41.46	32.00	°C
Outlet water temperature	70.24	60.97	51.17	41.46	°C
Water heat load	6207.2	6568.9	6505.5	6335.0	kW(R)

Table 9.100 Evaporator refrigerant circuit

Evaporator	Evap. 4	Evap. 3	Evap. 2	Evap. 1	Unit
Refrigerant flowrate	39.90	41.69	39.85	37.26	kg/s
Refrigerant temperature	16.28	12.16	8.43	4.92	°C
Refrigerant pressure	509.77	451.58	403.25	361.49	kPa
Inlet refrigerant enthalpy	79.28	73.08	67.12	61.52	kJ/kg
Outlet refrigerant enthalpy	194.29	192.62	191.08	189.62	kJ/kg
Tube thermal resistance	0.0521	0.0521	0.0521	0.0521	°C/MW
Fouling thermal resistance	0.7150	0.7150	0.7150	0.7150	°C/MW
Water thermal resistance	0.2426	0.2527	0.2641	0.2763	°C/MW
Ref. thermal resistance	0.4834	0.4563	0.4591	0.4703	°C/MW
Overall UA	669.76	677.49	671.00	660.64	kW/°C
Refrigerant heat load	4589.3	4984.2	4939.8	4773.2	kW(R)

Table 9.101 Condenser refrigerant circuit

Condenser	Cond. 4	Cond. 3	Cond. 2	Cond. 1	Unit
Refrigerant flowrate	54.05	53.48	48.46	43.27	kg/s
Refrigerant temperature	74.17	65.26	55.52	45.81	°C
Refrigerant pressure	2052.13	1707.73	1381.91	1105.02	kPa
Inlet refrigerant enthalpy	226.96	224.47	225.08	226.93	kJ/kg
Outlet refrigerant enthalpy	112.12	101.64	90.82	80.54	kJ/kg
Tube thermal resistance	0.0422	0.0422	0.0422	0.0422	°C/MW
Fouling thermal resistance	0.5801	0.5801	0.5801	0.5801	°C/MW
Water thermal resistance	0.1980	0.2134	0.2319	0.2534	°C/MW
Ref. thermal resistance	0.4116	0.4190	0.4192	0.4177	°C/MW
Overall UA	811.71	796.98	785.30	773.14	kW/°C
Refrigerant heat load	6207.2	6568.9	6505.5	6335.0	kW(R)

Table 9.102 Stage 1 compressor performance

Compressor 1	**Chiller 4**	**Chiller 3**	**Chiller 2**	**Chiller 1**	**Unit**
Vane angle	0.00	0.00	0.00	0.00	degrees
Refrigerant flowrate	39.90	41.69	39.85	37.26	kg/s
Inlet volumetric flowrate	1.36	1.60	1.71	1.77	m^3/s
Inlet refrigerant temperature	16.28	12.16	8.43	4.92	°C
Inlet refrigerant pressure	509.77	451.58	403.25	361.49	kPa
Inlet specific volume	0.03417	0.03844	0.04287	0.04762	m^3/kg
Inlet enthalpy	194.29	192.62	191.08	189.62	kJ/kg
Outlet refrigerant temp.	54.68	48.24	44.39	41.52	°C
Outlet refrigerant pressure	1073.60	925.94	796.20	685.28	kPa
Outlet specific volume	0.01726	0.02000	0.02351	0.02764	m^3/kg
Outlet enthalpy	212.75	210.16	209.37	209.05	kJ/kg
Isentropic head	13.16	12.67	11.98	11.23	kJ/kg
Isentropic efficiency	71.27	72.26	65.52	57.78	%
Absorbed power	736.6	731.3	728.8	724.2	kW(M)
Operating region	STABLE	STABLE	STABLE	STABLE	-

Table 9.103 Stage 2 compressor performance

Compressor 2	**Chiller 4**	**Chiller 3**	**Chiller 2**	**Chiller 1**	**Unit**
Vane angle	0.00	0.00	0.00	0.00	degrees
Refrigerant flowrate	54.05	53.48	48.46	43.27	kg/s
Inlet volumetric flowrate	0.92	1.06	1.13	1.18	m^3/s
Inlet refrigerant temperature	52.01	46.08	42.27	39.47	°C
Inlet refrigerant pressure	1073.60	925.94	796.20	685.28	kPa
Inlet specific volume	0.01699	0.01976	0.02325	0.02736	m^3/kg
Inlet enthalpy	210.65	208.52	207.81	207.58	kJ/kg
Outlet refrigerant temp.	89.47	80.83	75.98	73.71	°C
Outlet refrigerant pressure	2052.13	1707.73	1381.91	1105.02	kPa
Outlet specific volume	0.00903	0.01103	0.01417	0.01844	m^3/kg
Outlet enthalpy	226.96	224.47	225.08	226.93	kJ/kg
Isentropic head	11.73	11.19	10.25	9.03	kJ/kg
Isentropic efficiency	71.96	70.10	59.36	46.65	%
Absorbed power	881.3	853.4	836.9	837.6	kW(M)
Operating region	STABLE	STABLE	STABLE	STABLE	-

9.2.6 Tau Tona mine, 2 chillers operating at full load

Table 9.104 Installation performance, with $t_{(w)Co[max]}$ = 55°C

Installation	Value	Unit
Return water available temperature	32.00	°C
Return water final temperature	42.40	°C
Cool water available temperature	18.89	°C
Chilled water final temperature	5.50	°C
Lorenz COP	11.40	-
System COP	3.14	-
Mass flowrate of return water	266.00	kg/s
Total evaporator water heat load	8786.60	kW(R)
Total return water utilization	33.03	kW(R)/(kg/s)

Table 9.105 Chiller performance

Chiller	Chiller 2	Chiller 1	Unit
Carnot COP	7.31	7.22	-
COP	3.06	3.25	-
Cycle efficiency	42	45	%
Return water utilization	17.82	15.21	kW(R)/(kg/s)

Table 9.106 Evaporator water circuit

Evaporator	**Evap. 2**	**Evap. 1**	**Unit**
Fouling factor	0.00009	0.00009	m^2 °C/W
Water flowrate	156.71	156.71	kg/s
Tube water velocity	2.90	2.90	m/s
Inlet water temp.	18.89	11.66	°C
Outlet water temp.	11.66	5.50	°C
Water heat load	4740.7	4045.9	kW(R)

Table 9.107 Condenser water circuit

Condenser	**Cond. 2**	**Cond. 1**	**Unit**
Fouling factor	0.00018	0.00018	m^2 °C/W
Water flowrate	266.00	266.00	kg/s
Tube water velocity	2.94	2.94	m/s
Inlet water temperature	36.75	32.00	°C
Outlet water temperature	42.40	36.75	°C
Water heat load	6292.2	5289.8	kW(R)

Table 9.108 Evaporator refrigerant circuit

Evaporator	Evap. 2	Evap. 1	Unit
Refrigerant flowrate	34.99	29.08	kg/s
Refrigerant temperature	8.73	2.67	°C
Refrigerant pressure	406.93	336.41	kPa
Inlet refrigerant enthalpy	55.71	49.53	kJ/kg
Outlet refrigerant enthalpy	191.20	188.66	kJ/kg
Tube thermal resistance	0.0826	0.0826	°C/MW
Fouling thermal resistance	0.3014	0.3014	°C/MW
Water thermal resistance	0.3558	0.3874	°C/MW
Refrigerant thermal resistance	0.4886	0.5460	°C/MW
Overall UA	814.05	759.06	kW/°C
Refrigerant heat load	4740.7	4045.9	kW(R)

Table 9.109 Condenser refrigerant circuit

Condenser	Cond. 2	Cond. 1	Unit
Refrigerant flowrate	43.08	34.46	kg/s
Refrigerant temperature	47.31	40.85	°C
Refrigerant pressure	1144.80	980.52	kPa
Inlet refrigerant enthalpy	228.14	224.62	kJ/kg
Outlet refrigerant enthalpy	82.10	75.44	kJ/kg
Tube thermal resistance	0.0660	0.0660	°C/MW
Fouling thermal resistance	0.4976	0.4976	°C/MW
Water thermal resistance	0.2213	0.2327	°C/MW
Refrigerant thermal resistance	0.3877	0.3709	°C/MW
Overall UA	852.77	856.76	kW/°C
Refrigerant heat load	6292.2	5289.8	kW(R)

Table 9.110 Stage 1 compressor performance

Compressor 1	**Chiller 2**	**Chiller 1**	**Unit**
Vane angle	0.00	0.00	degrees
Refrigerant flowrate	34.99	29..08	kg/s
Inlet volumetric flowrate	1.49	1.48	m^3/s
Inlet refrigerant temperature	8.73	2.67	°C
Inlet refrigerant pressure	406.93	336.41	kPa
Inlet specific volume	0.04250	0.05101	m^3/kg
Inlet enthalpy	191.20	188.66	kJ/kg
Outlet refrigerant temperature	31.42	25.20	°C
Outlet refrigerant pressure	581.28	482.86	kPa
Outlet specific volume	0.03178	0.03807	m^3/kg
Outlet enthalpy	203.57	200.95	kJ/kg
Isentropic head	6.23	6.28	kJ/kg
Isentropic efficiency	50.40	51.11	%
Absorbed power	432.8	357.4	kW(M)
Operating region	STABLE	STABLE	-

Table 9.111 Stage 2 compressor performance

Compressor 2	**Chiller 2**	**Chiller 1**	**Unit**
Vane angle	0.00	0.00	degrees
Refrigerant flowrate	43.08	35.46	kg/s
Inlet volumetric flowrate	1.36	1.34	m^3/s
Inlet refrigerant temperature	29.43	23.25	°C
Inlet refrigerant pressure	581.28	482.86	kPa
Inlet specific volume	0.03146	0.03771	m^3/kg
Inlet enthalpy	202.17	199.62	kJ/kg
Outlet refrigerant temperature	75.95	68.53	°C
Outlet refrigerant pressure	1144.80	980.52	kPa
Outlet specific volume	0.01787	0.02073	m^3/kg
Outlet enthalpy	228.14	224.62	kJ/kg
Isentropic head	12.55	13.12	kJ/kg
Isentropic efficiency	48.34	52.48	%
Absorbed power	1118.7	886.5	kW(M)
Operating region	STABLE	STABLE	-

9.2.7 Tau Tona mine, 3 chillers operating at full load

Table 9.112 Installation performance, with $t_{(w)Co[max]}$ = 55°C

Installation	Value	Unit
Return water available temperature	32.00	°C
Return water final temperature	46.88	°C
Cool water available temperature	18.89	°C
Chilled water final temperature	5.50	°C
Lorenz COP	10.47	-
System COP	3.26	-
Mass flowrate of return water	266.00	kg/s
Total evaporator water heat load	12679.60	kW(R)
Total return water utilization	47.67	kW(R)/(kg/s)

Table 9.113 Chiller performance

Chiller	Chiller 3	Chiller 2	Chiller 1	Unit
Carnot COP	6.65	6.82	6.97	-
COP	3.17	3.27	3.36	-
Cycle efficiency	48	48	48	%
Return water utilization	17.47	15.82	14.38	kW(R)/(kg/s)

Table 9.114 Evaporator water circuit

Evaporator	**Evap. 3**	**Evap. 2**	**Evap. 1**	**Unit**
Fouling factor	0.00009	0.00009	0.00009	m^2 °C/W
Water flowrate	226.20	226.20	226.20	kg/s
Tube water velocity	1.39	1.39	1.39	m/s
Inlet water temp.	18.89	13.98	9.54	°C
Outlet water temp.	13.98	9.54	5.50	°C
Water heat load	4647.1	4207.6	3824.9	kW(R)

Table 9.115 Condenser water circuit

Condenser	**Cond. 3**	**Cond. 2**	**Cond. 1**	**Unit**
Fouling factor	0.00018	0.00018	0.00018	m^2 °C/W
Water flowrate	266.00	266.00	266.00	kg/s
Tube water velocity	2.94	2.94	2.94	m/s
Inlet water temperature	41.39	36.46	32.00	°C
Outlet water temperature	46.88	41.39	36.46	°C
Water heat load	6114.0	5493.4	4963.0	kW(R)

Table 9.116 Evaporator refrigerant circuit

Evaporator	Evap. 3	Evap. 2	Evap. 1	Unit
Refrigerant flowrate	34.58	30.65	27.35	kg/s
Refrigerant temperature	9.14	4.86	0.97	°C
Refrigerant pressure	412.12	360.73	318.38	kPa
Inlet refrigerant enthalpy	57.00	52.29	48.10	kJ/kg
Outlet refrigerant enthalpy	191.38	189.59	187.94	kJ/kg
Tube thermal resistance	0.0826	0.0826	0.0826	°C/MW
Fouling thermal resistance	0.3014	0.3014	0.3014	°C/MW
Water thermal resistance	0.6299	0.6674	0.7056	°C/MW
Refrigerant thermal resistance	0.4955	0.5312	0.5679	°C/MW
Overall UA	662.52	631.86	603.34	kW/°C
Refrigerant heat load	4647.1	4207.6	3824.9	kW(R)

Table 9.117 Condenser refrigerant circuit

Condenser	Cond. 3	Cond. 2	Cond. 1	Unit
Refrigerant flowrate	43.88	38.16	33.55	kg/s
Refrigerant temperature	51.58	45.61	40.28	°C
Refrigerant pressure	1263.83	1099.75	966.79	kPa
Inlet refrigerant enthalpy	225.93	224.29	222.78	kJ/kg
Outlet refrigerant enthalpy	86.59	80.33	74.85	kJ/kg
Tube thermal resistance	0.0660	0.0660	0.0660	°C/MW
Fouling thermal resistance	0.4976	0.4976	0.4976	°C/MW
Water thermal resistance	0.2122	0.2227	0.2331	°C/MW
Refrigerant thermal resistance	0.3840	0.3739	0.3646	°C/MW
Overall UA	862.21	861.94	861.15	kW/°C
Refrigerant heat load	6114.0	5493.4	4963.0	kW(R)

Table 9.118 Stage 1 compressor performance

Compressor 1	**Chiller 3**	**Chiller 2**	**Chiller 1**	**Unit**
Vane angle	0.00	0.00	0.00	degrees
Refrigerant flowrate	34.58	30.65	27.35	kg/s
Inlet volumetric flowrate	1.45	1.46	1.47	m^3/s
Inlet refrigerant temperature	9.14	4.86	0.97	°C
Inlet refrigerant pressure	412.12	360.73	318.38	kPa
Inlet specific volume	0.04198	0.04771	0.05377	m^3/kg
Inlet enthalpy	191.38	189.59	187.94	kJ/kg
Outlet refrigerant temperature	31.18	26.97	23.19	°C
Outlet refrigerant pressure	603.48	525.31	461.66	kPa
Outlet specific volume	0.03040	0.03491	0.03966	m^3/kg
Outlet enthalpy	203.03	201.43	199.95	kJ/kg
Isentropic head	6.67	6.55	6.45	kJ/kg
Isentropic efficiency	57.30	55.30	53.67	%
Absorbed power	402.8	363.0	328.6	kW(M)
Operating region	STABLE	STABLE	STABLE	-

Table 9.119 Stage 2 compressor performance

Compressor 2	**Chiller 3**	**Chiller 2**	**Chiller 1**	**Unit**
Vane angle	0.00	0.00	0.00	degrees
Refrigerant flowrate	43.88	38.16	33.55	kg/s
Inlet volumetric flowrate	1.32	1.32	1.32	m^3/s
Inlet refrigerant temperature	29.27	25.06	21.28	°C
Inlet refrigerant pressure	603.48	525.31	461.66	kPa
Inlet specific volume	0.03010	0.03457	0.03929	m^3/kg
Inlet enthalpy	201.67	200.11	198.65	kJ/kg
Outlet refrigerant temperature	75.05	70.14	65.82	°C
Outlet refrigerant pressure	1263.83	1099.75	966.79	kPa
Outlet specific volume	0.01577	0.01822	0.02081	m^3/kg
Outlet enthalpy	225.93	224.29	222.78	kJ/kg
Isentropic head	13.58	13.63	13.66	kJ/kg
Isentropic efficiency	56.01	56.36	56.61	%
Absorbed power	1064.1	922.7	809.5	kW(M)
Operating region	STABLE	STABLE	STABLE	-

9.2.8 Tau Tona mine, 4 chillers operating at full load

Table 9.120 Installation performance, with $t_{(w)Co[max]}$ = 55°C

Installation	Value	Unit
Return water available temperature	32.00	°C
Return water final temperature	51.84	°C
Cool water available temperature	18.89	°C
Chilled water final temperature	5.50	°C
Lorenz COP	9.61	-
System COP	3.29	-
Mass flowrate of return water	266.00	kg/s
Total evaporator water heat load	16946.50	kW(R)
Total return water utilization	63.71	kW(R)/(kg/s)

Table 9.121 Chiller performance

Chiller	Chiller 4	Chiller 3	Chiller 2	Chiller 1	Unit
Carnot COP	6.17	6.43	6.71	6.99	-
COP	3.22	3.28	3.33	3.35	-
Cycle efficiency	52	51	50	48	%
Return water utilization	17.49	16.40	15.38	14.43	kW(R)/(kg/s)

Table 9.122 Evaporator water circuit

Evaporator	**Evap. 4**	**Evap. 3**	**Evap. 2**	**Evap. 1**	**Unit**
Fouling factor	0.00009	0.00009	0.00009	0.00009	m^2 °C/W
Water flowrate	302.29	302.29	302.29	302.29	kg/s
Tube water velocity	1.86	1.86	1.86	1.86	m/s
Inlet water temp.	18.89	15.21	11.77	8.53	°C
Outlet water temp.	15.21	11.77	8.53	5.50	°C
Water heat load	4653.1	4363.4	4091.4	3838.6	kW(R)

Table 9.123 Condenser water circuit

Condenser	**Cond. 4**	**Cond. 3**	**Cond. 2**	**Cond. 1**	**Unit**
Fouling factor	0.00018	0.00018	0.00018	0.00018	m^2 °C/W
Water flowrate	266.00	266.00	266.00	266.00	kg/s
Tube water velocity	2.94	2.94	2.94	2.94	m/s
Inlet water temperature	46.36	41.25	36.47	32.00	°C
Outlet water temperature	51.84	46.36	41.25	36.47	°C
Water heat load	6098.6	5692.7	5321.5	4983.2	kW(R)

Table 9.124 Evaporator refrigerant circuit

Evaporator	Evap. 4	Evap. 3	Evap. 2	Evap. 1	Unit
Refrigerant flowrate	35.06	32.25	29.72	27.46	kg/s
Refrigerant temperature	10.48	7.14	4.01	1.08	°C
Refrigerant pressure	429.28	387.44	351.13	319.49	kPa
Inlet refrigerant enthalpy	59.20	55.23	51.57	48.19	kJ/kg
Outlet refrigerant enthalpy	191.93	190.54	189.23	187.98	kJ/kg
Tube thermal resistance	0.0826	0.0826	0.0826	0.0826	°C/MW
Fouling thermal resistance	0.3014	0.3014	0.3014	0.3014	°C/MW
Water thermal resistance	0.4958	0.5178	0.5404	0.5633	°C/MW
Refrigerant thermal resistance	0.4951	0.5178	0.5417	0.5664	°C/MW
Overall UA	727.34	704.38	682.10	660.60	kW/°C
Refrigerant heat load	4653.1	4363.4	4091.4	3838.6	kW(R)

Table 9.125 Condenser refrigerant circuit

Condenser	Cond. 4	Cond. 3	Cond. 2	Cond. 1	Unit
Refrigerant flowrate	45.89	41.15	37.12	33.67	kg/s
Refrigerant temperature	56.47	50.70	45.33	40.31	°C
Refrigerant pressure	1411.25	1238.72	1092.36	967.63	kPa
Inlet refrigerant enthalpy	224.76	224.02	223.40	222.90	kJ/kg
Outlet refrigerant enthalpy	91.85	85.66	80.03	74.89	kJ/kg
Tube thermal resistance	0.0660	0.0660	0.0660	0.0660	°C/MW
Fouling thermal resistance	0.4976	0.4976	0.4976	0.4976	°C/MW
Water thermal resistance	0.2031	0.2129	0.2228	0.2331	°C/MW
Refrigerant thermal resistance	0.3830	0.3767	0.3707	0.3650	°C/MW
Overall UA	869.79	867.19	864.22	860.87	kW/°C
Refrigerant heat load	6098.6	5692.7	5321.5	4983.2	kW(R)

Table 9.126 Stage 1 compressor performance

Compressor 1	**Chiller 4**	**Chiller 3**	**Chiller 2**	**Chiller 1**	**Unit**
Vane angle	0.00	0.00	0.00	0.00	degrees
Refrigerant flowrate	35.06	32.25	29.72	27.46	kg/s
Inlet volumetric flowrate	1.41	1.44	1.46	1.47	m^3/s
Inlet refrigerant temperature	10.48	7.14	4.01	1.08	°C
Inlet refrigerant pressure	429.28	387.44	351.13	319.49	kPa
Inlet specific volume	0.04036	0.04455	0.04896	0.05359	m^3/kg
Inlet enthalpy	191.93	190.54	189.23	187.98	kJ/kg
Outlet refrigerant temp.	32.06	28.88	25.97	23.32	°C
Outlet refrigerant pressure	642.46	573.23	513.95	462.96	kPa
Outlet specific volume	0.02839	0.03188	0.03561	0.03955	m^3/kg
Outlet enthalpy	202.98	201.93	200.94	200.02	kJ/kg
Isentropic head	7.07	6.85	6.64	6.44	kJ/kg
Isentropic efficiency	63.95	60.13	56.66	53.50	%
Absorbed power	387.4	367.1	348.1	330.4	kW(M)
Operating region	STABLE	STABLE	STABLE	STABLE	-

Table 9.127 Stage 2 compressor performance

Compressor 2	**Chiller 4**	**Chiller 3**	**Chiller 2**	**Chiller 1**	**Unit**
Vane angle	0.00	0.00	0.00	0.00	degrees
Refrigerant flowrate	45.89	41.15	37.12	33.67	kg/s
Inlet volumetric flowrate	1.29	1.30	1.31	1.32	m^3/s
Inlet refrigerant temperature	30.27	27.03	24.09	21.41	°C
Inlet refrigerant pressure	642.46	573.23	513.95	462.96	kPa
Inlet specific volume	0.02812	0.03158	0.03527	0.03918	m^3/kg
Inlet enthalpy	201.69	200.63	199.64	198.71	kJ/kg
Outlet refrigerant temp.	76.08	72.19	68.85	65.99	°C
Outlet refrigerant pressure	1411.25	1238.72	1092.36	967.63	kPa
Outlet specific volume	0.01380	0.01592	0.01825	0.02080	m^3/kg
Outlet enthalpy	224.76	224.02	223.40	222.90	kJ/kg
Isentropic head	14.35	14.13	13.89	13.63	kJ/kg
Isentropic efficiency	62.22	60.43	58.45	56.34	%
Absorbed power	1058.2	962.3	882.1	814.2	kW(M)
Operating region	STABLE	STABLE	STABLE	STABLE	-

9.2.9 Tau Tona mine, 5 chillers operating at full load

Table 9.128 Installation performance, with $t_{(w)Co[max]}$ = 70°C

Installation	Value	Unit
Return water available temperature	32.00	°C
Return water final temperature	56.57	°C
Cool water available temperature	18.89	°C
Chilled water final temperature	5.50	°C
Lorenz COP	8.92	-
System COP	3.33	-
Mass flowrate of return water	266.00	kg/s
Total evaporator water heat load	21036.00	kW(R)
Total return water utilization	79.08	kW(R)/(kg/s)

Table 9.129 Chiller performance

Chiller	Chiller 5	Chiller 4	Chiller 3	Chiller 2	Chiller 1	Unit
Carnot COP	5.73	6.01	6.32	6.64	7.00	-
COP	3.27	3.32	3.35	3.36	3.35	-
Cycle efficiency	57	55	53	51	48	%
Return w. utilizat.	17.15	16.50	15.82	15.14	14.47	kW(R)/(kg/s)

Table 9.130 Evaporator water circuit

Evaporator	**Evap. 5**	**Evap. 4**	**Evap. 3**	**Evap. 2**	**Evap. 1**	**Unit**
Fouling factor	0.00009	0.00009	0.00009	0.00009	0.00009	m^2 °C/W
Water flowrate	375.32	375.32	375.32	375.32	375.32	kg/s
Tube water velocity	2.31	2.31	2.31	2.31	2.31	m/s
Inlet water temp.	18.89	15.99	13.19	10.51	7.95	°C
Outlet water temp.	15.99	13.19	10.51	7.95	5.50	°C
Water heat load	4562.9	4389.4	4208.4	4026.8	3848.5	kW(R)

Table 9.131 Condenser water circuit

Condenser	**Cond. 5**	**Cond. 4**	**Cond. 3**	**Cond. 2**	**Cond. 1**	**Unit**
Fouling factor	0.00018	0.00018	0.00018	0.00018	0.00018	m^2 °C/W
Water flowrate	266.00	266.00	266.00	266.00	266.00	kg/s
Tube water velocity	2.94	2.94	2.94	2.94	2.94	m/s
Inlet water temp.	51.22	46.09	41.18	36.49	32.00	°C
Outlet water temp.	56.57	51.22	46.09	41.18	36.49	°C
Water heat load	5958.9	5711.7	5465.5	5226.6	4997.8	kW(R)

Table 9.132 Evaporator refrigerant circuit

Evaporator	Evap. 5	Evap. 4	Evap. 3	Evap. 2	Evap. 1	Unit
Ref. flowrate	34.75	32.85	30.99	29.21	27.54	kg/s
Ref. temperature	11.38	6.84	6.03	3.53	1.15	°C
Ref. pressure	441.16	405.91	374.27	345.85	320.29	kPa
Inlet ref. enthalpy	60.99	57.53	54.26	51.17	48.25	kJ/kg
Outlet ref. enthalpy	192.30	191.17	190.08	189.03	188.02	kJ/kg
Tube thermal res.	0.0826	0.0826	0.0826	0.0826	0.0826	°C/MW
Fouling thermal res.	0.3014	0.3014	0.3014	0.3014	0.3014	°C/MW
Water thermal res.	0.4151	0.4296	0.4446	0.4599	0.4756	°C/MW
Ref. thermal res.	0.5019	0.5157	0.5311	0.5478	0.5654	°C/MW
Overall UA	768.65	752.26	735.44	718.53	701.72	kW/°C
Ref. heat load	4562.9	4389.4	4208.4	4026.8	3848.5	kW(R)

Table 9.133 Condenser refrigerant circuit

Condenser	Cond. 5	Cond. 4	Cond. 3	Cond. 2	Cond. 1	Unit
Ref. flowrate	47.04	43.15	39.66	36.54	33.75	kg/s
Ref. temperature	61.02	55.52	50.23	45.17	40.34	°C
Ref. pressure	1559.69	1381.72	1225.42	1088.36	968.25	kPa
Inlet ref. enthalpy	223.53	223.17	222.97	222.91	222.98	kJ/kg
Outlet ref. enthalpy	96.86	90.82	85.16	79.87	74.91	kJ/kg
Tube thermal res.	0.0660	0.0660	0.0660	0.0660	0.0660	°C/MW
Fouling thermal res.	0.4976	0.4976	0.4976	0.4976	0.4976	°C/MW
Water thermal res.	0.1951	0.2039	0.2132	0.2229	0.2330	°C/MW
Ref. thermal res.	0.3799	0.3763	0.3726	0.3689	0.3653	°C/MW
Overall UA	878.29	874.25	870.02	865.51	860.67	kW/°C
Ref. heat load	5958.9	5711.7	5465.5	5226.6	4997.8	kW(R)

Table 9.134 Stage 1 compressor performance

Compressor 1	Chiller 5	Chiller 4	Chiller 3	Chiller 2	Chiller 1	Unit
Vane angle	0.00	0.00	0.00	0.00	0.00	degrees
Ref. flowrate	34.75	32.85	30.99	29.21	27.54	kg/s
Inlet vol. flowrate	1.37	1.40	1.43	1.45	1.47	m^3/s
Inlet ref. temp.	11.38	8.64	6.03	3.53	1.15	°C
Inlet ref. pressure	441.16	405.91	374.27	345.85	320.29	kPa
Inlet specific volume	0.03931	0.04260	0.04606	0.04968	0.05346	m^3/kg
Inlet enthalpy	192.30	191.17	190.08	189.03	188.02	kJ/kg
Outlet ref. temp.	32.60	29.98	27.59	25.41	23.41	°C
Outlet ref. pressure	675.38	612.79	557.11	507.72	463.91	kPa
Outlet specific vol.	0.02685	0.02968	0.03273	0.03600	0.03948	m^3/kg
Outlet enthalpy	202.79	202.01	201.31	200.66	200.06	kJ/kg
Isentropic head	7.47	7.21	6.95	6.68	6.43	kJ/kg
Isentropic efficiency	71.24	66.50	61.85	57.45	53.38	%
Absorbed power	364.4	356.1	348.0	339.8	331.7	kW(M)
Operating region	STABLE	STABLE	STABLE	STABLE	STABLE	-

Table 9.135 Stage 2 compressor performance

Compressor 2	Chiller 5	Chiller 4	Chiller 3	Chiller 2	Chiller 1	Unit
Vane angle	0.00	0.00	0.00	0.00	0.00	degrees
Ref. flowrate	47.04	43.15	39.66	36.54	33.75	kg/s
Inlet vol. flowrate	1.25	1.27	1.29	1.30	1.32	m^3/s
Inlet ref. temp.	30.96	28.25	25.79	23.54	21.50	°C
Inlet ref. pressure	675.38	612.79	557.11	507.72	463.91	kPa
Inlet specific volume	0.02661	0.02941	0.03243	0.03567	0.03911	m^3/kg
Inlet enthalpy	201.60	200.78	200.04	199.37	198.76	kJ/kg
Outlet ref. temp.	77.15	73.61	70.61	68.13	66.11	°C
Outlet ref. pressure	1559.69	1381.72	1225.42	1088.38	968.25	kPa
Outlet specific vol.	0.01218	0.01398	0.01600	0.01827	0.02080	m^3/kg
Outlet enthalpy	223.53	223.17	222.97	222.91	222.98	kJ/kg
Isentropic head	15.14	14.81	14.44	14.04	13.60	kJ/kg
Isentropic efficiency	69.06	66.15	63.01	59.65	56.15	%
Absorbed power	1031.5	966.1	909.2	860.0	817.6	kW(M)
Operating region	STABLE	STABLE	STABLE	STABLE	STABLE	-

9.2.10 Tau Tona mine, 5 chillers with 4 operating at full load and the lag chiller at part load

Table 9.136 Installation performance, with $t_{(w)Co[max]}$ = 55°C

Installation	Value	Unit
Return water available temperature	32.00	°C
Return water final temperature	55.01	°C
Cool water available temperature	18.89	°C
Chilled water final temperature	5.50	°C
Lorenz COP	9.14	-
System COP	3.29	-
Mass flowrate of return water	266.00	kg/s
Total evaporator water heat load	19654.6	kW(R)
Total return water utilization	73.89	kW(R)/(kg/s)

Table 9.137 Chiller performance

Chiller	Chiller 5	Chiller 4	Chiller 3	Chiller 2	Chiller 1	Unit
Carnot COP	5.86	6.14	6.44	6.75	7.78	-
COP	3.26	3.31	3.34	3.36	3.17	-
Cycle efficiency	56	54	52	50	41	%
Return w. utilizat.	17.27	16.48	15.69	14.93	9.51	kW(R)/(kg/s)

Table 9.138 Evaporator water circuit

Evaporator	**Evap. 5**	**Evap. 4**	**Evap. 3**	**Evap. 2**	**Evap. 1**	**Unit**
Fouling factor	0.00009	0.00009	0.00020	0.00009	0.00009	m^2 °C/W
Water flowrate	350.50	350.50	350.50	350.50	350.50	kg/s
Tube water velocity	2.16	2.16	2.16	2.16	2.16	m/s
Inlet water temp.	18.89	15.76	12.77	9.93	7.22	°C
Outlet water temp.	15.76	12.77	9.93	7.22	5.50	°C
Water heat load	4594.5	4384.4	4174.8	3970.5	2530.4	kW(R)

Table 9.139 Condenser water circuit

Condenser	**Cond. 5**	**Cond. 4**	**Cond. 3**	**Cond. 2**	**Cond. 1**	**Unit**
Fouling factor	0.00018	0.00018	0.00018	0.00018	0.00018	m^2 °C/W
Water flowrate	266.00	266.00	266.00	266.00	266.00	kg/s
Tube water velocity	2.94	2.94	2.94	2.94	2.94	m/s
Inlet water temp.	49.61	44.49	39.62	34.99	32.00	°C
Outlet water temp.	55.01	49.61	44.49	39.62	34.99	°C
Water heat load	6005.3	5709.0	5424.1	5153.9	3328.4	kW(R)

Table 9.140 Evaporator refrigerant circuit

Evaporator	Evap. 5	Evap. 4	Evap. 3	Evap. 2	Evap. 1	Unit
Ref. flowrate	34.87	32.68	30.61	28.67	17.36	kg/s
Ref. temperature	11.08	8.17	5.40	2.77	2.11	°C
Ref. pressure	437.19	400.00	366.95	337.53	330.44	kPa
Inlet ref. enthalpy	60.41	56.80	53.41	50.23	42.66	kJ/kg
Outlet ref. enthalpy	192.18	190.97	189.82	188.71	188.43	kJ/kg
Tube thermal res.	0.0826	0.0826	0.0826	0.0826	0.0826	°C/MW
Fouling thermal res.	0.3082	0.3082	0.3082	0.3082	0.3082	°C/MW
Water thermal res.	0.4390	0.4556	0.4726	0.4901	0.5049	°C/MW
Ref. thermal res.	0.4995	0.5161	0.5341	0.5532	0.7583	°C/MW
Overall UA	752.25	733.90	715.50	697.28	604.56	kW/°C
Ref. heat load	4594.5	4384.4	4174.8	3970.5	2530.4	kW(R)

Table 9.141 Condenser refrigerant circuit

Condenser	Cond. 5	Cond. 4	Cond. 3	Cond. 2	Cond. 1	Unit
Ref. flowrate	46.70	42.53	38.86	35.63	21.66	kg/s
Ref. temperature	59.59	53.99	48.68	43.62	37.48	°C
Ref. pressure	1511.71	1335.25	1181.98	1048.77	901.99	kPa
Inlet ref. enthalpy	223.87	223.41	223.10	222.92	225.69	kJ/kg
Outlet ref. enthalpy	95.27	89.17	83.53	78.28	72.02	kJ/kg
Tube thermal res.	0.0660	0.0660	0.0660	0.0660	0.0660	°C/MW
Fouling thermal res.	0.5089	0.5089	0.5089	0.5089	0.5089	°C/MW
Water thermal res.	0.1977	0.2068	0.2163	0.2262	0.2348	°C/MW
Ref. thermal res.	0.3819	0.3774	0.3730	0.3686	0.3284	°C/MW
Overall UA	866.24	862.74	858.97	854.90	878.65	kW/°C
Ref. heat load	6005.3	5709.0	5424.1	5153.9	3328.4	kW(R)

Table 9.142 Stage 1 compressor performance

Compressor 1	Chiller 5	Chiller 4	Chiller 3	Chiller 2	Chiller 1	Unit
Vane angle	0.00	0.00	0.00	0.00	-47.50	degrees
Ref. flowrate	34.87	32.68	30.61	28.67	17.36	kg/s
Inlet vol. flowrate	1.38	1.41	1.44	1.46	0.90	m^3/s
Inlet ref. temp.	11.08	8.17	5.40	2.77	2.11	°C
Inlet ref. pressure	437.19	400.00	366.95	337.53	330.44	kPa
Inlet specific volume	0.03966	0.04321	0.04694	0.05085	0.05189	m^3/kg
Inlet enthalpy	192.18	190.97	189.82	188.71	188.43	kJ/kg
Outlet ref. temp.	32.40	29.62	27.08	24.76	32.93	°C
Outlet ref. pressure	664.67	600.05	543.26	493.37	387.27	kPa
Outlet specific vol.	0.02733	0.03036	0.03361	0.03708	0.05032	m^3/kg
Outlet enthalpy	202.83	201.98	201.20	200.47	207.72	kJ/kg
Isentropic head	7.35	7.10	6.85	6.60	2.74	kJ/kg
Isentropic efficiency	68.98	64.46	60.14	56.12	14.19	%
Absorbed power	371.4	359.7	348.4	337.3	334.9	kW(M)
Operating region	STABLE	STABLE	STABLE	STABLE	STABLE	-

Table 9.143 Stage 2 compressor performance

Compressor 2	Chiller 5	Chiller 4	Chiller 3	Chiller 2	Chiller 1	Unit
Vane angle	0.00	0.00	0.00	0.00	0.00	degrees
Ref. flowrate	46.70	42.53	38.86	35.63	21.66	kg/s
Inlet vol. flowrate	1.26	1.28	1.29	1.31	1.07	m^3/s
Inlet ref. temp.	30.70	27.85	25.25	22.88	27.80	°C
Inlet ref. pressure	664.67	600.05	543.26	493.37	387.27	kPa
Inlet specific volume	0.02708	0.03008	0.03329	0.03673	0.04922	m^3/kg
Inlet enthalpy	201.61	200.73	199.92	199.18	204.31	kJ/kg
Outlet ref. temp.	76.73	73.10	70.02	67.45	68.63	°C
Outlet ref. pressure	1511.71	1335.25	1181.98	1048.77	901.99	kPa
Outlet specific vol.	0.01266	0.01456	0.01668	0.01904	0.02286	m^3/kg
Outlet enthalpy	223.87	223.41	223.10	222.92	225.69	kJ/kg
Isentropic head	14.90	14.60	14.27	13.90	16.56	kJ/kg
Isentropic efficiency	66.96	64.36	61.55	58.55	77.43	%
Absorbed power	1039.4	964.8	900.9	846.1	463.2	kW(M)
Operating region	STABLE	STABLE	STABLE	STABLE	STABLE	-

9.2.11 Tau Tona mine, 5 chillers with 2 operating at full load and 3 at part load

Table 9.144 Installation performance, with $t_{(w)Co[max]}$ = 55°C

Installation	Value	Unit
Return water available temperature	32.00	°C
Return water final temperature	55.00	°C
Cool water available temperature	18.89	°C
Chilled water final temperature	5.50	°C
Lorenz COP	9.14	-
System COP	3.33	-
Mass flowrate of return water	266.00	kg/s
Total evaporator water heat load	19700.10	kW(R)
Total return water utilization	74.06	kW(R)/(kg/s)

Table 9.145 Chiller performance

Chiller	Chiller 5	Chiller 4	Chiller 3	Chiller 2	Chiller 1	Unit
Carnot COP	5.86	6.14	6.58	6.96	7.27	-
COP	3.26	3.31	3.37	3.37	3.37	-
Cycle efficiency	56	54	51	48	46	%
Return w. utilizat.	17.28	16.49	14.46	13.20	12.62	kW(R)/(kg/s)

Table 9.146 Evaporator water circuit

Evaporator	**Evap. 5**	**Evap. 4**	**Evap. 3**	**Evap. 2**	**Evap. 1**	**Unit**
Fouling factor	0.00009	0.00009	0.00020	0.00009	0.00009	m^2 °C/W
Water flowrate	351.50	351.50	351.50	351.50	351.50	kg/s
Tube water velocity	2.16	2.16	2.16	2.16	2.16	m/s
Inlet water temp.	18.89	15.77	12.79	10.17	7.79	°C
Outlet water temp.	15.77	12.79	10.17	7.79	5.50	°C
Water heat load	4596.0	4386.9	3846.8	3512.3	3358.1	kW(R)

Table 9.147 Condenser water circuit

Condenser	**Cond. 5**	**Cond. 4**	**Cond. 3**	**Cond. 2**	**Cond. 1**	**Unit**
Fouling factor	0.00018	0.00018	0.00018	0.00018	0.00018	m^2 °C/W
Water flowrate	266.00	266.00	266.00	266.00	266.00	kg/s
Tube water velocity	2.94	2.94	2.94	2.94	2.94	m/s
Inlet water temp.	49.61	44.48	40.00	35.91	32.00	°C
Outlet water temp.	55.00	49.61	44.48	40.00	35.91	°C
Water heat load	6007.5	5712.6	4988.1	4553.5	4354.2	kW(R)

Table 9.148 Evaporator refrigerant circuit

Evaporator	Evap. 5	Evap. 4	Evap. 3	Evap. 2	Evap. 1	Unit
Ref. flowrate	34.88	32.70	27.87	24.96	23.58	kg/s
Ref. temperature	11.09	8.18	5.89	3.69	1.47	°C
Ref. pressure	437.30	400.18	372.61	347.59	323.65	kPa
Inlet ref. enthalpy	60.42	56.81	51.97	48.37	45.72	kJ/kg
Outlet ref. enthalpy	192.18	190.98	190.02	189.09	188.15	kJ/kg
Tube thermal res.	0.0826	0.0826	0.0826	0.0826	0.0826	°C/MW
Fouling thermal res.	0.3082	0.3082	0.3082	0.3082	0.3082	°C/MW
Water thermal res.	0.4380	0.4545	0.4708	0.4863	0.5018	°C/MW
Ref. thermal res.	0.4993	0.5159	0.5656	0.6028	0.6220	°C/MW
Overall UA	752.89	734.60	700.66	675.68	660.19	kW/°C
Ref. heat load	4596.0	4386.9	3846.8	3512.3	3358.1	kW(R)

Table 9.149 Condenser refrigerant circuit

Condenser	Cond. 5	Cond. 4	Cond. 3	Cond. 2	Cond. 1	Unit
Ref. flowrate	46.71	42.55	35.65	31.42	29.19	kg/s
Ref. temperature	59.59	53.99	48.29	43.48	39.26	°C
Ref. pressure	1511.63	1335.16	1171.34	1045.14	942.93	kPa
Inlet ref. enthalpy	223.88	223.43	223.03	223.04	223.00	kJ/kg
Outlet ref. enthalpy	95.27	89.17	83.12	78.13	73.82	kJ/kg
Tube thermal res.	0.0660	0.0660	0.0660	0.0660	0.0660	°C/MW
Fouling thermal res.	0.5089	0.5089	0.5089	0.5089	0.5089	°C/MW
Water thermal res.	0.1977	0.2068	0.2159	0.2248	0.2337	°C/MW
Ref. thermal res.	0.3819	0.3775	0.3646	0.3565	0.3529	°C/MW
Overall UA	866.21	862.68	865.46	864.96	860.98	kW/°C
Ref. heat load	6007.5	5712.6	4988.1	4553.4	4354.2	kW(R)

Table 9.150 Stage 1 compressor performance

Compressor 1	Chiller 5	Chiller 4	Chiller 3	Chiller 2	Chiller 1	Unit
Vane angle	0.00	0.00	-13.70	-20.00	-20.00	degrees
Ref. flowrate	34.88	32.70	27.87	24.96	23.58	kg/s
Inlet vol. flowrate	1.38	1.41	1.29	1.23	1.25	m^3/s
Inlet ref. temp.	11.09	8.18	5.89	3.69	1.47	°C
Inlet ref. pressure	437.30	400.18	372.61	347.59	323.65	kPa
Inlet specific volume	0.03965	0.04319	0.04626	0.04944	0.05293	m^3/kg
Inlet enthalpy	192.18	190.98	190.02	189.09	188.15	kJ/kg
Outlet ref. temp.	32.41	29.64	28.90	28.31	26.74	°C
Outlet ref. pressure	664.78	600.23	520.32	465.66	428.02	kPa
Outlet specific vol.	0.02732	0.03035	0.03562	0.04025	0.04388	m^3/kg
Outlet enthalpy	202.84	201.99	202.85	203.37	202.93	kJ/kg
Isentropic head	7.35	7.09	5.82	5.08	4.84	kJ/kg
Isentropic efficiency	68.95	64.42	45.34	35.57	32.74	%
Absorbed power	371.6	360.0	357.6	356.3	348.3	kW(M)
Operating region	STABLE	STABLE	STABLE	STABLE	STABLE	-

Table 9.151 Stage 2 compressor performance

Compressor 2	Chiller 5	Chiller 4	Chiller 3	Chiller 2	Chiller 1	Unit
Vane angle	0.00	0.00	0.00	0.00	0.00	degrees
Ref. flowrate	46.71	42.55	35.65	31.42	29.19	kg/s
Inlet vol. flowrate	1.26	1.28	1.25	1.25	1.26	m^3/s
Inlet ref. temp.	30.71	27.87	26.29	25.19	23.58	°C
Inlet ref. pressure	664.78	600.23	520.32	465.66	428.02	kPa
Inlet specific volume	0.02707	0.03007	0.03517	0.03966	0.04324	m^3/kg
Inlet enthalpy	201.62	200.74	201.05	201.24	200.81	kJ/kg
Outlet ref. temp.	76.74	73.12	69.74	67.54	65.69	°C
Outlet ref. pressure	1511.63	1335.16	1171.34	1045.14	942.93	kPa
Outlet specific vol.	0.01267	0.01456	0.01684	0.01912	0.02141	m^3/kg
Outlet enthalpy	223.88	223.43	223.03	223.04	223.00	kJ/kg
Isentropic head	14.90	14.60	15.10	15.24	14.95	kJ/kg
Isentropic efficiency	66.93	64.31	68.71	69.91	67.35	%
Absorbed power	1039.9	965.7	783.7	684.9	647.8	kW(M)
Operating region	STABLE	STABLE	STABLE	STABLE	STABLE	-

9.2.12 Tau Tona mine, 5 chillers operating at part load

Table 9.152 Installation performance, with $t_{(w)Co[max]}$ = 55°C

Installation	Value	Unit
Return water available temperature	32.00	°C
Return water final temperature	55.00	°C
Cool water available temperature	18.89	°C
Chilled water final temperature	5.50	°C
Lorenz COP	9.14	-
System COP	3.35	-
Mass flowrate of return water	266.00	kg/s
Total evaporator water heat load	19727.10	kW(R)
Total return water utilization	74.16	kW(R)/(kg/s)

Table 9.153 Chiller performance

Chiller	Chiller 5	Chiller 4	Chiller 3	Chiller 2	Chiller 1	Unit
Carnot COP	5.96	6.22	6.51	6.81	7.13	-
COP	3.29	3.34	3.37	3.38	3.38	-
Cycle efficiency	55	54	52	50	47	%
Return w. utilizat.	16.23	15.52	14.81	14.13	13.47	kW(R)/(kg/s)

Table 9.154 Evaporator water circuit

Evaporator	**Evap. 5**	**Evap. 4**	**Evap. 3**	**Evap. 2**	**Evap. 1**	**Unit**
Fouling factor	0.00009	0.00009	0.00009	0.00009	0.00009	m^2 °C/W
Water flowrate	352.00	352.00	352.00	352.00	352.00	kg/s
Tube water velocity	2.17	2.17	2.17	2.17	2.17	m/s
Inlet water temp.	18.89	15.96	13.16	10.49	7.94	°C
Outlet water temp.	15.96	13.16	10.49	7.94	5.50	°C
Water heat load	4316.0	4127.5	3940.6	3758.9	3584.1	kW(R)

Table 9.155 Condenser water circuit

Condenser	**Cond. 5**	**Cond. 4**	**Cond. 3**	**Cond. 2**	**Cond. 1**	**Unit**
Fouling factor	0.00018	0.00018	0.00018	0.00018	0.00018	m^2 °C/W
Water flowrate	266.00	266.00	266.00	266.00	266.00	kg/s
Tube water velocity	2.94	2.94	2.94	2.94	2.94	m/s
Inlet water temp.	49.95	45.13	40.55	36.17	32.00	°C
Outlet water temp.	55.00	49.95	45.13	40.55	36.17	°C
Water heat load	5627.2	5363.7	5111.2	4871.5	4645.4	kW(R)

Table 9.156 Evaporator refrigerant circuit

Evaporator	Evap. 5	Evap. 4	Evap. 3	Evap. 2	Evap. 1	Unit
Ref. flowrate	32.44	30.50	28.67	26.97	25.38	kg/s
Ref. temperature	11.48	8.74	6.14	3.66	1.30	°C
Ref. pressure	442.42	407.17	375.60	347.29	321.86	kPa
Inlet ref. enthalpy	59.28	55.89	52.69	49.69	46.86	kJ/kg
Outlet ref. enthalpy	192.34	191.21	190.13	189.08	188.08	kJ/kg
Tube thermal res.	0.0826	0.0826	0.0826	0.0826	0.0826	°C/MW
Fouling thermal res.	0.3082	0.3082	0.3082	0.3082	0.3082	°C/MW
Water thermal res.	0.4370	0.4524	0.4682	0.4843	0.5007	°C/MW
Ref. thermal res.	0.5218	0.5384	0.5561	0.5748	0.5943	°C/MW
Overall UA	740.92	723.77	706.63	689.66	672.99	kW/°C
Ref. heat load	4316.0	4127.5	3940.6	3758.9	3584.1	kW(R)

Table 9.157 Condenser refrigerant circuit

Condenser	Cond. 5	Cond. 4	Cond. 3	Cond. 2	Cond. 1	Unit
Ref. flowrate	46.69	40.00	36.74	33.85	31.29	kg/s
Ref. temperature	59.26	54.03	49.05	44.30	39.77	°C
Ref. pressure	1500.95	1336.34	1192.18	1065.82	954.91	kPa
Inlet ref. enthalpy	223.70	223.30	223.03	222.87	222.82	kJ/kg
Outlet ref. enthalpy	94.91	89.21	83.91	78.97	74.34	kJ/kg
Tube thermal res.	0.0660	0.0660	0.0660	0.0660	0.0660	°C/MW
Fouling thermal res.	0.5089	0.5089	0.5089	0.5089	0.5089	°C/MW
Water thermal res.	0.1974	0.2059	0.2147	0.2239	0.2334	°C/MW
Ref. thermal res.	0.3752	0.3710	0.3669	0.3629	0.3590	°C/MW
Overall UA	871.49	868.18	864.62	860.79	856.66	kW/°C
Ref. heat load	5627.2	5363.7	5111.2	4871.5	4645.4	kW(R)

Table 9.158 Stage 1 compressor performance

Compressor 1	Chiller 5	Chiller 4	Chiller 3	Chiller 2	Chiller 1	Unit
Vane angle	-11.00	-11.00	-11.00	-11.00	-11.00	degrees
Ref. flowrate	32.44	30.50	28.67	26.97	25.38	kg/s
Inlet vol. flowrate	1.27	1.30	1.32	1.33	1.35	m^3/s
Inlet ref. temp.	11.48	8.74	6.14	3.66	1.30	°C
Inlet ref. pressure	442.42	407.17	375.60	347.29	321.86	kPa
Inlet specific volume	0.03920	0.04248	0.04590	0.04948	0.05321	m^3/kg
Inlet enthalpy	192.34	191.21	190.13	189.08	188.08	kJ/kg
Outlet ref. temp.	33.30	30.93	28.75	26.75	24.91	°C
Outlet ref. pressure	643.99	584.34	531.67	485.14	443.96	kPa
Outlet specific vol.	0.02850	0.03151	0.03474	0.03816	0.04178	m^3/kg
Outlet enthalpy	203.84	203.18	202.56	201.98	201.43	kJ/kg
Isentropic head	6.58	6.32	6.06	5.81	5.57	kJ/kg
Isentropic efficiency	57.23	52.80	48.75	45.07	41.76	%
Absorbed power	372.9	364.9	356.4	347.7	338.7	kW(M)
Operating region	STABLE	STABLE	STABLE	STABLE	STABLE	-

Table 9.159 Stage 2 compressor performance

Compressor 2	Chiller 5	Chiller 4	Chiller 3	Chiller 2	Chiller 1	Unit
Vane angle	0.00	0.00	0.00	0.00	0.00	degrees
Ref. flowrate	43.69	40.00	36.74	33.85	31.29	kg/s
Inlet vol. flowrate	1.23	1.25	1.26	1.28	1.29	m^3/s
Inlet ref. temp.	31.04	28.57	26.32	24.27	22.39	°C
Inlet ref. pressure	643.99	584.34	531.67	485.14	443.96	kPa
Inlet specific volume	0.02816	0.03114	0.03432	0.03770	0.04127	m^3/kg
Inlet enthalpy	202.22	201.52	200.87	200.27	199.72	kJ/kg
Outlet ref. temp.	76.33	72.98	70.11	67.68	65.65	°C
Outlet ref. pressure	1500.95	1336.34	1192.18	1065.82	954.91	kPa
Outlet specific vol.	0.01275	0.01453	0.01651	0.01869	0.02109	m^3/kg
Outlet enthalpy	223.70	223.30	223.03	222.87	222.82	kJ/kg
Isentropic head	15.49	15.25	14.97	14.66	14.33	kJ/kg
Isentropic efficiency	72.14	70.01	67.57	64.90	62.03	%
Absorbed power	938.3	871.4	814.1	765.0	722.6	kW(M)
Operating region	STABLE	STABLE	STABLE	STABLE	STABLE	-

9.3 CHILLER comparison with spreadsheet

9.3.1 Kloof mine, 1 chiller operating at full load

This section combines the results from Sections 9.1.1 and 9.2.1.

Table 9.160 Installation performance, with $t_{(w)Co[max]}$ = 55°C

	CHILLER	S-sheet	
Installation	**Value**	**Value**	**Unit**
Return water available temp.	32.00	32.00	°C
Return water final temp.	42.28	42.00	°C
Cool water available temp.	25.00	25.00	°C
Chilled water final temp.	10.50	10.50	°C
Lorenz COP	14.97	15.08	-
System COP	2.92	4.25	-
Mass flowrate of return water	160.00	160.00	kg/s
Total evap. water heat load	5131.10	5423.98	kW(R)
Total return w. utilization	32.07	33.90	kW(R)/(kg/s)

Table 9.161 Chiller performance

	CHILLER	S-sheet	
Chiller	**Chiller 1**	**Chiller 1**	**Unit**
Carnot COP	7.06	7.09	-
COP	2.92	4.25	-
Cycle efficiency	41	60	%
Return w. utilization	32.07	33.90	kW(R)/(kg/s)

Table 9.162 Evaporator water circuit

	CHILLER	S-sheet	
Evaporator	**Evap. 1**	**Evap. 1**	**Unit**
Fouling factor	0.00020	-	m^2 °C/W
Water flowrate	84.50	89.34	kg/s
Tube water velocity	2.30	-	m/s
Inlet water temp.	25.00	25.00	°C
Outlet water temp.	10.50	10.50	°C
Water heat load	5131.10	5423.98	kW(R)

Table 9.163 Condenser water circuit

	CHILLER	S-sheet	
Condenser	**Cond. 1**	**Cond. 1**	**Unit**
Fouling factor	0.00020	-	m^2 °C/W
Water flowrate	160.00	160.00	kg/s
Tube water velocity	2.65	-	m/s
Inlet water temp.	32.00	32.00	°C
Outlet water temp.	42.28	42.00	°C
Water heat load	6886.10	6699.13	kW(R)

Table 9.164 Evaporator refrigerant circuit

	CHILLER	S-sheet	
Evaporator	**Evap. 1**	**Evap. 1**	**Unit**
Refrigerant flowrate	40.45	-	kg/s
Refrigerant temperature	7.34	6.85	°C
Refrigerant pressure	389.86	-	kPa
Inlet refrigerant enthalpy	63.77	-	kJ/kg
Outlet refrigerant enthalpy	7.34	-	kJ/kg
Tube thermal resistance	0.0521	-	°C/MW
Fouling thermal resistance	0.7150	-	°C/MW
Water thermal resistance	0.4283	-	°C/MW
Refrigerant thermal resistance	0.4471	-	°C/MW
Overall UA	608.83	600.00	kW/°C
Refrigerant heat load	5131.10	5423.98	kW(R)

Table 9.165 Condenser refrigerant circuit

	CHILLER	S-sheet	
Condenser	**Cond. 1**	**Cond. 1**	**Unit**
Refrigerant flowrate	46.67	-	kg/s
Refrigerant temperature	47.07	46.35	°C
Refrigerant pressure	1138.22	-	kPa
Inlet refrigerant enthalpy	229.39	-	kJ/kg
Outlet refrigerant enthalpy	81.84	-	kJ/kg
Tube thermal resistance	0.0422	-	°C/MW
Fouling thermal resistance	0.5801	-	°C/MW
Water thermal resistance	0.2523	-	°C/MW
Refrigerant thermal resistance	0.4271	-	°C/MW
Overall UA	768.18	800.00	kW/°C
Refrigerant heat load	6886.1	6699.13	kW(R)

Table 9.166 Stage 1 compressor performance

	CHILLER	S-sheet	
Compressor 1	**Chiller 1**	**Chiller 1**	**Unit**
Vane angle	0.00	-	degrees
Refrigerant flowrate	40.45	-	kg/s
Inlet volumetric flowrate	1.79	-	m^3/s
Inlet refrigerant temperature	7.34	-	°C
Inlet refrigerant pressure	389.86	-	kPa
Inlet specific volume	0.04429	-	m^3/kg
Inlet enthalpy	190.63	-	kJ/kg
Outlet refrigerant temperature	44.40	-	°C
Outlet refrigerant pressure	728.68	-	kPa
Outlet specific volume	0.02611	-	m^3/kg
Outlet enthalpy	210.44	-	kJ/kg
Isentropic head	11.00	-	kJ/kg
Isentropic efficiency	55.49	-	%
Absorbed power	801.6	1275.15 (combined)	kW(M)
Operating region	STABLE	-	-

Table 9.167 Stage 2 compressor performance

	CHILLER	S-sheet	
Compressor 2	**Chiller 1**	**Chiller 1**	**Unit**
Vane angle	0.00	-	degrees
Refrigerant flowrate	46.67	-	kg/s
Inlet volumetric flowrate	1.21	-	m^3/s
Inlet refrigerant temperature	42.35	-	°C
Inlet refrigerant pressure	728.68	-	kPa
Inlet specific volume	0.02584	-	m^3/kg
Inlet enthalpy	208.96	-	kJ/kg
Outlet refrigerant temperature	77.49	-	°C
Outlet refrigerant pressure	1138.22	-	kPa
Outlet specific volume	0.01812	-	m^3/kg
Outlet enthalpy	229.39	-	kJ/kg
Isentropic head	8.45	-	kJ/kg
Isentropic efficiency	41.37	-	%
Absorbed power	953.5	Refer to Compr. 1	kW(M)
Operating region	STABLE	-	

9.3.2 Kloof mine, 2 chillers operating at full load

This section combines the results from Sections 9.1.2 and 9.2.2.

Table 9.168 Installation performance, with $t_{(w)Co[max]}$ = 55°C

	CHILLER	S-sheet	
Installation	**Value**	**Value**	**Unit**
Return water available temp.	32.00	32.00	°C
Return water final temp.	52.50	52.36	°C
Cool water available temp.	25.00	25.00	°C
Chilled water final temp.	10.50	10.50	°C
Lorenz COP	11.90	11.93	-
System COP	3.00	3.89	-
Mass flowrate of return water	160.00	160.00	kg/s
Total evap. water heat load	10302.20	10847.96	kW(R)
Total return w. utilization	64.39	67.80	kW(R)/(kg/s)

Table 9.169 Chiller performance

	CHILLER		S-sheet		
Chiller	**Chiller 2**	**Chiller 1**	**Chiller 2**	**Chiller 1**	**Unit**
Carnot COP	6.24	6.84	6.34	6.62	-
COP	2.97	3.03	3.80	3.97	-
Cycle efficiency	48	44	60	60	%
Return w. utilization	34.20	30.19	33.90	33.90	kW(R)/(kg/s)

Table 9.170 Evaporator water circuit

	CHILLER		S-sheet		
Evaporator	**Evap. 2**	**Evap. 1**	**Evap. 2**	**Evap. 1**	**Unit**
Fouling factor	0.00020	0.00020	-	-	m^2 °C/W
Water flowrate	169.70	169.70	178.68	178.68	kg/s
Tube water velocity	2.31	2.31	-	-	m/s
Inlet water temp.	25.00	17.30	25.00	17.75	°C
Outlet water temp.	17.30	10.50	17.75	10.50	°C
Water heat load	5472.10	4830.10	5423.98	5423.98	kW(R)

Table 9.171 Condenser water circuit

	CHILLER		S-sheet		
Condenser	**Cond. 2**	**Cond. 1**	**Cond. 2**	**Cond. 1**	**Unit**
Fouling factor	0.00020	0.00020	-	-	m^2 °C/W
Water flowrate	160.00	160.00	160.00	160.00	kg/s
Tube water velocity	2.65	2.65	-	-	m/s
Inlet water temp.	41.59	32.00	42.13	32.00	°C
Outlet water temp.	52.50	41.59	52.36	42.13	°C
Water heat load	7312.30	6421.90	6849.62	6788.73	kW(R)

Table 9.172 Evaporator refrigerant circuit

	CHILLER		S-sheet		
Evaporator	**Evap. 2**	**Evap. 1**	**Evap. 2**	**Evap. 1**	**Unit**
Refrigerant flowrate	44.81	37.76	-	-	kg/s
Refrigerant temperature	11.81	5.31	11.86	4.61	°C
Refrigerant pressure	446.86	365.94	-	-	kPa
Inlet refrigerant enthalpy	70.36	61.88	-	-	kJ/kg
Outlet refrigerant enthalpy	192.48	189.78	-	-	kJ/kg
Tube thermal resistance	0.0521	0.0521	-	-	°C/MW
Fouling thermal resistance	0.7150	0.7150	-	-	°C/MW
Water thermal resistance	0.4104	0.4473	-	-	°C/MW
Ref. thermal resistance	0.4274	0.4664	-	-	°C/MW
Overall UA	623.11	594.96	600.00	600.00	kW/°C
Refrigerant heat load	5472.10	4830.10	5423.98	5423.98	kW(R)

Table 9.173 Condenser refrigerant circuit

	CHILLER		S-sheet		
Condenser	**Cond. 2**	**Cond. 1**	**Cond. 2**	**Cond. 1**	**Unit**
Refrigerant flowrate	54.11	43.81	-	-	kg/s
Refrigerant temperature	57.48	46.01	56.80	46.54	°C
Refrigerant pressure	1443.17	1110.20	-	-	kPa
Inlet refrigerant enthalpy	228.08	227.33	-	-	kJ/kg
Outlet refrigerant enthalpy	92.95	80.74	-	-	kJ/kg
Tube thermal resistance	0.0422	0.0422	-	-	°C/MW
Fouling thermal resistance	0.5801	0.5801	-	-	°C/MW
Water thermal resistance	0.2304	0.2532	-	-	°C/MW
Ref. thermal resistance	0.4324	0.4192	-	-	°C/MW
Overall UA	778.13	772.33	800.00	800.00	kW/°C
Refrigerant heat load	7312.30	6421.90	6849.62	6788.73	kW(R)

Table 9.174 Stage 1 compressor performance

	CHILLER		S-sheet		
Compressor 1	**Chiller 2**	**Chiller 1**	**Chiller 2**	**Chiller 1**	**Unit**
Vane angle	0.00	0.00	-	-	degrees
Refrigerant flowrate	44.81	37.76	-	-	kg/s
Inlet volumetric flowrate	1.74	1.78	-	-	m^3/s
Inlet refrigerant temperature	11.81	5.31	-	-	°C
Inlet refrigerant pressure	446.86	365.94	-	-	kPa
Inlet specific volume	0.03883	0.04706	-	-	m^3/kg
Inlet enthalpy	192.48	189.78	-	-	kJ/kg
Outlet refrigerant temp.	48.40	41.99	-	-	°C
Outlet refrigerant pressure	865.35	692.08	-	-	kPa
Outlet specific volume	0.02174	0.02739	-		m^3/kg
Outlet enthalpy	211.25	209.28	-	-	kJ/kg
Isentropic head	11.65	11.19	-	-	kJ/kg
Isentropic efficiency	62.08	57.39	-	-	%
Absorbed power	841.20	736.30	1425.64 (combined)	1364.75 (combined)	kW(M)
Operating region	STABLE	STABLE	-	-	-

Table 9.175 Stage 2 compressor performance

	CHILLER		S-sheet		
Compressor 2	**Chiller 2**	**Chiller 1**	**Chiller 2**	**Chiller 1**	**Unit**
Vane angle	0.00	0.00	-	-	degrees
Refrigerant flowrate	54.11	43.81	-	-	kg/s
Inlet volumetric flowrate	1.16	1.19	-	-	m^3/s
Inlet refrigerant temperature	46.21	39.93	-	-	°C
Inlet refrigerant pressure	865.35	692.08	-	-	kPa
Inlet specific volume	0.02148	0.02711	-	-	m^3/kg
Inlet enthalpy	209.61	207.80	-	-	kJ/kg
Outlet refrigerant temp.	80.74	74.31	-	-	°C
Outlet refrigerant pressure	1443.17	1110.20	-	-	kPa
Outlet specific volume	0.01376	0.01839	-	-	m^3/kg
Outlet enthalpy	228.08	227.33	-	-	kJ/kg
Isentropic head	9.53	8.94	-	-	kJ/kg
Isentropic efficiency	51.64	45.76	-	-	%
Absorbed power	999.00	855.50	Refer to Compr. 1	Refer to Compr. 1	kW(M)
Operating region	STABLE	STABLE	-	-	-

9.3.3 Tau Tona mine, 2 chillers operating at full load

This section combines the results from Sections 9.1.7 and 9.2.6

Table 9.176 Installation performance, with $t_{(w)Co[max]}$ = 55°C

	CHILLER	S-sheet	
Installation	**Value**	**Value**	**Unit**
Return water available temp.	32.00	32.00	°C
Return water final temp.	42.40	41.98	°C
Cool water available temp.	18.89	18.89	°C
Chilled water final temp.	5.50	5.50	°C
Lorenz COP	11.40	11.49	-
System COP	3.14	4.32	-
Mass flowrate of return water	266.00	266.00	kg/s
Total evap. water heat load	8786.60	9024.00	kW(R)
Total return w. utilization	33.03	33.92	kW(R)/(kg/s)

Table 9.177 Chiller performance

	CHILLER		S-sheet		
Chiller	**Chiller 2**	**Chiller 1**	**Chiller 2**	**Chiller 1**	**Unit**
Carnot COP	7.31	7.22	7.47	6.96	-
COP	3.06	3.25	4.48	4.17	-
Cycle efficiency	42	45	60	60	%
Return w. utilization	17.82	15.21	16.96	16.96	kW(R)/(kg/s)

Table 9.178 Evaporator water circuit

	CHILLER		S-sheet		
Evaporator	**Evap. 2**	**Evap. 1**	**Evap. 2**	**Evap. 1**	**Unit**
Fouling factor	0.00009	0.00009	-	-	m^2 °C/W
Water flowrate	156.71	156.71	160.96	160.96	kg/s
Tube water velocity	2.90	2.90	-	-	m/s
Inlet water temp.	18.89	11.66	18.89	12.20	°C
Outlet water temp.	11.66	5.50	12.20	5.50	°C
Water heat load	4740.7	4045.9	4512.00	4512.00	kW(R)

Table 9.179 Condenser water circuit

	CHILLER		S-sheet		
Condenser	**Cond. 2**	**Cond. 1**	**Cond. 2**	**Cond. 1**	**Unit**
Fouling factor	0.00018	0.00018	-	-	m^2 °C/W
Water flowrate	266.00	266.00	266.00	266.00	kg/s
Tube water velocity	2.94	2.94	-	-	m/s
Inlet water temp.	36.75	32.00	37.02	32.00	°C
Outlet water temp.	42.40	36.75	41.98	37.02	°C
Water heat load	6292.2	5289.8	5519.07	5592.78	kW(R)

Table 9.180 Evaporator refrigerant circuit

	CHILLER		S-sheet		
Evaporator	**Evap. 2**	**Evap. 1**	**Evap. 2**	**Evap. 1**	**Unit**
Refrigerant flowrate	34.99	29.08	-	-	kg/s
Refrigerant temperature	8.73	2.67	8.92	2.22	°C
Refrigerant pressure	406.93	336.41	-	-	kPa
Inlet refrigerant enthalpy	55.71	49.53	-	-	kJ/kg
Outlet refrigerant enthalpy	191.20	188.66	-	-	kJ/kg
Tube thermal resistance	0.0826	0.0826	-	-	°C/MW
Fouling thermal resistance	0.3014	0.3014	-	-	°C/MW
Water thermal resistance	0.3558	0.3874	-	-	°C/MW
Ref. thermal resistance	0.4886	0.5460	-	-	°C/MW
Overall UA	814.05	759.06	750.00	750.00	kW/°C
Refrigerant heat load	4740.7	4045.9	4512.00	4512.00	kW(R)

Table 9.181 Condenser refrigerant circuit

	CHILLER		S-sheet		
Condenser	**Cond. 2**	**Cond. 1**	**Cond. 2**	**Cond. 1**	**Unit**
Refrigerant flowrate	43.08	34.46	-	-	kg/s
Refrigerant temperature	47.31	40.85	46.69	41.80	°C
Refrigerant pressure	1144.80	980.52	-	-	kPa
Inlet refrigerant enthalpy	228.14	224.62	-	-	kJ/kg
Outlet refrigerant enthalpy	82.10	75.44	-	-	kJ/kg
Tube thermal resistance	0.0660	0.0660	-	-	°C/MW
Fouling thermal resistance	0.4976	0.4976	-	-	°C/MW
Water thermal resistance	0.2213	0.2327	-	-	°C/MW
Ref. thermal resistance	0.3877	0.3709	-	-	°C/MW
Overall UA	852.77	856.76	750.00	750.00	kW/°C
Refrigerant heat load	6292.2	5289.8	4512.00	4512.00	kW(R)

Table 9.182 Stage 1 compressor performance

	CHILLER		S-sheet		
Compressor 1	**Chiller 2**	**Chiller 1**	**Chiller 2**	**Chiller 1**	**Unit**
Vane angle	0.00	0.00	-	-	degrees
Refrigerant flowrate	34.99	29..08	-	-	kg/s
Inlet volumetric flowrate	1.49	1.48	-	-	m^3/s
Inlet refrigerant temperature	8.73	2.67	-	-	°C
Inlet refrigerant pressure	406.93	336.41	-	-	kPa
Inlet specific volume	0.04250	0.05101	-	-	m^3/kg
Inlet enthalpy	191.20	188.66	-	-	kJ/kg
Outlet refrigerant temp.	31.42	25.20	-	-	°C
Outlet refrigerant pressure	581.28	482.86	-	-	kPa
Outlet specific volume	0.03178	0.03807	-	-	m^3/kg
Outlet enthalpy	203.57	200.95	-	-	kJ/kg
Isentropic head	6.23	6.28	-	-	kJ/kg
Isentropic efficiency	50.40	51.11	-	-	%
Absorbed power	432.8	357.4	1007.07 (combined)	1080.78 (combined)	kW(M)
Operating region	STABLE	STABLE	-	-	-

Table 9.183 Stage 2 compressor performance

	CHILLER		S-sheet		
Compressor 2	**Chiller 2**	**Chiller 1**	**Chiller 2**	**Chiller 1**	**Unit**
Vane angle	0.00	0.00	-	-	degrees
Refrigerant flowrate	43.08	35.46	-	-	kg/s
Inlet volumetric flowrate	1.36	1.34	-	-	m^3/s
Inlet refrigerant temperature	29.43	23.25	-	-	°C
Inlet refrigerant pressure	581.28	482.86	-	-	kPa
Inlet specific volume	0.03146	0.03771	-	-	m^3/kg
Inlet enthalpy	202.17	199.62	-	-	kJ/kg
Outlet refrigerant temp.	75.95	68.53	-	-	°C
Outlet refrigerant pressure	1144.80	980.52	-	-	kPa
Outlet specific volume	0.01787	0.02073	-	-	m^3/kg
Outlet enthalpy	228.14	224.62	-	-	kJ/kg
Isentropic head	12.55	13.12	-	-	kJ/kg
Isentropic efficiency	48.34	52.48	-	-	%
Absorbed power	1118.7	886.5	Refer to Compr. 1	Refer to Compr. 1	kW(M)
Operating region	STABLE	STABLE	-	-	-

9.3.4 Kloof mine, 3 chillers operating at part load

This section combines the results from Sections 9.1.3 and 9.2.3

Table 9.184 Installation performance, with $t_{(w)Co[max]}$ = 55°C

	CHILLER	S-sheet	
Installation	**Value**	**Value**	**Unit**
Return water available temp.	32.00	32.00	°C
Return water final temp.	55.00	55.00	°C
Cool water available temp.	25.00	25.00	°C
Chilled water final temp.	10.50	10.50	°C
Lorenz COP	11.33	11.33	-
System COP	2.93	4.25	-
Mass flowrate of return water	160.00	160.00	kg/s
Total evap. water heat load	11491.20	12473.63	kW(R)
Total return w. utilization	71.82	77.96	kW(R)/(kg/s)

Table 9.185 Chiller performance

	CHILLER			S-sheet			
Chiller	**Chiller 3**	**Chiller 2**	**Chiller 1**	**Chiller 3**	**Chiller 2**	**Chiller 1**	**Unit**
Carnot COP	6.66	7.18	7.76	6.71	7.08	7.50	-
COP	2.90	2.95	2.96	4.03	4.25	4.50	-
Cycle efficiency	44	41	38	60	60	60	%
Return w. utilization	25.70	23.94	22.18	25.99	25.99	25.99	kW(R)/(kg/s)

Table 9.186 Evaporator water circuit

	CHILLER			S-sheet			
Evaporator	**Evap. 3**	**Evap. 2**	**Evap. 1**	**Evap. 3**	**Evap. 2**	**Evap. 1**	**Unit**
Fouling factor	0.00020	0.00020	0.00020	-	-	-	m^2 °C/W
Water flowrate	189.33	189.33	189.33	205.46	205.46	205.46	kg/s
Tube water velocity	2.58	2.58	2.58	-	-	-	m/s
Inlet water temp.	25.00	19.81	14.98	25.00	20.17	15.33	°C
Outlet water temp.	19.81	14.98	10.50	20.17	15.33	10.50	°C
Water heat load	4112.2	3829.6	3549.4	4157.88	4157.88	4157.88	kW(R)

Table 9.187 Condenser water circuit

	CHILLER			S-sheet			
Condenser	**Cond. 3**	**Cond. 2**	**Cond. 1**	**Cond. 3**	**Cond. 2**	**Cond. 1**	**Unit**
Fouling factor	0.00020	0.00020	0.00020	-	-	-	m^2 °C/W
Water flowrate	160.00	160.00	160.00	160.00	160.00	160.00	kg/s
Tube water velocity	2.65	2.65	2.65	-	-	-	m/s
Inlet water temp.	46.75	39.09	32.00	47.25	39.59	32.00	°C
Outlet water temp.	55.00	46.75	39.09	55.00	47.25	39.59	°C
Water heat load	5531.3	5128.0	4749.4	5190.48	5136.01	5081.68	kW(R)

Table 9.188 Evaporator refrigerant circuit

	CHILLER			S-sheet			
Evaporator	**Evap. 3**	**Evap. 2**	**Evap. 1**	**Evap. 3**	**Evap. 2**	**Evap. 1**	**Unit**
Refrigerant flowrate	32.66	29.35	26.40	-	-	-	kg/s
Refrigerant temperature	15.26	10.56	6.22	15.37	10.54	5.71	°C
Refrigerant pressure	494.81	430.31	376.58	-	-	-	kPa
Inlet refrigerant enthalpy	67.96	61.48	55.70	-	-	-	kJ/kg
Outlet refrigerant enthalpy	193.88	191.96	190.16	-	-	-	kJ/kg
Tube thermal resistance	0.0521	0.0521	0.0521	-	-	-	°C/MW
Fouling thermal resistance	0.7150	0.7150	0.7150	-	-		°C/MW
Water thermal resistance	0.3707	0.3928	0.4158	-	-	-	°C/MW
Ref. thermal resistance	0.5220	0.5487	0.5786	-	-	-	°C/MW
Overall UA	602.50	585.30	567.69	600.00	600.00	600.00	kW/°C
Refrigerant heat load	4112.2	3829.6	3549.4	4157.88	4157.88	4157.88	kW(R)

Table 9.189 Condenser refrigerant circuit

	CHILLER			S-sheet			
Condenser	**Cond. 3**	**Cond. 2**	**Cond. 1**	**Cond. 3**	**Cond. 2**	**Cond. 1**	**Unit**
Refrigerant flowrate	40.67	35.44	31.08	-	-	-	kg/s
Refrigerant temperature	58.57	50.10	42.24	58.37	50.58	42.88	°C
Refrigerant pressure	1478.44	1221.54	1014.21	-	-	-	kPa
Inlet refrigerant enthalpy	230.15	229.71	229.67	-	-	-	kJ/kg
Outlet refrigerant enthalpy	94.15	85.02	76.85	-	-	-	kJ/kg
Tube thermal resistance	0.0422	0.0422	0.0422	-	-	-	°C/MW
Fouling thermal resistance	0.5801	0.5801	0.5801	-	-	-	°C/MW
Water thermal resistance	0.2229	0.2390	0.2563	-	-	-	°C/MW
Ref. thermal resistance	0.4008	0.3938	0.3870	-	-	-	°C/MW
Overall UA	802.57	796.66	790.12	800.00	800.00	800.00	kW/°C
Refrigerant heat load	5531.3	5128.0	4749.4	5190.48	5136.01	5081.68	kW(R)

Table 9.190 Stage 1 compressor performance

	CHILLER			S-sheet			
Compressor 1	**Chiller 3**	**Chiller 2**	**Chiller 1**	**Chiller 3**	**Chiller 2**	**Chiller 1**	**Unit**
Vane angle	-37.52	-37.52	-37.52	-	-	-	degrees
Refrigerant flowrate	32.66	29.35	26.40	-	-	-	kg/s
Inlet volumetric flowrate	1.15	1.18	1.21	-	-	-	m^3/s
Inlet refrigerant temp.	15.26	10.56	6.22	-	-	-	°C
Inlet refrigerant pressure	494.81	430.31	376.58	-	-	-	kPa
Inlet specific volume	0.03517	0.04027	0.04579	-	-		m^3/kg
Inlet enthalpy	193.88	191.96	190.16	-	-	-	kJ/kg
Outlet refrigerant temp.	55.65	52.82	50.39	-	-	-	°C
Outlet ref. pressure	813.75	684.66	581.16	-	-	-	kPa
Outlet specific volume	0.02425	0.02919	0.03472	-	-	-	m^3/kg
Outlet enthalpy	217.36	217.11	216.81	-	-	-	kJ/kg
Isentropic head	8.76	8.15	7.59	-	-	-	kJ/kg
Isentropic efficiency	37.29	32.41	28.46	-	-	-	%
Absorbed power	766.9	738.1	703.6	1032.60 (combined)	978.13 (combined)	923.80 (combined)	kW(M)
Operating region	STABLE	STABLE	STABLE	-	-	-	-

Table 9.191 Stage 2 compressor performance

	CHILLER			S-sheet			
Compressor 2	**Chiller 3**	**Chiller 2**	**Chiller 1**	**Chiller 3**	**Chiller 2**	**Chiller 1**	**Unit**
Vane angle	0.00	0.00	0.00	-	-	-	degrees
Refrigerant flowrate	40.67	35.44	31.08	-	-	-	kg/s
Inlet volumetric flowrate	0.97	1.01	1.06	-	-	-	m^3/s
Inlet refrigerant temp.	51.21	48.30	45.91	-	-	-	°C
Inlet refrigerant pressure	813.75	684.66	581.16	-	-	-	kPa
Inlet specific volume	0.02373	0.02859	0.03404	-	-	-	m^3/kg
Inlet enthalpy	214.11	213.90	213.70	-	-	-	kJ/kg
Outlet refrigerant temp.	83.90	79.24	75.87	-	-	-	°C
Outlet ref. pressure	1478.44	1221.54	1014.21	-	-	-	kPa
Outlet specific volume	0.01358	0.01679	0.02061	-	-	-	m^3/kg
Outlet enthalpy	230.15	229.71	229.67	-	-	-	kJ/kg
Isentropic head	11.61	11.46	11.17	-	-	-	kJ/kg
Isentropic efficiency	72.37	72.49	69.95	-	-	-	%
Absorbed power	652.2	560.2	496.4	Refer to Comp. 1	Refer to Comp. 1	Refer to Comp. 1	kW(M)
Operating region	STABLE	STABLE	STABLE	-	-	-	-

9.3.5 Kloof mine, 3 chillers operating at full load

This section combines the results from Sections 9.1.5 and 9.2.4

Table 9.192 Installation performance, with $t_{(w)Co[max]}$ = 70°C

	CHILLER	S-sheet	
Installation	**Value**	**Value**	**Unit**
Return water available temp.	32.00	32.00	°C
Return water final temp.	62.14	63.29	°C
Cool water available temp.	25.00	25.00	°C
Chilled water final temp.	10.50	10.50	°C
Lorenz COP	9.98	9.79	-
System COP	3.07	3.47	-
Mass flowrate of return water	160.00	160.00	kg/s
Total evap. water heat load	15231.30	16271.94	kW(R)
Total return w. utilization	95.20	101.70	kW(R)/(kg/s)

Table 9.193 Chiller performance

	CHILLER			S-sheet			
Chiller	**Chiller 3**	**Chiller 2**	**Chiller 1**	**Chiller 3**	**Chiller 2**	**Chiller 1**	**Unit**
Carnot COP	5.46	6.06	6.81	5.25	5.79	6.44	-
COP	3.06	3.10	3.05	3.15	3.47	3.87	-
Cycle efficiency	56	51	45	60	60	60	%
Return w. utilization	33.39	31.87	29.94	33.90	33.90	33.90	kW(R)/(kg/s)

Table 9.194 Evaporator water circuit

	CHILLER			S-sheet			
Evaporator	**Evap. 3**	**Evap. 2**	**Evap. 1**	**Evap. 3**	**Evap. 2**	**Evap. 1**	**Unit**
Fouling factor	0.00020	0.00020	0.00020	-	-	-	m^2 °C/W
Water flowrate	250.93	250.93	250.93	268.02	268.02	268.02	kg/s
Tube water velocity	3.42	3.42	3.42	-	-	-	m/s
Inlet water temp.	25.00	19.91	15.06	25.00	20.17	15.33	°C
Outlet water temp.	19.91	15.06	10.50	20.17	15.33	10.50	°C
Water heat load	5342.4	5098.4	4790.5	5423.98	5423.98	5423.98	kW(R)

Table 9.195 Condenser water circuit

	CHILLER			S-sheet			
Condenser	**Cond. 3**	**Cond. 2**	**Cond. 1**	**Cond. 3**	**Cond. 2**	**Cond. 1**	**Unit**
Fouling factor	0.00020	0.00020	0.00020	-	-	-	m^2 °C/W
Water flowrate	160.00	160.00	160.00	160.00	160.00	160.00	kg/s
Tube water velocity	2.65	2.65	2.65	-	-	-	m/s
Inlet water temp.	51.56	41.50	32.00	52.62	42.19	32.00	°C
Outlet water temp.	62.14	51.56	41.50	63.29	52.62	42.19	°C
Water heat load	7088.5	6743.0	6361.4	7146.71	6985.64	6826.85	kW(R)

Table 9.196 Evaporator refrigerant circuit

	CHILLER			S-sheet			
Evaporator	**Evap. 3**	**Evap. 2**	**Evap. 1**	**Evap. 3**	**Evap. 2**	**Evap. 1**	**Unit**
Refrigerant flowrate	45.17	41.31	37.41	-	-	-	kg/s
Refrigerant temperature	14.19	9.44	5.04	13.33	8.50	3.66	°C
Refrigerant pressure	479.59	415.95	362.84	-	-	-	kPa
Inlet refrigerant enthalpy	75.17	68.08	61.62	-	-	-	kJ/kg
Outlet refrigerant enthalpy	193.45	191.50	189.66	-	-	-	kJ/kg
Tube thermal resistance	0.0521	0.0521	0.0521	-	-	-	°C/MW
Fouling thermal resistance	0.7150	0.7150	0.7150	-	-	-	°C/MW
Water thermal resistance	0.2957	0.3132	0.3317	-	-	-	°C/MW
Ref. thermal resistance	0.4346	0.4491	0.4691	-	-	-	°C/MW
Overall UA	667.81	653.88	637.79	600.00	600.00	600.00	kW/°C
Refrigerant heat load	5342.4	5098.4	4790.5	5423.98	5423.98	5423.98	kW(R)

Table 9.197 Condenser refrigerant circuit

	CHILLER			S-sheet			
Condenser	**Cond. 3**	**Cond. 2**	**Cond. 1**	**Cond. 3**	**Cond. 2**	**Cond. 1**	**Unit**
Refrigerant flowrate	57.93	50.13	43.44	-	-	-	kg/s
Refrigerant temperature	66.82	56.10	45.87	67.92	57.15	46.62	°C
Refrigerant pressure	1764.53	1399.75	1106.59	-	-	-	kPa
Inlet refrigerant enthalpy	225.78	225.97	227.05	-	-	-	kJ/kg
Outlet refrigerant enthalpy	103.43	91.45	80.60	-	-	-	kJ/kg
Tube thermal resistance	0.0422	0.0422	0.0422	-	-	-	°C/MW
Fouling thermal resistance	0.5801	0.5801	0.5801	-	-	-	°C/MW
Water thermal resistance	0.2121	0.2314	0.2533	-	-	-	°C/MW
Ref. thermal resistance	0.4275	0.4232	0.4182	-	-	-	°C/MW
Overall UA	792.44	783.11	772.89	800.00	800.00	800.00	kW/°C
Refrigerant heat load	7088.5	6743.0	6361.4	7146.71	6985.64	6826.85	kW(R)

Table 9.198 Stage 1 compressor performance

	CHILLER			S-sheet			
Compressor 1	**Chiller 3**	**Chiller 2**	**Chiller 1**	**Chiller 3**	**Chiller 2**	**Chiller 1**	**Unit**
Vane angle	0.00	0.00	0.00	-	-	-	degrees
Refrigerant flowrate	45.17	41.31	37.41	-	-	-	kg/s
Inlet volumetric flowrate	1.64	1.72	1.78	-	-	-	m^3/s
Inlet refrigerant temp.	14.19	9.44	5.04	-	-	-	°C
Inlet refrigerant pressure	479.59	415.95	362.84	-	-	-	kPa
Inlet specific volume	0.03626	0.04161	0.04745	-	-	-	m^3/kg
Inlet enthalpy	193.45	191.50	189.66	-	-	-	kJ/kg
Outlet refrigerant temp.	50.47	45.59	41.67	-	-	-	°C
Outlet ref. pressure	974.34	816.27	687.34	-	-	-	kPa
Outlet specific volume	0.01902	0.02297	0.02757	-	-	-	m^3/kg
Outlet enthalpy	211.08	209.94	209.12	-	-	-	kJ/kg
Isentropic head	12.51	11.88	11.22	-	-	-	kJ/kg
Isentropic efficiency	70.97	64.44	57.66	-	-	-	%
Absorbed power	796.5	761.5	727.9	1722.73 (combined)	1561.66 (combined)	1402.87 (combined)	kW(M)
Operating region	STABLE	STABLE	STABLE	-	-	-	-

Table 9.199 Stage 2 compressor performance

	CHILLER			S-sheet			
Compressor 2	**Chiller 3**	**Chiller 2**	**Chiller 1**	**Chiller 3**	**Chiller 2**	**Chiller 1**	**Unit**
Vane angle	0.00	0.00	0.00	-	-	-	degrees
Refrigerant flowrate	57.93	50.13	43.44	-	-	-	kg/s
Inlet volumetric flowrate	1.09	1.14	1.19	-	-	-	m^3/s
Inlet refrigerant temp.	48.27	43.44	36.61	-	-	-	°C
Inlet refrigerant pressure	974.34	816.27	687.34	-	-	-	kPa
Inlet specific volume	0.01878	0.02271	0.02728	-	-	-	m^3/kg
Inlet enthalpy	209.39	208.35	207.64	-	-	-	kJ/kg
Outlet refrigerant temp.	83.32	77.40	73.89	-	-	-	°C
Outlet ref. pressure	1764.53	1399.75	1106.59	-	-	-	kPa
Outlet specific volume	0.01072	0.01405	0.01842	-	-	-	m^3/kg
Outlet enthalpy	225.78	225.97	227.05	-	-	-	kJ/kg
Isentropic head	10.84	10.04	9.00	-	-	-	kJ/kg
Isentropic efficiency	66.14	56.96	46.37	-	-	-	%
Absorbed power	949.6	883.1	843.0	Refer to Compr. 1	Refer to Compr. 1	Refer to Compr. 1	kW(M)
Operating region	STABLE	STABLE	STABLE	-	-	-	-

9.3.6 Kloof mine, 4 chillers operating at full load

This section combines the results from Sections 9.1.6 and 9.2.5

Table 9.200 Installation performance, with $t_{(w)Co[max]}$= 70°C

	CHILLER	S-sheet	
Installation	**Value**	**Value**	**Unit**
Return water available temp.	32.00	32.00	°C
Return water final temp.	70.24	70.00	°C
Cool water available temp.	25.00	25.00	°C
Chilled water final temp.	10.50	10.50	°C
Lorenz COP	8.80	8.83	-
System COP	3.05	3.39	-
Mass flowrate of return water	160.00	160.00	kg/s
Total evap. water heat load	19286.50	19653.18	kW(R)
Total return w. utilization	120.54	122.83	kW(R)/(kg/s)

Table 9.201 Chiller performance

	CHILLER				S-sheet				
Chiller	**Chill. 4**	**Chill. 3**	**Chill. 2**	**Chill. 1**	**Chill. 4**	**Chill. 3**	**Chill. 2**	**Chill. 1**	**Unit**
Carnot COP	5.00	5.37	5.98	6.80	4.85	5.36	5.98	6.74	-
COP	2.84	3.15	3.16	3.06	2.91	3.21	3.59	4.04	-
Cycle efficiency	0.57	0.59	0.53	0.45	60	60	60	60	%
Ret. w. utiliz.	28.68	31.15	30.87	29.83	30.71	30.71	30.71	30.71	kW(R)/(kg/s)

Table 9.202 Evaporator water circuit

	CHILLER				S-sheet				
Evaporator	**Evap. 4**	**Evap. 3**	**Evap. 2**	**Evap. 1**	**Evap. 4**	**Evap. 3**	**Evap. 2**	**Evap. 1**	**Unit**
Fouling factor	0.00020	0.00020	0.00020	0.00020	-	-	-	-	m^2 °C/W
Water flowrate	317.75	317.75	317.75	317.75	323.71	323.71	323.71	323.71	kg/s
Tube w. vel.	4.33	4.33	4.33	4.33	-	-	-	-	m/s
Inlet w. temp.	25.00	21.55	17.80	14.09	25.00	21.38	17.75	14.13	°C
Outlet w. temp.	21.55	17.80	14.09	10.50	21.38	17.75	14.13	10.50	°C
Water heat load	4589.3	4984.2	4939.8	4773.2	4913.29	4913.29	4913.29	4913.29	kW(R)

Table 9.203 Condenser water circuit

	CHILLER				S-sheet				
Condenser	**Cond. 4**	**Cond. 3**	**Cond. 2**	**Cond. 1**	**Cond. 4**	**Cond. 3**	**Cond. 2**	**Cond. 1**	**Unit**
Fouling factor	0.00020	0.00020	0.00020	0.00020	-	-	-	-	m^2 °C/W
Water flowrate	160.00	160.00	160.00	160.00	160.00	160.00	160.00	160.00	kg/s
Tube w. vel.	2.65	2.65	2.65	2.65	-	-	-	-	m/s
Inlet w. temp.	60.27	51.17	41.46	32.00	60.14	50.53	41.15	32.00	°C
Outlet w. temp.	70.24	60.97	51.17	41.46	70.00	60.14	50.53	41.15	°C
Water heat load	6207.2	6568.9	6505.5	6335.0	6602.66	6441.78	6283.80	6128.71	kW(R)

Table 9.204 Evaporator refrigerant circuit

	CHILLER				S-sheet				
Evaporator	**Evap. 4**	**Evap. 3**	**Evap. 2**	**Evap. 1**	**Evap. 4**	**Evap. 3**	**Evap. 2**	**Evap. 1**	**Unit**
Ref. flowrate	39.90	41.69	39.85	37.26	-	-	-	-	kg/s
Ref. temp.	16.28	12.16	8.43	4.92	14.87	11.24	7.62	3.99	°C
Ref. pressure	509.77	451.58	403.25	361.49	-	-	-	-	kPa
Inlet ref. enth.	79.28	73.08	67.12	61.52	-	-	-	-	kJ/kg
Outlet ref. enth.	194.29	192.62	191.08	189.62	-	-	-	-	kJ/kg
Tube therm. res.	0.0521	0.0521	0.0521	0.0521	-	-	-	-	°C/MW
Fouling therm. res.	0.7150	0.7150	0.7150	0.7150	-	-	-	-	°C/MW
Water therm. res.	0.2426	0.2527	0.2641	0.2763	-	-	-	-	°C/MW
Ref. therm. res.	0.4834	0.4563	0.4591	0.4703	-	-	-	-	°C/MW
Overall UA	669.76	677.49	671.00	660.64	600.00	600.00	600.00	600.00	kW/°C
Ref. heat load	4589.3	4984.2	4939.8	4773.2	4913.29	4913.29	4913.29	4913.29	kW(R)

Table 9.205 Condenser refrigerant circuit

	CHILLER				S-sheet				
Condenser	**Cond. 4**	**Cond. 3**	**Cond. 2**	**Cond. 1**	**Cond. 4**	**Cond. 3**	**Cond. 2**	**Cond. 1**	**Unit**
Ref. flowrate	54.05	53.48	48.46	43.27	-	-	-	-	kg/s
Ref. temp.	74.17	65.26	55.52	45.81	74.28	64.32	54.61	45.12	°C
Ref. pressure	2052.13	1707.73	1381.91	1105.02	-	-	-	-	kPa
Inlet ref. enth.	226.96	224.47	225.08	226.93	-	-	-	-	kJ/kg
Outlet ref. enth.	112.12	101.64	90.82	80.54	-	-	-	-	kJ/kg
Tube therm. res.	0.0422	0.0422	0.0422	0.0422	-	-	-	-	°C/MW
Fouling therm. res.	0.5801	0.5801	0.5801	0.5801	-	-	-	-	°C/MW
Water therm. res.	0.1980	0.2134	0.2319	0.2534	-	-	-	-	°C/MW
Ref. therm. res.	0.4116	0.4190	0.4192	0.4177	-	-	-	-	°C/MW
Overall UA	811.71	796.98	785.30	773.14	800.00	800.00	800.00	800.00	kW/°C
Ref. heat load	6207.2	6568.9	6505.5	6335.0	6602.66	6441.78	6283.80	6128.71	kW(R)

Table 9.206 Stage 1 compressor performance

	CHILLER				S-sheet				
Compressor 1	**Chill. 4**	**Chill. 3**	**Chill. 2**	**Chill. 1**	**Chill. 4**	**Chill. 3**	**Chill. 2**	**Chill. 1**	**Unit**
Vane angle	0.00	0.00	0.00	0.00	-	-	-	-	deg.
Ref. flowrate	39.90	41.69	39.85	37.26	-	-	-	-	kg/s
Inlet vol. flowrate	1.36	1.60	1.71	1.77	-	-	-	-	m^3/s
Inlet ref. temp.	16.28	12.16	8.43	4.92	-	-	-	-	°C
Inlet ref. pressure	509.77	451.58	403.25	361.49	-	-	-	-	kPa
Inlet specific vol.	0.03417	0.03844	0.04287	0.04762	-	-	-	-	m^3/kg
Inlet enthalpy	194.29	192.62	191.08	189.62	-	-	-	-	kJ/kg
Outlet ref. temp.	54.68	48.24	44.39	41.52	-	-	-	-	°C
Outlet ref. pressure	1073.60	925.94	796.20	685.28	-	-	-	-	kPa
Outlet specific vol.	0.01726	0.02000	0.02351	0.02764	-	-	-	-	m^3/kg
Outlet enthalpy	212.75	210.16	209.37	209.05	-	-	-	-	kJ/kg
Isentropic head	13.16	12.67	11.98	11.23	-	-	-	-	kJ/kg
Isentropic efficiency	71.27	72.26	65.52	57.78	-	-	-	-	%
Absorbed power	736.6	731.3	728.8	724.2	1689.37 (comb.)	1528.49 (comb.)	1370.51 (comb.)	1215.42 (comb.)	kW(M)
Operating region	STABLE	STABLE	STABLE	STABLE	-	-	-	-	-

Table 9.207 Stage 2 compressor performance

	CHILLER				S-sheet				
Compressor 2	**Chill. 4**	**Chill. 3**	**Chill. 2**	**Chill. 1**	**Chill. 4**	**Chill. 3**	**Chill. 2**	**Chill. 1**	**Unit**
Vane angle	0.00	0.00	0.00	0.00	-	-	-	-	deg.
Ref. flowrate	54.05	53.48	48.46	43.27	-	-	-	-	kg/s
Inlet vol. flowrate	0.92	1.06	1.13	1.18	-	-	-	-	m^3/s
Inlet ref. temp.	52.01	46.08	42.27	39.47	-	-	-	-	°C
Inlet ref. pressure	1073.60	925.94	796.20	685.28	-	-	-	-	kPa
Inlet specific vol.	0.01699	0.01976	0.02325	0.02736	-	-	-	-	m^3/kg
Inlet enthalpy	210.65	208.52	207.81	207.58	-	-	-	-	kJ/kg
Outlet ref. temp.	89.47	80.83	75.98	73.71	-	-	-	-	°C
Outlet ref. pressure	2052.13	1707.73	1381.91	1105.02	-	-	-	-	kPa
Outlet specific vol.	0.00903	0.01103	0.01417	0.01844	-	-	-	-	m^3/kg
Outlet enthalpy	226.96	224.47	225.08	226.93	-	-	-	-	kJ/kg
Isentropic head	11.73	11.19	10.25	9.03	-	-	-	-	kJ/kg
Isentropic efficiency	71.96	70.10	59.36	46.65	-	-	-	-	%
Absorbed power	881.3	853.4	836.9	837.6	Refer to compr.1	Refer to compr.1	Refer to compr.1	Refer to compr.1	kW(M)
Operating region	STABLE	STABLE	STABLE	STABLE	-	-	-	-	-

9.3.7 Tau Tona mine, 4 chillers operating at full load

This section combines the results from Sections 9.1.8 and 9.2.8

Table 9.208 Installation performance, with $t_{(w)Co[max]}$= 70°C

	CHILLER	S-sheet	
Installation	**Value**	**Value**	**Unit**
Return water available temp.	32.00	32.00	°C
Return water final temp.	51.84	52.42	°C
Cool water available temp.	18.89	18.89	°C
Chilled water final temp.	5.50	5.50	°C
Lorenz COP	9.61	9.52	-
System COP	3.29	3.85	-
Mass flowrate of return water	266.00	266.00	kg/s
Total evap. water heat load	16946.50	18048.00	kW(R)
Total return w. utilization	63.71	67.85	kW(R)/(kg/s)

Table 9.209 Chiller performance

	CHILLER				S-sheet				
Chiller	**Chill. 4**	**Chill. 3**	**Chill. 2**	**Chill. 1**	**Chill. 4**	**Chill. 3**	**Chill. 2**	**Chill. 1**	**Unit**
Carnot COP	6.17	6.43	6.71	6.99	6.14	6.32	6.51	6.71	-
COP	3.22	3.28	3.33	3.35	3.69	3.79	3.91	4.03	-
Cycle efficiency	52	51	50	48	60	60	60	60	%
Ret. w. utiliz.	17.49	16.40	15.38	14.43	16.96	16.96	16.96	16.96	kW(R)/(kg/s)

Table 9.210 Evaporator water circuit

	CHILLER				S-sheet				
Evaporator	**Evap. 4**	**Evap. 3**	**Evap. 2**	**Evap. 1**	**Evap. 4**	**Evap. 3**	**Evap. 2**	**Evap. 1**	**Unit**
Fouling factor	0.00009	0.00009	0.00009	0.00009	-	-	-	-	m^2 °C/W
Water flowrate	302.29	302.29	302.29	302.29	321.92	321.92	321.92	321.92	kg/s
Tube w. vel.	1.86	1.86	1.86	1.86	-	-	-	-	m/s
Inlet w. temp.	18.89	15.21	11.77	8.53	18.89	15.54	12.20	8.85	°C
Outlet w. temp.	15.21	11.77	8.53	5.50	15.54	12.20	8.85	5.50	°C
Water heat load	4653.1	4363.4	4091.4	3838.6	4512.00	4512.00	4512.00	4512.00	kW(R)

Table 9.211 Condenser water circuit

	CHILLER				S-sheet				
Condenser	**Cond. 4**	**Cond. 3**	**Cond. 2**	**Cond. 1**	**Cond. 4**	**Cond. 3**	**Cond. 2**	**Cond. 1**	**Unit**
Fouling factor	0.00018	0.00018	0.00018	0.00018	-	-	-	-	m^2 °C/W
Water flowrate	266.00	266.00	266.00	266.00	266.00	266.00	266.00	266.00	kg/s
Tube w. vel.	2.94	2.94	2.94	2.94	-	-	-	-	m/s
Inlet w. temp.	46.36	41.25	36.47	32.00	47.27	42.15	37.06	32.00	°C
Outlet w. temp.	51.84	46.36	41.25	36.47	52.42	47.27	42.15	37.06	°C
Water heat load	6098.6	5692.7	5321.5	4983.2	5736.37	5701.90	5667.43	5632.98	kW(R)

Table 9.212 Evaporator refrigerant circuit

	CHILLER				S-sheet				
Evaporator	**Evap. 4**	**Evap. 3**	**Evap. 2**	**Evap. 1**	**Evap. 4**	**Evap. 3**	**Evap. 2**	**Evap. 1**	**Unit**
Ref. flowrate	35.06	32.25	29.72	27.46	-	-	-	-	kg/s
Ref. temp.	10.48	7.14	4.01	1.08	11.05	7.70	4.35	1.00	°C
Ref. pressure	429.28	387.44	351.13	319.49	-	-	-	-	kPa
Inlet ref. enth.	59.20	55.23	51.57	48.19	-	-	-	-	kJ/kg
Outlet ref. enth.	191.93	190.54	189.23	187.98	-	-	-	-	kJ/kg
Tube therm. res.	0.0826	0.0826	0.0826	0.0826	-	-	-	-	°C/MW
Fouling therm. res.	0.3014	0.3014	0.3014	0.3014	-	-	-	-	°C/MW
Water therm. res.	0.4958	0.5178	0.5404	0.5633	-	-	-	-	°C/MW
Ref. therm. res.	0.4951	0.5178	0.5417	0.5664	-	-	-	-	°C/MW
Overall UA	727.34	704.38	682.10	660.60	750.00	750.00	750.00	750.00	kW/°C
Ref. heat load	4653.1	4363.4	4091.4	3838.6	4512.00	4512.00	4512.00	4512.00	kW(R)

Table 9.213 Condenser refrigerant circuit

	CHILLER				S-sheet				
Condenser	**Cond. 4**	**Cond. 3**	**Cond. 2**	**Cond. 1**	**Cond. 4**	**Cond. 3**	**Cond. 2**	**Cond. 1**	**Unit**
Ref. flowrate	45.89	41.15	37.12	33.67	-	-	-	-	kg/s
Ref. temp.	56.47	50.70	45.33	40.31	57.32	52.14	46.99	41.87	°C
Ref. pressure	1411.25	1238.72	1092.36	967.63	-	-	-	-	kPa
Inlet ref. enth.	224.76	224.02	223.40	222.90	-	-	-	-	kJ/kg
Outlet ref. enth.	91.85	85.66	80.03	74.89	-	-	-	-	kJ/kg
Tube therm. res.	0.0660	0.0660	0.0660	0.0660	-	-	-	-	°C/MW
Fouling therm. res.	0.4976	0.4976	0.4976	0.4976	-	-	-	-	°C/MW
Water therm. res.	0.2031	0.2129	0.2228	0.2331	-	-	-	-	°C/MW
Ref. therm. res.	0.3830	0.3767	0.3707	0.3650	-	-	-	-	°C/MW
Overall UA	869.79	867.19	864.22	860.87	800.00	800.00	800.00	800.00	kW/°C
Ref. heat load	6098.6	5692.7	5321.5	4983.2	5736.37	5701.90	5667.43	5632.98	kW(R)

Table 9.214 Stage 1 compressor performance

	CHILLER				S-sheet				
Compressor 1	**Chill. 4**	**Chill. 3**	**Chill. 2**	**Chill. 1**	**Chill. 4**	**Chill. 3**	**Chill. 2**	**Chill. 1**	**Unit**
Vane angle	0.00	0.00	0.00	0.00	-	-	-	-	deg.
Ref. flowrate	35.06	32.25	29.72	27.46	-	-	-	-	kg/s
Inlet vol. flowrate	1.41	1.44	1.46	1.47	-	-	-	-	m^3/s
Inlet ref. temp.	10.48	7.14	4.01	1.08	-	-	-	-	°C
Inlet ref. pressure	429.28	387.44	351.13	319.49	-	-	-	-	kPa
Inlet specific vol.	0.04036	0.04455	0.04896	0.05359	-	-	-	-	m^3/kg
Inlet enthalpy	191.93	190.54	189.23	187.98	-	-	-	-	kJ/kg
Outlet ref. temp.	32.06	28.88	25.97	23.32	-	-	-	-	°C
Outlet ref. pressure	642.46	573.23	513.95	462.96	-	-	-	-	kPa
Outlet specific vol.	0.02839	0.03188	0.03561	0.03955	-	-	-	-	m^3/kg
Outlet enthalpy	202.98	201.93	200.94	200.02	-	-	-	-	kJ/kg
Isentropic head	7.07	6.85	6.64	6.44	-	-	-	-	kJ/kg
Isentropic efficiency	63.95	60.13	56.66	53.50	-	-	-	-	%
Absorbed power	387.4	367.1	348.1	330.4	1224.37 (comb.)	1189.90 (comb.)	1155.43 (comb.)	1120.98 (comb.)	kW(M)
Operating region	STABLE	STABLE	STABLE	STABLE	-	-	-	-	-

Table 9.215 Stage 2 compressor performance

	CHILLER				S-sheet				
Compressor 2	**Chill. 4**	**Chill. 3**	**Chill. 2**	**Chill. 1**	**Chill. 4**	**Chill. 3**	**Chill. 2**	**Chill. 1**	**Unit**
Vane angle	0.00	0.00	0.00	0.00	-	-	-	-	deg.
Ref. flowrate	45.89	41.15	37.12	33.67	-	-	-	-	kg/s
Inlet vol. flowrate	1.29	1.30	1.31	1.32	-	-	-	-	m^3/s
Inlet ref. temp.	30.27	27.03	24.09	21.41	-	-	-	-	°C
Inlet ref. pressure	642.46	573.23	513.95	462.96	-	-	-	-	kPa
Inlet specific vol.	0.02812	0.03158	0.03527	0.03918	-	-	-	-	m^3/kg
Inlet enthalpy	201.69	200.63	199.64	198.71	-	-	-	-	kJ/kg
Outlet ref. temp.	76.08	72.19	68.85	65.99	-	-	-	-	°C
Outlet ref. pressure	1411.25	1238.72	1092.36	967.63	-	-	-	-	kPa
Outlet specific vol.	0.01380	0.01592	0.01825	0.02080	-	-	-	-	m^3/kg
Outlet enthalpy	224.76	224.02	223.40	222.90	-	-	-	-	kJ/kg
Isentropic head	14.35	14.13	13.89	13.63	-	-	-	-	kJ/kg
Isentropic efficiency	62.22	60.43	58.45	56.34	-	-	-	-	%
Absorbed power	1058.2	962.3	882.1	814.2	Refer to compr.1	Refer to compr.1	Refer to compr.1	Refer to compr.1	kW(M)
Operating region	STABLE	STABLE	STABLE	STABLE	-	-	-	-	-

10 APPENDIX C SPREADSHEET SIMULATION MODEL

The model allows investigation of multiple-chiller series-counterflow arrangements by calculating, amongst other outputs, evaporator chilling load, return water utilization, COP and compressor absorbed power.

For all spreadsheet simulations, the machine cycle efficiency is assumed constant at 60%. The assumption suggests that the machines are infinitely flexible, meaning that they are able to maintain constant cycle efficiency for a range of operating conditions.

The spreadsheet model was developed for a single chiller. Successive machines are added by using the basic model, with inputs to the new machine being governed by outputs from the previous machine. In this way, any combination of chillers may be modelled.

The procedure used to select constant UA_E and UA_C terms is given in Appendix E. The maximum chilling load for a single machine was set for Kloof mine and Tau Tona mine by running a CHILLER simulation for the same operating regime and observing the maximum return water temperature reached. The evaporator water flowrate for a single spreadsheet machine was varied to deliver a similar return water outlet temperature and the resulting evaporator water heat load was taken as the maximum load achievable by a single machine.

If the nominal maximum chilling load of several chillers would cause the return water temperature to exceed its maximum allowed value, the individual equal chiller loads were reduced so as not to exceed this maximum.

Table 10.1 Spreadsheet solution criteria

Scenario type	Adjust	Solution criteria	Supporting variable
A. The operating regime limits the refrigerating load because of the limited heat rejection facility provided by available return water. The final temperature of the return water is regulated to remain at, without exceeding, its specified maximum allowed value	$\dot{m}_{wE}$	$t_{(w)Co} = t_{(w)Co[max]}$ that is, when the return water temperature reaches its specified maximum allowed value at the condenser outlet of the lead chiller	$\sum \dot{Q}_E < \sum \dot{Q}_{E[max]}$ The total evaporator water chilling load is less than the chilling load achieved when all machines are at full capacity
B. The capacity of the installation limits refrigerating load. The final temperature of the return water is below its specified maximum allowed value, with all machines running at full capacity		$\sum \dot{Q}_E = \sum \dot{Q}_{E[max]}$ that is, when each chiller delivers an evaporator water chilling load equal to the maximum, as defined in sections 3.2.2 and 3.3.2	$t_{(w)Co} < t_{(w)Co[max]}$ The return water temperature does not reach its specified maximum allowed value at the condenser outlet of the lead chiller

For an evaporator of constant *UA* and where the evaporating refrigerant temperature $t_{(r)E}$ is constant, Bailey-McEwan (2004) gives the derivation of COP of a water chilling machine when the condenser outlet water temperature is unknown, as follows.

$$t_{(r)E} = \frac{t_{(w)Eo} - t_{(w)Ei}\exp\left(\dfrac{-UA_E}{m_{(w)E}c_{(w)}}\right)}{1-\exp\left(\dfrac{-UA_E}{m_{(w)E}c_{(w)}}\right)} \qquad \text{(C.1a)}$$

Writing $NTU_E \equiv \dfrac{UA_E}{m_{(w)E}c_{(w)}}$, this becomes

$$t_{(r)E} = \frac{t_{(w)Eo} - t_{(w)Ei}\exp(-NTU_E)}{1-\exp(-NTU_E)}$$, and similarly $t_{(r)C} = \frac{t_{(w)Co} - t_{(w)Ci}\exp(-NTU_C)}{1-\exp(-NTU_C)}$,(C.1b)

where $NTU_C \equiv \dfrac{UA_C}{m_{(w)C}c_{(w)}}$.

The Carnot COP is

$$COP_{\text{Car}} = \frac{T_{(r)E}}{T_{(r)C} - T_{(r)E}} = \frac{273{,}15 + t_{(r)E}}{t_{(r)C} - t_{(r)E}} \qquad \text{(C.2)}$$

with $t_{(r)E}$ and $t_{(r)C}$ given by (C.1b) above. Now since the COP is given by $COP = COP_{\text{Car}}\eta_{\text{Car}}$, where η_{Car} is the Carnot cycle efficiency,

$$COP = \frac{\eta_{\text{Car}}(273{,}15 + t_{(r)E})}{t_{(r)C} - t_{(r)E}} \qquad \text{(C.3)}$$

Now the condenser heat load is given by

$$Q_{(w)C} = m_{(w)C}c_{(w)}(t_{(w)Co} - t_{(w)Ci}) = -Q_{(w)E}(1 + 1/COP) = m_{(w)E}c_{(w)}(t_{(w)Ei} - t_{(w)Eo})(1 + 1/COP)$$

Solving for $t_{(w)Co}$,

$$t_{(w)Co} = \frac{m_{(w)E}(t_{(w)Ei} - t_{(w)Eo})(1 + 1/COP)}{m_{(w)C}} + t_{(w)Ci} \qquad \text{(C.4)}$$

Substituting (C.4) in the second relation of (C.1b), it follows that

$$t_{(r)C} = \frac{t_{(w)Co} - t_{(w)Ci}\exp(-NTU_C)}{1-\exp(-NTU_C)} = \frac{m_{(w)E}\left(t_{(w)Ei} - t_{(w)Eo}\right)(1+1/COP)}{m_{(w)C}\left[1-\exp(-NTU_C)\right]} + t_{(w)Ci} \qquad \text{(C.5)}$$

Substituting (C.5) into (C.3),

$$COP = \frac{\eta_{Cat}\left(273{,}15 + t_{(r)E}\right)}{\dfrac{m_{(w)E}\left(t_{(w)Ei} - t_{(w)Eo}\right)}{m_{(w)C}\left[1-\exp(-NTU_C)\right]}(1+1/COP) + t_{(w)Ci} - t_{(r)E}} \qquad \text{(C.6)}$$

Apart from *COP,* all quantities in (C.6) are known. Writing

$R_{E/C} \equiv \dfrac{m_{(w)E}}{m_{(w)C}\left[1-\exp(-NTU_C)\right]}$ and solving (C.6) for *COP,*

$$COP = \frac{\eta_{Car}\left(273{,}15 + t_{(r)E}\right) + R_{E/C}\cdot\Delta t_{(w)E}}{-R_{E/C}\cdot\Delta t_{(w)E} + t_{(w)Ci} - t_{(r)E}} \qquad \text{(C.7)}$$

where $\Delta t_{(w)E} \equiv t_{(w)Eo} - t_{(w)Ei}$. Equation (C.7) is the one used in the spreadsheet

11 APPENDIX D MACHINE SPECIFICATIONS FOR THE CHILLER PROGRAM

11.1 Kloof mine

Table 11.1 Evaporator specification for chiller at Kloof gold mine

Description of attribute	Unit	Value
Amount of passes		4
Amount of tubes		1040
Diameter of tube	mm	13.4
Tube wall thickness	mm	1.3
Total inside wall area of tubes	m^2	279.71
Total outside wall area of tubes	m^2	1006.41
Tube thermal conductivity	W/m.K	44.00

Table 11.2 Condenser specification for chiller at Kloof gold mine

Description of attribute	Unit	Value
Amount of passes		3
Amount of tubes		1282
Diameter of tube	mm	13.4
Tube wall thickness	mm	1.3
Total inside wall area of tubes	m^2	344.76
Total outside wall area of tubes	m^2	1240.59
Tube thermal conductivity	W/m.K	44.00

Table 11.3 Compressor specification (First stage) for chiller at Kloof gold mine

Description of attribute	Unit	Value
Max. guide vane setting (fully open)	deg.	0
Min. guide vane setting (fully closed)	deg.	-80.00
Design refrigerant	R12	
Compressor curve family	Chamber of Mines	
Slope of full-capacity curve	very flat	
Design suction vol. flow-rate	m^3/s	1.58
Design isentropic head	kJ/kg	12.74
Design isentropic efficiency	%	72.50

Table 11.4 Compressor specification (Second stage) for chiller at Kloof gold mine

Description of attribute	Unit	Value
Max. guide vane setting (fully open)	deg.	Stage unregulated - no capacity control
Min. guide vane setting (fully closed)	deg.	
Design refrigerant	R12	
Compressor curve family	Chamber of Mines	
Slope of full-capacity curve	very flat	
Design suction vol. flow-rate	m^3/s	1.01
Design isentropic head	kJ/kg	11.47
Design isentropic efficiency	%	72.50

11.2 Tau Tona mine

Table 11.5 Evaporator specification for chiller at Tau Tona gold mine

Description of attribute	Unit	Value
Amount of passes		3
Amount of tubes		1040
Diameter of tube	mm	14.1
Tube wall thickness	mm	1.0
Total inside wall area of tubes	m^2	292.00
Total outside wall area of tubes	m^2	1003.00
Tube thermal conductivity	W/m.K	21.00

Table 11.6 Condenser specification for chiller at Tau Tona gold mine

Description of attribute	Unit	Value
Amount of passes		2
Amount of tubes		1282
Diameter of tube	mm	13.4
Tube wall thickness	mm	1.0
Total inside wall area of tubes	m^2	353.70
Total outside wall area of tubes	m^2	1284.00
Tube thermal conductivity	W/m.K	21.00

Table 11.7 Compressor specification (First stage) for chiller at Tau Tona gold mine

Description of attribute	Unit	Value
Max. guide vane setting (fully open)	deg.	0.00
Min. guide vane setting (fully closed)	deg.	-80.00
Design refrigerant	R12	
Compressor curve family	Chamber of Mines	
Slope of full-capacity curve	very flat	
Design suction vol. flow-rate	m^3/s	1.27
Design isentropic head	kJ/kg	7.89
Design isentropic efficiency	%	77.80

Table 11.8 Compressor specification (Second stage) for chiller at Tau Tona gold mine

Description of attribute	Unit	Value
Max. guide vane setting (fully open)	deg.	Stage unregulated - no capacity control
Min. guide vane setting (fully closed)	deg.	
Design refrigerant	R12	
Compressor curve family	Chamber of Mines	
Slope of full-capacity curve	very flat	
Design suction vol. flow-rate	m^3/s	1.15
Design isentropic head	kJ/kg	16.25
Design isentropic efficiency	%	77.80

12 APPENDIX E SPREADSHEET HEAT EXCHANGER MODELS

The evaporator water load is given by

$$Q_{(W)E}=m_{(W)E}c_{(W)}\left(t_{(W)Eo}-t_{(W)Ei}\right) \qquad \text{(Equation E.1)}$$

The heat transferred through the evaporator is

$$Q_E=UA_E\ LMTD_E \qquad \text{(Equation E.2)}$$

Where the log-mean temperature difference

$$LMTD_E=\frac{t_{(W)Eo}-t_{(W)Ei}}{ln\left(\frac{t_{(W)Eo}-t_{(r)E}}{t_{(W)Ei}-t_{(r)E}}\right)} \qquad \text{(Equation E.3)}$$

The condenser water heat load, the heat transferred through the condenser, and the condenser log-mean temperature difference are given by exactly analogous versions of Equations E.1, E.2 and E.3 respectively.

Initial estimates for the *constant* overall thermal conductance values for spreadsheet evaporator and condenser models were calculated for the spreadsheet using the work of Bailey-McEwan (1998) using the environmental conditions and constraints for Kloof mine and Tau Tona mine. With reference to Appendix F

- Evaporator overall thermal conductance is given by Equation F.5.

- The water side coefficient of heat transfer in the evaporator is given by Equation F.6.

- The coefficient of heat transfer to evaporating refrigerant is given by Equation F.9.

- Condenser overall thermal conductance is given by Equation F.14

- The water side coefficient of heat transfer in the condenser is given by an exactly analogous version of Equation F.6

- For a condenser, the coefficient of heat transfer from condensing refrigerant is given by Equation F.15.

These initial estimates were compared and confirmed for suitability with the range of expected overall thermal conductance values calculated by the CHILLER program, shown in Figures 12.1 to 12.4.

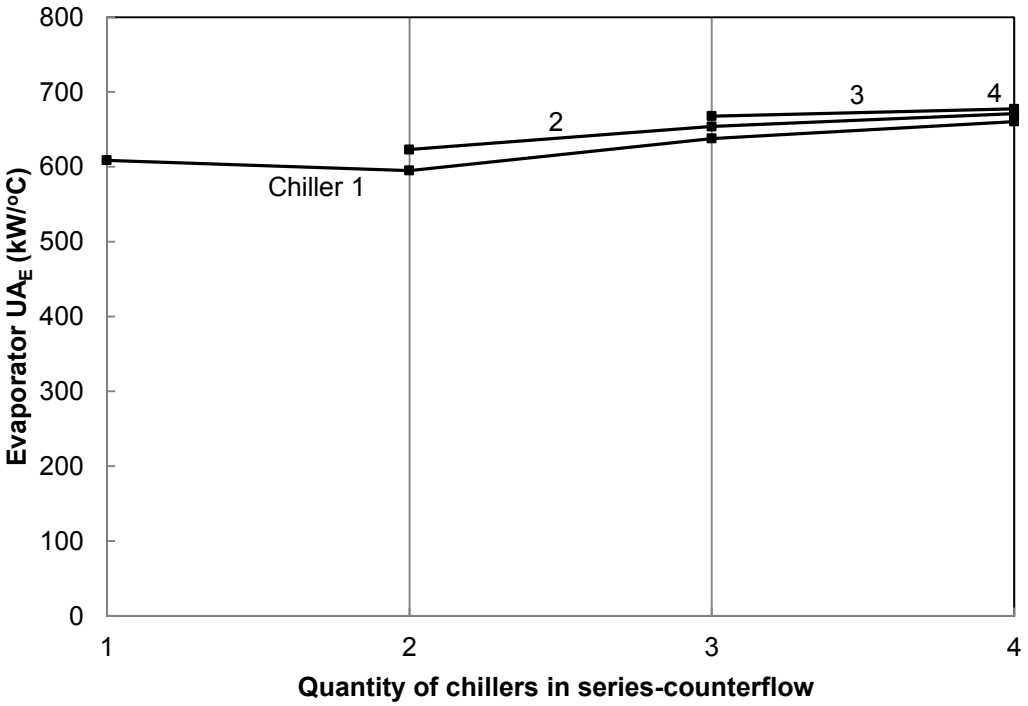

Figure 12.1 Variation in evaporator overall thermal conductance from CHILLER simulations, Kloof gold mine

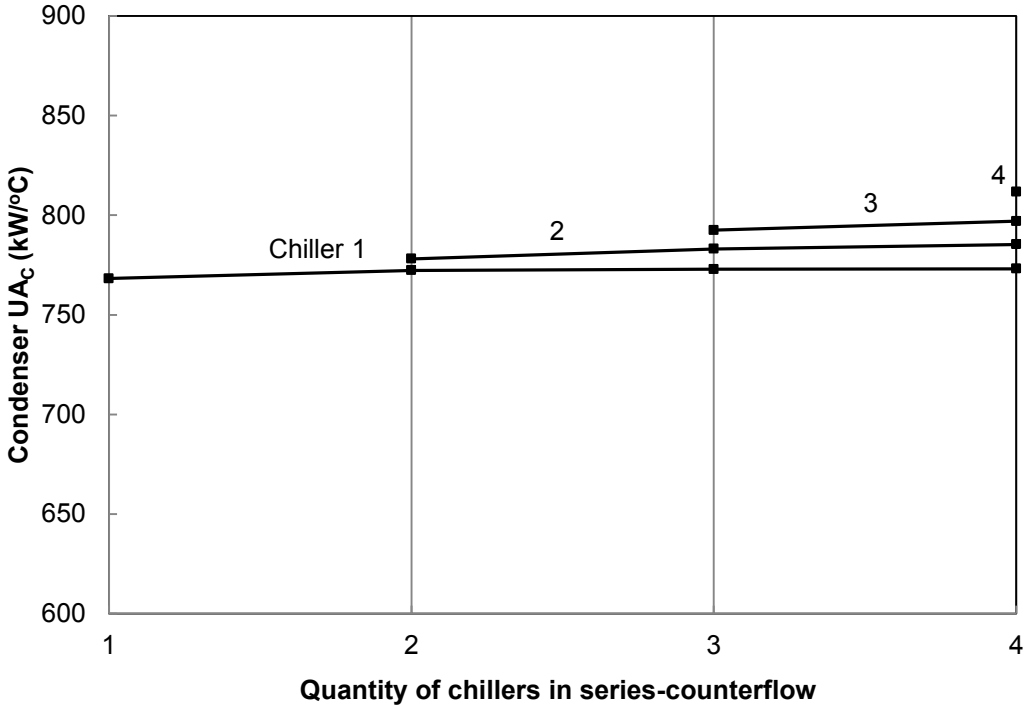

Figure 12.2 Variation in condenser overall thermal conductance from CHILLER simulations, Kloof gold mine

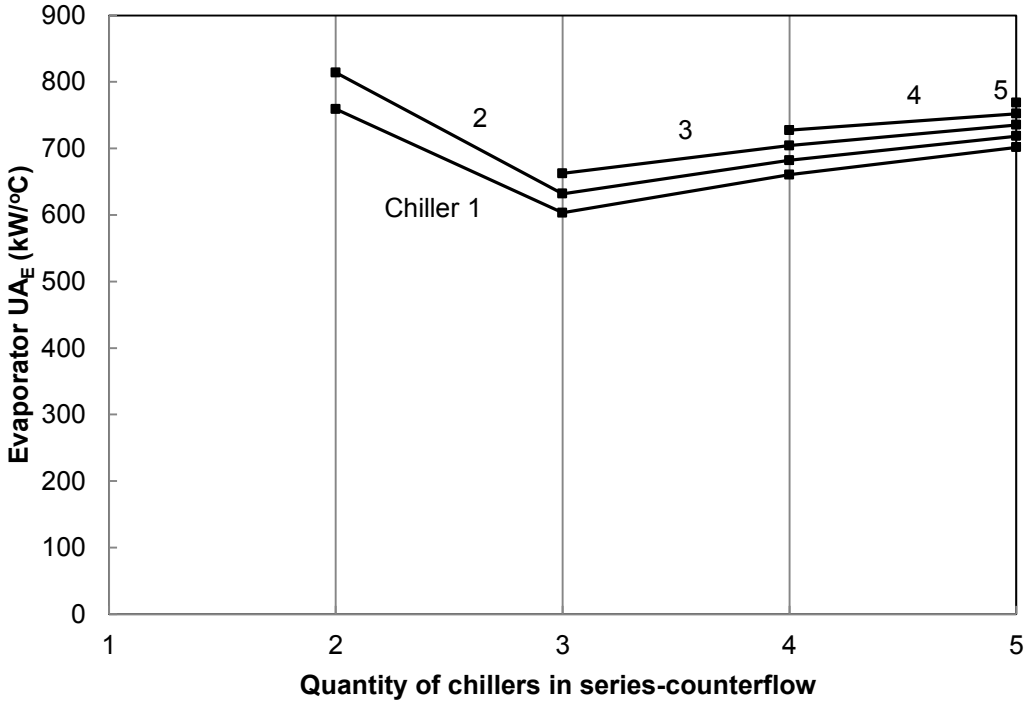

Figure 12.3 Variation in evaporator overall thermal conductance from CHILLER simulations, Tau Tona gold mine

Figure 12.4 Variation in condenser overall thermal conductance from CHILLER simulations, Tau Tona gold mine

13 APPENDIX F MODELLING OF CENTRIFUGAL CHILLERS IN THE CHILLER COMPUTER PROGRAM

All information in this appendix is from Bailey-McEwan (1998) and describes the modelling of centrifugal chillers in the CHILLER computer program.

Evaporator model in CHILLER

The evaporator water load is given by

$$Q_{(W)E}=m_{(W)E}c_{(W)}\left(t_{(W)Eo}-t_{(W)Ei}\right) \qquad \text{(Equation F.1)}$$

The evaporator refrigerant load $Q_{(r)E}$ is the product of the refrigerant mass flow rate and enthalpy change through the evaporator.

$$Q_{(r)E}=m_{(r)E}\left(h_{Eo}-h_{Ei}\right) \qquad \text{(Equation F.2)}$$

The heat transferred through the evaporator is

$$Q_E=UA_E\ LMTD_E \qquad \text{(Equation F.3)}$$

Where the log-mean temperature difference

$$LMTD_E=\frac{t_{(W)Eo}-t_{(W)Ei}}{ln\left(\frac{t_{(W)Eo}-t_{(r)E}}{t_{(W)Ei}-t_{(r)E}}\right)} \qquad \text{(Equation F.4)}$$

and

$$\frac{1}{UA_E}=\frac{1}{h'_{(W)E}A_{T[W]E}}+\frac{1}{h'_{f(W)E}A_{T[W]E}}+\frac{y_{TE}}{k_{TE}\bar{A}_{TE}}+\frac{1}{h'_{(r)E}A_{T[r]E}} \qquad \text{(Equation F.5)}$$

Bailey-McEwan (1998, p. 392) describes the water-side heat transfer coefficient.

$$h'_{[W]} = \frac{5\,680\left[1+0{,}015\left(t_{(W)i} + t_{(W)o}\right)/2\right]v_{(W)}^{0,8}}{d_T^{0,2}} \qquad \text{(Equation F.6)}$$

where $t_{(W)i}$ and $t_{(W)o}$ are the inlet and outlet water temperatures; d_T is the internal tube diameter in millimetres; and $v_{(W)}$ is the water velocity through the tube, given by

$$v_{(W)} = \frac{N_{pa} m_{(W)}}{N_T a_T \rho_{(W)}} \qquad \text{(Equation F.7)}$$

where N_{pa} and N_T are the amounts of passes and tubes respectively; a_T is the internal cross-sectional area of a tube, and $\rho_{(W)}$ is the density of water.

$A_{T[W]}$ is the total inside wall area of the tubes, with $A_{T[r]}$ the total outside wall area. The mean area $\overline{A_T}$ for calculation of the tube thermal resistance is correctly the logarithmic mean area. However, because the tube wall thickness is small (rarely exceeding 2mm), and the tube thermal resistance is thus likely to be the smallest of all four resistances in equation F.6, it is sufficiently accurate to use the arithmetic mean for $\overline{A_T}$:

$$\overline{A_T} \cong \left(A_{T[W]} + A_{T[r]}\right)/2 \qquad \text{(Equation F.8)}$$

The coefficient of heat transfer to evaporating refrigerant $h'_{(r)E}$ is expressed as a function of a constant C and the heat flux through the tubes in the following correlation, described by Bailey-McEwan (1998, p. 396).

$$h'_{(r)E} = C \cdot \left(Q_E / A_{T[W]}\right)^{0,7} \qquad \text{(Equation F.9)}$$

where $A_{T[W]}$ is the total inside wall area of the tubes. C=290 for refrigerant R12, used in all simulations.

Condenser model in CHILLER

Similarly to the evaporator model, the condenser water load and refrigerant load are given by

$$Q_{(W)C}=m_{(W)C}c_{(W)}\left(t_{(W)Co}-t_{(W)Ci}\right) \qquad \text{(Equation F.10)}$$

$$Q_{(r)C}=m_{(r)C}\left(h_{Co}-h_{Ci}\right) \qquad \text{(Equation F.11)}$$

The heat transferred through the condenser is

$$Q_C=UA_C\ LMTD_C \qquad \text{(Equation F.12)}$$

and similarly to the evaporator

$$LMTD_C=\frac{t_{(W)Co}-t_{(W)Ci}}{ln\left(\frac{t_{(W)Co}-t_{(r)C}}{t_{(W)Ci}-t_{(r)C}}\right)} \qquad \text{(Equation F.13)}$$

$$\frac{1}{UA_C}=\frac{1}{h'_{(W)C}A_{T[W]E}}+\frac{1}{h'_{f(W)C}A_{T[W]C}}+\frac{y_{TC}}{k_{TC}\bar{A}_{TC}}+\frac{1}{h'_{(r)C}A_{T[r]C}}$$

(Equation F.14)

$h'_{[W]C}$ and $\overline{A_{TC}}$ are given by exactly analogous versions of equations above. The coefficient $h'_{(r)C}$ of heat transfer from condensing refrigerant is given by Bailey-McEwan (1998, p. 400).

$$h'_{(r)C} = \frac{C}{\left[t_{(r)C} - \left(t_{(W)Ci} + t_{(W)Co}\right)/2\right]^{0,25}} \qquad \text{(Equation F.15)}$$

where C = 3 350 for Refrigerant 12.

Single compressor stage model in CHILLER

“Version 1.01 of CHILLER uses isentropic analysis in modelling individual stages of a centrifugal compressor”.
“Isentropic work and efficiency can be directly ascertained from the thermodynamic properties of the refrigerant employed.”

“A centrifugal compressor stage, assumed to be equipped with variable inlet guide vanes, is modelled in the form of maps of curves of fraction-of-design isentropic head and fraction of design isentropic efficiency, both being functions of fraction –of-design volumetric flow-rate and inlet guide vane opening. “

“The design point (100% of volumetric flow-rate, 100% of isentropic head) is always defined to be on the curve for a guide vane angle of 0^{o} (i.e. when the guide vanes are fully open). For each position of the vanes, different curves of isentropic head and efficiency obtain.”

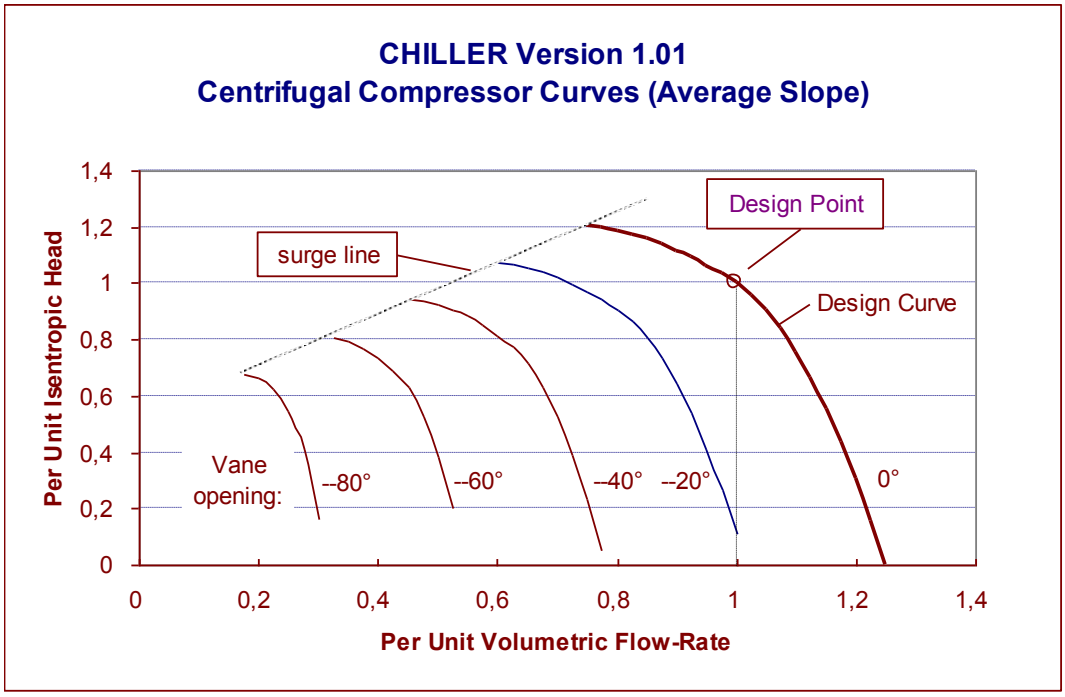

Figure 13.1 CHILLER Version 1.01: Isentropic Head Curve Map for Centrifugal Compressor Stage with Inlet Guide Vanes

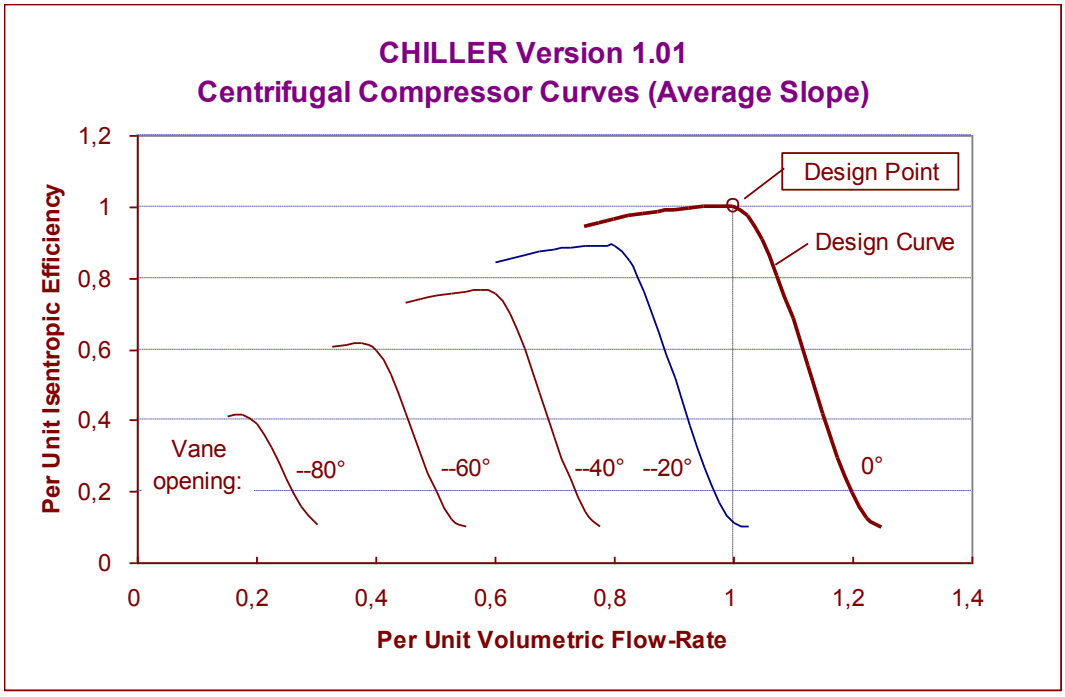

Figure 13.2 CHILLER Version 1.01: Efficiency Curve Map for Centrifugal Compressor Stage with Inlet Guide Vanes

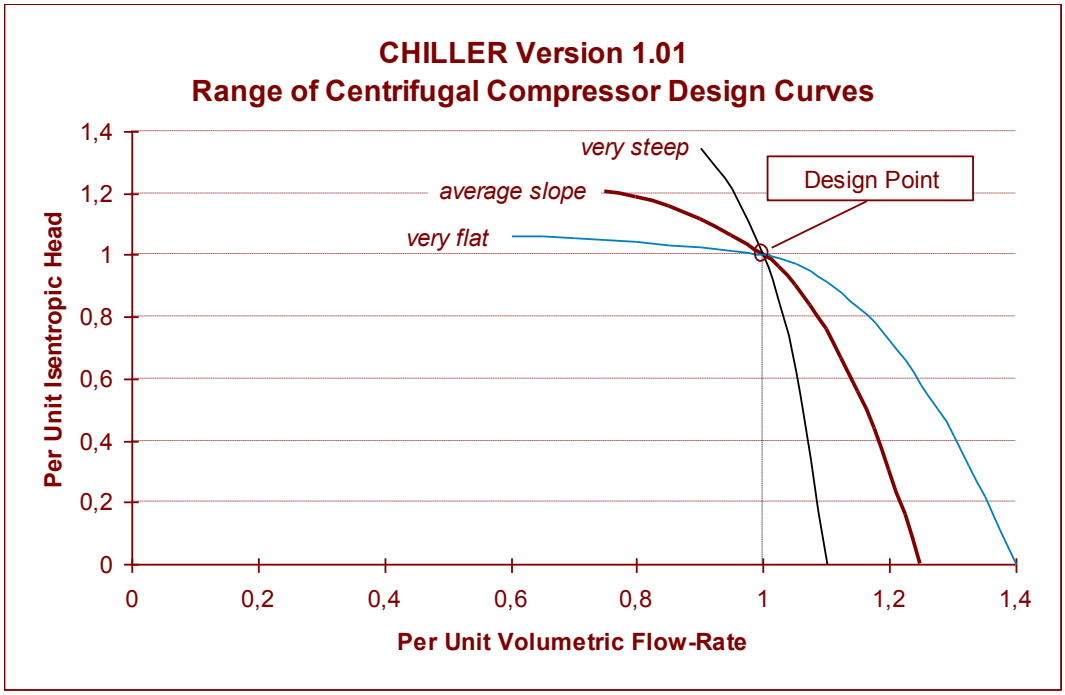

Figure 13.3 CHILLER Version 1.01: Range of Design Curves of Per Unit Isentropic Head versus Per Unit Volumetric Flow-Rate

The curves in the above figures are of per unit (i.e. fraction of design) isentropic head $\Delta h|_s / \Delta h|_{s.des}$ and per unit isentropic efficiency $\eta|_s / \eta|_{s.des}$ are expressed as functions of inlet guide-vane opening ψ and per unit (fraction-of-design) volumetric flow-rate $\dot{V}_{Pi} / \dot{V}_{Pi.des}$ as follows.

$$\frac{\Delta h|_s}{\Delta h|_{s.des}} = \frac{\Delta h|_s}{\Delta h|_{s.des}} \left(\psi , \frac{\dot{V}_{Pi}}{\dot{V}_{Pi.des}} \right) \qquad \text{(Equation F.16)}$$

and

$$\frac{\eta|_s}{\eta|_{s.des}} = \frac{\eta|_s}{\eta|_{s.des}} \left(\psi , \frac{\dot{V}_{Pi}}{\dot{V}_{Pi.des}} \right) \qquad \text{(Equation F.17)}$$

Characteristic curves of compressors may differ in the overall slope of the design curve, expressed relatively in terms of “steepness” or “flatness”. CHILLER version 1.01 allows seven different slopes of the design curve.

In this analysis, all compressor curves are modelled as “very flat”. So, as far as possible for less than design volumetric flow rate, a compressor maintains as high a fraction as possible of isentropic head and isentropic efficiency. Generally, isentropic efficiency falls off rapidly for refrigerant flow-rates above the design point.